A Study of Fouling on Ceramic Ultrafiltration Membranes by Model Solutions and Natural Waters

by

Leila Munla

A thesis
presented to the University of Waterloo
in fulfillment of the
thesis requirement for the degree of
Doctor of Philosophy
in
Civil Engineering

Waterloo, Ontario, Canada, 2013

AUTHOR'S DECLARATION

I hereby declare that I am the sole author of this thesis. This is a true copy of the thesis, including any required final revisions, as accepted by my examiners.

I understand that my thesis may be made electronically available to the public.

Abstract

Over the last decade polymeric membranes have emerged as an economically viable treatment option to produce drinking water. Due to higher capital costs, the use of ceramic membranes has generally been limited to industrial applications that deal with challenging water quality. Ceramic membranes are superior to polymeric membranes in their physical and chemical resistance, which allows for higher fluxes and backwash pressures as well as rigorous chemical cleaning. As a result, these membranes can potentially operate for longer periods of time, which can decrease the lifetime cost of the membrane. Furthermore, decreased production costs coupled with an increased desire for economical sustainability may open the door for the use of ceramic membranes in drinking water treatment, particularly for highly polluted waters.

The loss of membrane permeability as a result of fouling remains one of the biggest challenges for sustainable membrane operation. Therefore, a thorough understanding of fouling behavior and the identification of key foulants is essential for optimizing membrane performance. However, fouling has not been researched in detail for ceramic membranes in drinking water treatment, particularly ultrafiltration, since most research has focused on ceramic microfiltration membranes combined with coagulation.

The thesis is divided into four main stages. The first stage involved developing a factorial design to establish a procedure to determine sustainable flux that can adequately compare the fouling between a ceramic and polymeric membrane without compromising the functional potential or operating parameters of either membrane. In this stage, the significance of three different variables (interval length, increment increase, and a hydraulic backwash) in determining sustainable flux were statistically analyzed following a factorial design and consequently included or removed from the sustainable flux determination approach. The increment increase was not significant while the backwash was the most significant variable. The method established was used in later experiments to allow for a comparison of fouling behavior and performance between a polymeric and ceramic membrane.

The second stage investigated the fouling behavior of flat-sheet ceramic membranes with model solutions at constant pressure to identify foulants of concern and likely fouling mechanisms for

ceramic membranes as well as perform surface characterization techniques not possible with tubular membranes. In this stage the contributions of different model foulants (bovine serum albumin i.e. a protein, alginate i.e. a carbohydrate, humic acid, and colloidal silica) to reversible and irreversible fouling on a flat-sheet ceramic membrane at constant pressure were quantitatively evaluated. Both single foulant solutions and all possible combinations of mixtures of model foulants were investigated. The bovine serum albumin and humic acid were main contributors to hydraulically irreversible fouling and their removal mechanism is postulated to be largely through adsorption. Colloidal silica was the most influential factor governing fouling behavior and diminished the irreversible fouling effect of these organics, thus increasing hydraulic reversibility. Additionally, synergistic fouling effects were also observed.

The third stage investigated the same model solutions with tubular ceramic membranes at constant flux to determine the fouling behavior under different conditions and quantitatively assess the effectiveness of different fouling mitigation techniques. The rate of fouling was very high for bovine serum albumin but extremely low for humic acid; however, they both showed high irreversible fouling. The results obtained were consistent with the previous stage using flat-sheet ceramic membranes; particularly regarding the significant role colloidal silica plays in fouling. The ability to compare these two very different configurations and operating parameters is largely due to the use of a hydraulic backwash in both configurations. Therefore, this highlights the importance of investigating fouling reversibility, especially in simplified experiments.

The last stage investigated tubular ceramic fouling behavior and organic matter rejection with surface water at constant flux. Tubular ceramic membrane fouling behavior was investigated for river water. A very high initial organic carbon removal was observed at the initial stages of filtration and after each backwash cycle indicating a high affinity of organics to the membrane surface as well as partially reversible adsorption. Humic acid rejection decreased throughout the filtration cycle. On the contrary, biopolymer rejection remained constant indicating size exclusion as a primary removal mechanism. After several modifications to the design and setup, the sustainable flux method established in Stage 1 could not be applied to the ceramic membrane or to the polymeric membrane using highly turbid water; a few hypotheses were made as to why this occurred. It is likely that one or more variables that were not included in the sustainable flux method were influencing the fouling rate

over time. Overall, the robustness of ceramic membranes opens the door for some creative fouling mitigation techniques to be used such as backwash pulses and chemical maintenance cleaning.

Acknowledgements

I wholeheartedly want to express my gratitude to my supervisors Dr. Sigrid Peldszus and Dr. Peter Huck. Their support and understanding, both academically and personally, have made this long journey less arduous and more rewarding.

I cannot possibly fully express my appreciation for the love and support of my family and friends. Their unconditional understanding and grace have carried me to the light at the end of the tunnel (the good kind of light). I also want to thank all the angels that have crossed my path and have helped direct my course and encouraged me to keep fighting but without struggling.

I would like to thank Terry Ridgway who has really been the backbone of all three of my setups. His patience and countless efforts to explain (mA, volts, resistors, valves, pressure transducers, pump, flow meters, wiring, soldering, and the list goes on) are very much appreciated. I would also like to thank Rob Sluban who helped tremendously in bringing the Labview program to life.

I would like to thank Monica Tudorancea for her unbelievable patience and support with the LC-OCD instrument. There are too many names to list but a huge thank you to everyone in the NSERC chair research group both past and present. The wonderful support of this group has been a blessing.

I would also like to acknowledge and thank all the members of my thesis defense committee for their valuable feedback and guidance: Prof. Christine Moresoli, Prof. Wayne Parker, and Prof. Gary Amy.

This research was funded by the Natural Sciences and Engineering Research Council of Canada (NSERC) and Partners of the NSERC Chair in Water Treatment at the University of Waterloo.

Dedication

I would like to dedicate my work both past and future to the creativity of mankind. This journey has been both of breaking and building. My hope is that this is just the start of a path that leads me in the direction of helping others along their quest towards a life of love, laughter and health.

Table of Contents

AUTHOR'S DECLARATION ..... **ii**
Abstract ..... **iii**
Acknowledgements ..... **vi**
Dedication ..... **vii**
Table of Contents ..... **viii**
List of Figures ..... **xii**
List of Tables ..... **xv**
List of Acronyms ..... **xvii**
Chapter 1 Introduction and Research Objectives **1**
1.1 Statement of problem 1
1.2 Research objectives and scope 3
1.3 Thesis structure 4
Chapter 2 Background Information **6**
2.1 Membrane filtration processes 6
2.2 Fouling 7
2.2.1 Types of fouling 8
2.2.2 Fouling mechanisms 10
2.2.3 Removal mechanisms 11
2.3 Fouling countermeasures 12
2.3.1 Backwashing 12
2.3.2 Chemical cleaning 12
2.4 Polymeric membranes 13
2.5 Ceramic membranes 14
2.6 Application of ceramic membranes in drinking water treatment 17
2.7 Summary of research needs 23
Chapter 3 Stage 1: Developing a Sustainable Flux Methodology **25**
3.1 Introduction 25
3.2 Sustainable flux 26
3.2.1 Defining sustainable flux 26
3.2.2 Methods for sustainable flux determination 28
3.3 Materials and methods 31

3.3.1 Factorial design 33
3.3.2 Data analysis 36
3.3.3 Polymeric membrane setup 37
3.4 Results of the sustainable flux factorial 38
3.5 Long-term operation at sustainable flux with a polymeric membrane 42
3.5.1 TMP profile 42
3.5.2 Fluorescence 44
3.6 Conclusions 46
Chapter 4 Stage 2: Reversible and Irreversible Fouling of Ultrafiltration Ceramic Membranes by Model Solutions 47
4.1 Introduction 48
4.2 Materials and methods 50
4.2.1 Setup and experimental approach 50
4.2.2 Model solutions 52
4.2.3 Surface characterization 54
4.2.4 Data analysis 54
4.3 Results and discussion 56
4.3.1 Virgin membrane properties 56
4.3.2 Fouling behavior 57
4.3.3 Blocking filtration laws 62
4.3.4 Effect of backwashing 63
4.3.5 Chemically irreversible fouling 69
4.3.6 Contact angle/hydrophobicity 71
4.4 Conclusions 74
Chapter 5 Stage 3: Fouling Behavior of Tubular Ceramic Ultrafiltration Membranes Using Model Solutions 76
5.1 Introduction 77
5.2 Materials and methods 78
5.2.1 Ceramic membrane properties and operation 78
5.2.2 Water quality analysis techniques 80
5.2.3 Model foulant properties 81
5.2.4 Mass balance 81

5.3 Results 83
5.3.1 Fouling rates 83
5.3.1.1 Hydraulically irreversible fouling rates 85
5.3.1.2 Hydraulically reversible fouling rates 87
5.3.2 Fouling control 92
5.3.2.1 Hydraulic backwash 92
5.3.2.2 Alternative fouling mitigation techniques: Several backpulses and maintenance cleaning 94
5.3.3 Rejection 96
5.3.4 Mass balance results 101
5.4 Conclusions 104
Chapter 6 Stage 4: Sustainable Flux Experiments and NOM Rejection in Natural Waters with a Tubular Ceramic Membrane 106
6.1 Introduction 106
6.2 Materials and methods 107
6.3 Results 108
6.3.1 The sustainable flux story: A series of confounding events 108
6.3.1.1 Long-term sustainable flux experiment #4 110
6.3.1.2 Long-term sustainable flux experiment #5 113
6.3.1.3 Long-term sustainable flux experiment #6: The Final Frontier 117
6.3.2 Discussion on the limitations of the sustainable flux method 121
6.3.3 Rejection of different NOM fractions in surface water 124
6.3.3.1 NOM rejection 128
6.3.3.2 NOM in backwash 134
6.3.4 Mass balance 139
6.4 Conclusions 142
Chapter 7 Summary, Conclusions and Recommendations 144
7.1 Summary of findings and conclusions 145
7.2 Experimental approach guidelines and recommendations 149
7.3 Overall significant conclusions and contributions 150
7.4 Implications and recommendations for future ceramic membrane work for drinking water treatment 151

Copyright Permissions **153**
References **169**
Appendix A Pictures of the Membranes Used and Their Setups **182**
Appendix B Additional Figures for Chapter 3: Sustainable Flux Factorial Results **186**
Appendix C Additional Information and Figures for Chapter 5: Tubular Ceramic Membranes with Model Solution Filtration **196**
Appendix D Additional Information and Figures for Chapter 6: Tubular Ceramic Membranes with Natural Water **198**

List of Figures

Figure 2.1: Images of different types of ceramic membranes....15
Figure 3.1: TMP and observed rejection vs. flux (Source: Chan *et al.* 2002)....29
Figure 3.2: TMP vs flux to evaluate the critical flux (Source: Choi 2003)....30
Figure 3.3: Sustainable flux determination using flux curves (Source: Chiu and James 2006) 31
Figure 3.4: An example of the TMP and flux changes occurring over time with the flux stepping method....34
Figure 3.5: An example of how the sustainable flux is determined using the TMP and flux data acquired from the flux stepping method 37
Figure 3.6: Half-normal plot of factorial experimental results 41
Figure 3.7: Flux stepping results of sustainable flux determination test for long-term experiment 43
Figure 3.8: Sustainable flux determination for long-term experiment....43
Figure 3.9: TMP and flux over 5 days at sustainable flux with the polymeric membrane setup....44
Figure 3.10: Rejection of fulvic acid, humic acid, protein-like, and scattering/turbidity from fluorescence excitation/emission....45
Figure 4.1: Image of flat-sheet disc-shaped ceramic membrane and a 15 μm cross-section of the membrane surface taken with atomic force microscopy....57
Figure 4.2: Relative flux decline for single solutions over 1 h at (a) 20, (b) 30, and (c) 40 psi. 59
Figure 4.3: Relative flux decline over 1 h for combinations of model foulants. (a) effect of silica and (b) effect of humic acid. 60
Figure 4.4: Average final relative flux versus average total volume filtered at 40 psi for 1 h (a) all solutions and (b) only solutions with silica (b is a close-up of left oval in part a)....61
Figure 4.5: Fouling mechanism determination for humic acid alone (H) and humic acid combined with bovine serum albumin (BH). 63
Figure 4.6: Average flux recovered with hydraulic backwash (BW) versus average final relative flux for all solutions at 40 psi. 65
Figure 4.7: Log-log plot of specific cake resistance for single solutions at different pressures. 68
Figure 4.8: Average percent flux recovery (of clean water flux) after hydraulic backwash and after each consecutive cleaning step starting with sodium hypochlorite (NaOCl)....70
Figure 4.9: Average contact angle versus the average percent flux recovery following hydraulic backwash (BW) at 40 psi. 72
Figure 5.1: Schematic of tubular ceramic membrane setup at constant flux 79

Figure 5.2: Diagram depicting the sample locations taken for the mass balance 83
Figure 5.3: An illustration of how reversible and irreversible fouling is calculated. 85
Figure 5.4: TMP profiles for the model solutions run through a tubular ceramic membrane at a constant flux of 120 LMH. 86
Figure 5.5: The rate of hydraulically reversible and irreversible fouling for each model solution over three cycles. 87
Figure 5.6: Percent of initlal clean water permeability recovered after hydraulic backwashing 93
Figure 5.7: LC-OCD chromatograms for the feed and permeates (P) for each of the four cycles a) ABH and b) ABHS filtration. 100
Figure 5.8: Bovine serum albumin mass balance results 102
Figure 5.9: Alginate mass balance results 102
Figure 5.10: Humic acid mass balance results 103
Figure 6.1: Flux stepping with ultrapure water for the tubular ceramic membrane 109
Figure 6.2: Flux stepping results for sustainable flux experiment #4 110
Figure 6.3: Sustainable flux determination for experiment #4 111
Figure 6.4: Long-term experiment #4 at different fluxes 112
Figure 6.5: Long-term sustainable flux experiment #5 with different operating procedures at 64 LMH (10 mL/min). 116
Figure 6.6: Flux stepping results for sustainable flux experiment #6 118
Figure 6.7: Sustainable flux determination for experiment #6 118
Figure 6.8: TMP during long-term experiment #6 starting at 109 LMH (17 mL/min). 119
Figure 6.9: LC-OCD chromatograms of raw waters for all experiments 126
Figure 6.10: LC-OCD chromatograms for raw water during experiment #3 126
Figure 6.11: LC-OCD chromatograms for raw water in experiment #5 127
Figure 6.12: LC-OCD chromatograms for raw water during experiment #6 127
Figure 6.13: Raw and permeate LC-OCD chromatograms for cycle 1 and 2 for experiment #1 129
Figure 6.14: Comparison of rejections at the beginning to the end of the end of the filtration cycle for experiment #3. 130
Figure 6.15: Rejection at the beginning of the cycle during experiment #3 131
Figure 6.16: Rejection at the end of the cycle during experiment #3 131
Figure 6.17: Ceramic rejection of different NOM fractions during experiment #5 with a 15 minute filtration cycle 133

Figure 6.18: Rejection for experiment #6 133
Figure 6.19: LC-OCD chromatograms for backwash water in experiment #3 136
Figure 6.20: LC-OCD chromatograms for backwash water during experiment #5 with a 15 minute filtration cycle. 136
Figure 6.21: LC-OCD chromatograms for backwash water in experiment #6 137
Figure 6.22: LC-OCD chromatograms for feed channel water during the mass balance in experiment #4 138
Figure 6.23: Mass balance results for biopolymers and humics with LC-OCD analysis of natural waters in experiment #4. a) Biopolymers b) Humics 141

List of Tables

Table 2.1: Overview of pressure-driven membrane processes and their characteristics* 6
Table 2.2: Major categories of membrane cleaning chemicals* 13
Table 2.3: Advantages and disadvantages of ceramic membranes* 16
Table 2.4: The iso-electric point of different ceramic membrane materials 18
Table 3.1: Variables investigated for sustainable flux experiments 35
Table 3.2: Factorial experimental design to investigate variable in sustainable flux experiments using three different parameters. 2^3 design 35
Table 3.3: Polymeric membrane properties 38
Table 3.4: Water quality of Grand River 39
Table 3.5: Sustainable flux determined for each run of the factorial design 39
Table 3.6: ANOVA table for determining significant variables in the factorial design 40
Table 3.7: Main peak intensity values of fluorescence EEMs (excitation/emissions) of raw, permeate, and backwash water throughout the 5 day experiment 45
Table 4.1: Summary of virgin ceramic membrane properties 51
Table 4.2: Summary of model substance properties 53
Table 4.3: Calculations of cake compressibility index (n) and the 95% confidence interval for single solutions 69
Table 5.1: Model foulant properties 81
Table 5.2: A summary of the qualitative extent of the fouling rate and hydraulic reversibility with model solutions for both flat-sheet and tubular membranes 91
Table 5.3: %Net clean water permeability recovered* with hydraulic backwash 95
Table 5.4: Rejection of each model foulant when filtered individually for each permeate cycle 97
Table 6.1:%TMP recovered with either a series of 6 backwashes or a maintenance clean 120
Table 6.2: Fouling rate prediction using membrane resistance after backwash 123
Table 6.3: Summary of raw water quality for all experimental runs* 124
Table 6.4: Summary of DOC (mgC/L) values for the permeates 129
Table 6.5: The %NOM for different fractions in the backwash water for experiment #3* 135
Table 6.6: Concentration of biopolymers and humics in ugC/L in the backwash water at the beginning and end of the day for experiment #6 137

Table 7.1: Best practices approach to bench-scale studies for maximizing data from model solutions of low-pressure membranes in drinking water treatment (DWT) applications.....149

List of Acronyms

A	Alginate
AB	Alginate with bovine serum albumin
ABH	Alginate with bovine serum albumin and humic acid
ABHS	Alginate with bovine serum albumin, humic acid, and silica
ABS	Alginate with bovine serum albumin and silica
AH	Alginate with humic acid
AHS	Alginate with humic acid and silica
AS	Alginate with silica
B	Bovine Serum Albumin
BB	Building Blocks
BH	Bovine serum albumin with humic acid
BHS	Bovine serum albumin with humic acid and silica
BP	Biopolymers
BS	Bovine serum albumin with silica
BW	Backwash
CEB	Chemically Enhanced Backwash
CPR	Center Point Replicates
CWF	Clean Water Flux
CWP	Clean Water Permeability
Da	Daltons
DOC	Dissolved Organic Carbon
DBP	Disinfection By-Product
DWT	Drinking Water Treatment
FCW	Feed Channel Water
H	Humic Acid
HS	Humic acid and silica
kDa	KiloDaltons
LC-OCD	Liquid Chromatography with Organic Carbon Detection
LMH	Liters per Meter squared per Hour ($L/m^2.h$)
LMW (a)	Low Molecular Weight Acids

LMW (n)	Low Molecular Weight Neutrals
LTJ	Long-term sustainable flux experiment
MC	Maintenance Clean
MF	Microfiltration
NF	Nanofiltration
NOM	Natural Organic Matter
Pe	Peclet
PEG	Polyethylene Glycol
PVDF	Polyvinylidene Fluoride
RO	Reverse Osmosis
S	Silica
SRHA	Suwannee River Humic Acid
SUVA	Specific UV Absorbance
TMP	Transmembrane Pressure
TOC	Total Organic Carbon
UF	Ultrafiltration

Chapter 1
Introduction and Research Objectives

1.1 Statement of problem

The use of polymeric membranes in drinking water treatment has gained wide acceptance as an effective technology. More recently, ceramic membranes are raising interest in this field due to their unique physical properties, which may prove to be valuable in moving towards more robust and sustainable treatment methods. The main advantages of ceramic membranes lies in their strong mechanical, thermal, and chemical stability, which make them ideal for industrial applications such as in food and beverage production. However, these characteristics can also prove valuable in drinking water treatment applications due to their robustness and in particular the higher fluxes and backwash pressures that can be applied. Unfortunately, a major limitation preventing their widespread use over polymeric membranes in drinking water treatment is cost. Nevertheless, the cost of production due to technological advances has substantially decreased (Heidenreich 2011). Furthermore, their higher capital cost is compensated by lower operating costs due to higher permeabilities and longer lifetimes (Garmash *et al.* 1995). As a result, ceramic membranes are becoming cost-competitive even at full-scale operations and may potentially become the more economical alternative to polymeric membranes, which are now well established in drinking water treatment (Lehman *et al.* 2008). However, the major foulants and fouling mechanisms have not been investigated in detail for ceramic membranes in drinking water treatment applications.

Fouling remains the largest challenge for membranes in surface water filtration, and membrane characteristics can have a significant impact on the extent and type of fouling. Fouling can decrease membrane efficiency, increase operating costs, and ultimately decrease the lifetime of the membrane. Therefore, appropriate and effective fouling mitigation tools can play an integral role in maintaining stable and sustainable operation.

Foulant studies use many different approaches and operating conditions. Bench-scale experiments using model solutions are mostly operated at constant pressure as flux is monitored over time.

However, full-scale plants operate at constant flux that has different hydrodynamic conditions, which can potentially influence fouling behavior. Additionally, most experiments are limited to investigating only single solutions of model substances as opposed to combinations of two or more. In order to infer relevant fouling behavior similar to surface water quality, single solutions are far too simplistic. Therefore, investigating mixtures of foulants is desirable when using model solutions but is often not done.

Although model solution experiments allow for a great deal of control over the quality of the feedwater and composition, they are unable to represent the complexity of organic matter and colloids in raw surface water. The challenge in using natural water lies in characterizing the different components of the raw water and relating it to subsequent fouling behavior. Improved surface water quality characterization techniques, such as Liquid Chromatography Organic Carbon Detection (LC-OCD), can help bridge the gap between model solutions and natural water and possibly decrease the need to resort to model solution experimentation to investigate membrane fouling behavior.

The incorporation of a backwash procedure into membrane operation dramatically reduces membrane fouling, which allows for long-term sustainable operation, and minimizes the need for chemical cleaning. Membranes are typically backwashed at frequent intervals at full-scale plants to control fouling over time. Backwashing is a key component for long-term sustainable operation by removing hydraulically reversible fouling. However, many times bench scale experiments do not incorporate a backwash procedure to identify the extent of hydraulically reversible and irreversible fouling. Without this key information, extrapolating fouling behavior to full-scale operation becomes a difficult task. Thus, reversibility of fouling should constitute a key component of any membrane fouling investigation.

Currently, large-scale ceramic membrane filtration plants for drinking water treatment are limited to Japan, which uses Metawater membranes. The main limitation is that only microfiltration membranes are available from this manufacturer and is often combined with coagulation pretreatment. Coagulation has a significant effect on the water chemistry and can influence the interaction of the water constituents with the membrane surface. Furthermore, this is the most commonly researched ceramic membrane for drinking water treatment, which leaves a significant gap in research outside of

this specific membrane composition and configuration preceded by coagulation. Another research gap is that there have been very few studies investigating fouling with ceramic ultrafiltration membranes.

A comprehensive understanding of problematic foulants allows for optimized operation, which could ultimately translate into decreased costs due to the minimization of chemicals or treatment processes required. Considering that very few studies have investigated the primary foulants in ceramic membranes for drinking water treatment, it is important to identify and characterize their effects before membrane pretreatment can be optimized. Since the surface chemistry and membrane properties are quite different in polymeric membranes to that of ceramic membranes, the major foulants may vary drastically.

1.2 Research objectives and scope

The objectives of this research were to identify and characterize the fouling observed in an ultrafiltration ceramic membrane under conditions anticipated in drinking water treatment and to gain a fundamental understanding of the fouling behavior of major foulants. The membrane material and characteristics, as well as the operating conditions, such as backwashing and cleaning regimes, can influence the susceptibility of these membranes to different types of fouling. Therefore, to optimize membrane performance for surface water treatment, the primary foulants need to be identified and characterized. Although most studies have chosen to implement a pretreatment prior to ceramic filtration, this study focuses on identifying major foulants using direct filtration only.

The specific objectives of this research were to:

1) Assess the advantages of applying ceramic membranes for drinking water treatment as compared to polymeric membranes by establishing a procedure to adequately compare fouling between a polymeric and ceramic membrane without compromising the functional potential or operating parameters of either membrane
    a. Use a factorial design that takes into account the relevant operating parameters to experimentally determine sustainable flux

b. Establish a method to analyze the data from these experiments to determine sustainable flux

2) Quantitatively evaluate the extent that different foulants, both model and natural, contribute to reversible and irreversible fouling on an ultrafiltration ceramic membrane
    a. Identify the susceptibility of this particular ceramic membrane material to specific types of foulants focusing primarily on particulates and natural organic matter
    b. Quantitatively assess the effectiveness of a hydraulic backwash in removing reversible fouling
    c. Quantitatively evaluate the ability of cleaning regimes in removing irreversible fouling

3)
    a. Characterize the effect of fouling on the surface characteristics and morphology of the membrane and suggest likely fouling mechanisms
    b. Contribute to the fundamental understanding of foulants and fouling mechanisms on ceramic membranes

4) Contribute to the assessment of ceramic membranes as a suitable and economical choice for drinking water treatment and evaluate the potential operational advantages of ceramic membranes in a drinking water treatment setting

1.3 Thesis structure

The thesis is divided into four main stages; generally each stage builds upon the previous. The chapters were written in journal article format. Chapter 4 has already been published, Chapter 5 was submitted to a scientific journal in May 2013, while Chapter 3 and Chapter 6 may be considered for publication.

Chapter 1: introduces the research statement and specific objectives of the research presented.

Chapter 2: is a short background section that covers general information that is relevant to the research but not discussed in the other chapters. Literature results related to specific experiments are already contained in those chapters.

Chapter 3: presents the results of the first stage, which uses a factorial design to establish a sustainable flux procedure to allow for the comparison of fouling behavior between a polymeric and ceramic membrane.

Chapter 4: presents the results of the second stage, which investigates the fouling behavior of flat-sheet ceramic membranes at constant pressure using four different model solutions representing foulants that have been identified as problematic for polymeric membranes in drinking water treatment. Foulants of concern were identified and the reversibility of fouling was quantified. Surface characterization of the virgin ceramic membrane, as well as the contact angle of the fouled membrane surface was performed to determine the effect of fouling on the membrane surface characteristics.

Chapter 5: presents the results of the third stage, which investigates the fouling behavior of a tubular ceramic membrane at constant flux with the same four model solutions used in Chapter 4. These results are compared to those obtained in the flat-sheet experiments. The effectiveness of hydraulic backwashing and chemical cleaning regimes for removing reversible and irreversible fouling are also quantitatively assessed.

Chapter 6: presents the results of the final stage, which investigates the fouling behavior of a tubular ceramic membrane with surface water operating at constant flux. Foulants of concern are evaluated using natural organic matter characterization techniques and their contributions to reversible and irreversible fouling are quantitatively determined using a hydraulic backwash and cleaning regimes.

Chapter 7: summarizes the research work with a focus on significant conclusions and contributions and discusses recommendations and potential applications of the ceramic membrane in drinking water treatment

.

Chapter 2
Background Information

This section provides background information on membranes and a brief review on the literature with a focus on ceramic membrane filtration for drinking water treatment. The literature discussion is mainly on that which is not included in other chapters since each chapter already contains a literature review that is relevant to that specific set of objectives and experimental results.

2.1 Membrane filtration processes

In drinking water treatment applications there are currently four major membrane separation processes used: microfiltration (MF), ultrafiltration (UF), nanofiltration (NF), and reverse osmosis (RO). The characteristics of these membrane types are summarized in Table 2.1. These four membrane types are generally categorized into low-pressure (MF/UF) and high-pressure (NF/RO) membranes.

Table 2.1: Overview of pressure-driven membrane processes and their characteristics*

	MF	UF	NF	RO
Permeability ($l/h.m^2.bar$)	> 1,000	10 – 1000	1.5 – 3.0	0.05 – 1.5
Applied Pressure	0.1 – 2 bar 10 – 100 kPa	0.1 – 5 bar 10 – 500 kPa	3 – 20 bar 300 – 1000 kPa	5 – 120 bar 5000–120000 kPa
Pore size (nm) or MWCO	100 – 10000	2 – 100 > 1000 Da	0.5 – 2 200 – 400 Da	< 0.5 50 – 200 Da
Rejection/ Application	Particle/turbidity, bacteria, algae, protozoa	Small colloids, macromolecule, viruses	Dissolved organic matter, multivalent ions (softening)	Monovalent ions (desalination)
Separation Mechanism	Sieving/size exclusion	Sieving/size exclusion	Sieving, charge effects	Differences in solubility or diffusivity

* Adapted from Van der Bruggen *et al.* (2003).

The retention rating or the size of the material retained by the membrane can be expressed as pore size or molecular weight cutoff (MWCO). Pore size and its distribution is determined using a variety of methods such as microscopic techniques (atomic force microscopy, scanning electron microscopy), bubble-point technique, mercury porosimetry, solute transport, thermometry, permporometry, and others (Lee *et al.* 2002; Nakao 1994; Singh *et al.* 1998). On the other hand, MWCO is a measure of the atomic weight or mass (expressed in daltons) of the material retained. The MWCO is defined as the molecular weight of the solute that exhibits a rejection of 90% by the membrane. This value gives only a rough indication of the membranes characteristics and rejection potential due to differences in molecular shapes and possible steric interactions (Van der Bruggen *et al.* 2003). Furthermore, manufacturers often provide MWCO values from solute rejection tests that use uncharged macromolecules such as proteins, dextrans, and PEGs, thereby not accounting for possible rejection through electrostatic repulsion (Cho *et al.* 2000). In addition to membrane pore size, several other membrane surface properties such as hydrophobicity, surface charge, and surface roughness affect the performance of the membrane system.

Membrane systems can be operated under either constant flux or constant pressure mode. Constant pressure filtration has been shown to create cake layers with higher resistances than during constant flux operations (Carrère *et al.* 2001; Decloux and Tatoud 2000; Defrance and Jaffrin 1999; Field *et al.* 1995). However, Vyas *et al.* (2002) observed that irreversible fouling was greater under constant flux mode than that in constant pressure mode. Although constant pressure operation may be simpler to apply in a lab setting, most full-scale membrane systems for drinking water treatment operate with constant flux to ensure sufficient production.

2.2 Fouling

The main challenge for membranes in drinking water treatment is the accumulation of foulants, near, on, or within the membrane, which can heavily impact sustainable operation and operating cost. Membrane fouling causes an increase in transmembrane pressure (at constant flux), as a result of particles accumulating on the surface, forming a cake layer, or the adsorption of both suspended particles and dissolved material (AWWA 2005). Fouling is characterized by whether it can be removed (reversible or irreversible), by the material causing it (particulate, dissolved, organic, or

biological), and by the mechanism of formation (pore adsorption, cake formation or pore blockage) (MWH 2005). The extent to which fouling occurs is dependent on the source water characteristics (such as organic matter concentration and characteristics, pH, ionic strength, and calcium concentration) and the membrane surface properties (zeta potential, roughness, pore size, and hydrophobicity) (Howe and Clark 2002).

2.2.1 Types of fouling

The different types of fouling that can be categorized in membrane processes include colloidal/particulate fouling, organic fouling, microbial fouling, and inorganic fouling. Colloidal and organic fouling are the most relevant types of fouling for low-pressure membrane surface water applications.

Colloidal/particulate fouling

Colloidal and particulate fouling is caused by the deposition and accumulation of suspended and colloidal solids in the feed water on the membrane surface or inside the pores, resulting in the reduction of permeate flux. Colloids are fine suspended particles (nm to μm range) and their presence in natural surface water is ubiquitous. Colloidal foulants in UF membranes include inorganic (clays, silica, salt precipitates, and metal oxides), organic (natural and synthetic substances), and biological matter (bacteria, viruses, and proteins) (AWWA 2005). Colloidal matter is typically charged in aqueous solutions due to the presence of charged functional groups on the surface of the colloid or through the adsorption of ions from the surrounding water. The resulting cake structure porosity and the hydraulic resistance are influenced by the surface charge of the colloids.

Organic fouling

Another major cause of fouling in membrane filtration of natural waters is dissolved naturally occurring organic substances. The rejection of natural organic matter (NOM) by membranes is primarily a physical removal process, however, the charged functional groups of both the membrane and NOM can also impact rejection (Cho *et al.* 2000). While the majority of dissolved NOM will pass through MF/UF membranes due to their smaller size, organic constituents can still contribute significantly to fouling by plugging membrane pores, adsorbing to the internal matrix of the

membrane, and forming a cohesive gel on the cake layer (AWWA 2005). The mechanisms of NOM fouling are very complex and the rate and extent is influenced by factors such as membrane characteristics, properties of organic matter, feedwater solution characteristics, and membrane module hydrodynamics (Aoustin *et al.* 2001; AWWA 2005).

Certain factions of NOM in surface water may have a higher fouling potential than others, however, the identification of which particular fraction has the highest potential has been inconsistent. Several studies have attributed the greatest fouling components of NOM to be colloidal and the hydrophilic neutral fraction of NOM (Fan *et al.* 2001; Howe and Clark 2002; Lee *et al.* 2008). Carroll *et al.* (2000) concluded that the low molecular weight and neutral hydrophilic fraction of NOM caused the most fouling. Fan *et al.* (2001) classified potential foulants in the order of hydrophilic neutral > hydrophobic acids > transphilic acids > hydrophilic charged. The fouling potential of each fraction will also vary depending on different membrane types investigated. The adsorption of NOM has been reported to be higher on hydrophobic membranes than on hydrophilic membranes (Fan *et al.* 2001; Gray *et al.* 2007; Howe and Clark 2002; Jucker and Clark 1994; Jung and Kang 2003; Jung *et al.* 2006; Lee *et al.* 2008). Jung and Kang (2003) suggested the use of hydrophilic membranes for reduced membrane fouling rates due to their reduced adsorption capacity towards both hydrophobic and hydrophilic organics.

Microbial/biological fouling

Biofouling occurs as a result of the accumulation and growth of living organisms (bacteria, algae, and fungi) at the membrane surface or within the pores. As the bacteria multiply they produce extracellular polymeric substances (EPS) which form a viscous biofilm, which reduces permeability, causes flux decline, and causes pore blocking. This type of fouling can be well controlled in the operation of low-pressure membranes by frequent hydraulic backwashing as well as chemical maintenance cleaning.

Inorganic fouling

Scaling on the membrane occurs due to the precipitation or crystallization of salts on the membrane surface or inside the pores. This occurs when the ion concentration of inorganic precipitates and metals exceed their solubility limit due to their accumulation near the membrane surface. The precipitation of inorganic scalants can reduce the permeate flux, damage the membrane surface and

cause irreversible pore blocking. This type of fouling can also be well controlled through targeted chemical cleaning.

2.2.2 Fouling mechanisms

The characteristics of both the membrane and the foulants have an important impact on the resulting fouling mechanisms. The fouling mechanisms can be categorized as pore constriction, intermediate pore blocking, complete pore blocking, and cake layer formation. This concept is based on the modeling of particulates as spheres.

Standard pore blocking/Pore constriction

Standard pore blocking occurs when the diameter of the particle is smaller than that of the pore and is consequently deposited on the membrane by attaching internally to the pore walls of the membrane. The resulting constriction of the pores decreases the overall pore volume and causes flux decline.

Complete pore blocking

Pore blocking occurs when the feedwater contains particles with similar or larger diameters to the membrane pores. Each particle arriving to the membrane participates in blocking some pore or pores with no superposition of particles. The blocked pores reduce the pore volume and cause rapid and severe flux decline.

Intermediate pore blocking

Intermediate pore blocking occurs when each particle reaching the membrane may block the membrane pores (i.e. complete pore blocking) or also attach to other particles on the membrane surface.

Cake layer formation

The formation of a cake layer occurs when the feedwater contains particles that are too large to enter the pores and are deposited on the surface of the membrane. This cake layer creates additional resistance during filtration that increases transmembrane pressure (during constant flux operation).

2.2.3 Removal mechanisms

The primary mechanism for particle removal in membrane filtration (MF/UF) is straining through size exclusion, but removal can also occur by adsorption or as a result of cake formation. In some cases when the particle size is close to the membrane retention rating, interactions between the particles and membrane can impact removal (MWH 2005).

Size exclusion, which is the dominant removal mechanism in membrane filtration, occurs when particles or solutes larger than the membrane pore size are retained. Since membranes have a distribution of pore sizes, particles both larger and smaller than the nominal retention rating may be rejected. Additionally, large proteins or other macromolecules that are spherical in solution may become linear when forced through a membrane under pressure (MWH 2005).

The interactions between particles and the membrane can affect rejection and contribute to non-ideal filtration particularly when the particle size is similar to the membrane pore size. Since membrane surfaces are typically negatively charged, particles with a negative charge often observe higher retentions than uncharged or positively charged particles with similar sizes. This occurs due to electrostatic interaction, which prevents the particle from passing through the membrane even if its physical size would allow it to (MWH 2005). Therefore, although the rejection is primarily a physical removal process that is dependent on the chemical's molecular size, the charged functional groups of both the membrane and solute can also have a significant impact on rejection (Cho *et al.* 2000).

Adsorption can play a significant role during the initial stages of filtration (Bellona *et al.* 2004; Nghiem *et al.* 2005). However, once the adsorption capacity of the membrane is exhausted, adsorption ceases to be an effective mechanism in long-term operation unless it is reversible through hydraulic backwashing (MWH 2005). Nevertheless, the foulants adsorbed on the membrane surface can modify the initial membrane characteristics and consequently impact subsequent membrane performance.

Similar to adsorption, cake formation, which is the accumulation of solids on the membrane surface due to straining, will impact the membrane's surface characteristics and acts as a filtration medium by providing an additional mechanism for rejection. The cake layer builds over filtration time and can be partially or completely removed during backwashing.

2.3 Fouling countermeasures

2.3.1 Backwashing

Incorporating a backwash (BW) step into the operation cycle of the membrane can dramatically reduce membrane fouling. Backwashing controls the deposition and accumulation of solids on the membrane surface by removing the surface cake that develops during the filtration cycle. Both liquid and gas backwashing can be employed with low-pressure membranes. The frequency of BW can range between 30 and 120 minutes for most low-pressure systems and usually lasts from 1 to 5 minutes (AWWA 2005; MWH 2005). Periodic backwashing improves membrane permeability and reduces fouling, thus leading to optimal, stable hydraulic operating conditions. Additionally, combined with air sparging in submerged membrane reactors, the flux can be increased up to fivefold (Hilal *et al*. 2005).

The frequency of backwashing is not only dependent upon the feedwater quality (e.g. total suspended solids) but can be influenced by the imposed operating flux. It has been suggested that if the membrane were operated at lower fluxes, less energy would be required to control fouling and less chemical cleaning would be needed (Fane *et al.* 2005). The efficiency of this technique often depends on both the type of suspension being filtered and the type of fouling that occurs. For ceramic membranes the BW pressure is typically 20 to 40 psi higher than the feed pressure or 2 to 3 times the transmembrane pressure (Hsieh 1996). Higher BW pressures for polymeric membranes are limited by the polymeric membrane properties and tend to be much lower. Foulant removal through effective backwashing can control fouling in ceramic membranes and consequently reduce the operating costs.

2.3.2 Chemical cleaning

Chemical cleaning is performed once the BW cycle is ineffective in removing the clogged or adsorbed material on the membrane and restoring the flux to an acceptable level. The manufacturer usually gives a preset maximum limit for the transmembrane pressure for a particular membrane. The frequency of recovery cleaning with chemicals ranges from a few days to several months depending on the membrane system characteristics and source water quality (MWH 2005). However, this step is preferably avoided or minimized due to the use of chemicals and temporary loss in production.

Shorter, more frequent maintenance cleans using lower chemical concentrations are also used and can often be an effective tool in controlling fouling. There are five categories of chemicals that can be applied to remove the fouling materials from the membrane and restore flux. These categories are summarized in Table 2.2.

Table 2.2: Major categories of membrane cleaning chemicals*

Category	Major Functions	Typical Chemicals	Primary Foulant Targeted
Caustic	Hydrolysis, solubilization	NaOH	Organic and microbial
Oxidants/Disinfectants	Oxidation, disinfection	NaOCl, Ozone, H_2O_2	Organic & microbial
Acids	Solubilization	Citric, Nitric, Oxalic acid	Scales, metal dioxides, & inorganic deposits
Chelating Agents	Chelation	Citric acid, EDTA	
Surfactants	Emulsifying, dispersion	Surfactants, detergents	Biofilms

* Adapted from Liu *et al.* (2001)

2.4 Polymeric membranes

Polymeric membranes largely dominate the application of membrane filtration in drinking water treatment (de la Rubia *et al.* 2006; Lee and Cho 2004; Loi-Brügger *et al.* 2006). The physical and chemical properties of the membrane material strongly influence the performance of the membrane. Ideally, the membrane material can produce high fluxes without fouling, is physically durable, chemically stable, non-biodegradable, chemically resistant, and inexpensive (MWH 2005). The most common membrane materials used in water treatment are polypropylene, polyvinylidene fluoride (PVDF), polysulfone, polyethersulfone, and cellulose acetate. Most of the time these membranes are modified by blending bulk polymers with hydrophilic polymers to provide better antifouling properties (Mallevialle *et al.* 1996). Hydrophilic polymers tend to have ionized functional groups, polar groups, like oxygen-containing and hydroxyl groups. PVDF membranes are widely used in many UF processes due to their excellent oxidative, thermal and hydrolytic stability as well as good mechanical and film-forming properties (Yan *et al.* 2005). However, their tendency to foul due to their intrinsic hydrophobicity limits their use without surface or bulk polymer modification. Although these surface modifications may enhance surface properties such as fouling resistance, they may also

negatively impact membrane characteristics such as pore size distribution as well as degrade the mechanical, thermal, and/or chemical stability (Hester and Mayes 2002). Additionally, the added layers may lack long-term stability resulting in decreased hydrophilicity over time (Zhao *et al.* 2008).

In drinking water treatment applications common membrane configurations are spiral wound, hollow fiber, and tubular. Hollow fiber membrane configurations, which can be backwashed, are particularly popular for low pressure membrane filtration applications. Tubular membrane configurations can be composed of polymeric or ceramic material.

2.5 Ceramic membranes

Ceramic membranes are available as metal oxides, composites, and sintered clay. The most commonly used membranes are composed of metal oxides such as aluminum oxide or alumina (α-Al_2O_3 and γ-Al_2O_3), titanium dioxide (TiO_2), zirconium dioxide (ZrO_2), and silicon dioxide (SiO_2) or a combination of these. Ceramic membranes, similar to polymeric membranes, are usually constructed from multiple layers into an asymmetric, multi-channel element. The asymmetric structure consists of a supporting system with large pores (to decrease flow resistance) with adequate mechanical strength on top of which are layers with gradually decreasing pore size (Burggraaf and Cot 1996). The shape of these membranes is usually a tubular configuration with the membrane surface cast on the inside wall on top of the support material. The tube can be round or hexagonal with multiple channels that can vary in shape. New products are moving towards smaller open channel diameters with more channels in an element (Hsieh 1996, Heidenreich 2011). Other available configurations include hollow fiber and flat-sheet ceramic membranes (Figure 2.1). The types of modules can either be a multi-channel monolithic or one consisting of multiple membrane elements. An operational advantage of a module having multi-channel monolithic elements is that installation and maintenance are much easier (Hsieh 1996). Additionally, this configuration allows for effective cleaning through backwashing and the ability to tolerate much higher loads of suspended materials (Kanaya *et al*. 2007; Loi-Brügger *et al.* 2007). However, their main disadvantage is their low packing density, which is constantly being addressed by manufacturers through several ranges of channel shapes and number of channels (Figure 2.1) (Heidenreich 2011).

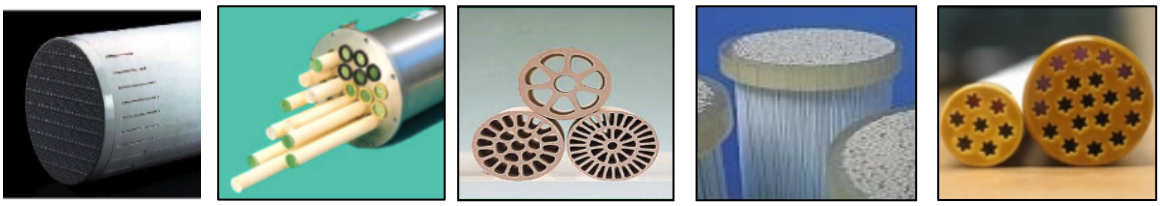

Figure 2.1: Images of different types of ceramic membranes[1]

From left to right: multi-channel monolithic membrane element by Metawater, membrane module consisting of several elements arranged in a stainless steel housing by TAMI, tubular membranes showing different numbers and shapes of flow channels by TAMI, hollow fiber ceramic membrane by Hyflux, tubular star-shaped channels by Fairey Industrial Ceramics.

Ceramic membranes have several advantages over polymeric membranes particularly in industrial applications that operate at extreme conditions and require aggressive cleaning at extreme pHs and/or temperatures. Although these advantages would still be relevant in a drinking water treatment setting, their high production costs have generally limited their application to industrial processes. The advantages of ceramic membranes are summarized in (Table 2.3). Increased chemical resistance allows for higher concentrations and longer exposure times to chemicals and thus, more efficient foulant removal without compromising the integrity of the membrane, which could decrease the membrane's lifetime. Furthermore, the higher permeability allows for higher fluxes at lower pressures. The high mechanical strength of ceramic membranes also allows for higher backwash pressures and potentially more effective hydraulic fouling mitigation techniques without the need for chemicals. All of these advantages can translate into decreased operating and lifetime costs, thus offsetting the initial capital cost of manufacturing or procuring ceramic membranes.

[1] http://www.ngk.co.jp/english/research/ecology.html

http://www.membranesystem.co.in/oil_grease_sep.html

http://www.membranesystem.co.in/oil_grease_sep.html

http://tami.exportpages.com/productdetail/1066202374-1.htm

http://www.membrane-guide.com/membrane-directory/europe/nederland-membraanfiltratie.htm

http://www.membrane-guide.com/inorganic-membranes/ceramic-membranes/uk-ceramic-membrane.htm

Accessed April 17, 2013

Table 2.3: Advantages and disadvantages of ceramic membranes*

Advantages	Disadvantages
- **Mechanical strength:** can withstand very high pressures (10-90 bars), which allows for high backwash pressures. - **Chemical resistance:** resistant to high chemical concentrations and all pH levels. Allows for more rigorous cleaning without degrading the membrane - **Thermal stability:** can withstand very high temperatures (greater than 100°C) - **High permeability:** due to very high hydrophilic surface. Allows for higher possible fluxes. - **Lifetime:** have a longer lifetime (>10 yrs) than polymeric membranes (3 – 6 yrs) - **Narrow pore size distribution:** separation efficiency based on steric exclusion is high due to greater selectivity	- **Brittleness:** sensitive to crack formation - **Cost:** the high manufacturing costs of ceramic membranes is the main limitation for their use in drinking water treatment, which is why they are generally limited to treating and recovering high value-added products like industrial effluents, food, beverages, pharmaceuticals, etc. However, the cost over the last decade has significantly decreased due to technological advances in membrane materials and manufacturing processes and is expected to continue to decrease.

*Adapted from Hsieh (1996)

An important advantage of ceramic membranes in drinking water treatment is their chemical resistance, which can play a critical role in maintaining the integrity of the membrane as well as impact the membrane's lifetime. Some investigators have observed the significant impact that chemical cleaning can have on polymeric membranes. Abdullah and Bérubé (2012) observed that over time, extended exposure to sodium hypochlorite could significantly degrade the physical/chemical characteristics of the polymeric membrane and likely decrease the operating lifetime. The surface characteristics of a modified hydrophilic PVDF membrane, after longer exposures to sodium hypochlorite, showed that large portions of the hydrophilic additive are removed, which could make the membrane more vulnerable and susceptible to fouling due to the increased affinity of certain foulants to the membrane (such as proteins) (Abdullah and Bérubé 2012). Levitsky *et al.* (2011) also observed increased protein fouling for a polyethersulphone membrane after sodium hypochlorite cleaning. This further highlights the long-term benefits of using ceramic membranes particularly if organic matter is an issue and frequent chemical cleanings might be necessary. Furthermore, it allows for increased chemical use in backwashes with ceramic membranes if necessary and if chemical cost is not a concern.

Guerra *et al.* (2012) investigated the impact of operating conditions for an alumina ultrafiltration membrane (0.01μm) filtering surface water. Although increased fouling occurred at higher fluxes, it was argued that in order to take full advantage of the ceramic membrane's properties, it would still be best to operate at higher fluxes despite increased fouling, instead of lower fluxes to minimize the fouling rate. Additionally, increased backwash frequency was found to be beneficial. Therefore, the authors suggested that future research should focus on optimizing backwash conditions so that flux decline and irreversible fouling is minimized while still meeting production goals and costs. Furthermore, the emphasis should be primarily focused on strategies for removing fouling within an economic objective or framework.

Very little information is available on ceramic membrane fouling by typical foulants encountered in drinking water treatment. Most of the information available from other applications using ceramic membranes is not applicable to drinking water treatment due to the different operating conditions and feed characteristics used. Other applications, such as the food industry, primarily operate using crossflow configurations and employ batch operations, often without backwash cycles (e.g. Daufin *et al.* 2001; Hsieh 1996; Mourouzidis-Mourouzis and Karabelas 2006; Weber *et al.* 2003). Therefore, the conclusions regarding fouling and fouling rates are not easily transferable.

2.6 Application of ceramic membranes in drinking water treatment

Although there is limited research available on the performance of ceramic membranes for drinking water treatment, there have been several promising results. Due to the particularly different surface characteristics of ceramic to polymeric membranes, specific foulants and fouling mechanisms will not necessarily apply to both materials. The following discussion summarizes several studies that have applied ceramic membranes for the filtration of natural waters. It is important to note that most studies combined coagulation pretreatment with a MF ceramic membrane. Combining coagulation with filtration can help decrease fouling for both polymeric and ceramic membranes by minimizing pore blocking and pore adsorption and allow stable operation due to pure cake filtration as well as improve rejection (e.g. viruses) to increase permeate quality (Carroll *et al.* 2000; Lerch *et al.* 2005; Matsushita *et al.* 2005).

Full-scale drinking water treatment plants in Japan using Metawater ceramic membranes operate at moderate fluxes without any chemically enhanced backwash (CEB) (Loi-Brügger *et al.* 2006). Metawater membranes are monolitihic MF membranes (0.1 μm) composed of Al_2O_3. Standard operating conditions of a full scale ceramic membrane drinking water treatment plant in Japan (10 MGD or 1620 m^3/h) practicing coagulation and flocculation prior to MF use a coagulant dose of 0.75 mg Al^{+3}/L and use a rapid and slow mixing tank in series with a retention time of 10 to 20 minutes without the need for a sedimentation step (Kanaya *et al.* 2007). Most studies using ceramic membranes for drinking water treatment applications have used the Metawater membranes. According to the literature, the iso-electric point of Al_2O_3 can be between 8-9.4 (Table 2.4). Although some surface waters such as the Grand River (Ontario) can have a pH of approximately 8, the widespread use of coagulation as a pretreatment will likely require a pH adjustment making the feedwater slightly acidic. Therefore, these membranes will likely have a positive charge unlike other ceramic membrane materials, such as SiC (Table 2.4). In the case of ceramic membranes composed of mixtures, it would be difficult to estimate the surface charge of the membrane without directly measuring it. However, it is extremely challenging to measure the surface charge of tubular membranes, which is likely why there is very limited information available in the literature.

Table 2.4: The iso-electric point of different ceramic membrane materials

Material	Iso-electric point
Al_2O_3	8-9.4 [1,2,3]
TiO_2	5.1-6.4 [1,2]
ZrO_2	6.3-7.1 [1, 4, 5]
SiC	2.5-3.5 [3, 6, 7]

[1] Kosmulski (2009)
[2] Mullet *et al.* (1997)
[3] Wang and Hirata (2004)
[4] Leong *et al.* (1993)
[5] Mao *et al.* (1994)
[6] Sano *et al.* (1996)
[7] Yeh and Wan (1994)

Konieczny *et al.* (2006) used two MF membranes (0.1 and 0.2 μm) (Kerasep® by Orelis SA – composed of a monolithic support layer of TiO_2/Al_2O_3 and an active layer of ZrO_2/TiO_2) to compare synthetic humic acid (7 and 10 mg/L) removal by coagulation alone, MF alone, and coagulation followed by membrane filtration. The membrane filtration process was operated using a crossflow configuration at constant pressure. Total organic carbon (TOC) removals with the combined coagulation – MF process (100% removal) were higher than coagulation alone. Although the MF membranes both showed complete TOC removal as well, they exhibited significantly greater flux declines. This indicates that removal by MF alone is not sustainable. Furthermore, the addition of coagulation prior to membrane filtration showed improved and more stable fluxes. The complete removal of the humic acids by MF membranes was unexpected but the mechanism of humic acid removal was not investigated. It is likely some form of binding interaction with the membrane surface (metal oxide surface chemistry of ceramic membrane). Overall, combining coagulation with MF did seem to improve membrane performance but it would be of interest to run long-term filtration experiments (they only filtered for 300 minutes) and incorporate backwash cycles (Konieczny *et al.* 2006).

A study by de la Rubia *et al.* (2006) used a 15 kDa UF ceramic membrane (Orelis SA – composed of a mixture of $Al_2O_3/ZrO_2/TiO_2$) to filter a synthetic humic acid solution (10 mg/L) at different pH levels and varying ionic strengths. A molecular weight distribution of the humic acid showed that the majority (~70-75%) of the humic acid was larger (30 kDa) than the MWCO of the membrane (15 kDa). At a pH value of 7.9 and with a low ionic strength, a 99% rejection of dissolved organic carbon (DOC) was observed. At higher ionic strengths, the DOC rejection decreased to 74%. These results indicated that the pH and the ionic strength affect the UF of the humic acid solution by changing the surface properties of both the ceramic membrane and humic solution.

Loi-Brügger *et al.* (2006) used a 0.1 μm MF membrane (Metawater – composed of Al_2O_3) operated at constant flux in a dead-end filtration mode with regular backwashes at varied intervals to filter raw surface water. Raw water with a DOC of 2-3.5 mg/L was coagulated with 3.5 mg Al^{+3}/L and resulted in a DOC reduction of 20-35%. This DOC removal is surprisingly low compared to the results by Konieczny *et al.* (2006), which could be due to either the feed water or the different membranes used. The results of this pilot study indicated that with proper coagulation and a CEB, neither temperature variations nor turbidity peaks (up to 100 FNU, which is equivalent to NTU) disrupted stable

membrane performance. If membrane operation was kept at fluxes below 200 LMH, the application of CEB was not necessary but could be useful in the case of high organic loadings or to extend the interval between more rigorous chemical cleanings. Ultimately it is a tradeoff between chemical consumption, power consumption, and chemical cleaning intervals. It is difficult to compare the membrane performance and DOC removals of this study to that by Konieczny *et al.* (2006) due to the significant differences in filtration mode and feed water quality.

Lerch *et al.* (2005) observed the importance of optimizing coagulation conditions using a setup similar to Loi-Brügger *et al.* (2006). The Metawater MF membrane (composed of Al_2O_3) was operated at a flux of 80 LMH and showed no significant influence of coagulant dosage on the permeability decline of the membrane (Lerch *et al.* 2005). One hypothesis was that the percentage retention of TOC by the coagulation/flocculation unit was too low to prevent the adsorption of organics on the membrane surface (especially humic substances). Once the operating conditions were modified to where co-precipitation or sweep coagulation of the organics could occur, coupled with a doubling of the coagulant dosage, the permeability decline was virtually eliminated. Therefore, optimization of the pretreatment step is crucial for an effective fouling mitigation tool.

Bottino *et al.* (2001) used a 0.2 μm MF ceramic membrane (Membralox by Pall – composed of Al_2O_3) for the treatment of raw lake water with no pretreatment. In this investigation, a cross-flow configuration at constant pressure was used and due to the recirculation of the retentate into the feed, the turbidity continued to gradually increase over the filtration run (0.5 – 80 NTU). After 80 hours the flux decreased rapidly from the initial 600 LMH, and slowly leveled off at around 200 LMH. The turbidity, total suspended solids, microorganisms, algae, and some disinfection by-product (DBP) precursors were completely rejected while TOC and chloroform rejection was 64% and 56% respectively. The high TOC removal could be due to formation of a cake layer that resulted in increased removal of contaminants; therefore, retention may not be consistent and vary between the beginning and end of each filtration run.

Zhu *et al.* (2012) observed that coagulation is an effective pretreatment for the control of ceramic MF (Metawater – composed of Al_2O_3) fouling. Additionally, there seemed to be a "transmembrane pressure (TMP) turning point" in which once this point was exceeded, both the reversible and irreversible fouling rate dramatically increased making it more difficult to thoroughly clean the

membrane even with chemical cleaning. Dissolved and colloidal organic matter, as well as inorganic ions contributed the greatest to irreversible fouling. Since three membrane sizes were used (0.1, 0.5, and 1 μm) and the 0.1 μm experienced the lowest fouling rate, followed by the 0.5 μm membrane, the authors hypothesized that foulants with a size between 0.5-1 μm likely played an important role in irreversible fouling. It was also observed that sodium hypochlorite solution washing recovered more flux than citric acid.

Several studies have shown that in-line coagulation is just as effective, if not more so, than flocculation/sedimentation in maintaining stable operation (Cho *et al.* 2005; Fujiura *et al.* 2006; Lehman *et al.* 2007; Yonekawa *et al*. 2004). This is in part due to the fact that the coagulation rate is very fast and the aggregates rapidly reach sizes larger than the membrane's pore size soon after coagulant addition. Matsushita *et al.* (2005) showed that virus removal using coagulation – ceramic MF (Metawater – composed of Al_2O_3) was a tradeoff between coagulant dose and time. For in-line filtration, coagulant dose was significantly more important than coagulation time, and using in-line systems can save considerable space compared to flocculation tanks. However, to properly assess the economical benefits of in-line filtration coupled with higher coagulant doses, further investigation into the effects on subsequent fouling of the membrane and flux decline would be needed. Consequently, although in-line coagulation at higher coagulant doses may have its benefits, drinking water treatment systems need to be robust and prepared to handle varying feedwater characteristics such as turbidity spikes.

Few papers have compared the performance of polymeric membranes to ceramic membranes for drinking water treatment purposes. In a study by Bodzek and Konieczny (1998), both ceramic (MF and UF) (Kerasep® by Orelis SA – composed of a support layer TiO_2/Al_2O_3 and active layer ZrO_2/TiO_2) membranes and a polymeric (0.2 μm polypropylene) membrane were used to investigate their potential application for disinfection of natural waters. Both membrane types exhibited effective removal of bacteria and turbidity (Bodzek and Konieczny 1998). However, TOC removals for the ceramic membranes (~30%) were higher than the polymeric membrane (~12%). Furthermore, the TOC removal by the UF ceramic (300 kDa) was only 1% higher than the ceramic MF membranes, suggesting that some rejection of the organic matter may be occurring through adsorption onto the membrane.

Guerra and Pellegrino (2012) compared a UF ceramic membrane (CerCor® by Corning Inc. – composed of Al_2O_3) and a UF polyethersulfone polymeric membrane under similar hydrodynamic conditions to filter a solution of bentonite to simulate water with a high concentration of particulates. The ceramic membrane had a lower rate of fouling at higher peclet (Pe) numbers compared to the polymeric membrane (Pe is a number used to describe the hydrodynamic conditions within the membrane channel; it relates the rate of advection of a flow to its rate of diffusion). Furthermore, a preliminary cost analysis using the results did show that both polymeric and ceramic membranes have higher costs at lower fluxes (same Pe number) with a minimum cost at 100 and 125 LMH. The authors suggested that in order to fully reap the advantages of ceramic membranes and to minimize their greater cost over polymeric membranes, ceramic membranes should be operated at as high a flux as possible while still maintaining the ability to recover the fouling that occurs.

Lee and Cho (2004) used two polymeric (8 kDa UF and 250 Da NF) and two ceramic UF (8 and 1 kDa) (TAMI – composed of TiO_2) membranes to compare their removals of NOM and haloacetic acid formation potential. The results showed that the ceramic membranes had several advantages: they exhibited the potential to more effectively remove DBP precursors than NOM in terms of DOC versus the tested polymeric membranes, and the ceramic membranes also exhibited higher permeability than the equivalent polymeric membranes (Lee and Cho 2004).

Hofs *et al.* (2011) compared the performance and fouling of several different ceramic membranes (TiO_2, ZrO_2, Al_2O_3, and SiC) to a polymeric membrane under the same flux and BW procedure. Higher removals of NOM and UV_{254} were observed for the different ceramic membranes (around 30%) compared to the polymeric membrane (13-25%). Additionally, the TiO_2 and SiC showed the lowest TMP increase due to low reversible and irreversible fouling.

Lee *et al.* (2013) compared the fouling mechanisms by Suwannee River Humic Acid (SRHA) and polyethylene glycol (PEG) for a flat-sheet ceramic MF (0.2 μm) membrane (TAMI – composed of a support layer of $Al_2O_3/ZrO_2/TiO_2$ and an active layer of TiO_2) and two polymeric MF membranes made from PVDF (0.22 μm) and polycarbonate (0.2 μm). The majority of fouling for the ceramic membrane consisted of physically removable resistances (i.e. backwashable) and with a much smaller percentage of fouling requiring chemical cleaning as compared to the polymeric membranes. This

was concluded to likely be due to the more hydrophilic nature of ceramic membranes and the earlier occurrence (despite similar pore sizes) of cake formation.

Newer research shows the versatility of the application of ceramic membranes in drinking water. For example, Alpatova *et al.* (2013) used a hybrid ozonation pretreatment for a 1 kDa UF ceramic membrane (TAMI – composed of Al_2O_3 and TiO_2) to investigate the effect of ozone dose on fouling and the removal of DBP precursors, as well as antibiotics. This combination would not be possible due to the sensitivity of polymeric membranes to ozone. It was observed that ozone helped control fouling and showed significant reductions in TOC and specific UV absorbance (SUVA); however, high TOC and alkalinity adversely affected the ability of the ozone to control fouling. Additionally, the promising results observed could make this combination a potentially effective tool for removing DBP precursors and possibly micropollutants such as pharmaceuticals.

Some studies have also investigated the application of ceramic ultrafiltration (80 nm pore size made with a silica support coated with alumina) as a pretreatment to reverse osmosis (Dramas and Croué 2012) as well as the use of ultrasound to minimize fouling with a 0.2 μm MF membrane composed of Al_2O_3 (by Anodisc™) (Gao *et al.* 2012).

From the studies discussed above, there are several surprising results particularly with respect to TOC removals. Despite these promising results, further investigation is needed.

2.7 Summary of research needs

The application of ceramic membranes to drinking water treatment is an area that has not been researched in depth. The types of foulants and extent of fouling as well as fouling mechanisms when filtering natural waters needs to be identified. Additionally, if model solutions are investigated, appropriate concentrations reflective of natural waters need to be used. Furthermore, the incorporation of combinations of model foulants occurring in natural waters is significantly lacking but necessary.

Most research on fouling of ceramic membranes in drinking water treatment has focused on MF membranes, usually combined with coagulation pretreatment. The addition of coagulants complicates the identification of foulants in natural water and the associated fouling mechanisms. Therefore, direct membrane filtration can provide an approach to identify foulants in natural water. Once foulants have been identified an optimal pretreatment can be chosen if necessary. Furthermore, particularly for the application of ceramic membranes to drinking water treatment, an emphasis needs to be placed on researching the reversibility of fouling by incorporating a hydraulic backwash in the experimental design.

Chapter 3
Stage 1: Developing a Sustainable Flux Methodology

3.1 Introduction

Since the application of ceramic membranes to drinking water treatment is an area that has not been well researched, the types of foulants and fouling behavior, as well as fouling mechanisms when filtering natural waters requires more in-depth investigation. The majority of research on fouling of ceramic membranes in drinking water treatment has focused on microfiltration (MF), which is often combined with coagulation pretreatment. The addition of coagulants changes the water chemistry and thus affects the interaction of foulants with the membrane surface, which can alter the type of fouling behavior. Therefore, direct membrane filtration without any pretreatment, as performed in this research, is optimal for identifying foulants specific to ceramic membranes, which can be essential information for selecting an effective pretreatment.

Currently, there is a shift towards minimizing chemical usage and increasing the membrane's lifetime to achieve greater economic and operational sustainability. Studies investigating the importance of operating at critical or sustainable flux suggest that operating at fluxes where low rates of fouling are observed can potentially minimize the extent of irreversible fouling, and thus decrease the frequency of cleaning. However, the approach to determining these lower, sustainable fluxes is not well defined and the accuracy of the results has not been appropriately tested. Since the operating flux can have a significant impact on fouling rates, foulants, and fouling mechanisms, consistent operational standards are needed if two different membrane systems are being compared based on performance. Employing the concept of sustainable flux and establishing a method with which to determine it can accurately compare the two different membrane materials with respect to fouling at a sustainable mode of operation.

It is useful to compare the ceramic membrane performance to that of polymeric membranes, since this is the current norm in drinking water treatment plants. Therefore, it will be essential to utilize an appropriate method to compare the fouling rates observed in both membranes. Such a comparison is challenging due to the differences in membrane material as well as operating conditions. Since the

ceramic membrane will likely have a much higher operating flux than the polymeric membrane, it would not reflect realistic conditions if both membranes were operated at the same flux. The concept of sustainable flux can be used in this scenario to provide a platform for the comparison of these two membranes with respect to fouling while operating at a realistic and sustainable rate. The sustainable flux distinguishes between low and higher fouling rates and is somewhat subjective. The value is dependent on membrane and feed characteristics, as well as the process design and operational requirements, such as an acceptable cleaning frequency. Therefore, this value is case specific and pilot trials can be used to determine the relationship between the flux and fouling rate for a particular set of circumstances, which can be further evaluated to establish a sustainable flux for a commercially competitive design and operation (Bacchin *et al.* 2006, Pearce and Field 2007). However, the approach or method to determine this sustainable flux needs to be developed.

3.2 Sustainable flux

One of the main objectives of membrane filtration is stable operation with minimal or at least an acceptable level of fouling. Sustainable flux allows the membrane filtration process to operate at fluxes that result in low levels of fouling, which ultimately increases the lifespan of the membrane and decreases the frequency of cleaning. It also allows for the comparison of fouling between two different membrane systems, by setting the same objectives in terms of acceptable fouling without compromising the operational parameters of the two membrane systems. This is important because in some studies that compare different membranes, the goal is to create identical hydrodynamic conditions, which can be both difficult and not reflective of full-scale operation. Furthermore, such conditions do not necessarily take advantage of the ability of ceramic membranes to operate at higher fluxes than polymeric membranes.

3.2.1 Defining sustainable flux

The concept of sustainable flux is derived from the idea of critical flux, which describes the relationship between flux and the rate of fouling in a controlled steady state environment (Pearce and Field 2007). Initially, critical flux definitions were theoretical; the flux at which the hydrodynamic

force transporting the particle toward the membrane pore is exactly balanced by the opposing back-transport forces (Field *et al.* 1995; Lahoussine-Turcaud *et al.* 1990). Field *et al.* (1995) defined critical flux as "a flux below which a decline of flux with time does not occur; above it fouling is observed". There are two forms of this flux: strong and weak. The strong form is the flux at which the transmembrane pressure (TMP) begins to deviate from the linear pure water line. For the weak form, very rapid fouling is assumed on start-up and so the flux-TMP relationship is below that of the pure water line. Therefore, the critical flux (weak form) in this case would be the point at which this line becomes non-linear. In practice, however, this definition is not necessarily appropriate for all membrane applications, particularly drinking water treatment.

Generally, the original definition of critical flux (strong or weak form), does not apply to natural feed waters and non-steady state modes of operation. The difficulty in determining the critical flux for natural waters is due to both the mode of operation and the nature of the feed water. Most ultrafiltration (UF) and MF membranes in the water industry are operated using dead end filtration (also known as direct flow filtration) as opposed to cross-flow filtration since it is less energy intensive. However, dead end filtration is only a pseudo steady state operation and will have different fouling characteristics than the steady state operation of cross-flow filtration (Pearce and Field 2007). Since there is some unavoidable fouling in non-steady state operations even at low fluxes, there is a trade-off between this mode and the higher energy costs in cross-flow.

The nature of the feedwater is an additional challenge due to the polydisperse particle sizes in natural water, the statistical nature (and distribution) of back-transport flow paths, and TMP changes along the length of a hollow fiber (Zhang and Song 2000). Furthermore, the occurrence of local supercritical fluxes have been demonstrated even when the membrane system was operated at global subcritical conditions (Cho and Fane 2002). This occurs as a result of heterogeneous fouling in the membrane, which causes a distribution of local fluxes. Additionally, low-pressure membrane filtration of natural waters usually results in perceptible increases in TMP with filtration time, even if operated at fluxes well below the design production for the system (Choi and Dempsey 2005). As a result of these observations, it is unlikely that a unique critical flux with absolutely no fouling at subcritical fluxes exists for typical operation of membranes in drinking water treatment applications. Hence, a more practical approach for natural waters would be to operate at conditions that result in

only slow fouling. Therefore, the focus now shifts towards differentiating between slow fouling and rapid fouling as opposed to slow fouling and no fouling.

In some cases, the critical flux has been redefined to indicate that it is the flux above which there is a rapid increase in the rate of fouling (Chan *et al.* 2002; Cho and Fane 2002; Espinasse *et al.* 2002; Huisman *et al.* 1999). Since this flux does not actually reflect the true definition of critical flux, the term "apparent critical flux" has sometimes been used to signify that deposition may still occur below this flux but it is relatively slow (Bacchin *et al.* 2006; Chan *et al.* 2002). An extension of this idea is the concept of sustainable flux, above which the rate of fouling is economically and environmentally unsustainable (Bacchin *et al.* 2006). For instance, an economically sustainable flux is one that meets a cost objective over the projected life of the membrane plant (Pearce and Field 2007). Therefore, the concept of sustainable flux can be used for comparing two different membrane systems by unifying them through a common treatment objective in order to directly assess their performance.

It is clear that the methods to determine and quantify the sustainable flux can vary and are not well defined. Consequently, the definition of sustainable flux is not very strict or rigorous and is largely dependent upon the objectives of the designer and operator of the plant. Therefore, a more in depth investigation to establish a well-defined approach to quantifying the sustainable flux is needed.

3.2.2 Methods for sustainable flux determination

The term critical flux has been misused in several cases, and often the label 'apparent critical flux' has been applied to indicate some divergence from the original definition. Although sustainable flux encompasses a range of possible fluxes (depending on performance objectives) and "apparent critical flux" would fall within this range, the terms are used in the literature almost interchangeably. For consistency with the cited papers, the terms used by the authors in these papers are used in the following discussion. Several different experimental approaches have been used to identify the sustainable flux. The most common method is either stepwise increases in the permeate flux or TMP and maintaining each for a certain amount of time. For example, Choi and Dempsey (2005) used stepwise increases in permeate flux and maintained each flux for 10 minutes, while continuously recording the flux and TMP. Similarly, the TMP can be increased stepwise at regular intervals and

held at 20 or 30-minute durations for each step. Chan *et al.* (2002) examined the linearity in the plot of TMP averaged over each 15-minute flux step versus the applied flux. The last value of flux remaining on the straight line was considered to be the apparent critical flux. In Figure 3.1, the authors determined that the apparent critical flux was approximately 30 LMH, which corresponds to the approximate location of the last data point forming a linear slope.

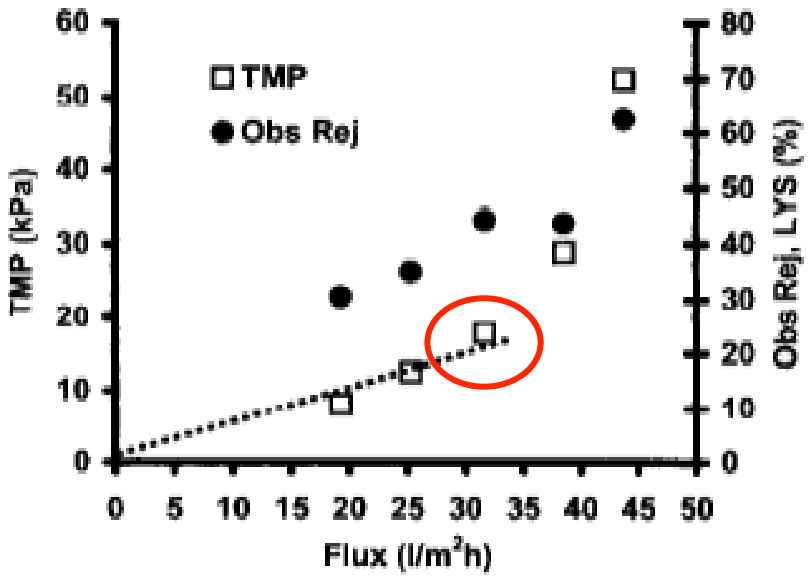

Figure 3.1: TMP and observed rejection vs. flux (Source: Chan *et al.* 2002)

In another flux stepping experiment, Choi (2003) separated the results according to their different flux-TMP behavior. The results were divided into a lower flux group (with little to no fouling) and a higher flux group. The author used dP/dJ (change in pressure over change in flux) to differentiate between these two groups but did not explicitly define a specific cut-off point. Then, each group was regressed to get the linear equation of the line and the intersection of these two lines was considered to be the critical flux (Figure 3.2) (Choi 2003). The limitation in this method is that once the flux exceeds this critical point, the resulting effect on TMP behavior is not necessarily linear. Therefore, linear regression may not accurately account for the behavior observed.

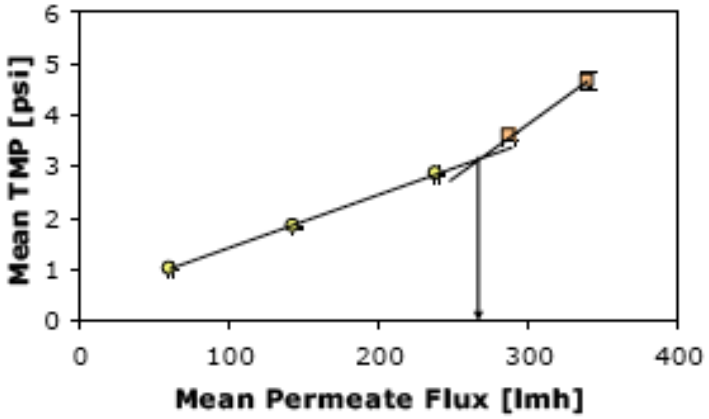

Figure 3.2: TMP vs flux to evaluate the critical flux (Source: Choi 2003)

Chiu and James (2006) recognized that critical flux would not be applicable to the complexity of wastewater filtration and used the term sustainable flux, which they defined as the flux that allows acceptable operating periods without the need for cleaning. In their experiment, the transmembrane pressure was increased at fixed time intervals of 30 minutes prior to the onset of non-linearity in the increase of permeate flux. Once this point was reached, the time interval was decreased to 15 minutes. The experiments continued until a maximum TMP of 1.2 bar was reached. The sustainable flux (Figure 3.3) was then determined to be the average between the last time independent flux step (linear flux-TMP behavior i.e. does not deviate from pure water flux) and the first time dependent step (non-linear behavior) (Chiu and James 2006; Gesan-Guiziou *et al.* 2002). Overall, these experiments chose sustainable fluxes at points near the onset of non-linearity. The method of choice, however, was arbitrary.

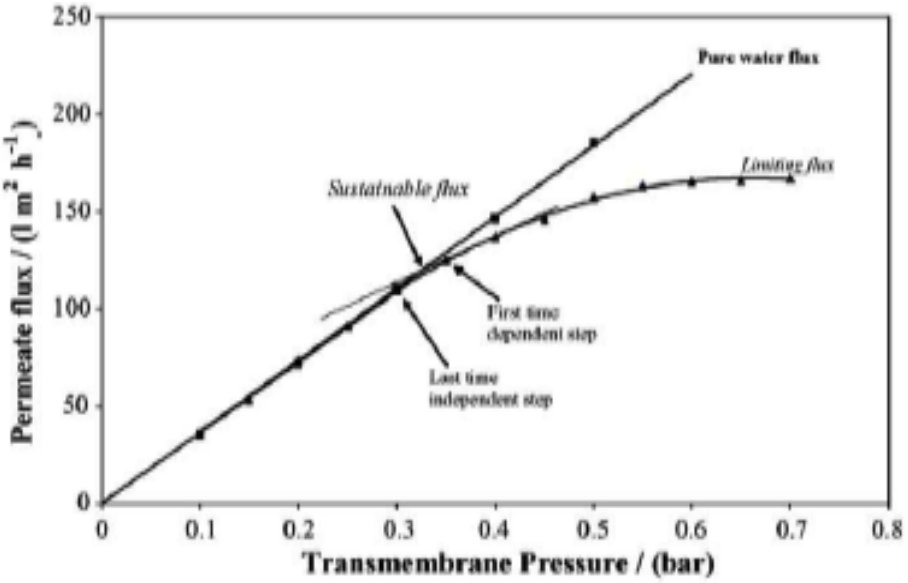

Figure 3.3: Sustainable flux determination using flux curves (Source: Chiu and James 2006)

In conclusion, it is evident that several methods have been used for determining critical or sustainable fluxes. The most common type is flux or pressure stepping and measuring the effect on performance. The length of each time interval was also inconsistent, however, they are comparable to the length of filtration runs between hydraulic cleanings in full-scale UF or MF facilities (usually between 15 minutes to 1 hour). Furthermore, the data analyses methods are not well defined and vary significantly.

3.3 Materials and methods

The objective of the first stage of this study was to establish a procedure to compare these two membrane materials without compromising the functional potential or operating parameters of either membrane. The challenge arises from the potentially significantly different operating fluxes of a ceramic and polymeric membrane as well as their different configurations. Consequently, by drawing upon the concept of critical flux, a parameter with which to compare the rate of fouling in both

membranes is possible. However, since the definition of sustainable flux is somewhat user defined and the methodology of determination is subjective, the intent of this stage was to develop an appropriate procedure through a factorial design for this particular set of experiments.

Source water quality was characterized using several parameters: temperature, pH, turbidity, total and dissolved organic carbon, the UV absorbance at 254 nm, hardness (Mg^{+2}/Ca^{+2}), alkalinity, and fluorescence to characterize the natural organic matter in the water. Turbidity was measured using a calibrated turbidimeter and the Standard Methods #2130. Alkalinity and hardness were determined using titration as outlined in method Standard Methods #2320 and #2340 respectively. UV absorbance at 254 nm was determined using a spectrophotometer (HP 8453, Palo Alto, CA) with a 1 cm quartz cell. No sample preparation is required prior to measurement. Specific UV absorbance (SUVA) is an indicator of the aromaticity of the organic matter and was calculated using the following equation:

$$SUVA\,(L/mg*L) = UV_{254}\,(cm^{-1}) * \frac{100}{DOC\,(mg/L)} \qquad \textbf{Equation 3.1}$$

The total and dissolved organic matter (TOC and DOC, respectively) was measured using the OI-Analytical TOC analyzer (Model 1010, College Station, TX). The analysis follows the wet-oxidation method outlined in Standard methods (2005). DOC samples were filtered through a 0.45 μm polyethersulfone filter prior to analysis.

Grand River water was used for all the experiments and a 200 μm prefilter (reusable filtration cartridge – 10 gpm - Cole Palmer) was the only pretreatment. The water was stored at 4°C for a maximum of 2 weeks to minimize inconsistencies in the raw water quality due to organic matter degradation.

3.3.1 Factorial design

The primary objective of this stage was to build upon previous methodologies in order to establish an appropriate and suitable procedure to determine a representative sustainable flux and compare the rate of fouling in the ceramic and polymeric membrane.

In order to determine the rate of fouling in the membranes, changes in TMP are measured at constant flux operation. The sustainable flux can be determined from the rate of fouling, which is given by the derivative of the transmembrane pressure, dTMP/dt, for constant flux experiments. Several studies have observed significant differences above and below clearly defined fluxes. This distinct point indicates the transition from a membrane process that is operationally and economically sustainable to one that is unsustainable (Bacchin *et al.* 2006). It is important that the criteria chosen is appropriate for the application since duration times of filtration can differ greatly. Therefore, the acceptable fouling rate needs to be sustainable over the desired time scale of filtration.

Several different approaches have been utilized to identify the sustainable flux. The most common method was either stepwise increases in the permeate flux or TMP and maintaining each for a certain amount of time. The approach used in this study was flux stepping and the TMP was monitored and recorded with a pressure transducer (Cole Palmer, 4-20 mA). Since flux stepping maintains constant fluxes during a given step, it is more applicable in full-scale systems where a consistent output is required. Furthermore, since vacuum pumping drives the polymeric membrane filtration, it is designed for constant fluxes and cannot be operated at constant pressures. Therefore, to ensure both membrane systems are evaluated using the same method, the flux stepping approach is most suited for this study. As demonstrated in Figure 3.4, the flux is kept constant while the TMP is measured for each predetermined interval length. Although this method may seem straightforward, several variables such as the length of each time interval, the increments between each interval, and the use of a backwash between each interval can all influence the resulting sustainable flux. Therefore, the membrane needs to undergo adequate fouling during the sustainable flux determination experiment to accurately reflect longer filtration time fouling behavior.

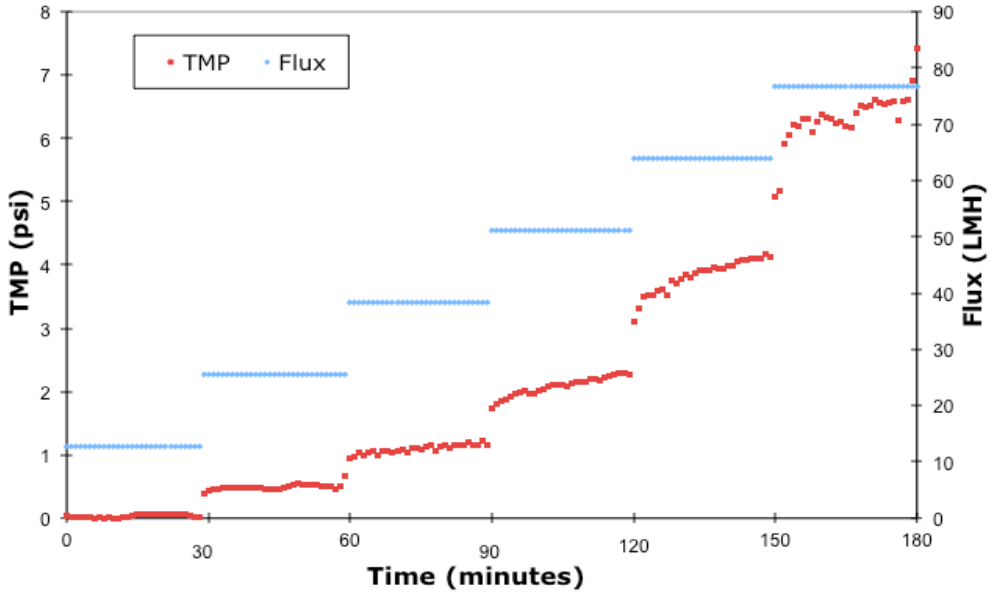

Figure 3.4: An example of the TMP and flux changes occurring over time with the flux stepping method

In order to investigate the importance and impact of the previously mentioned variables, a factorial experiment was designed (Table 3.1). Then a series of experiments running at different combinations of high and low levels of the relevant variables (Table 3.1) were performed as outlined in Table 3.2. The water used for this experiment was taken from the Grand River at the Kaufmann Flats in Waterloo, Ontario, Canada during October 2008. The experiments were operated at room temperature (~20°C); however, temperature was still recorded to monitor any possible changes and the flux data was temperature corrected to 20°C. To avoid any bias in the sequence of experimental tests, the sequence of runs was randomized. Two center point runs (CPR) were also performed with an interval length of 20 minutes, an increment increase of 75%, and with backwash either on or off.

Table 3.1: Variables investigated for sustainable flux experiments

Parameters	High Level	Low Level
1 Interval length	30 minutes	10 minutes
2 Increment increase	100% *	50% *
3 Backwash	Yes	No

* Percent of starting flux value

Table 3.2: Factorial experimental design to investigate variable in sustainable flux experiments using three different parameters. 2^3 design

Run	Parameters		
	1	2	3
1	+	+	+
2	+	+	-
3	+	-	-
4	-	-	-
5	-	+	+
6	-	-	+
7	-	+	-
8	+	-	+
CPR 1	0	0	Yes
CPR 2	0	0	No

+ : high level, - : low level, CPR: center point run

The length of each time interval in most studies has varied between 10 and 30 minutes (Choi and Dempsey 2005; Espinasse *et al.* 2002; Gesan-Guiziou *et al.* 2002). Choosing the increase in flux after each time interval is challenging and since the ceramic membrane can operate at significantly higher fluxes, the initial flux, the increase in flux, and final flux will differ. Therefore, a constant percentage increase from a starting flux was used instead of a specific absolute value. Although backwashing has generally not been included in previous sustainable flux studies, it was incorporated in these

experiments to investigate the effect it would have. The backwash was performed every 30 minutes, even for the shorter time interval of 10 minutes (i.e. after every three filtration cycles). This was done because otherwise backwashing would not have been practical due to long fill times of the polymeric membrane housing after the backwash, which may require up to 10 minutes. Overall, the factorial design outlined in these experiments will indicate the effect and statistical significance of these three variables on the determined sustainable flux.

Once the full factorial design was completed and the sustainable flux methodology was determined through statistical analysis, a long-term experiment was run over 5 days. This step served as methodology verification that the sustainable flux determined would allow the membrane to operate sustainably for several days. A single batch of water taken from one location at the same time was used to determine the sustainable flux, then the membrane was chemically cleaned, and then it was operated at that sustainable flux for 5 days. A hydraulic backwash was also performed every 30 minutes during the long-term filtration experiment.

3.3.2 Data analysis

Once the experiments were completed there were several ways to analyze the data to determine the sustainable flux of the system. Although these methods were somewhat arbitrary, they all chose apparent critical fluxes or sustainable fluxes at points near the onset of non-linearity.

Once the flux and TMP measurements were collected, the first step was to graph the average TMP for each constant flux condition versus the permeate flux, or vice versa. From this graph, an increase in the slope of the line was observed once a critical value was exceeded. An example of this increase is shown in Figure 3.5 where just below 50 LMH the rate of fouling markedly increases.

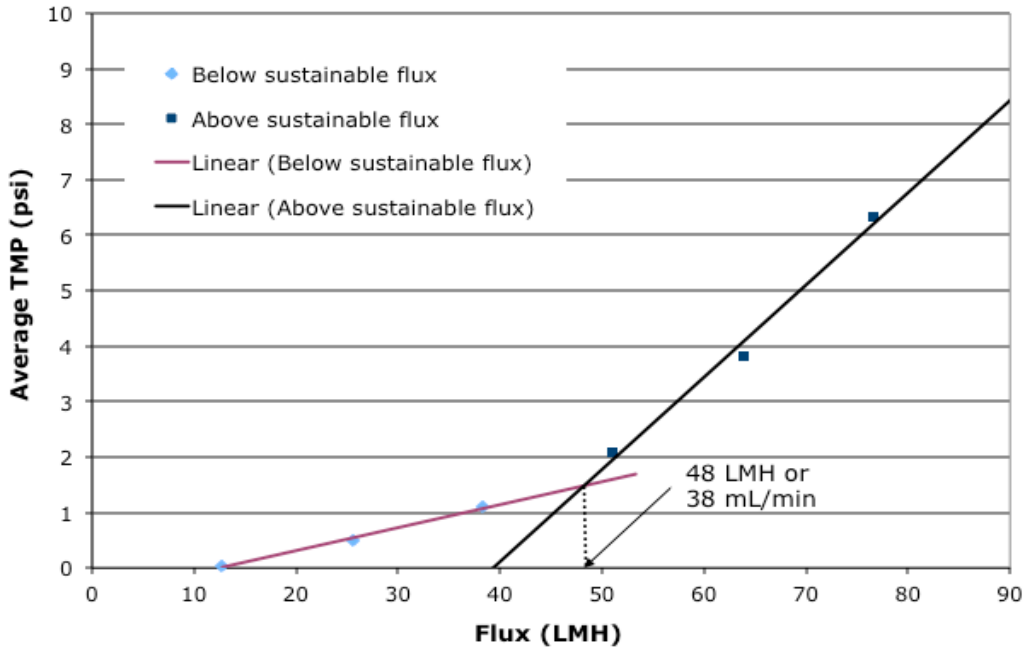

Figure 3.5: An example of how the sustainable flux is determined using the TMP and flux data acquired from the flux stepping method

To validate and confirm this methodology, a long-term experiment was performed once the sustainable flux was determined for a specific batch of water; the membrane was operated at this flux for 5 days. In order to identify foulants, the water composition of the feed water, permeate, and backwash were analyzed.

3.3.3 Polymeric membrane setup

The polymeric membrane used was a hollow fiber polyvinylidene fluoride (PVDF) UF polymeric membrane (General Electric) with a MWCO of approximately 400 kDa. Additional information on the membrane is provided in Table 3.3. The backwash cycle included a hydraulic backwash with the permeate combined with air sparging, which consisted of a 20 second reverse flow with air, followed by 25 seconds to drain the tank, then 10 minutes of tank fill time. The process was automated using a programmable logic controller. The membrane was cleaned between each sustainable flux experiment by soaking for 5 hours in a 200 mg/L sodium hypochlorite (NaOCl) solution followed by citric acid

(5 mg/L), with a rinsing after each cleaning solution. A picture of the setup is shown in Appendix A Figure 1.

Table 3.3: Polymeric membrane properties

Configuration	Hollow fiber (outside in)
Nominal Membrane Surface area	0.047 m^2
Molecular weight cut-off	400 kDa
Max transmembrane pressure	62 kPa (9 psi)
Max operating temperature	40°C
Operating pH range	5-9

3.4 Results of the sustainable flux factorial

The water used for this experiment was taken from the Grand River at the intake to the Manheim treatment plant in Waterloo, Ontario, Canada during February 2009. The water quality parameters tested are summarized in Table 3.4. The water quality is within the typical range for this river. The results of all the runs of the factorial design are summarized in Table 3.5. The flux stepping results and sustainable flux determination figures for each factorial design run are included in Appendix B. The interval length at a high level (i.e. 30 minutes) had a negative effect on the resulting sustainable flux, i.e. it resulted in lower sustainable flux determinations. Therefore, longer intervals provided increased time for the membrane to undergo fouling and consequently increased the resulting mean TMP values at each interval. When a hydraulic backwash was used (i.e. high level), there was a positive effect on the resulting sustainable flux. Since the backwash procedure targets the removal of hydraulically reversible fouling, some fouling is recovered with each backwash, thus allowing for a higher sustainable flux to be achieved overall. It is of interest to note that the extent of fouling removed with a backwash was not consistent and backwashing seemed to be more effective at higher fluxes. This is due to the fact that at lower fluxes where the overall rate of fouling is slower, the majority of the fouling is a result of hydraulically irreversible fouling.

Table 3.4: Water quality of Grand River

pH	8.1
Turbidity (NTU)	3.6
TOC (mg C/L)	6.4
DOC (mg C/L)	6.2
UV_{254} (cm^{-1})	0.188
SUVA (L/mg*L)	3.0
Conductivity (µS/cm)	413
Alkalinity (mg/L $CaCO_3$)	167
Hardness (mg/L $CaCO_3$)	208

Table 3.5: Sustainable flux determined for each run of the factorial design

	Variables			
Run	**Interval Length (min)**	**Increment Increase (%)**	**Backwash**	**Sustainable Flux (LMH)**
1	30	100	Yes	69
2	30	100	No	48
3	30	50	No	48
4	10	50	No	63
5	10	100	Yes	81
6	10	50	Yes	87
7	10	100	No	70
8	30	50	Yes	80
CPR 1	20	75	No	58
CPR 2	20	75	Yes	86

CPR: Center Point Run

Table 3.6: ANOVA table for determining significant variables in the factorial design

Source	Sum of squares	df	Mean Square	F-value	p-value Prob > F	
Model	1459.38	6	243.23	19.65	0.0166	Significant
A-Interval Length	231.13	1	231.13	18.68	0.0228	Significant
B-Increment Increase	6.13	1	6.13	0.49	0.5324	Not significant
C-Backwash	595.12	1	595.12	48.09	0.0061	Significant
AB	15.12	1	15.12	1.22	0.3496	Not significant
AC	21.13	1	21.13	1.71	0.2825	Not significant
BC	45.12	1	45.12	3.65	0.1522	Not significant
Curvature	122.42	2	61.21	4.95	0.1123	Not significant
Residual	37.12	3	12.37			
Lack of Fit	0.12	1	0.12	$6.757E^{-3}$	0.9420	Not significant
Pure Error	37	2	18.50			
Cor Total	1618.92	11				

In Table 3.6, ANOVA analysis of the model and the different terms are evaluated in order to determine which terms are significant in the model (significance level of 0.05). Values of "Prob > F" less than 0.0500 indicate model terms are significant, which in this case, A (Interval length) and C (Backwash) are significant model terms. Values greater than 0.1000 indicate the model terms are not significant, which in this case, B (Increment increase) and any interactions between the variables (i.e. AB, AC, and BC) are not considered significant. The curvature F-value of 4.95 implies the curvature (as measured by difference between the average of the center points and the average of the factorial points) in the design space is not significant relative to the noise. The Lack of Fit F-value of less than 0.01 implies the Lack of Fit is not significant relative to the pure error, which is desirable.

Even if no center point runs were performed, a normal probability plot can indicate the factors that are significant by observing any deviations from the linear plot. As can be seen in Figure 3.6, the interval length and the backwash are the only two factors that deviate from the straight line.

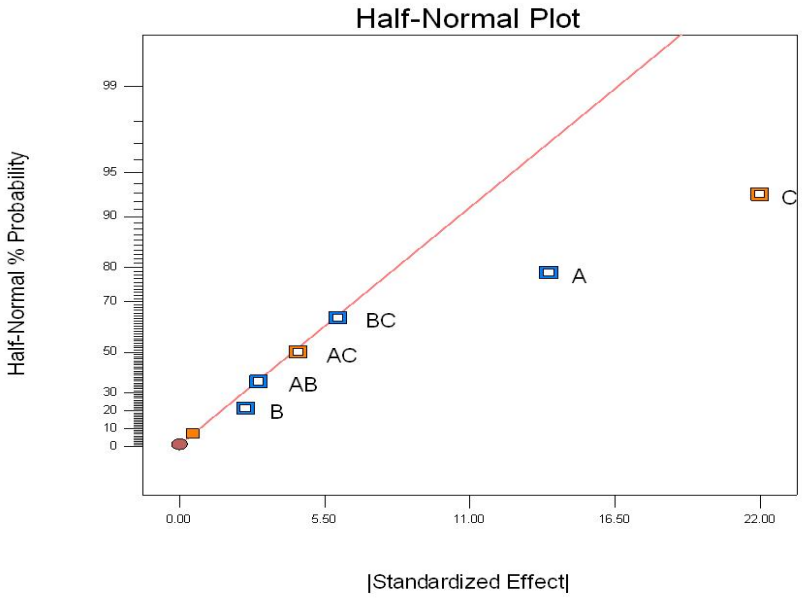

Figure 3.6: Half-normal plot of factorial experimental results

A: interval length; B: Increment increase; C: Backwash. Blue indicates negative effect and orange indicates a positive effect on the sustainable flux

Therefore, using statistical analysis the two factors that were considered significant in this model were the interval length and the use of backwash between each interval (Table 3.6). However, the third variable examined in the factorial experiment, the increment increase between each interval, was not found to be statistically significant, and thus had a minimal impact on the outcome of the sustainable flux. Therefore, to save time in such experiments, it is better to have longer interval times to adequately reflect fouling data at that flux instead of a greater number of flux intervals.

To establish whether the backwash might be skewing the results, the runs with no backwash can be observed. For example from Table 3.5, Runs 2 and 3 have an identical sustainable flux, despite Run 2 using larger increment increases. Similarly, Runs 4 and 7 have similar sustainable fluxes as well. Therefore, even in the absence of a backwash, a change in the increment increase resulted in only a small or negligible effect on the resulting sustainable flux determined.

Therefore, the method decided on for the determination of sustainable flux is as follows:

- 30 minute intervals
- Followed by a backwash
- With an increment increase of 100% of the initial flux

3.5 Long-term operation at sustainable flux with a polymeric membrane

3.5.1 TMP profile

A long-term experiment operating at sustainable flux was performed to verify the sustainable flux method established. A new water samples was used for this experiment and was taken from the Grand River at the intake to the Manheim treatment plant in Waterloo, Ontario, Canada during February 2009. To determine the sustainable flux for the long-term experiment flux stepping was used and the results are shown in Figure 3.7. Figure 3.8 shows the sustainable flux determination approach, which estimates the sustainable flux to be at 75 LMH. It is important to remember that the value obtained is specific to the water being tested and a different value will likely be obtained with a different water quality i.e. Grand River water sampled on a different day. This result is similar to Run 1 (Table 3.5), which used the same experimental approach and determined a sustainable flux of 69 LMH. Therefore, this result fell within the expected range for this type of water quality.

Figure 3.9 shows the TMP increase over the 5 day period. This increase is very small, starting at approximately 2.5 psi and does not surpass 4.5 psi, which is 50% of the maximum TMP for this polymeric membrane. Additionally, there is only a slight decrease in flux from 75 LMH to 67 LMH by the end of the fifth day. The results indicate that the sustainable flux method is appropriate to operate the polymeric membrane sustainably for several days with an acceptable fouling rate.

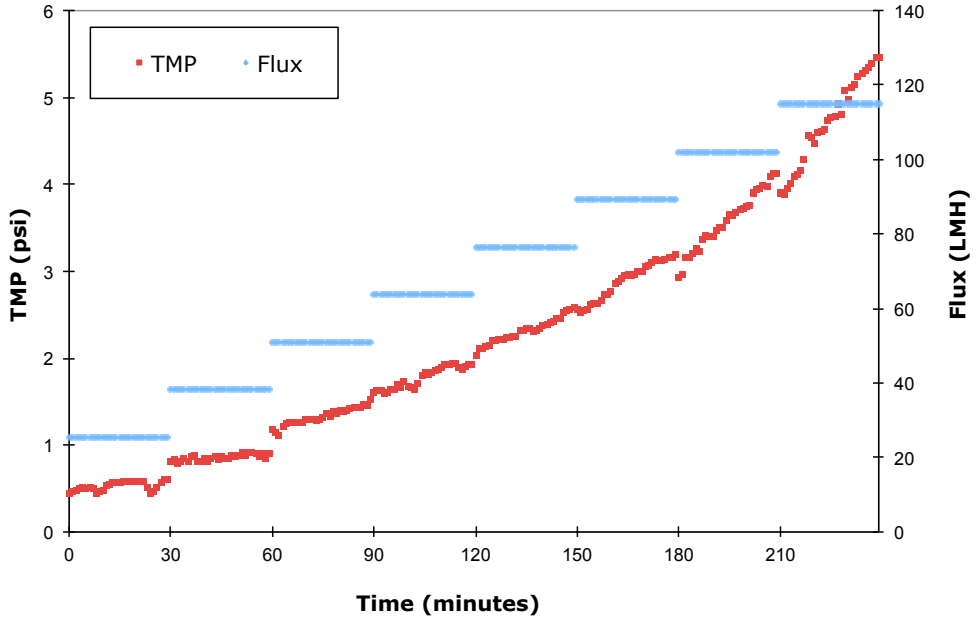

Figure 3.7: Flux stepping results of sustainable flux determination test for long-term experiment

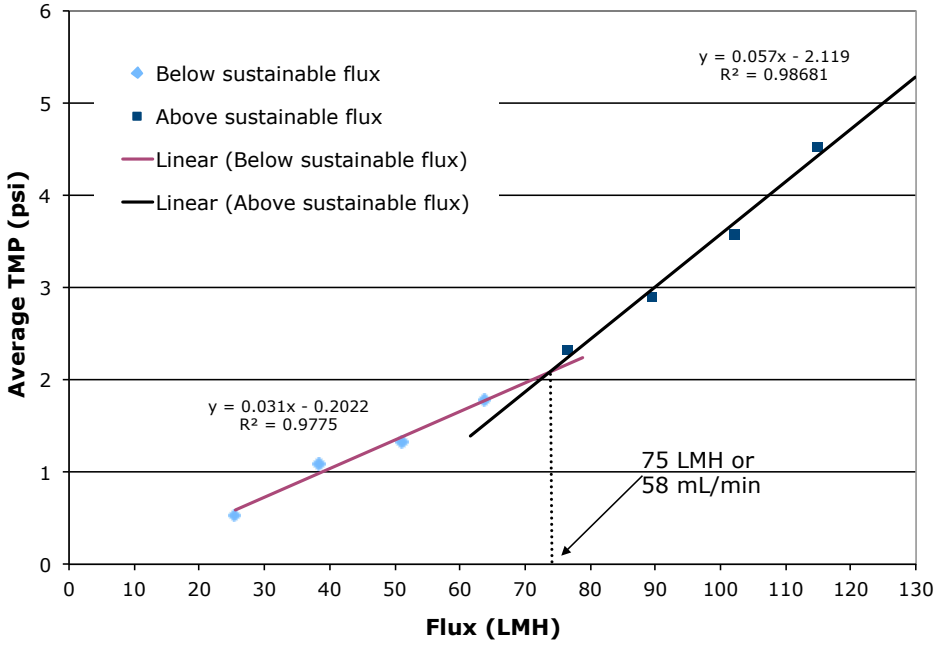

Figure 3.8: Sustainable flux determination for long-term experiment

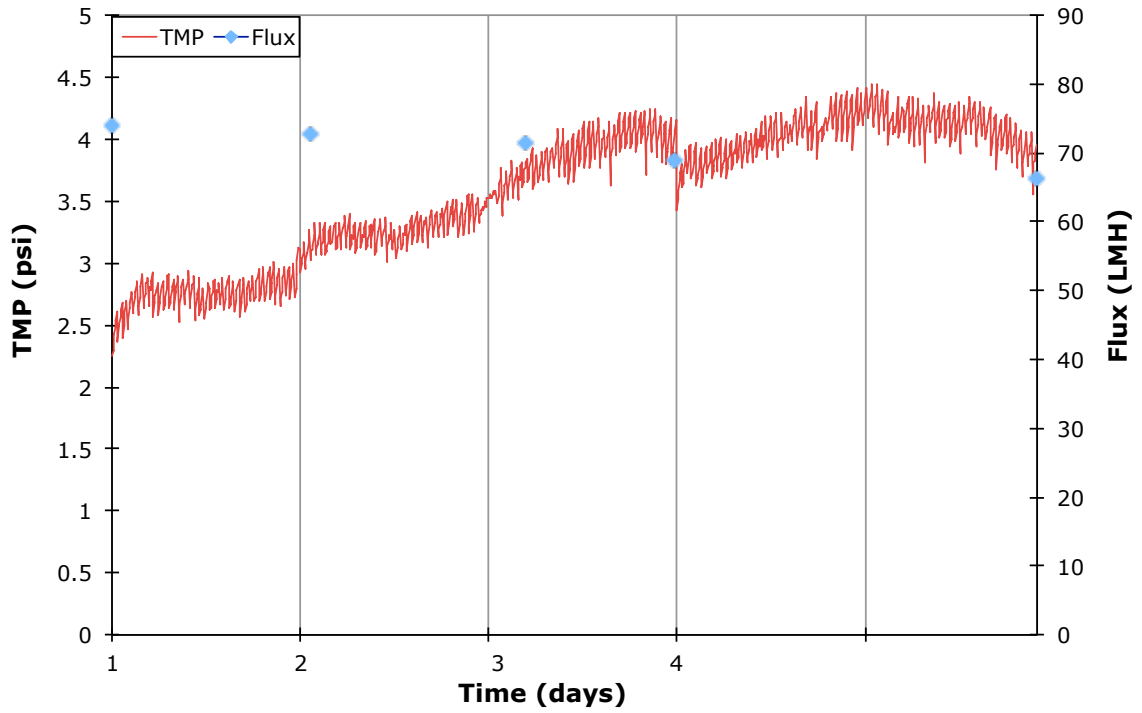

Figure 3.9: TMP and flux over 5 days at sustainable flux with the polymeric membrane setup

3.5.2 Fluorescence

Fluorescence samples were taken at the start of the long-term experiment and then every 24 hours. From Table 3.7 it can be seen that scattering decreases in the permeate, which is a reflection of particles in the water. This result is also reflected by the decrease in turbidity from the raw water of ~3.5 to less than 0.5 NTU. Protein-like material also seems to be slightly removed (Figure 3.10), however, it is present in much smaller concentrations than either fulvic or humic acid, therefore, the percentage removal only gives a rough indication as to the ability of the membrane to reject this foulant. Humic and fulvic acid were not rejected. These results are confirmed by the minimal DOC removal shown in the permeate, with DOC values ranging from 5.8-6.2 (raw DOC is 6.2). Additionally, the SUVA value did not decrease in the permeate indicating that humic concentrations remained the same. The results also do indicate some slight changes in the NOM composition over the 5 day period, which may be due to natural variation in the water sample or some expected degradation occurring over time.

Table 3.7: Main peak intensity values of fluorescence EEMs (excitation/emissions) of raw, permeate, and backwash water throughout the 5 day experiment

		Fulvic Acid (330/420)	Humic Acid (280/460)	Protein (280/330)	Scattering (260/520)
1st Hour	Raw	601	473	74	385
	Permeate	595	459	53	133
	BW	576	475	67	809
Day 2	Raw	579	468	62	492
	Permeate	598	493	58	159
	BW	591	468	71	449
Day 3	Raw	592	481	64	423
	Permeate	583	475	57	163
	BW	576	449	74	404
Day 4	Raw	629	502	70	500
	Permeate	627	512	54	163
	BW	620	490	80	479
Day 5	Raw	641	516	82	306
	Permeate	611	482	57	181
	BW	614	476	76	279

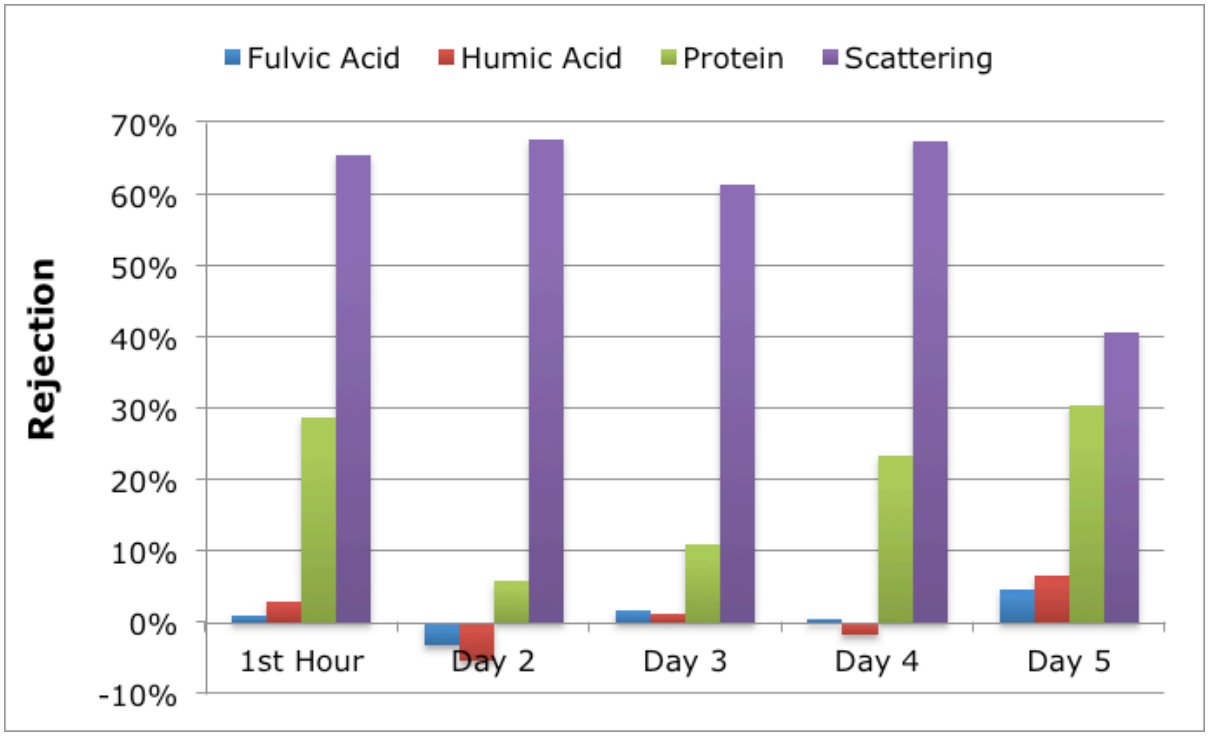

Figure 3.10: Rejection of fulvic acid, humic acid, protein-like, and scattering/turbidity from fluorescence excitation/emission

3.6 Conclusions

A factorial experiment was designed to establish the variables that are statistically significant in determining the sustainable flux using a polymeric membrane. Of the three variables investigated, backwashing and the interval length were significant, while the increment increase between flux steps was not significant. Therefore, the method to be used to determine sustainable flux for future experiments is:

- 30 minute intervals
- Followed by a backwash
- With an increment increase of 100% of the initial flux

The established method was verified by operating the polymeric membrane at the determined sustainable flux successfully over 5 days without exceeding 50% of the polymeric membrane's maximum TMP. Fluorescence results confirmed the removal of particles, however, as expected, minimal NOM was removed by the membrane.

Chapter 4
Stage 2: Reversible and Irreversible Fouling of Ultrafiltration Ceramic Membranes by Model Solutions

A version of this chapter titled "Reversible and Irreversible Fouling of Ultrafiltration Ceramic Membranes by Model Solutions" has been published in the Journal of American Water Works Association[2]. Cited references are in the consolidated list of references at the end of the thesis.

This chapter/article discusses the results of model solution fouling behavior using flat-sheet ceramic membranes and investigates fundamental fouling behavior of ceramic membranes as well as surface characterization techniques.

Summary

Although ceramic membranes are of increasing interest for drinking water treatment, there is little information available regarding their fouling behavior in this context. The objective of the current investigation was to understand the fouling behavior of ceramic membranes on a more fundamental level with foulants that have been identified as problematic for polymeric membranes in drinking water treatment. All solutions showed cake filtration except humic acid and the combination of humic acid and bovine serum albumin (BSA), which showed intermediate and complete blocking filtration, respectively. Silica played a substantial role in increasing the rates of flux decline. BSA was the only foulant that significantly increased the hydrophobicity of the membrane, suggesting that the contact angle of the fouled membrane is not an indication of fouling severity or reversibility. Synergistic fouling effects were observed when the model solutions were combined. These results will be helpful for the application of ceramic membranes in drinking water treatment.

Keywords: *biopolymers, chemical cleaning, contact angle, drinking water treatment, hydraulically reversible and irreversible fouling, model solutions*

[2] Reprinted from *Journal AWWA* Vol. 104 No.10 by permission. Copyright © 2013 the American Water Works Association. (October 2012) (online only) 104(10):E540-E554

4.1 Introduction

The use of polymeric membranes has been accepted in drinking water applications as an effective and sustainable treatment option. More recently, ceramic membranes are showing promise in this field because of their unique physical properties, which may be advantageous in moving towards a more robust treatment. Ceramic membranes can withstand higher pressures, are significantly more resistant to chemicals, and have a longer service life than polymeric membranes (Harman *et al.* 2010). Their surface is naturally quite hydrophilic, which is a membrane surface property that is desirable because of its correlation with lower fouling rates (Aoustin *et al.* 2001) and because it also imparts high permeabilities. The biggest challenge with operating membranes is fouling, which limits productivity and can reduce membrane lifetime. Therefore, effective fouling control methods, which are related to membrane properties, are crucial to a membrane's efficiency and longevity. Since ceramic membranes have thus far been largely limited to industrial and food applications, foulants of concern in typical drinking water treatment applications have not been studied in depth. However, some studies have shown the potential of ceramic membranes to perform better than polymeric membranes in drinking water treatment (Lee and Cho 2004; Bodzek and Konieczny 1998).

The unique properties of ceramic membranes may be advantageous as can be seen from a study by Konieczny *et al.* (2006) that used ceramic microfiltration (MF) membranes (active layer titanium dioxide/zirconium dioxide; pore size 0.1 and 0.2 μm) and compared total organic carbon (TOC) removal of synthetic humic acid solutions by coagulation alone, MF alone, and coagulation followed by membrane filtration. Despite the large pore size, complete removal of TOC was observed with MF alone and with coagulation–MF, which was higher than coagulation alone. However, the MF membranes alone exhibited significantly greater flux declines. These unexpected results indicate the need for further investigation into the fouling properties of ceramic membranes in drinking water treatment.

Few studies have compared the performance of polymeric membranes with ceramic membranes for drinking water treatment. However, several studies using ceramic membranes for different purposes have shown higher removal of natural organic matter (NOM) than would be expected based on the molecular weight cutoff (MWCO) of the ceramic membrane. The MWCO provides only an estimate of the size of the molecules rejected by the membrane. It does not account for differences in size and shape of molecules with the same molecular weight. In a study by Bodzek and Konieczny (1998),

both ceramic (MF and ultrafiltration [UF], 300-kDa) membranes and an MF polymeric membrane (polypropylene) were used to investigate their potential application for pathogen removal in natural waters. Although turbidity removals were similar for all membranes, the TOC removals for the ceramic membranes were higher than for the polymeric membrane. The TOC removal by the UF ceramic membrane was only slightly higher than the ceramic MF membranes; this is likely an indication of high preferential adsorption of organic matter onto ceramic membrane surfaces given that MF/UF membranes are not designed to target TOC removal. Lee and Cho (2004) used a tight UF (8-kDa) polymer membrane (polyamide) and two tight (8- and 1-kDa) ceramic UF (titanium dioxide) membranes to compare removals of NOM. The results showed that the ceramic membranes had several advantages: they exhibited the potential to more effectively remove dissolved organic carbon as well as higher permeabilities.

The unexpectedly high TOC removals observed with ceramic membranes in these studies require further investigation. It is possible that the higher removals were the result of initial adsorption on the membrane and might not have continued in longer experiments. An investigation into the reversibility of the foulants would also have been of interest and would have given additional insight into the fouling behavior observed. Considering that the composition of TOC can vary greatly, it is important to investigate removals and fouling potential of different TOC fractions for ceramic membranes to determine the most likely foulants as well as their reversibility.

NOM has been identified as a major contributor to polymeric membrane fouling (Yamamura *et al*. 2007; Fan *et al*. 2001; Hong and Elimelech 1997). However, the identification of the particular fraction of NOM that has the highest fouling potential has been inconsistent among different membranes. Peiris *et al.* (2010) identified colloidal/particulate substances as contributors to reversible fouling, whereas humic substances and protein-like matter were main contributors to irreversible fouling in a tight UF (60- and 20-kDa) polymeric membrane. Humic substances, proteins, and polysaccharides have also been identified in other studies as irreversible foulants through membrane adsorption and pore-blocking (Aoustin *et al.* 2001; Fan *et al.* 2001; Gray *et al*. 2011; Jermann *et al.* 2008a). Although colloidal particulates alone are generally associated with reversible fouling, synergistic interactions with NOM have not been greatly investigated and could in fact contribute to irreversible fouling (Peldszus *et al.* 2011; Jermann *et al.* 2008b). The importance of biopolymers in UF membrane fouling was observed by Hallé *et al.* (2009) when biofilter pretreatments with

increased biopolymer removal translated into decreased rates of fouling for a polyvinylidene fluoride (PVDF) UF membrane. Therefore, biopolymers, humic substances, and colloidal particulates have all been linked to fouling for polymeric UF membranes, which may or may not be similar for ceramic membranes.

The objective of this study was to investigate the fouling behavior of ceramic membranes using model solutions representative of foulants in drinking water sources alone and in combination. The effectiveness of hydraulic backwashing to identify reversible and irreversible foulants was also investigated because this can be a crucial factor for sustainable operation in drinking water treatment plants. Additionally, the surface properties of fouled and virgin membranes were analyzed to gain additional insight into the fouling behavior.

4.2 Materials and methods

4.2.1 Setup and experimental approach

Flat-sheet, disc-shaped ceramic membranes (DisRam, TAMI Industries, France) (47 mm in diameter) with a surface area of 0.0131 m^2 were used in constant pressure filtration experiments. Flat-sheet ceramic membranes were used to allow for surface characterization analysis, which is extremely difficult or not possible with other typical ceramic membrane configurations (generally tubular). Properties of the membranes used in this study are summarized in Table 4.1. Pictures of the membrane and setup are also included in Appendix A Figures 2 to 4. The membranes were pressurized with nitrogen gas, and the permeate flow was measured using a mass balance. Model solutions were filtered for 60 min at several pressures: 20, 30, and 40 psi (138, 207, and 276 kPa) for single solutions, at 40 psi for combinations, and at 20 and 40 psi for the solution containing all model substances. The solutions were filtered through three different cleaned membranes. The cleaning procedure, which is described in more detail later, was composed of sodium hypochlorite (NaOCl), sodium hydroxide (NaOH), and citric acid. At the end of the filtration cycle, two of these membranes were hydraulically backwashed, followed by a clean water permeability test. The contact angle of all three membranes was measured, providing results for fouled membranes before and after backwash. After contact angle measurements were completed, all membranes were chemically cleaned.

Table 4.1: Summary of virgin ceramic membrane properties

MWCO [a]	300 kDa
Active layer [a]	ZrO_2/TiO_2
Support layer [a]	TiO_2
Max operating pressure [a]	4 bar (58 psi)
Membrane surface area [a]	0.00131 m^2
Virgin contact angle [b]	22° ± 0.5
Average roughness [b]	50 nm ± 8
Mean pore radius	16.4 nm ± 1 [c] 13.6 nm ± 0.7 [d]

[a] Given by manufacturer (TAMI Industries)
[b] Measured in this experiment
[c] Calvo *et al.* (2008) using Scanning Electron Microscopy
[d] Calvo *et al.* (2008) using Liquid-Liquid Displacement Porosimetry

An inherent disadvantage of the ceramic membranes used for this study was the wide range of permeabilities within and between batches of membrane discs. Manufacturing standards allow for up to 40% variation in clean water permeability as long as an acceptable MWCO is achieved, according to the Association Française de Normalisation Standard NF X 45-103. Without previous screening of the membrane samples used, this would have posed a major challenge in obtaining reproducible and comparable flux decline curves during the fouling experiments. The approach taken, therefore, was to use only membranes with no more than a 15% deviation from the average clean water flux (CWF); as a result only six membranes in total were used for all experiments. Therefore, membranes were reused after each cleaning cycle when the CWF was fully recovered. The CWF of each membrane throughout these experiments was determined after each full cleaning cycle and before running fouling experiments; all membranes stayed within 15% of the average CWF during the entire study. In addition, all flux decline curves were run in triplicate, and membrane discs were selected randomly throughout to avoid bias. To allow for comparison, flux decline curves were normalized by plotting the relative flux, which is the observed flux divided by the CWF of that particular membrane (i.e., relative flux = J/CWF).

Backwashing was performed with ultrapure water for 5 min in order to collect a sufficient amount of

sample for analysis. Backwashing was run at the same pressure as filtration pressure. This was followed by a CWF measurement. Permeate was not used for backwashing due to limitations in the setup and inadequate permeate yield after 1 h. Some studies have found that the use of ultrapure or demineralized water instead of permeate water can enhance the effectiveness of backwashing in controlling fouling of both polymeric and ceramic UF membranes (Li *et al.* 2010; Abrahamse *et al.* 2008). The backwashing step was used to distinguish between reversible and hydraulically irreversible fouling. An additional 5-min backwash was performed to determine the importance of backwashing duration on flux recovery for a limited number of model solution experiments.

The chemical cleaning procedure used in this study was similar to that used for other ceramic membranes (Metawater, Japan). The cleaning method consisted of three cleaning solutions starting with NaOCl (3,000 mg/L), followed by NaOH (0.1 M), and ending with citric acid (1%), each with a soak time of 5 hours. The membranes were rinsed between each cleaning step with ultrapure water. The cleaning method originally suggested by the membrane manufacturer (TAMI) was not used due to its drastic nature (high concentrations of basic and acidic chemicals at high temperatures), which is not practical or necessary in a drinking water treatment facility.

4.2.2 Model solutions

The model substances investigated were a protein (bovine serum albumin [BSA], 5 mg/L), a polysaccharide (sodium alginate, 5 mg/L), an NOM fraction (humic acid, 5 mg/L), and an inorganic colloid (silica, [Ludox ® HS-30 colloidal silica] 200 mg/L). All model substance properties were supplied by Sigma Aldrich and their properties are summarized in Table 4.2. The pH of the solutions was between 5.7 and 6.3. Sodium alginate is a hydrophilic polysaccharide that is produced by algae and bacteria. Humic acid is a hydrophobic fraction of NOM, and BSA is a hydrophobic animal protein that is commonly used to represent protein-like foulants in surface water. Yuan and Zydney (1999) determined the apparent-molecular-weight distribution for this humic acid for approximately 60% > 50 kDa and for approximately 30% at ≈ 300 kDa, the latter fraction being in the same range as the MWCO of the ceramic membrane used in this study. The colloidal silica was supplied as a 30% w/w colloidal suspension having a density of 1.21 g/mL at 25°C. The surface area of the silica particles was 200 m^2/g and the average hydrodynamic size was ~9 nm (given by the manufacturer).

The size was chosen because small colloids in the size range of 3–20 nm have been identified as important membrane foulants (Howe and Clark 2002). The concentration of the colloidal silica was selected following a review of the literature. When nanofiltration/reverse osmosis membranes were used, the silica particle sizes ranged from 100 to 300 nm and concentrations were ~200 mg/L (Lee *et al.* 2005, Vrijenhoek *et al.* 2001). For UF membranes, the silica particle sizes ranged from ~12 to 100 nm, and the concentrations were 0.4 to 0.5% wt. (Wu *et al.* 1999; Chen *et al*. 1997). The turbidity of the 200 mg/L silica solutions used in these experiments was less than 0.5 NTU.

The feed solutions were prepared by adding 5 mL from a 1g/L stock solution into every liter of feed solution. The TOC of each individual single solution was 1.5, 2.5, and 2 mg C/L for alginate, BSA, and humic acid, respectively. Therefore, in mixtures, the TOC concentrations were higher than in single solutions. However, the concentration of the individual component remained constant between individual solutions and in mixtures thereby allowing for a direct comparison of the effect of an individual component in different mixtures.

In addition to providing important insights into fouling behavior, the investigations with these model substances are relevant to natural waters low in concentrations of divalent cations. Future work will examine the effect of dissolved calcium on fouling.

Table 4.2: Summary of model substance properties

Model Substance	Foulant Type	Average Molecular Weight (kDa)	Carbon Content (%)
Bovine Serum Albumin (B)	protein	67[1]	0.46[1] 0.47[3]
Humic Acid (H)	NOM fraction	~ 70[1]	0.31[1] 0.4[3]
Sodium Alginate (A)	polysaccharide	30-100[4]	0.29[3]
Silica (S)	inorganic colloid	~ 9 nm average hydrodynamic size[2]	Not applicable

[1] Xiao *et al*. (2009)
[2] Given by manufacturer Sigma Aldrich
[3] Measured
[4] Katsoufidou *et al.* (2007)

4.2.3 Surface characterization

The contact angle was measured using a 10-μL drop of ultrapure water (DSA100, KRÜSS GmbH, Germany). The average of five measurements was taken on each membrane within the first second of contact between the water drop and the membrane surface. The height–width method provided in the instrument software was used to analyze the contact angle. In this standard method, it is assumed that the contact angle for small drops is not influenced by the absolute drop size. The contact angle is calculated from:

$$\theta = \cos^{-1}\left(1 - \frac{h}{R_{\max}}\right) \qquad \textbf{Equation 4.1}$$

in which h is the height of the drop and R_{max} is the maximum radius of the drop. It is particularly important to analyze the first contact moment since the contact angle decreases rapidly as the drop vanishes into the membrane due to the hydrophilicity of the ceramic membrane.

The roughness of the membrane was measured using atomic force microscopy (Digital Instruments Nanoscope® multimode aromic force microscope, Veeco, Ontario, Canada). A cross-section scan size of 5 μm x 5 μm was taken at 10 different locations on the membrane in contact mode. The scanned images were plane-fitted and flattened with a second order polynomial approximation, which removes any curvature or slope induced by the scanner. The z-range, root mean square, and average roughness of all 10 cross sections were averaged. The settings were a scan rate of 0.5 kHz, silicon nitride tip (spring constant is 0.12 N/m, frequency is 14–26 kHz, and a cantilever thickness is 0.4–0.7 μm), tip velocity of 1 μm/s, integral gain of 2, proportional gain of 3, and deflection setpoint of 0V.

4.2.4 Data analysis

The flux decline curves were analyzed using blocking laws (Hermia, 1982) to determine the fouling mechanism.

$$\frac{d^2t}{dV^2} = \beta\left(\frac{dt}{dV}\right)^{\Phi} \qquad \textbf{Equation 4.2}$$

which can be rewritten as

$$\log\left(\frac{d^2t}{dV^2}\right) = \log\beta + \Phi\log\left(\frac{dt}{dV}\right) \qquad \textbf{Equation 4.3}$$

in which t is time (s), V is volume (L), β is blocking law filtration coefficient (units vary depending on Φ), and Φ is blocking law filtration exponent (unitless). Values of Φ that are 0, 1, 1.5, and 2 correspond to cake, intermediate, standard (pore constriction), and complete blocking filtration respectively.

Total membrane resistance can be determined using Darcy's Law:

$$R_t = \frac{\Delta P}{\mu J} \qquad \textbf{Equation 4.4}$$

If all fouling is assumed to be a result of cake filtration then cake resistance can be calculated using:

$$R_c = R_t - R_m \qquad \textbf{Equation 4.5}$$

and the specific cake resistance can be calculated using the flux decline results:

$$\alpha_c = \frac{R_c A}{CV} \qquad \textbf{Equation 4.6}$$

Where R_t is the total fouling resistance, ΔP is the transmembrane pressure drop, μ is the water viscosity, J is the permeate flux, R_c is cake resistance, R_m is the membrane resistance, α is specific cake resistance, A is the membrane surface area, C is the concentration, and V is the volume filtered.

The cake compressibility n can be estimated as follows (Foley 2006):

$$\alpha=\alpha_0 \Delta P^n$$ **Equation 4.7**

in which α is specific cake resistance, α_0 is a constant related primarily to the size and shape of the particles forming the cake, ΔP is pressure drop across the membrane, and *n* is the cake compressibility index, which ranges from zero (incompressible cake) to 1 or greater (for a highly compressible cake).

The quantities can be estimated by calculating the specific cake resistance from flux decline curves at several pressures using equations 4.4 to 4.6 and plotting the linearized form of Eq. 4.7 as represented by Eq 4.8:

$$\log \alpha = \log \alpha_0 + n \log \Delta P$$ **Equation 4.8**

4.3 Results and discussion

4.3.1 Virgin membrane properties

The virgin ceramic membranes (Table 4.1) have an average roughness of 50 nm, a root mean square of 65 nm, and a z-range of 450 nm. An image of the membrane surface taken with the atomic force microscopy is shown in Figure 4.1. These values are much higher than those for polymeric membranes of similar MWCO (Haberkamp *et al.* 2008). The contact angle of the virgin ceramic membrane was quite low (22°± 0.5), pointing to its hydrophilic nature. In contrast, contact angles for polymeric membranes are usually much higher, e.g., 75° for PVDF and 65° for polycarbonate membranes (Yao *et al.* 2010), and 64° for PVDF and 53° for a hydrophilized polyethersulfone membrane (Haberkamp *et al.* 2008). These differences in surface properties of the ceramic membrane used in this study compared with commonly used polymeric membranes may lead to differences in interactions with organic and inorganic foulants and thus affect fouling behavior. Additional virgin membrane properties are summarized in Table 4.1. The zeta potential of the virgin ceramic membrane

was measured once at a pH of 5.5 and found to be negative; due to the complexity of the measurement, it was not replicated.

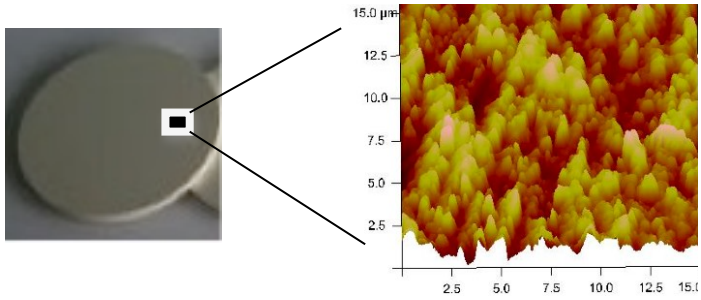

Figure 4.1: Image of flat-sheet disc-shaped ceramic membrane and a 15 µm cross-section of the membrane surface taken with atomic force microscopy

4.3.2 Fouling behavior

The flux decline curves in Figure 4.2 and Figure 4.3 provide an initial insight into the overall fouling behavior of typical model foulants. To distinguish between contributions of hydraulically reversible and irreversible fouling to these curves, a hydraulic backwash of the fouled membranes was performed (for details see Section 4.3.4: Effect of backwashing). Contributions to chemically irreversible fouling were identified after additional chemical cleaning (for details see Section 4.3.5: Chemically irreversible fouling).

The single solution flux decline curves (Figure 4.2) show that silica has the highest initial rate of fouling at all pressures. Although the concentration of silica was higher than that of the other model compounds, the fouling rates for silica were in the same general range as the other compounds. Alginate, BSA, and humic acid have similar initial fouling rates at 30 and 40 psi (Figure 4.2 parts b and c). However, at the end of the 40 psi test, the rate of flux decline with alginate appeared to be somewhat greater than that of the other substances. Humic acid and BSA seemed to reach a pseudo-steady state at approximately 10% of the clean water flux. At 20 psi (Figure 4.2 part a) humic acid fouling behavior differs, showing a slow but almost constant rate of flux decline, which may be related to its fouling mechanism, discussed in Section 4.3.3. The higher final flux for BSA and the

continuation of alginate fouling are consistent with results for a polymeric membrane found by Zhang *et al.* (2006), who identified polysaccharides as the major foulants—not proteins.

When the model solutions are combined with one another, all the solutions with silica demonstrate higher rates of fouling (Figure 4.3 part a). Colloids alone form a cake layer that is porous and highly permeable. However, when coupled with smaller organics (such as BSA and alginate), the cake resistance increases as a result of the combined fouling, which can hinder the back diffusion of foulants into the bulk solution, thus creating higher foulant concentrations at the membrane surface (Law *et al.* 2010). Another possible explanation is that the organic molecules serve as "glue" for the silica particles and through filling holes in the cake layer a more condensed cake layer is formed. Therefore, the higher fouling rates with silica are likely caused by the formation of a thicker and denser cake layer, thus increasing the overall membrane resistance at a faster rate. Also, the relatively high roughness of the membrane (around 50 nm) possibly enhances the fouling as a result of the accumulation of the silica particles in the valleys (Al-Amoudi, 2010). The effect of silica on the fouling rates is further demonstrated in Figure 4.4 by showing the average final relative flux versus average total volume filtered. In Figure 4.4, part a, it can be seen that once silica is added, it shifts and compresses the grouping to the bottom left by decreasing the total volume filtered and decreasing the average final relative flux, which is reflected by higher rates of flux decline experienced for solutions with silica. Figure 4.4 part b, looks at only solutions with silica, and from here a less significant effect of alginate on decreasing the average final relative flux and the average total volume filtered can be observed. Synergistic fouling effects when model solutions are combined were also observed by Jermann *et al.* (2008a) for a polymeric UF membrane.

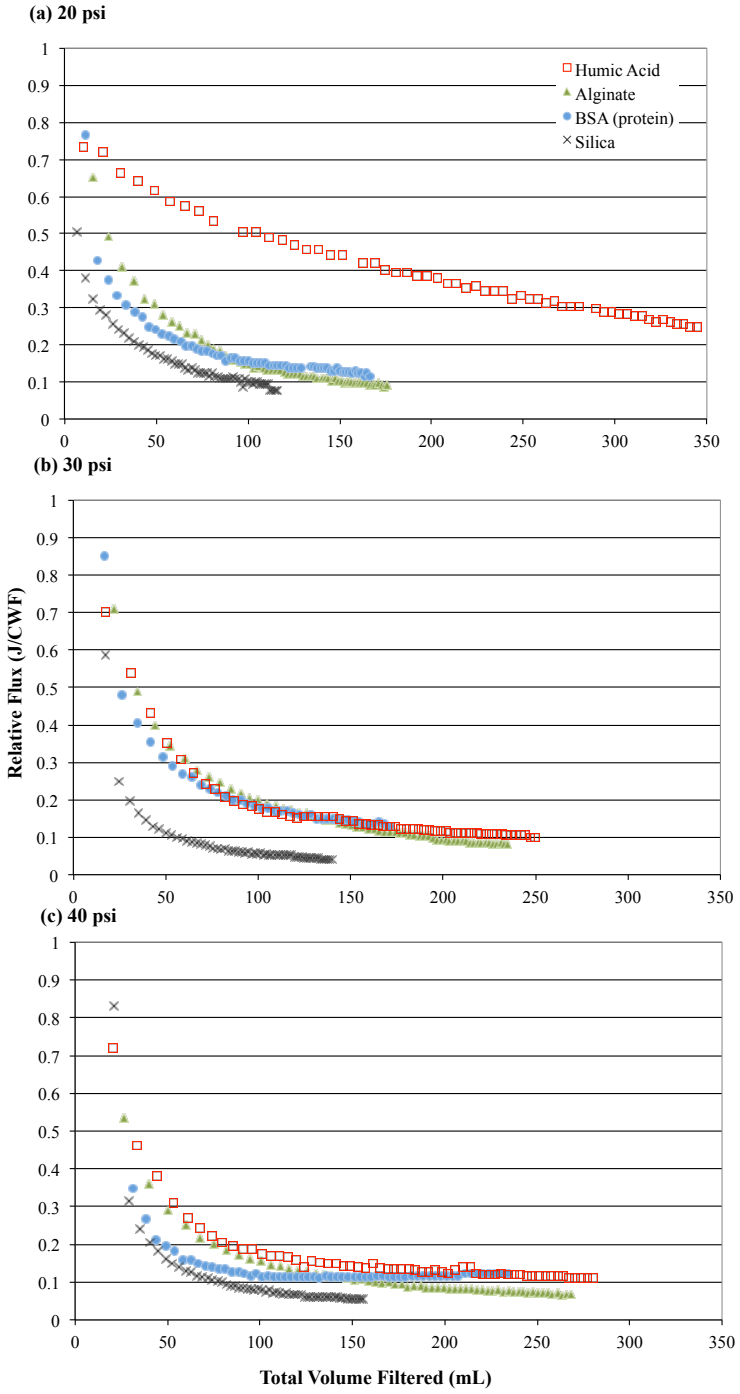

Figure 4.2: Relative flux decline for single solutions over 1 h at (a) 20, (b) 30, and (c) 40 psi.

The relative flux, which is the flux divided by the clean water flux (CWF) for that specific membrane, is plotted over the total volume filtered over 1 h; each flux decline curve is for one replicate; fluxes are temperature corrected to 20°C. BSA: Bovine Serum Albumin.

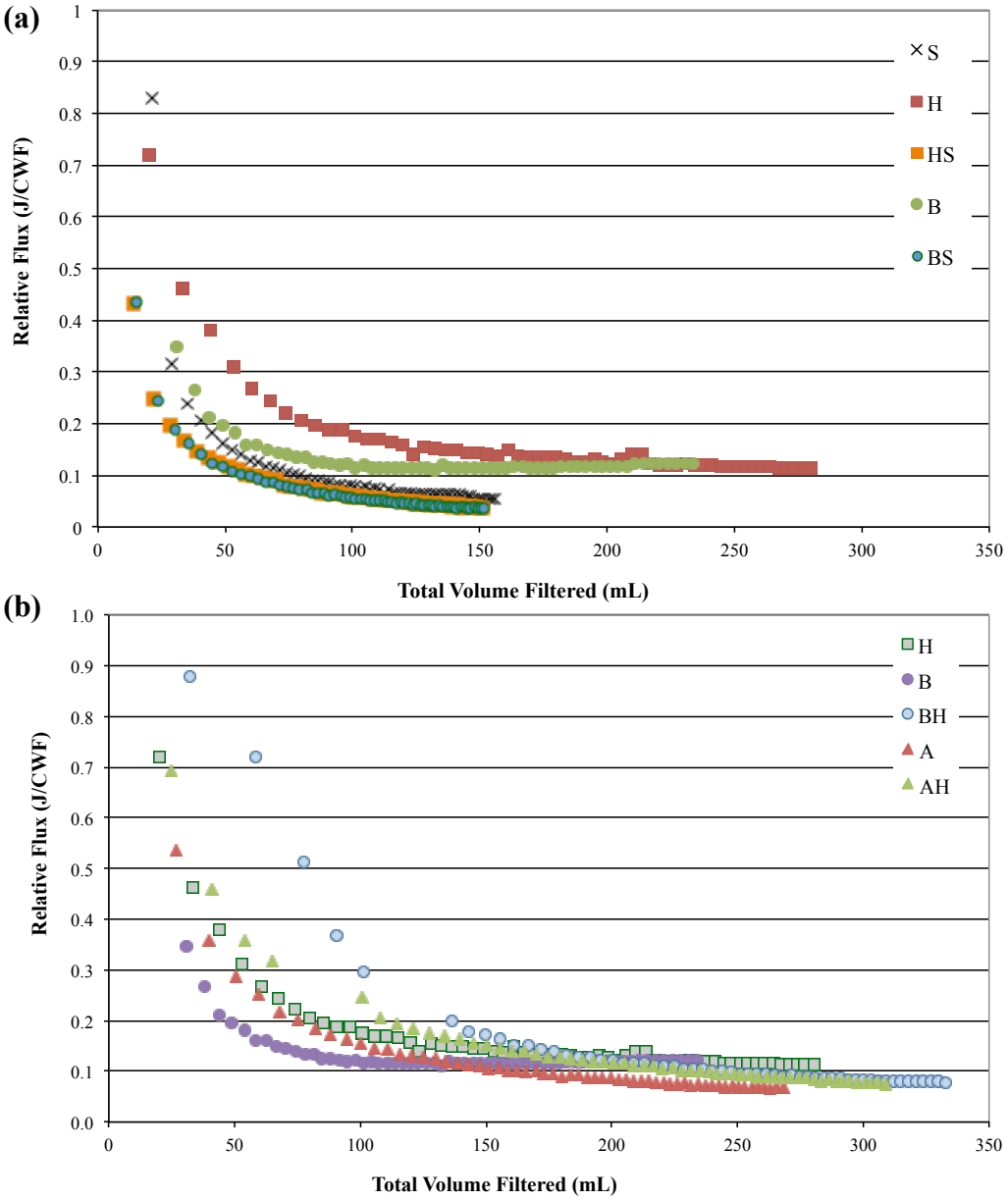

Figure 4.3: Relative flux decline over 1 h for combinations of model foulants. (a) effect of silica and (b) effect of humic acid.

For each solution three clean membranes were used to run three 1-h experiments. All three runs had a final flow within 15% of one another and a total volume filtered within less than 10% of one another. Although only one run is shown for the combination solutions, it is representative of the fouling behavior observed for all three runs of a particular solution Not all combination solutions filtered are shown. Fluxes have been temperature corrected to 20°C. A: Alginate; B: Bovine Serum Albumin; H: Humic acid; S: Silica.

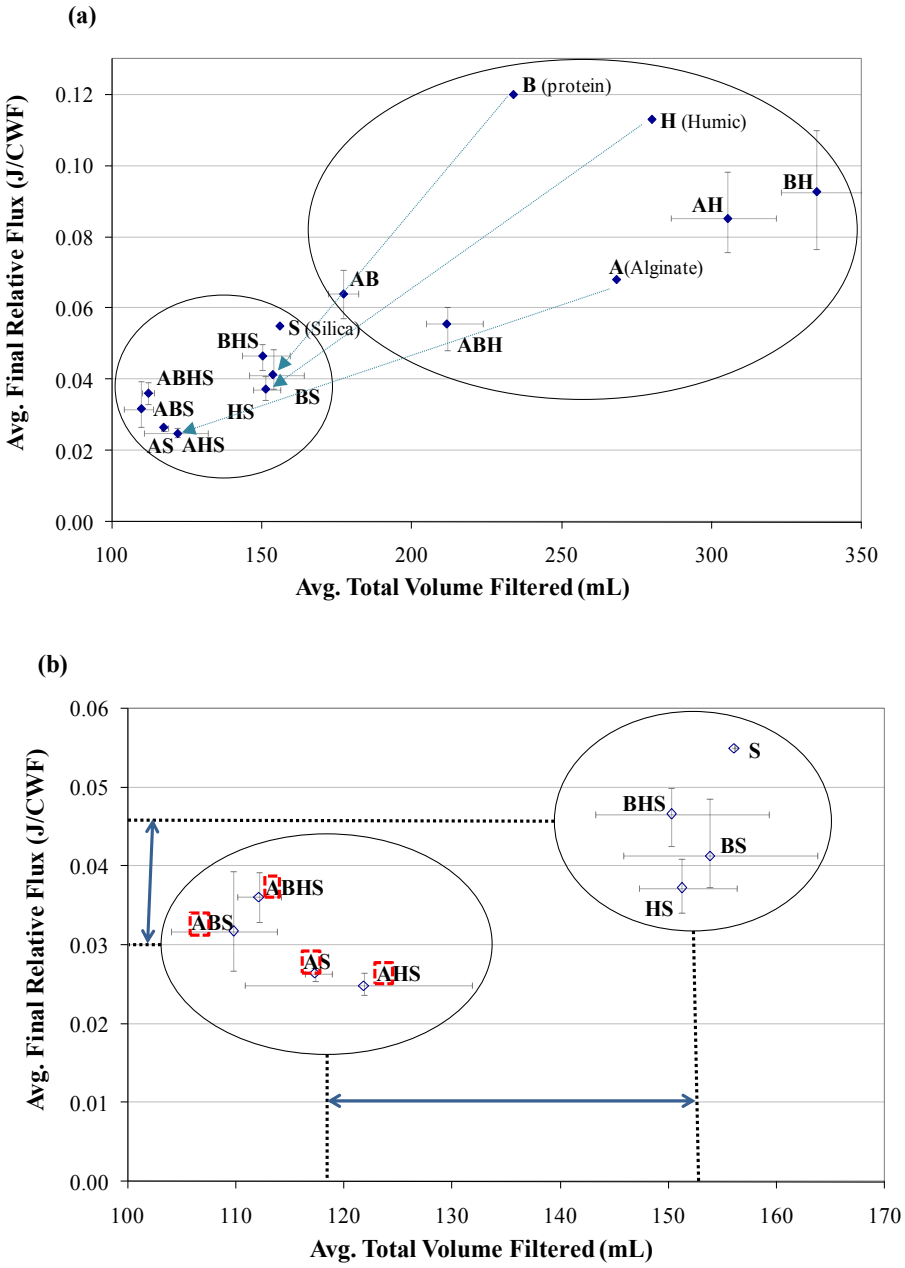

Figure 4.4: Average final relative flux versus average total volume filtered at 40 psi for 1 h (a) all solutions and (b) only solutions with silica (b is a close-up of left oval in part a).

Error bars indicate range of values (n=3) except for single solutions (n=1). A: Alginate; B: Bovine Serum Albumin; H: Humic acid; S: Silica.

4.3.3 Blocking filtration laws

Flux decline curve analysis using Hermia's model (Eq. 4.3) indicated that cake layer filtration was virtually instantaneous for almost all solutions (data not shown). This is similar to the observation by Lee *et al.* (2008) that cake formation occurred almost immediately with NOM filtration using polymeric UF membranes.

Humic acid alone showed an exponent of approximately 1 (n= 2) at 30 and 40 psi (Figure 4.5), which correlates to intermediate blocking filtration. This is an extension of complete blocking filtration as it allows for the superposition of particles in addition to pore-blocking. This may be the result of a greater affinity of humic acid molecules to each other than to the membrane surface and/or electrostatic repulsion between the negatively charged humic acid and the membrane surface. However, Costa *et al.* (2006) observed complete pore blocking with cellulose acetate UF membranes (filtration exponent of 2) when filtering humic acid, although at concentrations significantly higher than in this study (1,000 mg/L). The results between the different repetitions as well as pressures for humic acid filtration are consistent (Figure 4.5).

The only combination solution without instantaneous cake filtration was BSA combined with humic acid (BH; Figure 4.5). The average filtration exponent of 2.7 (n = 3) indicated complete blocking filtration, which normally causes rapid and severe flux decline. However, in this case, the rate of flux decline for BH was the lowest of all solutions, with the highest total volume filtered and one of the highest final flows (Figure 4.4). This inconsistency may be the result of the limitations of applying a model that was developed for spherical particles to dissolved macromolecules such as those in these experiments. Further observations showed that the membrane with the highest permeability among the three membranes used for each solution experienced cake layer formation earlier and after less total volume filtered. This observation is consistent with experiments by Costa *et al.* (2006) and Howe *et al.* (2007) that showed the onset of cake filtration earlier for the more permeable membrane.

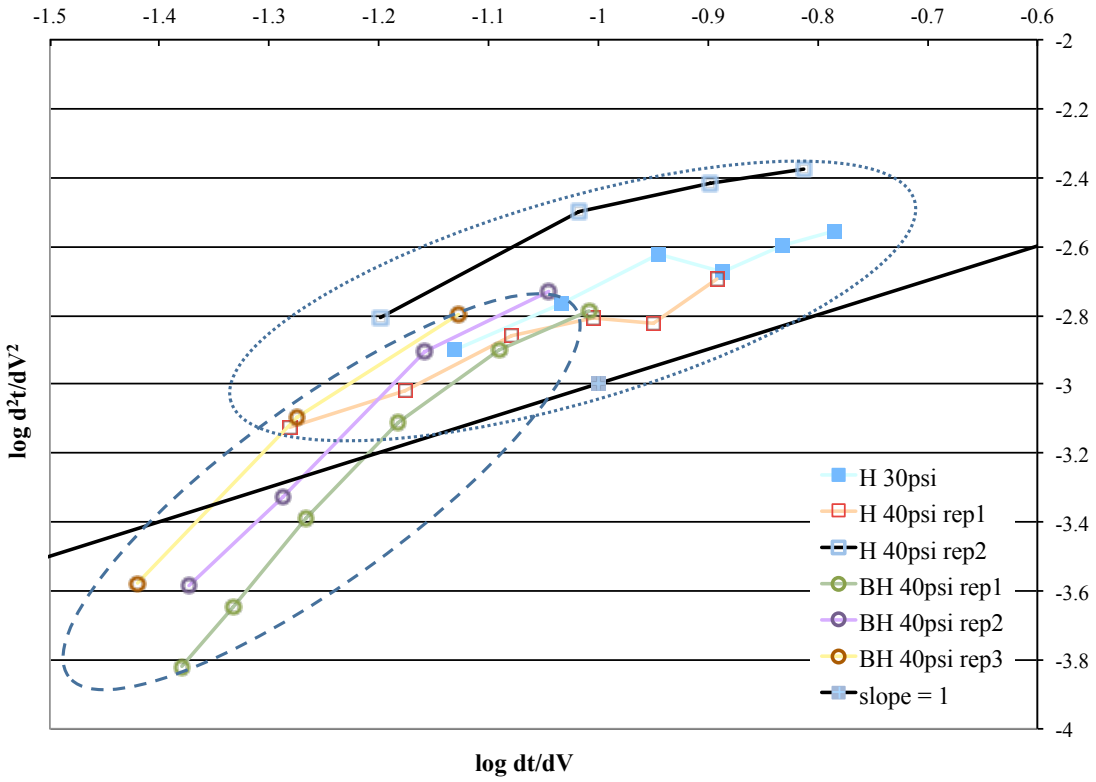

Figure 4.5: Fouling mechanism determination for humic acid alone (H) and humic acid combined with bovine serum albumin (BH).

Recall Equation 4.3: $\log\left(\frac{d^2t}{dV^2}\right) = \log\beta + \Phi\log\left(\frac{dt}{dV}\right)$ Equation 4.3. *Therefore, the slope of the line is Φ, which is the blocking law filtration exponent (a line with Φ = 1 is provided for reference).*

4.3.4 Effect of backwashing

Both a hydraulic backwash (BW) and chemical cleaning are used to remove the foulants and recover performance. Fouling that can be removed with a hydraulic backwash is considered hydraulically reversible (the remaining fouling is hydraulically irreversible). Fouling that can be removed with a chemical cleaning step is chemically reversible fouling (the remaining fouling is considered chemically irreversible).

Backwashing was used to determine the hydraulic reversibility of different model foulants and their combinations. Backwashing was performed using ultrapure water for 5 minutes at the same pressure as filtration. An increase in backwashing time by an additional 5 minutes showed only a marginal increase in flux recovery (2% on average, data not shown). Figure 4.6 shows flux recovery following a BW as a function of the average final flux before backwashing. Solutions with high hydraulically reversible fouling were characterized by rapid flux declines, whereas solutions with high hydraulically irreversible fouling had a much slower flux decline.

The fouling observed is clearly not simply a function of the TOC concentration present in the mixture. For example, comparing AS to AHS shows similar fouling behavior despite almost twice as much TOC in the AHS mixture. Therefore, this illustrates that there is no obvious effect due to the TOC concentration being higher in mixtures and that the TOC concentration may only be a factor contributing to fouling. To evaluate reproducibility flux decline curves for each solution were repeated 2-3 times. Ranges (i.e. minimum and maximum values) as opposed to standard deviations are shown for the individual data points in all figures in Chapter 4 because the number of replicates for each solution was too low to calculate a standard deviation. Comparisons are being made between major groupings where differences are clearly evident, even when taking into account the ranges associated with the individual data points. Additional statistical significance tests were therefore not performed.

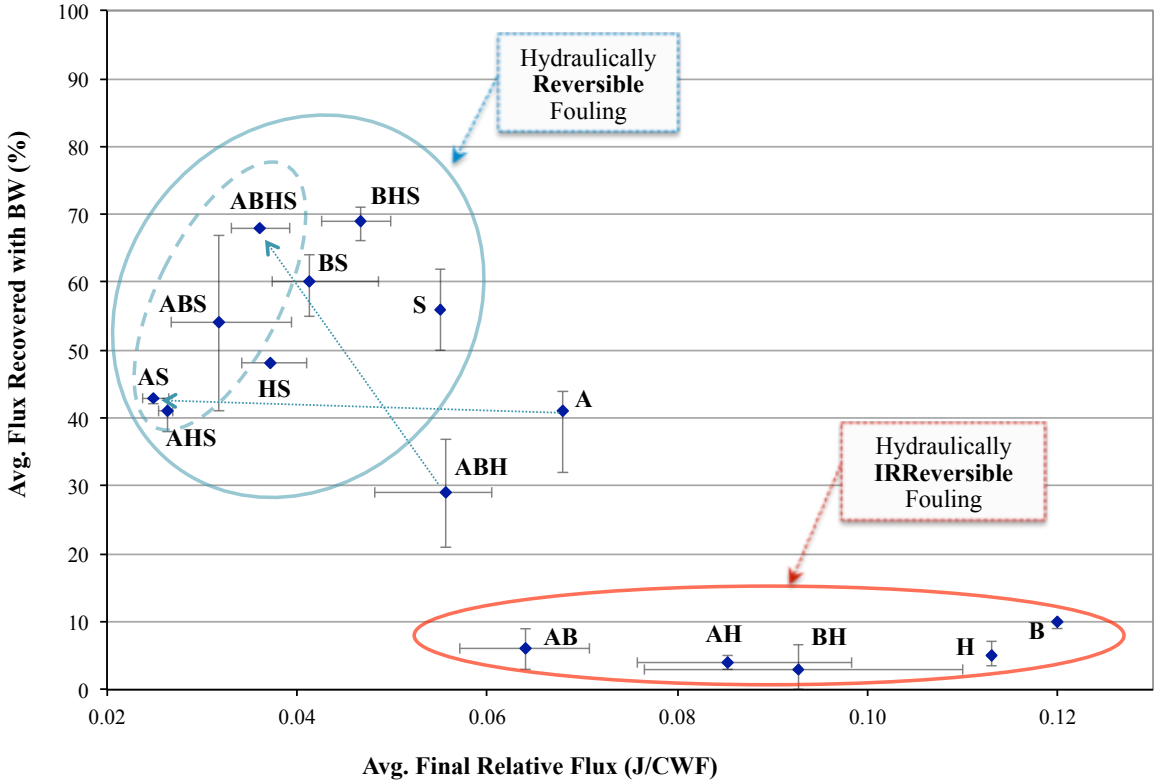

Figure 4.6: Average flux recovered with hydraulic backwash (BW) versus average final relative flux for all solutions at 40 psi.

Error bars indicate range of values for x-axis (n=3) and y-axis (n=2). A: Alginate; B: Bovine Serum Albumin; H: Humic acid; S: Silica; J: Flux, CWF: clean water flux.

Among the single solutions, the highest percentage flux recovery and therefore hydraulic reversibility was observed for silica despite its having the highest rate of fouling and lowest final relative flux. The lowest percentage flux recovery was with humic acid followed by BSA. Given that humic acid, BSA, or the two combined showed significant hydraulically irreversible fouling, the likely fouling mechanism for these substances is adsorption. Similarly, Peiris *et al.* (2010) identified colloidal/particulate substances as contributors to reversible fouling, whereas humic substances and protein-like matter were identified as contributors to irreversible fouling in a tight UF polymeric membrane.

Yuan and Zydney (1999) found that up to 80% of the clean water flux was recovered on a polymeric MF (nominal pore size 0.16 μm, polyethersulfone) membrane by wiping off the membrane surface with paper towels to remove the yellowish deposit left by humic acid. They concluded that the majority of fouling was thus located on the upper surface of the membrane as opposed to deeper in the pore structure. Although Yuan and Zydney's cleaning method differed from the current study, it can be assumed that a hydraulic backwash would at least partially remove the cake layer and recover some of the clean water flux. Since backwashing could not remove humic fouling in these experiments, it is unlikely that the majority of fouling is on the upper surface of the ceramic membrane; a result quite different from Yuan and Zydney (1999). Possible explanations are either strong bonding with the membrane or deep penetration into the pores. One hypothesis is that the high hydrophilic surface of the membrane decreases the strength of hydrophobic interactions and increases electrostatic repulsion between the membrane surface and humic acid, thereby discouraging the aggregation of the humic acid molecules on the membrane surface. However, at higher pressures the convective deposition is stronger and might outweigh the effect of the membrane surface–foulant interactions. This may explain why the rate of humic acid fouling increases dramatically with increasing filtration pressure (Figure 4.2). Therefore, despite lower rates of fouling associated with humic acid as discussed previously, humic acid fouling can lead to unsustainable operation as a result of high hydraulically irreversible fouling and thus a greater need for chemical cleaning.

Xiao *et al.* (2009) determined the affinity for a hydrophilically enhanced PVDF membrane as follows: humic acid > protein (BSA) > polysaccharide (dextran). This order is similar to the relative extent of hydraulically irreversible fouling caused by single model solution filtration discussed here.

Once the solutions were combined, the hydraulically irreversible fouling was similar to that observed for BSA and humic acid except when silica was present. Figure 4.6 illustrates the dramatic effect silica has on decreasing the hydraulically irreversible fouling, in which the results can be separated into two distinct clusters: hydraulically reversible and hydraulically irreversible fouling. If silica was not present, a maximum of 10% of the fouling was hydraulically reversible (except for alginate and the alginate/BSA/humic acid [ABH] combination). The lowest hydraulically irreversible fouling was observed either when all the model solutions were combined, or with BHS. The effect of alginate is more subtle (see dotted oval in Figure 4.6); the solutions with alginate are slightly shifted to the left, indicating decreased average final relative flux (i.e., higher total fouling). Although approximately

40% of the fouling with alginate alone was hydraulically reversible, this decreased significantly when combined with humic acid (4%) or with BSA (6%). Considering these results, it is interesting that the ABH combination is more similar to alginate than either humic acid or BSA. This indicates that the interactions between the foulants can be as important as the interactions between the foulants and the membrane surface. Although this finding may be intuitive and a few studies have also observed the importance of interactions between foulants for polymeric membranes (Jermann *et al.* 2007), it has not been specifically investigated. To quantify the relative importance of interactions between foulants compared with interactions with the membrane surface is an area that requires further work.

Overall, the addition of silica to any single solution or combination of solutions showed a dramatic increase in recovery, i.e., a decrease in hydraulically irreversible fouling. This was especially true when silica was added to humic acid or BSA and, in particular, the combination of both. Silica could possibly be inhibiting the ability of these components to interact and bond with the membrane surface. Therefore, silica consistently plays a positive role in creating a more backwashable foulant cake layer through interactions with the other model components.

In order to determine the compressibility of the different model foulants and the influence of pressure, the cake compressibility index was calculated from a log–log plot of specific cake resistance versus pressure (Eqs 4.4 and 4.5). From Figure 4.7, it can be seen that humic acid cake resistance is significantly affected by increasing pressure; changes in cake resistance with pressure indicate a compressible cake. The other three solutions show little to no variation in cake resistance between 20 and 40 psi, indicating that they do not form very compressible cakes and thus fouling is less affected by pressure. This is reflected in Figure 4.2, where the fouling trend for humic acid changes significantly, particularly between 20 and 30 psi. This may also partially be due to slower cake development at 30 and 40 psi for humic acid as seen in Figure 4.5. However, in most instances, cake filtration was instantaneous thus allowing for cake compressibility evaluation as outlined in 4.2.

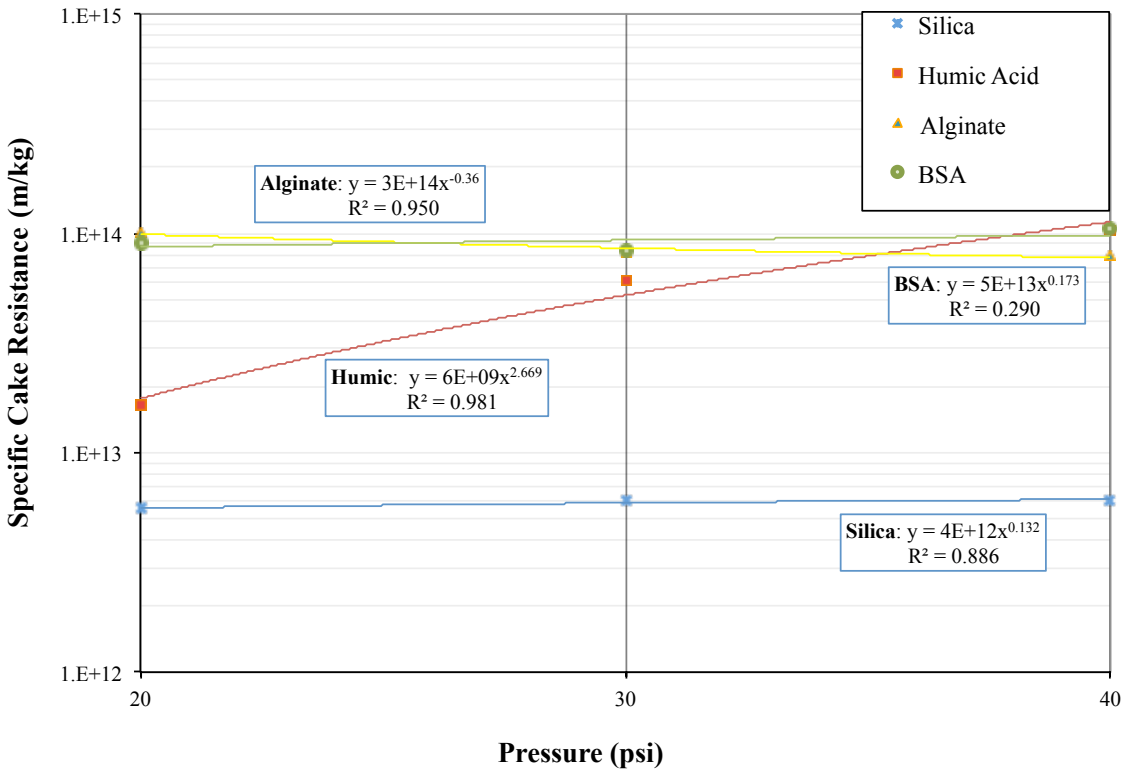

Figure 4.7: Log-log plot of specific cake resistance for single solutions at different pressures.

BSA: bovine serum albumin

Table 4.3 summarizes the cake compressibility index for the single solutions from Figure 4.7. For incompressible cakes, n is theoretically zero, and it increases with more compressible cakes. Constituents in solutions with a higher compressibility coefficient are more likely to have a wider size distribution, with the majority consisting of larger macromolecules or particles, which would be more susceptible to distortion at higher pressures (Boerlage *et al.* 2003). A wider molecular size distribution of humic acid compared with sodium alginate has been measured by others (Sioutopoulos *et al.* 2010; Katsoufidou *et al.* 2007; Katsoufidou *et al.* 2005). The results of the current study are confirmed by those of Sioutopoulos *et al.* (2010) who found that humic acid deposits are more compressible (n = 0.7) compared with alginate deposits (n = 0.4) with a polymeric UF membrane. The difference in the actual numerical value of n may be caused by the different membrane material

and/or the high concentration of total dissolved solids in the solutions used by Sioutopoulos *et al.* (2010). Furthermore, in the Sioutopoulos *et al.* (2010) study alginate fouling was also more severe than humic acid fouling; however, these authors did not distinguish between hydraulically reversible and irreversible fouling. Jermann *et al.* (2007) determined that despite the increased fouling occurring with alginate, it was to a large extent hydraulically reversible; this is also similar to the behavior observed in the experiments presented in this study and in later studies by Katsoufidou *et al*. (2008, 2010).

Table 4.3: Calculations of cake compressibility index (n) and the 95% confidence interval for single solutions

Model Foulant	*n*	R^2
Silica	0.13 ± 0.03	0.886
Humic Acid	2.7 ± 0.63	0.981
Alginate	-0.36 ± 0.16	0.950
Bovine Serum Albumin	0.17 ± 0.06	0.290

4.3.5 Chemically irreversible fouling

The fouled membranes were cleaned with three solutions, starting with NaOCl, followed by NaOH, and finally citric acid, following a procedure recommended by a manufacturer that uses ceramic membranes for drinking water treatment (Metawater) (see Section 4.2.1) To evaluate the effectiveness of each cleaning step and therefore the extent of chemically irreversible and reversible fouling, the CWF was measured for some of the experiments after each cleaning step. Not all solutions could be investigated because this is a time-intensive procedure. With one exception, chemically irreversible fouling was minimal. Only the AHS combination caused significant chemically irreversible fouling (greater than 15%, results not shown). However, the CWF and therefore membrane performance was fully recovered after an additional cleaning cycle. This demonstrates that for ceramic membranes, more thorough chemical cleaning can be used to eliminate chemically irreversible fouling. This option is usually not available for polymeric membranes because they are less resistant to chemical cleaning.

In terms of chemically reversible fouling, Figure 4.8 shows that the greatest improvement was generally seen following NaOCl addition. However, this may be due to the fact that it was the first cleaning agent used. Further work is required to assess various cleaning sequences.

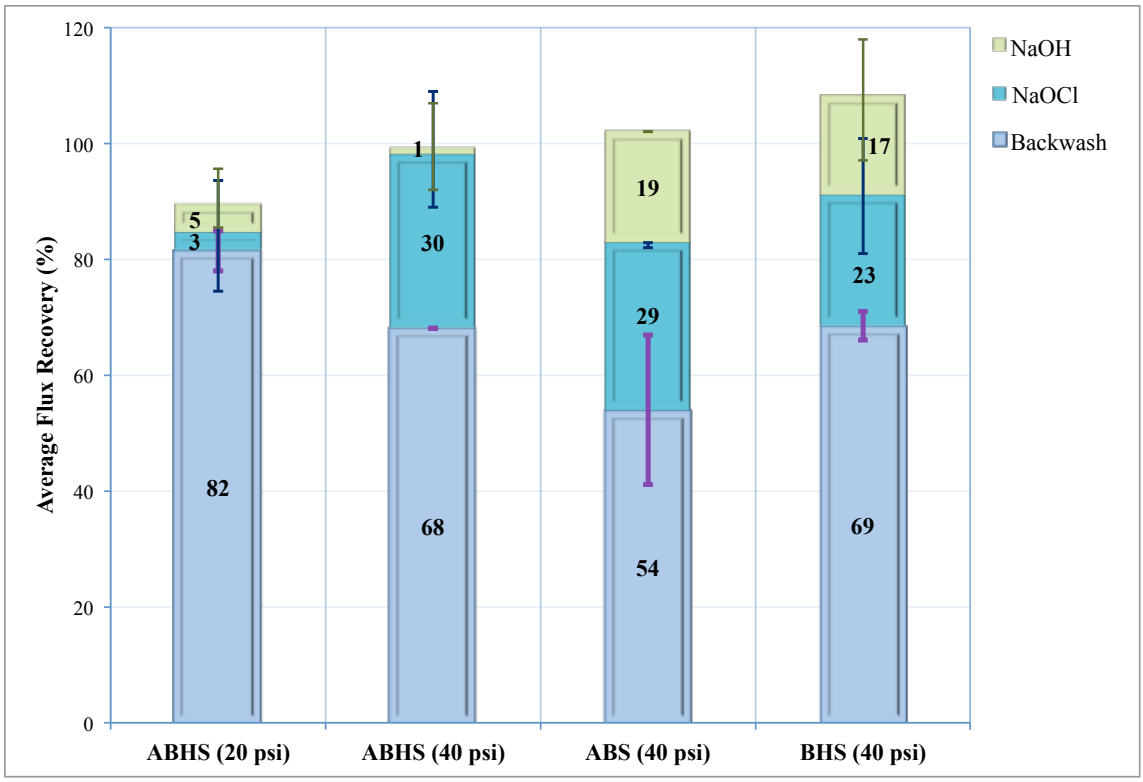

Figure 4.8: Average percent flux recovery (of clean water flux) after hydraulic backwash and after each consecutive cleaning step starting with sodium hypochlorite (NaOCl)

Error bars indicate range of values (n=3). A: Alginate; B: Bovine Serum Albumin; H: Humic acid; S: Silica

In terms of assessing any effect of filtration pressure, the cleaning efficiency for the solution with all model foulants was investigated at both 20 and 40 psi. The ABH and silica (ABHS) combination at 20 psi had the highest overall recovery with the hydraulic backwash (82% ±4), indicating that the majority of the overall clean water flux recovery could be achieved with backwashing alone. When the ABHS solution was filtered at 40 psi it had a relatively better flux recovery with NaOCl (average of 98% ±10) than when operated at 20 psi (average of 85% ±10). Also, the overall improvement in

the CWF for those solutions filtered at 20 psi only averaged around 90% (±2) compared with 99% (±4) at 40 psi.

Caustic (i.e., NaOH) is especially important for the removal of humic substances. It increases the repulsion between the negatively charged functional groups, which results in a stretched, linear configuration of NOM, thus loosening the fouling layer and enhancing the efficacy of cleaning (Hong and Elimelech. 1997). Nevertheless, the caustic cleaning step did not prove to be advantageous when humic acid was present; i.e., the net recovery with NaOH did not differ between the ABHS and BHS solutions. This could be a result specific to these experiments, particularly when taking into consideration that the flux recovery achieved by the previous hypochlorite cleaning step was already high.

The use of citric acid as a cleaning agent mainly targets the removal of scale, which is not an issue in the case of these experiments. Also, most, if not all, of the fouling was removed with the first two cleaning steps in these experiments, leaving little for the citric acid to do.

4.3.6 Contact angle/hydrophobicity

Contact angle measurements were carried out on both virgin and fouled membranes before and after backwash. Results reported in this article refer to the uppermost surface of a membrane and thus in the case of fouled membranes reflect the nature of the fouling layer rather than the membrane itself. The virgin membrane was very hydrophilic, with a contact angle of 22°. Detailed results comparing the contact angle before and after backwashing are not shown because, except for BHS, the alginate/humic acid combination (AH), and the alginate/BSA combination (AB), there were few differences. This may indicate that the composition of the foulant layer was largely unaffected by backwashing.

Results in Figure 4.9 show the contact angle of the backwashed membranes as a function of flux recovery following backwash. As is apparent from the contact angle values, BSA alone caused a dramatic increase in hydrophobicity (80°) compared with the virgin membrane contact angle of 22°. In contrast, the membrane remained hydrophilic when filtering single-solute solutions of alginate, silica, and humic acid, which resulted in contact angles of 28, 31, and 22°, respectively.

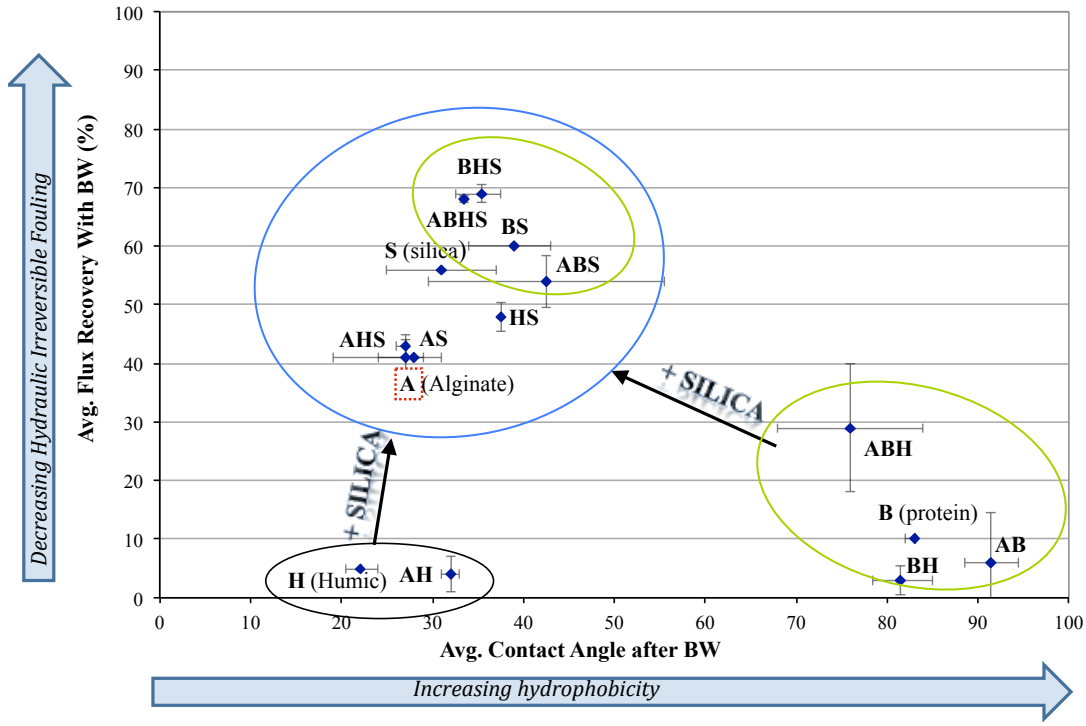

Figure 4.9: Average contact angle versus the average percent flux recovery following hydraulic backwash (BW) at 40 psi.

Error bars indicate range of values (n=2). A: Alginate; B: Bovine Serum Albumin; H: Humic acid; S: Silica

When combinations of model solutions are assessed, it is evident that all combinations with BSA had contact angles similar to BSA alone unless silica was present. In the latter cases, contact angles shifted to much lower values but were still higher than for the virgin membrane. Overall, once silica was added to any combination that included BSA, the contact angle was significantly decreased (to ~40°), thus maintaining a more hydrophilic surface.

When BSA was combined with humic acid (BH) and with alginate (AB), contact angles remained very hydrophobic, similar to BSA. For AB the contact angle increased from 71° before to 91° after backwash. This may be the result of the removal of alginate during the backwash cycle, thus indicating that alginate may have constituted the hydraulically reversible portion of the fouling layer.

Alternatively, when alginate was combined with humic acid, the contact angle of the fouled membrane before backwash was very hydrophobic (78°). This was unexpected because both alginate and humic acid alone maintain the hydrophilicity of the fouled membrane surface. Although this increase is largely rectified with a backwash (decreased to 32°), this does not translate into a more hydraulically reversible fouling layer compared with humic acid alone (only about 5% hydraulically reversible for both; Figure 4.9).

The results shown in Figure 4.9 can be roughly divided into three main groupings; a humic grouping with low contact angles and high hydraulically irreversible fouling, a BSA grouping with high contact angles and high hydraulically irreversible fouling, and a silica grouping with low contact angles and low hydraulically irreversible fouling. Additionally, there is a BSA subgroup within the silica grouping. Furthermore, alginate is the only single solution to fall within this silica grouping. This trend is somewhat similar to Figure 4.4, in which solutions containing silica are positioned closely and the remaining solutions are distributed much farther apart. The results clearly illustrate the dominating effect that silica has in combination solutions on the contact angle and on the flux recoveries.

Figure 4.9 shows that the hydrophobicity of the fouled membrane surface does not give an indication of the reversibility of fouling because humic acid and BSA both contributed to hydraulically irreversible fouling despite having drastically different contact angles. This trend can be further extended to chemically irreversible fouling, which was significant for the most hydrophilic fouled surface (AHS). Therefore, although hydrophilic membranes have been linked to lower rates of fouling (Aoustin *et al.* 2001), a fouled hydrophilic surface is not a reliable reflection of the severity of fouling.

Since BSA is the only foulant resulting in a highly hydrophobic fouled membrane surface, the contact angle of a fouled membrane could provide some indication of the composition of the fouling layer. For AB, BH, ABH, and B, the high contact angles of the backwashed membranes suggest a significant proportion of BSA in the foulant layer. However, once silica is present, the contact angle is lower, suggesting that BSA is a smaller component of the fouling layer or perhaps a patchy foulant layer where some of the membrane surface is not fully covered.

Overall, the addition of silica had a favorable effect on maintaining a hydrophilic membrane surface; as mentioned previously, hydrophilic membrane surfaces have been linked to lower rates of fouling in the literature (Aoustin *et al.* 2001). Possible reasons that silica decreases hydraulically irreversible fouling while still maintaining a hydrophilic membrane surface may be the result of a rapid cake layer formation (as discussed previously), thus minimizing the ability of BSA and/or humic acid to adsorb on the membrane surface or plug the pores, or a preferential adsorption onto silica. Also, backwashing rarely had a significant effect on altering the contact angle of the fouled membranes. In most cases, however, if the backwash could recover a minimum of 40% of the flux, the contact angle would likely be no more than 40°.

4.4 Conclusions

In this investigation, model solutions were used to determine foulants of concern for a bench-scale UF ceramic membrane. The solutions of BSA, alginate, humic acid, and silica were used individually and in combinations to simulate likely foulants in a drinking water treatment setting. The main conclusions follow.

- Synergistic fouling effects were observed when model foulants were combined.
- Colloidal silica was the most influential factor governing fouling behavior.
  - Colloidal silica dramatically increased the overall fouling rate, but it enhanced the effectiveness of a hydraulic backwash by making the foulant layer more hydraulically reversible.
  - Foulant layers containing colloidal silica remained relatively hydrophilic, even in the presence of BSA, which was the only solution that greatly increased the hydrophobicity of the membrane
- Despite having lower rates of overall fouling, humic acid and BSA contributed the most to hydraulically irreversible fouling. Since the molecular weight of both substances is lower than the MWCO of the membrane, their removal mechanism is postulated to be largely through adsorption.
- All single solutions and combinations showed fouling by cake layer filtration—except for humic acid alone and humic acid combined with BSA—their fouling mechanism was intermediate and complete pore-blocking filtration, respectively.

- A hydrophilic membrane surface after fouling is not necessarily a reflection of the extent or reversibility of fouling, because humic acid and BSA-fouled membranes had substantially different contact angles, although their fouling behavior was similar.
- Hydraulic backwashing had a negligible effect on the contact angle of the fouled membrane.
- Alginate did not have a discernable influence on the fouling behavior when combined with the other model foulants.

Since hydraulically irreversible fouling is the main concern in full-scale operations, implementing pretreatment strategies that target irreversible foulants having characteristics similar to BSA and humic acid will enhance operational sustainability and allow for more effective and long-term foulant removal. Maintenance cleaning frequency as well as off-line chemical cleaning frequency could potentially be reduced, thus reducing chemical cost and loss of production. However, a more comprehensive investigation of fouling behavior, including work with real waters, is needed to gain a better understanding of the interactions between the different constituents of the feedwater and the membrane surface.

Chapter 5
Stage 3: Fouling Behavior of Tubular Ceramic Ultrafiltration Membranes Using Model Solutions

A version of this chapter was submitted to Water Research for review in May 2013. Cited references are in the consolidated list of references at the end of the thesis.

This chapter/article discusses the results of model solution fouling behavior obtained with a tubular ceramic ultrafiltration membrane.

Summary

This study investigated the fouling behavior of a tubular ceramic membrane using model solutions representative of foulants problematic in drinking water treatment. Organic and inorganic model foulants were filtered alone and in mixtures through a tubular ceramic ultrafiltration membrane at constant flux including backwashing. The results of the current study were also compared to a previous study using the same model foulants and membrane material but with a flat-sheet configuration operated at constant pressure and a hydraulic backwash. Overall, the main qualitative conclusions drawn from the previous studies held true; both bovine serum albumin and humic acid showed high hydraulically irreversible fouling, while silica alone and in mixtures had significantly less hydraulically irreversible fouling. Furthermore, the combination of all model foulants, alginate, bovine serum albumin, humic acid, and silica had very high overall fouling rates with high contributions from hydraulically reversible fouling and fairly low hydraulically irreversible fouling. This indicates that flat-sheet studies, which included a backwash, could be used meaningfully to study the fouling behavior of a tubular ceramic membrane, which is extremely difficult to perform surface characterization analysis on. Fouling mitigation techniques were also investigated to determine their applicability as an alternative approach to a full chemical cleaning.

5.1 Introduction

Polymeric membranes have become an accepted technology for drinking water treatment. Ceramic membranes, however, have thus far been largely limited to industrial applications that require the filtration of more difficult water qualities. In these cases, the physical and chemical robustness of ceramic membranes is necessary and worth the higher membrane capital costs. The unique properties of ceramic membranes allow for higher pressures (both in filtration and backwashing) and higher chemical concentrations to be used, which contribute to their longer lifetimes over polymeric membranes (Fakhfakh *et al.* 2010; Harmann *et al.* 2010). A recent study (Guerra and Pellegrino 2012) has attempted to compare costs of operating ceramic versus polymeric membranes for drinking water treatment and has shown that they are now beginning to be considered as a viable alternative to polymeric membranes. Therefore, selecting an appropriate membrane will ultimately be case specific and dependent on the source water quality and, if applicable, other treatment processes already in place. Consequently, a strong understanding of which foulants are of concern and the extent of their fouling on a specific membrane is crucial to selecting a case-appropriate membrane.

Model solutions are often used for controlled and simplified fouling studies to gather information on fundamental fouling behavior associated with a particular membrane and to identify the foulants of concern. While the objective of fundamental fouling studies may not always be intended to predict full-scale treatment behavior, there are a few key points that should be considered to maximize the potential applicability of fouling study results. For example, many studies focus on only one model foulant and do not consider combinations of model solutions. Research findings have shown that inorganic colloids influence fouling behavior through natural organic matter (NOM) interaction. Studies conducted by Jermann *et al.* (2008a and 2008b) showed that the presence of inorganic particles could play a significant role on the extent and reversibility of fouling. Another common limitation in fouling studies is the lack of a backwash component thereby not distinguishing between hydraulically reversible and irreversible fouling. While any fouling is undesirable in membrane filtration, the extent of hydraulically irreversible fouling is the most crucial. For these reasons it is vital that the fouling study design include backwashing as well as combinations of model foulants in order to represent full-scale operating conditions as closely as possible.

Some studies with ceramic membranes have investigated total organic carbon (TOC) removal (Bottino *et al.* 2001; de la Rubia *et al.* 2006; Loi-Brugger *et al.* 2006). Konieczny *et al.* (2006)

reported 100% TOC removal of synthetic humic acid using two microfiltration (0.1 and 0.2 μm) ceramic membranes (active layer of zirconium dioxide/titanium dioxide). Such unexpectedly high removals for a microfiltration membrane clearly indicate the need for further examination into the fouling behavior of ceramic membranes.

In many cases when fouling behavior is investigated using model solutions, flat-sheet membranes operating at constant pressure are employed, which are conditions that are quite different than full-scale drinking water treatment practices. Therefore, it is important to establish the extent to which flat-sheet study results can be used to predict fouling behavior under conditions more similar to full-scale operation.

The objective of this study was to determine the fouling behavior of a tubular ceramic membrane with organic and inorganic model foulants previously identified as problematic in drinking water membrane filtration; they were studied alone and in mixtures at constant flux. Additionally, the results of this study were compared to a previous study using flat-sheet ceramic membranes of the same material and constant pressure filtration. Furthermore, fouling control measures such as a single backwash, multiple backwashes and a chemical maintenance cleaning were investigated.

5.2 Materials and methods

5.2.1 Ceramic membrane properties and operation

The membrane used was a tubular ceramic membrane (TAMI Industries, France) consisting of 3 channels with a length of 25 cm, a molecular weight cut-off (MWCO) of 300 kDa and a surface area of 0.0094 m^2. The support layer is pure titanium dioxide while the active layer is composed of a mixture of titanium dioxide and zirconium dioxide. The maximum operating pressure is 10 bar (145 psi). Surface properties of the same membrane but a flat-sheet configuration were assessed in a previous study (Munla *et al.* 2012) and determined a virgin contact angle of 22° ± 0.5 and an average roughness of 50 nm ± 8. The same tubular membrane module was used for all experiments with a chemical cleaning performed between each experiment followed by a clean water permeability

(CWP) test to confirm the complete effectiveness of the cleaning procedure. The schematic of the membrane setup is shown in Figure 5.1.

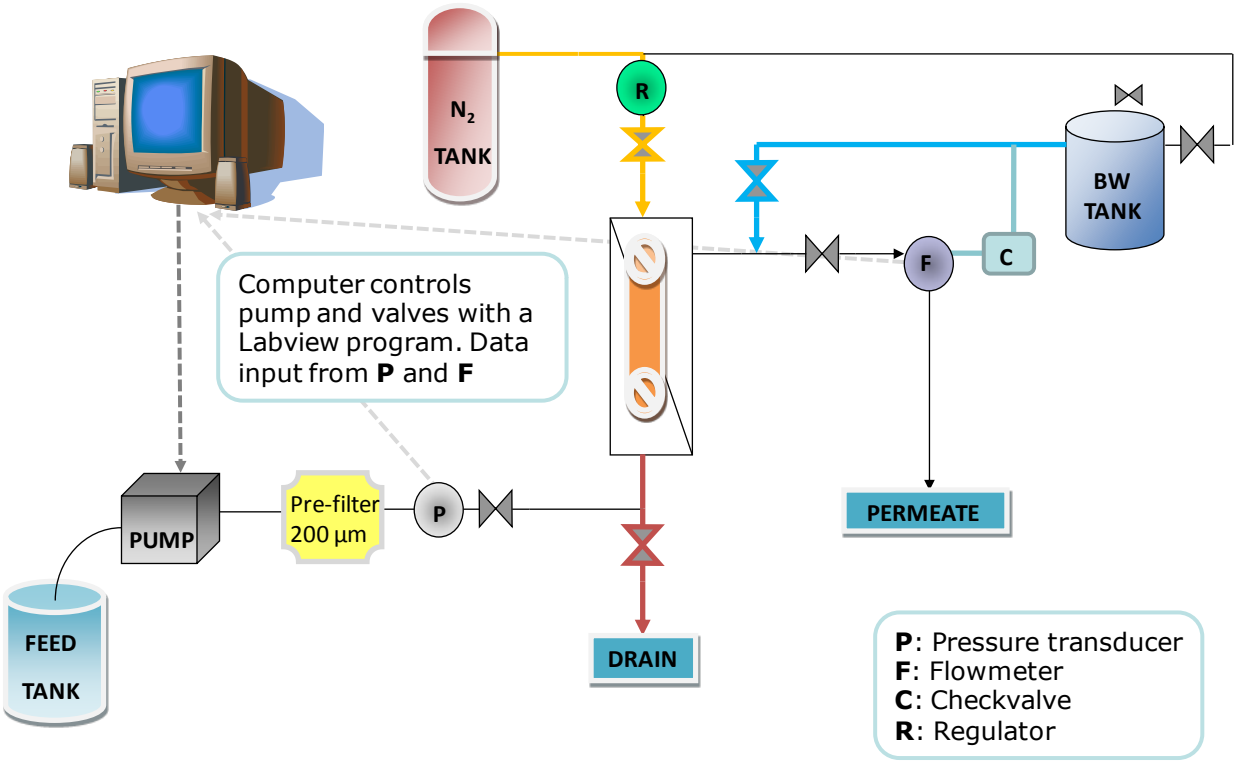

Figure 5.1: Schematic of tubular ceramic membrane setup at constant flux

This setup was optimized using natural water experiments and this set of experiments was performed after the experiments in Chapter 6.

The membrane was operated at a constant flux of 120 LMH for 2 hours consisting of four 30-minute filtration cycles in a dead end mode. The permeate was collected during each cycle and used for dissolved organic carbon (DOC) analysis. Each filtration cycle was followed by a backwash procedure, which consisted of a hydraulic pulse at 70 psi with ultrapure water for 15 seconds followed by an air flush at 30 psi for 5 seconds. After the fourth cycle of filtration was complete, a series of 6 backwash cycles (6-BW sequence) was performed, followed by a CWP test. Then a

maintenance clean using 1500 mg/L of NaOCl (half the concentration typically used during a regular full chemical cleaning) for 15 minutes was performed, which was also followed by a CWP test. These fouling mitigation techniques were not investigated in earlier studies using flat-sheet membranes (Chapter 4).

The chemical cleaning procedure was similar to that employed for ceramic membranes manufactured by Metawater (previously NGK). The cleaning method consisted of sodium hypochlorite (3000 mg/L), followed by NaOH (0.1M), and ending with citric acid (1%), each with a soak time of 5 hours. The membrane module was rinsed between each cleaning step with ultrapure water. The cleaning method suggested by the manufacturer, TAMI, was not used due to its drastic nature (high concentrations of basic and acidic chemicals at high temperatures), which is not practical or necessary in a drinking water treatment facility.

5.2.2 Water quality analysis techniques

Liquid Chromatography Organic Carbon Detection (LC-OCD) was used to qualitatively assess the composition of the permeates and backwash water when the model solutions were combined in order to differentiate between the various organic fractions. The LC-OCD instrument (DOC-Labor Dr. Huber, Karlsruhe, Germany) uses a size exclusion column (Toyopearl TSK HW-50S) with a fractionation range of 100-200,000 Da (Meylan *et al.* 2007). A phosphate buffer (0.02 M, pH 6.5) is used as the mobile phase. The sample is filtered through a 0.45 μm filter to remove particulates. The remaining DOC is then separated into five groups by chromatography according to their molecular size and subsequently detected by DOC and UV_{254} measurements: biopolymers (includes polysaccharides, polypeptides, proteins, organic colloids, and amino sugars), humic substances (humic and fulvic acids), building blocks (hydrolysates of humics), low molecular weight acids and neutrals (e.g. alcohols, aldehydes, ketones, and amino acids) (Cornelissen *et al.* 2008; Laabs *et al*. 2006). Since smaller molecular size substances have more access to the internal pore volume of the column, the larger molecules will elute first followed by the smaller compounds (Batsch *et al.* 2005). An inherent advantage with LC-OCD analysis is that it is not time consuming and does not require extensive sample preparation that could potentially alter the NOM characteristics.

The total and dissolved organic matter (TOC and DOC, respectively) were measured using the OI-Analytical TOC analyzer (Model 1010, College Station, TX). The analysis follows the wet-oxidation method outlined in Standard methods (2005). DOC samples were filtered through a 0.45 μm polyethersulfone filter prior to analysis.

5.2.3 Model foulant properties

The model substances investigated were a protein (bovine serum albumin [B], 5 mg/L), a polysaccharide (sodium alginate [A], 5 mg/L), a NOM fraction (Aldrich humic acid [H], 5 mg/L), and an inorganic colloid (silica [S], 200 mg/L). All model substance properties were obtained from Sigma Aldrich and are summarized in Table 5.1. The pH of all solutions was between 6-7.

Table 5.1: Model foulant properties

Model Substance	Foulant Type	Average Molecular Weight (kDa)	Carbon Content (%)
Bovine Serum Albumin (B)	Protein	67 [a]	0.46 [a] 0.47 [b]
Humic Acid (H)	NOM fraction	70 [a]	0.31 [a] 0.4 [b]
Sodium Alginate (A)	Polysaccharide	30 – 100	0.29 [b]
Silica (S)	Inorganic	~ 9 nm average hydrodynamic size [c]	NA

NA—not applicable
[a] Xiao *et al.* (2009)
[b] Measured
[c] From manufacturer Sigma Aldrich

5.2.4 Mass balance

A mass balance was performed for the different organic single model foulant solutions. A diagram of where the samples were taken is shown in Figure 5.2. Samples were taken from the feed, the permeate, the feed channel, and the backwash water once every cycle during the first 4 cycles of filtration. Samples were weighed to determine total volume and then analyzed with the LC-OCD to

calculate the mass. The feed channel water (i.e. retentate) was taken separately in order to determine the mass that was rejected but did not contribute to reversible or irreversible fouling. Mass balances were only performed on single solutions because the different organic foulants cannot be differentiated with TOC or LC-OCD (the peaks are not completely separated) analysis.

The mass balance was established as follows:

$$m_{feed}\,(1) = m_{perm}\,(2) + m_{adsorb,\,REV}\,(3) + m_{adsorb,\,IRR}\,(4) + m_{retentate}\,(5) \qquad \textbf{Equation 5.1}$$

where, the $m_{retentate}$ is the mass which is rejected and not reversibly or irreversibly adsorbed to the membrane and hence is not considered as contributing to fouling. All concentrations except for $m_{adsorb,IRREV}$ were independently measured and subsequently converted to mass.

The mass that is irreversibly fouled is calculated using:

$$m_{adsorb,\,IRR} = m_{feed} - m_{perm} - m_{adsorb,\,REV} - m_{retentate} \qquad \textbf{Equation 5.2}$$

The feed mass reflects 100% of the mass entering the system and was used as the basis to calculate the percentages of the other fractions accordingly. For example:

$$mass_{retentate} = \frac{mass_{retentate}}{mass_{feed}}\ x\ 100 \qquad \textbf{Equation 5.3}$$

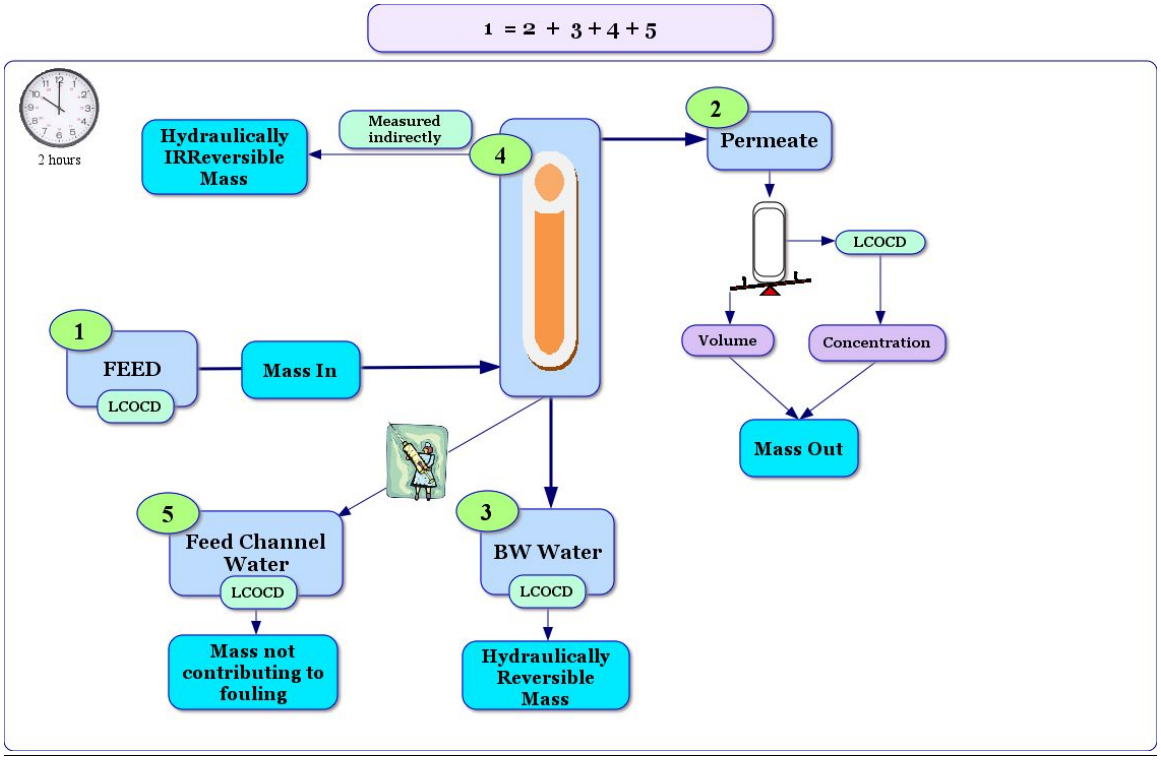

Figure 5.2: Diagram depicting the sample locations taken for the mass balance

5.3 Results

5.3.1 Fouling rates

Four different model compounds were chosen to represent problematic foulants identified for polymeric membranes in drinking water. The most common model substance used is humic acid, generally Aldrich, which is not ideal since it is soil-based but it is cheaper than Suwannee River humic acid, which is aquatic-based and more representative of humics that are likely present in surface waters. Alginate is also popularly used to represent a polysaccharide, especially to model extra polymeric substances (EPS), which is more typically an issue for wastewater treatment. Bovine serum albumin is also commonly used and cheap, and thus often used to represent proteins in water. These model foulants are discussed in more detail in Section 4.2.2.

The results obtained from the previous flat-sheet study using the same model solutions (Chapter 4) were compared to this study. Since both flat-sheet and tubular membranes were made from the same material with the same molecular weight cut-off and from the same manufacturer, it is likely that any variation in the type of fouling observed is primarily due to differences in the hydrodynamic conditions arising from a different membrane configuration and operating mode.

Single solutions of each foulant, the combination of all the organic model foulants, and the combination of all the model foulants including the inorganic colloidal silica were investigated at constant flux. Unlike the flat-sheet study, not all possible model foulant combinations were investigated with the tubular configuration due to time constraints. Initially, the single solutions were operated at a constant flux of 64 LMH, however, minimal fouling was observed for all solutions except for bovine serum albumin (Appendix C Figure 1). Therefore, the solutions were subsequently filtered but at a higher flux of 120 LMH in order to create sufficient fouling that could allow for proper fouling behavior analysis. Additionally, the resulting transmembrane pressures of 10 to 70 psi observed at a flux of 120 LMH for the tubular membrane were in a similar range of the pressures applied in the flat-sheet study (20 to 40 psi).

Throughout the filtration cycle both hydraulically reversible and irreversible fouling occurs. Once a backwash is performed, the portion of fouling that is irreversible can be determined by the starting TMP of the next cycle (Figure 5.3). The following discussion examines the fouling trends for the hydraulically reversible (backwashable) and hydraulically irreversible (non- backwashable) foulants encountered with the different model solutions.

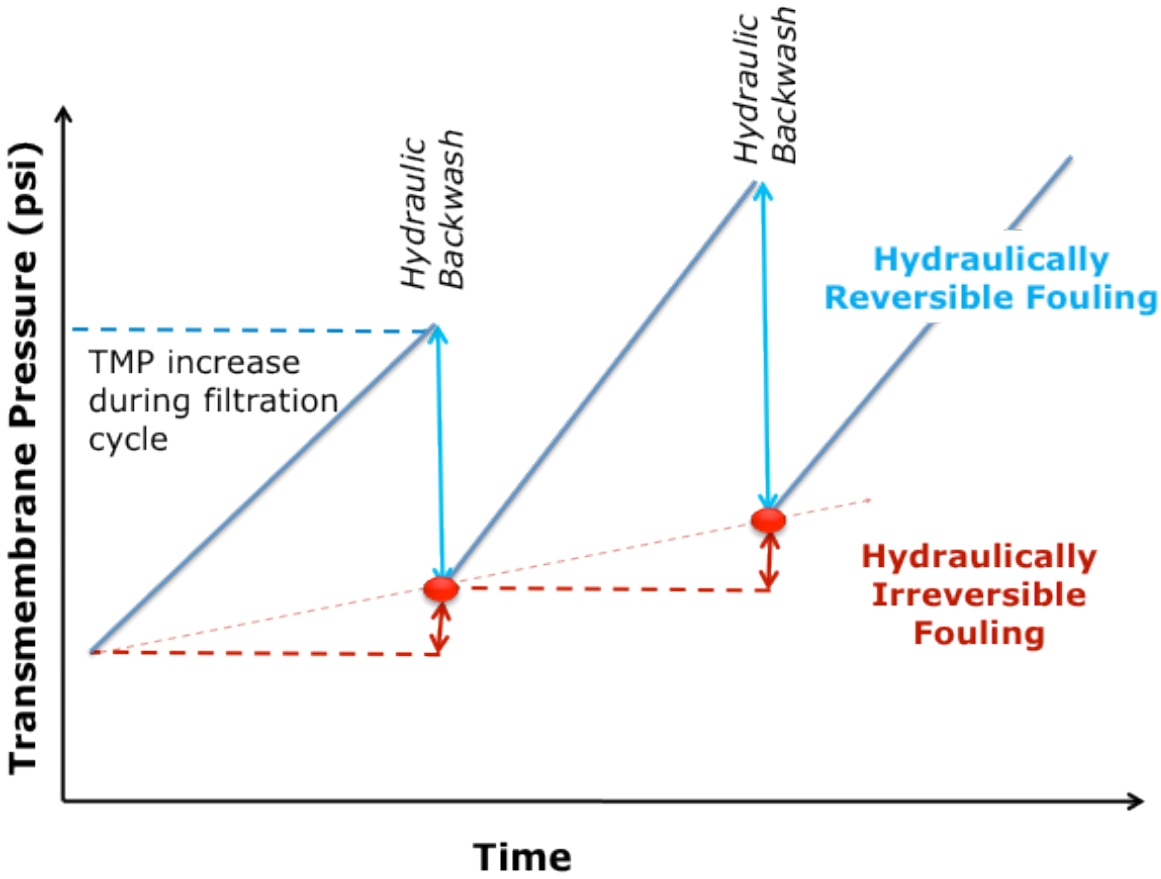

Figure 5.3: An illustration of how reversible and irreversible fouling is calculated.

5.3.1.1 Hydraulically irreversible fouling rates

The TMP increase in Figure 5.4, shows that bovine serum albumin resulted in a high rate of fouling over the four cycles investigated, most of which was hydraulically irreversible. The rate of hydraulically irreversible fouling increased with each cycle (from 8 then to 14 and then to 16 psi/cycle), while the rate of hydraulically reversible fouling ranged from 0 to 6 psi/cycle (Figure 5.5). In this case, the rate of hydraulically reversible fouling increased when the rate of hydraulically irreversible fouling increased. However, this was not the case for humic acid, which was the only other solution that exhibited increasing rates of hydraulically irreversible fouling albeit at a much slower rate than bovine serum albumin (from 0.2 to 0.6 to 1.4 psi/cycle). For the other single solutions, alginate and silica, the rate of hydraulically irreversible fouling was very low with values at or below 1 psi/cycle.

These results are similar to the flat-sheet study, where humic acid and bovine serum albumin contributed mostly to hydraulically irreversible fouling, while silica and alginate contributed mostly to hydraulically reversible fouling.

For the mixtures, the rates of hydraulically irreversible fouling were less than 1 psi/cycle with ABH, which had only a slightly higher fouling rate than ABHS. These results clearly point to a synergistic effect in that the irreversible fouling rates were not additive. On the contrary in the presence of other constituents bovine serum albumin's contribution to irreversible fouling seemed to be largely mitigated.

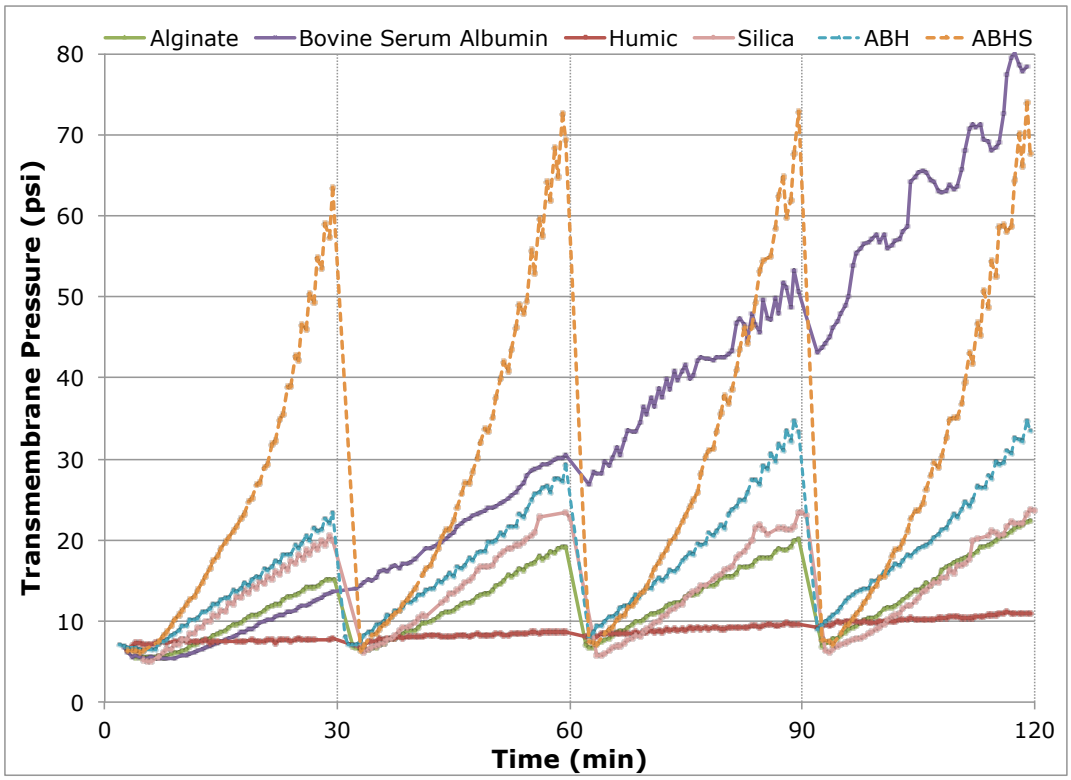

Figure 5.4: TMP profiles for the model solutions run through a tubular ceramic membrane at a constant flux of 120 LMH.

A backwash was performed every 30 minutes and is indicated by a dashed line. ABH: Alginate, Bovine Serum Albumin, and Humic Acid mixture; ABHS: Alginate, Bovine Serum Albumin, and Humic Acid and Silica mixture.

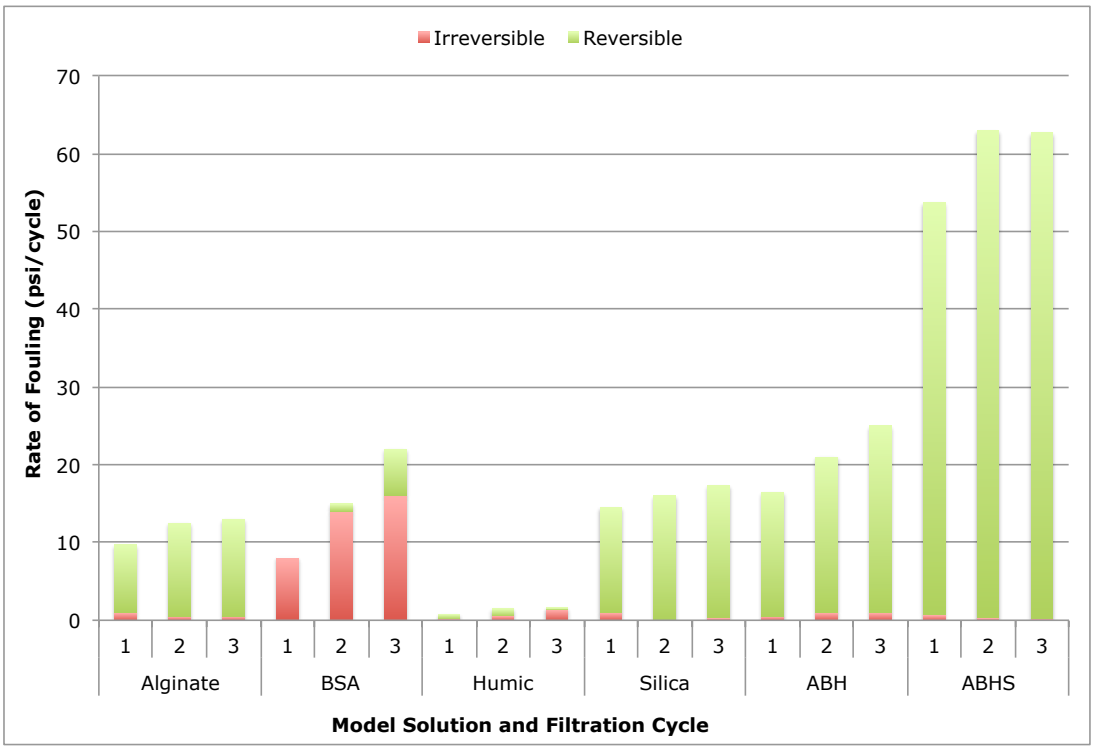

Figure 5.5: The rate of hydraulically reversible and irreversible fouling for each model solution over three cycles.

BSA: Bovine Serum Albumin; ABH: Alginate, Bovine Serum Albumin, and Humic Acid mixture; ABHS: Alginate, Bovine Serum Albumin, and Humic Acid and Silica mixture.

5.3.1.2 Hydraulically reversible fouling rates

For most solutions the majority of fouling occurring throughout each cycle was hydraulically reversible (Figure 5.5). During the first cycle, colloidal silica had the highest rate of hydraulically reversible fouling of all the single model foulant solutions. Nevertheless, the rate of hydraulically reversible fouling for silica only slightly increased (14 to 17 psi/cycle), indicating that once an initial foulant layer had formed subsequent fouling was reversible. The colloidal silica results observed in the current study differ from Jermann *et al.* (2008a and 2008b) who reported that kaolinite had a very low flux decline with a polyethersulfone 100 kDa flat-sheet membrane (hydrophobic). Since the MWCO of the membranes are on the same order of magnitude as in these experiments, possible explanations for this variation in results could be either due to the difference in membrane material

(i.e. more hydrophobic polymeric membrane vs. hydrophilic ceramic membrane), the size of the kaolinite (450 nm) compared to the size of silica (9 nm) used in the current study, or the difference in chemical composition of the kaolinite which is also partially an aluminum oxide. The size of the silica colloid chosen in this study was intended to induce fouling since this size range (3-20 nm) has been identified by Howe and Clark (2002) as a major foulant for natural colloids. It is similar in size to the pore size of the studied membrane, and this similarity in pore size has been identified as a contributing factor for polymeric membrane fouling.

Alginate displayed similar behavior to silica (Figure 5.4 and Figure 5.5) but with slightly lower rates of hydraulically reversible (9 to 12.5 psi/cycle) and slightly higher rates of hydraulically irreversible fouling, which ultimately resulted in an almost identical overall fouling trend compared to silica by the fourth cycle (Figure 5.4). It is likely that the overall fouling rate of alginate would eventually exceed that of silica. Similar behavior was observed with the flat-sheet membranes in which alginate fouling was initially slower than some of the other model foulants but continued at a slow and steady rate even after the membrane had reached a pseudo steady state of fouling for the other foulants (Munla *et al.* 2012).

The overall rate of humic acid fouling was very low in comparison to the other solutions (Figure 5.4). The rate of hydraulically reversible fouling remained at less than 1 psi/cycle but hydraulically irreversible fouling increased steadily at a low rate. Considering that the TMP only slightly increased to just above 10 psi even at the higher flux of 120 LMH, this behavior is quite similar to the humic acid behavior observed for the flat-sheet membranes at a constant pressure filtration at 20 psi (Figure 4.2 part a). With the tubular membranes, the humic acid flux decline curve had an almost linear shallow slope as opposed to the typical curved shape observed for the other model solutions (Figure 5.4). With the flat-sheet membrane study, humic acid fouling resembled the other model foulants at higher pressures (Figure 4.2 part c). Therefore, the fouling rate (i.e. change in TMP) would be expected to increase at higher fluxes for the tubular ceramic membrane. Furthermore, it may be concluded that the probable fouling mechanism of humic acid for this tubular ceramic membrane is likely the same as for the flat-sheet membranes, which was postulated to be largely through adsorption (Munla *et al.* 2012). These results are analogous to those by Jermann *et al*. (2007) and

Katsoufidou *et al.* (2008, 2010) in which humic acid had a gradual flux decline for polymeric membranes with a comparable MWCO and at pressures similar to this ceramic membrane study. Both investigators also similarly observed higher fouling rates with alginate than humic acid.

The model solution combinations investigated were mixtures of all organic model foulants (ABH) and the mixture of all the model foulants, both organic and inorganic (ABHS). The initial rate of hydraulically reversible fouling observed with ABH (16 psi/cycle) was higher than for any of the individual solutions (13.5 psi/cycle), but similar to alginate, the rate of ABH reversible and irreversible fouling increased with each cycle (up to 24 psi/cycle) (Figure 5.5). It can therefore be expected that over time, ABH fouling would continue to increase with each subsequent cycle. The rate of fouling increased dramatically once silica was included in the mixture (ABHS in Figure 5.4 and Figure 5.5); however, this was largely hydraulically reversible fouling with only minimal contribution from hydraulically irreversible fouling. Although there was a small increase in the rate of hydraulically reversible fouling between cycle 1 and 2 (from 53 to 63 psi/cycle), there was no increase in the rate of reversible fouling in subsequent cycles. These results are similar to the behavior of silica alone where the majority of the irreversible fouling has occurred in the first cycle. Thus, silica seems to influence the fouling behavior by increasing the reversible fouling rates but decreasing the irreversible fouling rates. Therefore, it is anticipated that despite the high rate of fouling observed in each cycle, that ABHS filtration is more sustainable at a constant flux of 120 LMH, unlike bovine serum albumin, alginate or the ABH combination.

Fouling was not additive in the case of these tubular membrane experiments since bovine serum albumin fouling alone reaches a similar TMP compared to the ABHS combination. However, the irreversible fouling was quite different for these two solutions (i.e. B alone and ABHS combination), which suggests that bovine serum albumin interacts with silica. Therefore, these results as well as those from the previous flat-sheet study (Munla *et al*. 2012) further highlight the need for more focused research on the foulant-foulant interactions as opposed to individual foulant-membrane interactions. Other studies have also observed interesting results that begin to highlight the importance of foulant-foulant interactions (Jermann *et al.* 2007, 2008a, 2008b; Katsoufidou *et al.* 2005, 2007, 2008, 2010). Such research is especially important since the properties of the membrane

surface will change at the onset of fouling and most likely will never fully return to its original surface characteristics.

Table 5.2 qualitatively summarizes the rate of fouling and hydraulic reversibility for the solutions in both the tubular and flat-sheet studies. With a few exceptions, the results are quite similar. The two main unexpected results observed in the tubular, constant flux experiments are the rapid rate of fouling with bovine serum albumin and the high hydraulic reversibility of ABH. Considering this outcome, it can be concluded that the flat-sheet experiments operated at constant pressure including a backwash, provided good qualitative data regarding fouling behavior that can be extrapolated to tubular membranes operating at constant flux with respect to the rate of fouling and hydraulic reversibility. These results are promising, however, further work using different membrane materials would need to be performed to verify this conclusion.

Comparing results obtained with the tubular membrane and the previous flat-sheet study (Munla *et al.* 2012) the following key observations can be made:

- Colloidal silica fouling behavior was similar for both membrane configurations.
- Humic acid caused the lowest overall rate of fouling for both membrane configurations, particularly at lower pressures.
- Bovine serum albumin and alginate had similar overall fouling rates in the flat-sheet membranes study, and also in the first cycle of the tubular membrane study. Since a backwash was performed for the flat-sheet membranes, it was evident (and confirmed by the tubular membranes) that fouling with bovine serum albumin was largely hydraulically irreversible, whereas alginate fouling was mostly hydraulically reversible. Based on the flat-sheet results, very different fouling trends were expected for these two foulants, which was then confirmed by the tubular membrane results.
- The inclusion of a backwash procedure in the previous flat-sheet study was crucial in minimizing the limitation of that study, and thus was still able to give important information and highlight bovine serum albumin as a problematic foulant, which was confirmed by this study using a tubular membrane.

- ABH is also similar in fouling rate for both the flat-sheet (at 40 psi) and tubular configuration.
- ABHS had the highest fouling rate in both configurations, which could indicate that foulant-foulant interactions may be less affected by the different membrane configurations and operating procedures than expected. Furthermore, it may indicate that these foulant-foulant interactions are one of the most important and critical factors governing fouling behavior.

Overall, the results are promising because they show consistency between the two different configurations (i.e. tubular vs. flat-sheet) and different operating conditions (i.e. constant flux vs. constant pressure). Qualitatively, the results observed in the previous flat-sheet study with the same model foulants can be extrapolated; for example, the effect of silica on the rate of fouling and reversibility of fouling is confirmed in this tubular study. Therefore, simplified fouling studies can be useful in establishing fundamental fouling knowledge for a particular membrane if a hydraulic backwash is included in the study. Nevertheless, experimental conditions that most closely resemble full-scale operation are always preferred.

Table 5.2: A summary of the qualitative extent of the fouling rate and hydraulic reversibility with model solutions for both flat-sheet and tubular membranes

	Rate of Fouling						Hydraulic Reversibility					
	A	**B**	**H**	**S**	**ABH**	**ABHS**	**A**	**B**	**H**	**S**	**ABH**	**ABHS**
Tubular	M	M-H to H	L	M-H	M-H	H	M	L	L	H	H	H
Flat	M	L	L	M-H	M-H	H	M	L	L	H	M	H

H: high; M: medium; L: low; A: Alginate; B: Bovine Serum Albumin; H: Humic acid; S: Silica
Red indicates where the results between flat-sheet and tubular qualitatively deviated from each other

Criteria for grouping into H, M, L

	Tubular				Flat-Sheet			
	L	**M**	**M-H**	**H**	**L**	**M**	**M-H**	**H**
Rate of Fouling (psi/cycle or final relative flux)	0-5	5-15	15-25	>25	0.1<	0.06-0.1	0.04-0.06	<0.04
Hydraulic Reversibility (%CWP)*	<50	50-75	75-90	>90	0-10	11-30	30-50	>50

* Discussed in Section 5.3.2.1
CWP: Clean Water Permeability

5.3.2 Fouling control

5.3.2.1 Hydraulic backwash

A hydraulic backwash is essential for sustainable membrane operation at any full-scale treatment plant and is thus an important parameter to incorporate into any fouling study that evaluates potential fouling behavior. In the current study, a hydraulic backwash was performed after each 30 minute filtration cycle for a total of four cycles. The results obtained with a hydraulic backwash are consistent with the results of the fouling rate analysis (Section 5.3.1).

Figure 5.6 shows the percent recovery of the clean water permeability after each backwash and the extent of fouling by the end of each cycle. Therefore, the greater the distance between the point (at the end of each cycle) and the clean water permeability recovered with backwash, the greater the net recovery with a hydraulic backwash i.e. the greater the hydraulic reversibility of the fouling layer. Additionally, the decrease in permeability at the end of each cycle, from cycle to cycle, is an indication of the hydraulically irreversible fouling accumulating with each cycle.

A decrease in the clean water permeability recovered with each consecutive cycle was observed in Figure 5.6 with all solutions except when colloidal silica was present (i.e. silica alone and ABHS). Considering that for these two solutions the majority of the hydraulically irreversible fouling occurred in the first filtration cycle, it would be expected that this stable rate of hydraulically reversible fouling would continue even after several more cycles (Figure 5.5). As a result, longer experiment duration times would not be as imperative for predicting long-term fouling behavior for these solutions. Therefore, although colloidal silica and ABHS exhibited high degrees of fouling at the end of each cycle it was also largely hydraulically reversible. Jermann *et al.* (2008b) also observed that kaolinite was completely reversible, however, the size of their kaolinite (450 nm) was much larger than the membrane pore size expected for the membrane they used (100 kDa) and much larger than the silica average hydrodynamic size of 9 nm used in the present study. Jermann *et al.* (2008a) observed that kaolinite could not prevent irreversible fouling by humic acid or alginate. This differed from the results in the current study in which the presence of colloidal silica minimized hydraulically irreversible fouling. The variation between these two results may be due to different inorganic particle sizes or setup differences.

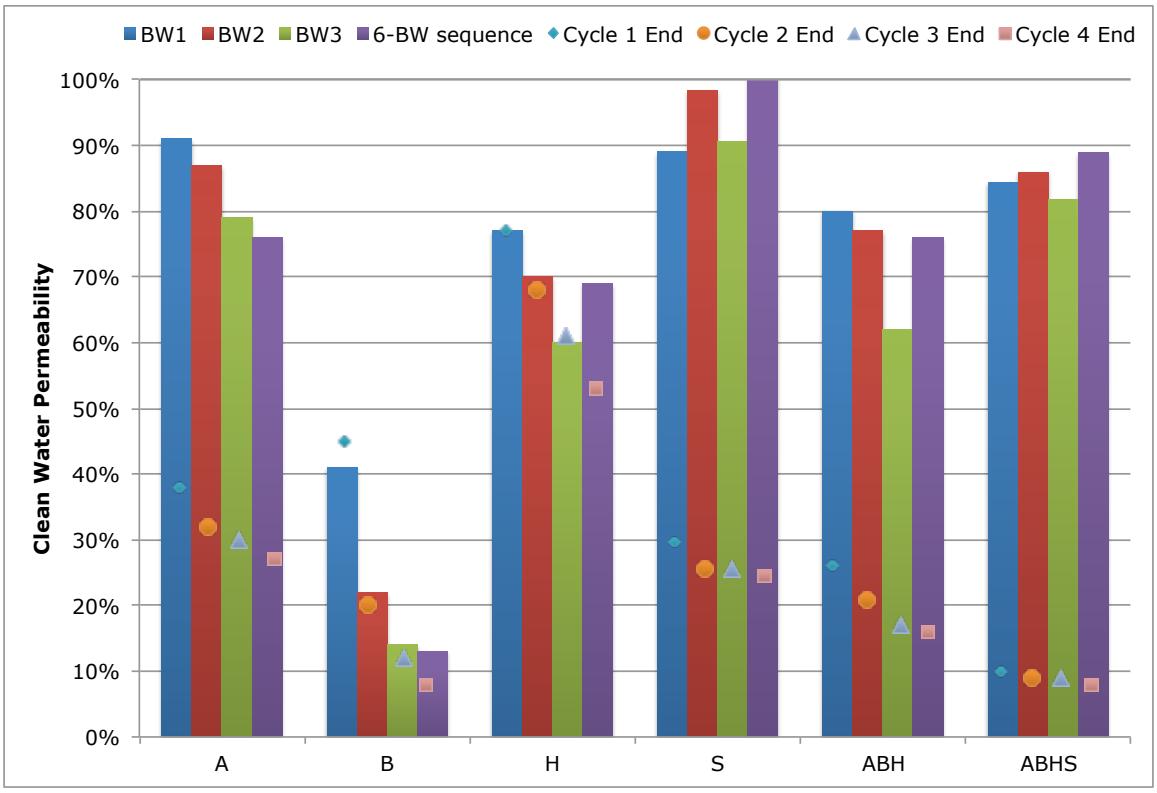

Figure 5.6: Percent of initlal clean water permeability recovered after hydraulic backwashing

The points indicate % of clean water permeability at the end of each fouling cycle and thereby the extent of fouling before backwash. The distance between the point and the top of the bar is an indication of the net clean water permeability recovered by a backwash (BW). A: Alginate; B: Bovine Serum Albumin; H: Humic acid; S: Silica; ABH: Alginate, Bovine Serum Albumin, and Humic Acid mixture; ABHS: Alginate, Bovine Serum Albumin, and Humic Acid and Silica mixture.

Alginate fouling was similar to colloidal silica and also largely reversible. However, alginate showed a downward trend in terms of the percent of the clean water permeability (%CWP) recovered by backwash similarly to the ABH combination, which decreased steadily with each consecutive cycle except for cycle 4 (Figure 5.6). Therefore, this may suggest that the hydraulically irreversible fouling rate is increasing for alginate and ABH and may even reach a steady state; however, additional filtration cycles would need to be performed to confirm this. Little to no %CWP was recovered with a backwash after humic acid and bovine serum albumin fouling (Figure 5.6). The same behavior was observed with the flat-sheet/constant pressure study, in which it was postulated that the majority of fouling with these model foulants was through adsorption. The results of the current study are

consistent with this hypothesis. Humic acid and bovine serum albumin had a high rate of continuing decline in the %CWP at the end of each cycle, which reflects a high and continuous rate of hydraulically irreversible fouling that is often associated with adsorption. The combination solutions highlight the significant influence that inorganic colloidal silica plays in the behavior of organic matter fouling. ABH showed a decreasing %CWP with each cycle (except for cycle 4) indicating slight irreversible fouling between each cycle. As mentioned earlier this could be an ongoing phenomenon, eventually resulting in severe fouling and increasing fouling rates (Figure 5.6). ABHS had the lowest %CWP at the end of each cycle; however, the majority of the CWP was recovered after each backwash at consistently high levels indicating that the fouling was almost entirely reversible.

The results for hydraulically reversible fouling for the single model solutions observed for the current study using tubular membranes are quite similar to the previous flat-sheet study (Chapter 4). The two variations observed were that although the irreversible nature of bovine serum albumin was expected, the high fouling rate was not, and the hydraulic reversibility of ABH was higher than expected. However, considering the differences in operation (i.e. configuration, etc.), the results from the flat-sheet study are qualitatively representative, which is very encouraging considering that surface characterization techniques on tubular ceramic membranes are extremely difficult to study and would require sacrificing the membrane. Therefore, if a backwash component is incorporated into the experimental design, the fouling behavior of ceramic membranes can be studied using flat-sheet membranes of the same composition, MWCO, and manufacturer. The comparability is very likely to diminish once the composition and characteristics of the flat-sheet membrane surface differ from those of the tubular membrane.

5.3.2.2 Alternative fouling mitigation techniques: Several backpulses and maintenance cleaning

When a hydraulic backwash is insufficient or ineffective at removing fouling and recovering membrane performance (i.e. clean water permeability), a chemical cleaning procedure is often the next option. Another option that has not been explored to the author's knowledge is running several hydraulic backwashes consecutively. The rationale for using this approach as opposed to a longer

backwash is that for ceramic membranes, due to their high stability, a high-pressure pulse backwash can be used, which can be advantageous in dislodging caked foulants on the membrane surface. This type of backwash is not used for polymeric membranes, which generally use a slower build up of backwash pressure with a pump. The benefit in using such a unique approach would be a quicker, chemical-free fouling removal option, particularly as the industry is moving towards more sustainable operations and minimizing chemical use. In the current study a series of 6 consecutive backwashes (6-BW sequence) was performed after the fourth cycle, followed by a clean water permeability test with ultrapure water to establish if there is a potential advantage in such an approach. In addition, a maintenance clean (a short 15 minute chemical soak with sodium hypochlorite) was done to determine if it could remove any further fouling that was not reversed with the additional backwashes. Another clean water permeability test was performed after this maintenance clean.

Table 5.3 shows the percent of the clean water permeability recovered with each fouling mitigation tool. In most cases, except for alginate and bovine serum albumin, the 6-BW sequence seemed to provide at least some additional clean water permeability recovered compared to only one backwash. However, this particular approach was not optimized and it is possible that fewer backwashes would have provided the same benefit. If the advantage is from the high pressure pulsing it may be more economical and effective if several short pulses are performed as opposed to several full cycle backwashes. It is noteworthy that the additional backwashes showed a considerable added benefit (16% as opposed to almost zero for a single backwash) for humic acid. This result is encouraging and suggests that there may be some potential in creative backwash procedures. Further investigations into optimizing this technique are needed and the potential benefits demonstrated in this study indicate that such studies could be worthwhile.

Table 5.3: %Net clean water permeability recovered* with hydraulic backwash

	Alginate	B	Humic	Silica	ABH	ABHS
BW Cycle 1	52	-5	0	59	54	74
BW Cycle 2	55	2	2	73	46	77
BW Cycle 3	49	2	0	65	45	73
6-BW sequence	48	5	16	76	60	82
MC	15	73	34	1	3	3

B: Bovine Serum Albumin; BW: Backwash; MC: Maintenance clean;
*The net clean water permeability recovered is calculated by taking the CWP after a backwash and subtracting the CWP from the end of the last cycle

The maintenance clean performed after the 6-BW sequence was most effective in recovering additional clean water permeability for humic acid and bovine serum albumin (Table 5.3). Alginate showed approximately 15% improvement to the clean water permeability after a maintenance clean. For inorganic colloidal silica and the combinations of ABH and ABHS, the maintenance clean did not add any significant further fouling removal, probably because most of the fouling was already recovered with the previous backwashes. These results suggest that even waters with a high fouling potential can be treated without a pretreatment step if a frequent chemical maintenance clean is performed. Considering the costs associated with a common pretreatment step such as coagulation due to infrastructure, chemical and residual treatment costs, this could translate into significant savings. Although frequent maintenance cleans are practiced with polymeric membranes, over time the chemical exposure can affect the physical/chemical characteristics of the membrane and ultimately, performance and lifetime (Abdullah and Bérubé 2012). However, ceramic membranes have an extremely high chemical stability and could withstand the chemical exposure without the negative side effects.

Although the focus of this discussion is on removing fouling that has already occurred, the results of this study have implications for applying pretreatment methods to prevent hydraulically irreversible fouling. The benefit of the presence of inorganic silica colloids could potentially play an important role in providing a novel pretreatment process for such membranes through the addition of particles. If on the contrary, pretreatment focuses on removing particles, this may cause the membrane to be more vulnerable to hydraulically irreversible fouling, and therefore could hinder membrane performance as opposed to improving it. A cake layer composed of particles seems to be particularly responsive to the pulse action of the backwash, which would thus allow a series of backwashes to be a potentially effective fouling mitigation tool.

5.3.3 Rejection

The rejection results discussed are from data collected during the initial lower flux experiments (at 60 LMH), since the analytical instrument was unavailable during the high flux experiments. The TOC values for the feed solutions of humic acid (70 kDa), bovine serum albumin (67 kDa), and alginate (3-100 kDa) are 1.7, 2.3, and 1.4 mg C/L respectively. The permeate samples were collected throughout

each cycle and then analyzed. Table 5.4 shows the rejection of each organic model foulant in single solution for all four permeate cycles as well as the combinations.

Table 5.4: Rejection of each model foulant when filtered individually for each permeate cycle

Cycle	Alginate	B	Humic Acid	ABH	ABHS
1	≥ 86%	≥ 91%	≥ 88%	52%	55%
2	≥ 86%	≥ 91%	≥ 88%	58%	55%
3	≥ 86%	≥ 91%	83%	64%	59%
4	≥ 86%	87%	85%	73%	62%

B: Bovine Serum Albumin
≥ is indicated for concentrations below the limit of quantification = 0.2 mg C/L
The single solutions were analyzed using the TOC instrument and the combinations were analyzed using LC-OCD

The rejection for all single model foulants was quite high and greater than 80% in all cases even though the size of the foulants is smaller than the membrane MWCO. However, despite the similar removals for all three model foulants with the tubular membranes, it is unlikely that the removal mechanism is the same since both humic acid and bovine serum albumin resulted in high levels of hydraulically irreversible fouling. Alginate rejection seems to remain relatively constant throughout all cycles. However, for humic acid and bovine serum albumin, by the fourth cycle rejection begins to decrease and this trend would be expected to continue considering the suspected fouling mechanism is adsorption, which can only occur temporarily at the beginning stages of filtration until adsorption sites are exhausted. Additional filtration cycles would be required to confirm this hypothesis. Konieczny *et al.* (2006) reported similarly high TOC removals of 100% of humic acid with microfiltration (MF). Considering that MF membranes are not expected to remove organics, adsorption is the most plausible removal mechanism.

The rejection results are somewhat higher compared to the flat-sheet study where the average TOC rejection was approximately 80% for bovine serum albumin, 75% for alginate and 50% for humic acid (Munla *et al.* 2011). If the mass filtered per membrane surface area is compared, the tubular membrane received approximately 600 mg/m^2 whereas the flat-sheet membrane was exposed to more than double that amount with approximately 1,300 mg/m^2. Therefore, it is possible that during the

flat-sheet experiments the membrane's adsorption capacity was reached or exceeded, thus resulting in lower TOC rejection of humic acid and bovine serum albumin.

Silica is not included in Table 5.4 because inorganic concentrations cannot be measured by TOC analysis. However, a few preliminary supporting measurements of silica concentration were obtained through a commercial lab. The observed rejection ranged from 70-80% and silica concentration was increased in the backwash water. Considering that the size of the silica is averaged at 9 nm and a previous study by Calvo *et al.* (2008) measured a membrane pore size of 16.4 nm ±1 with scanning electron microscopy and 13.6 nm ± 0.7 with liquid-liquid displacement porosimetry for this membrane, a high silica rejection is unexpected. Possible explanations include aggregation of particles, thus increasing particle size, or if both the membrane and colloid are negatively charged there may also be an electrostatic repulsion effect at play. Some rejection may also occur as a result of the pore size distribution of the membrane as well as the colloidal particles, in which case some particles may be rejected through size exclusion. This particle size was specifically chosen to induce fouling because it is close to the pore size of the membrane, which has been associated with higher rates of fouling. However, in this study silica mainly contributed to hydraulically reversible fouling.

From Table 5.4 it can be seen that the overall rejection of DOC increased for both ABHS and ABH, more so for the latter. Rejection for both combinations was approximately 60%, which is within the range of the results observed for the flat-sheet study (ABH ~ 50% and ABHS ~60-80%). However, it was much lower than the rejections observed for the individual solutions. LC-OCD analysis was used for the combination solutions ABH and ABHS at 120 LMH to qualitatively assess which of the foulants were being rejected. This result is relatively similar to Munla *et al.* (2011), in which a trend of lower rejections was observed for combinations of model foulants. One hypothesis is that in the presence of silica, the foulant layer is looser thus allowing more foulants to pass through the membrane; this is supported by the results in Munla *et al.* (2011) where the rejection of solutions with silica were generally lower. For ABH however, the rejection may be lower due to less pore constriction and more of a cake layer formation, which may prevent humic adsorption within the pores. This cake layer may also explain the high hydraulic reversibility of this combination solution (Figure 5.6).

The LC-OCD chromatograms for ABH and ABHS are shown in Figure 5.7. The different organic matter fractions are not baseline separated, however, they do have discernable peaks, particularly for the feed solutions. The LC-OCD chromatograms also confirm the use of BSA and alginate to represent biopolymers in natural water sources as they elute in the same time window biopolymers present in natural water elute.

For ABH, (Figure 5.7 part a) it can be seen that the biopolymer (in this case comprised of alginate and bovine serum albumin) concentrations in the permeate seem to decrease with each cycle but on average humic acid removal remained stable. Therefore, since humic acid rejection remained fairly consistent between cycles, while alginate and bovine serum albumin seem to show increased rejection with time, it is possible that theses two foulants are involved in the fouling layer build-up, which subsequently increased overall rejection from 52% to 73%.

For ABHS (Figure 5.7 part b) humic acid concentration was the lowest in the cycle 1 permeate. Therefore, rejection for humic acid was higher during the first cycle and then continued to decrease (peak in permeate increases), indicating likely initial adsorption. This trend is consistent with results of single humic acid filtration as shown in Table 5.4. Rejection of biopolymers (i.e. alginate and bovine serum albumin) remained quite constant throughout the cycles with only cycle 1 having a slightly higher concentration (i.e. lower rejection). Both simultaneously occurring opposite trends in concentration of these fractions resulted in a relatively constant DOC rejection over all four cycles (Table 5.4). The lower rejection for mixtures with silica was also observed for the flat-sheet study (Munla *et al.* 2011). One hypothesis is that silica interferes with humic acid adsorption either through interactions with the other model foulants or with the membrane surface itself.

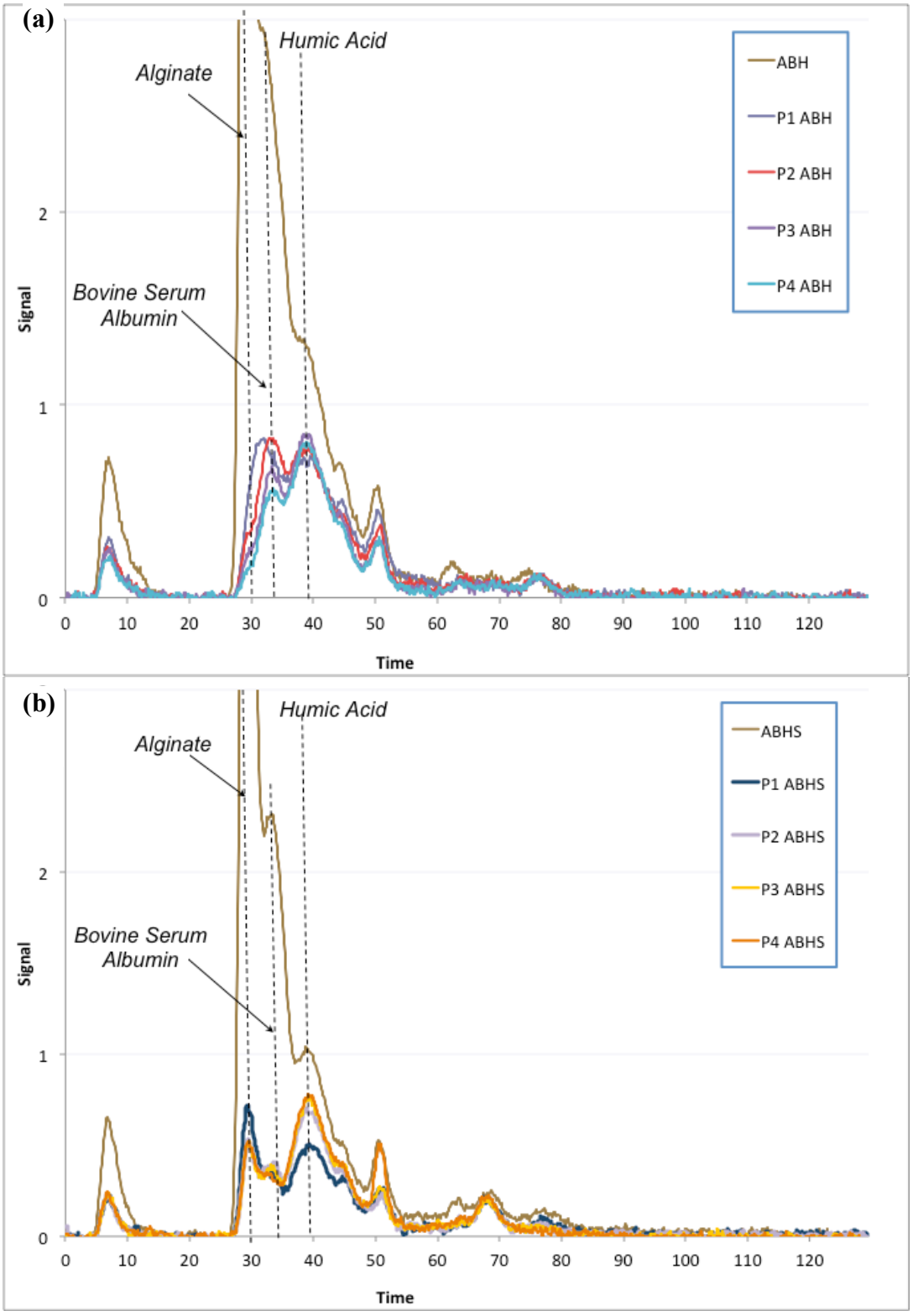

Figure 5.7: LC-OCD chromatograms for the feed and permeates (P) for each of the four cycles a) ABH and b) ABHS filtration.

5.3.4 Mass balance results

The results of the mass balance are shown in Figure 5.8 to Figure 5.10 for each individual organic foulant over four cycles. Since mass balances are inherently challenging, the focus of this discussion is on general trends observed. Generally, mass balance results are consistent with the other results reported herein.

Figure 5.8 shows that BSA fouling was mostly irreversible fouling and had the highest irreversible fouling of all the organic model foulants. This is confirmed by the high rate of irreversible fouling (Figure 5.5), the backwash efficiency results (Figure 5.6), and the high rejection (Table 5.4). From cycle 1 to 4 slight increases in reversibility combined with decreasing irreversibility were observed, which could be due to less BSA adsorbing onto the membrane surface. Almost no BSA was found in the feed channel water, further supporting its high affinity to the membrane surface.

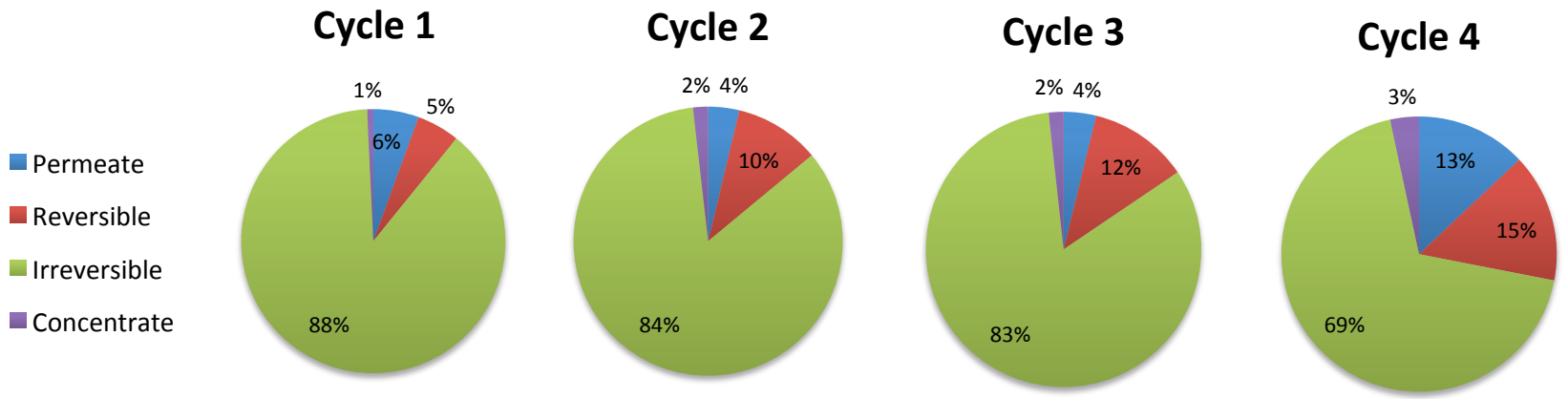

Figure 5.8: Bovine serum albumin mass balance results

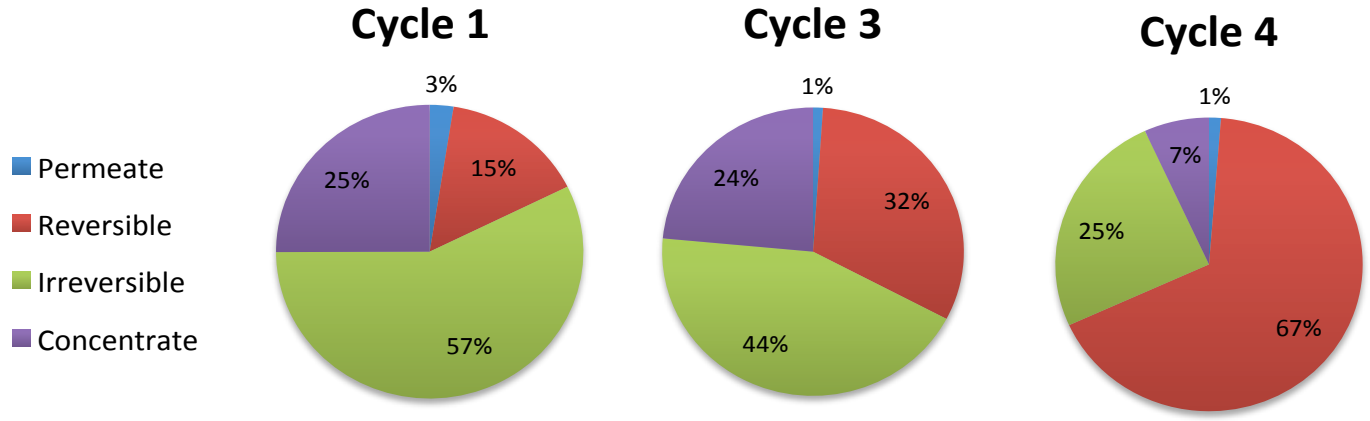

Figure 5.9: Alginate mass balance results (Cycle 2 is not included due to sample loss)

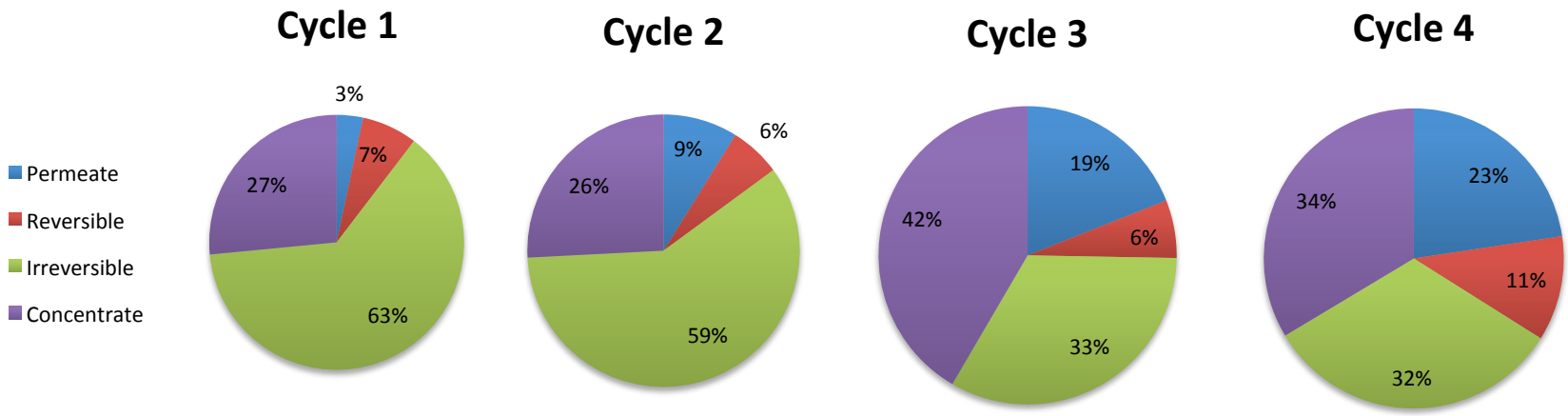

Figure 5.10: Humic acid mass balance results

Figure 5.9 shows that among the model foulants alginate was the least present in the permeate, which is confirmed by its high rejection results (Table 5.4). The reversibility increased while the irreversibility decreased with each cycle. The amount concentrated in the feed channel water also decreased.

Figure 5.10 shows that humic acid increased in the permeate with each cycle, which is reflected in the rejection results. The percent that was reversible remained consistent while the irreversibility decreased, which could be due to less adsorption onto the membrane surface and a greater amount being concentrated in the feed channel and to a lesser degree passing through the membrane.

Overall, all model foulants showed some decrease in irreversibility with each cycle, which is likely the result of the formation of a cake layer on the membrane surface.

5.4 Conclusions

In this investigation model foulants of concern for drinking water were used to evaluate fouling for a ceramic tubular ultrafiltration membrane at constant flux using dead end mode operation and backwashing. These experiments were intended to gauge the extent to which the results of a previous flat-sheet study operated at constant pressure with the same model foulants were relevant for different membrane configurations or operating conditions. The main conclusions are:

- For tubular membranes the bovine albumin serum single solution showed high fouling, which was almost entirely hydraulically irreversible fouling. However, when combined with other model foulants hydraulically irreversible decreased drastically.
- Although the overall rate of humic acid fouling was the lowest among the model foulants, it was largely comprised of hydraulically irreversible fouling.
- The mass balance results showed that the percent mass of all single organic model foulants contributing to irreversible fouling decreased over the first 4 cycles of filtration likely due to the formation of a cake layer, which thus decreased adsorption onto the membrane surface.
- ABHS showed the greatest overall rate of flux decline but was largely comprised of hydraulically reversible fouling. The results for silica alone were similar. These results

support the importance of investigating the reversibility of fouling in experiments through backwashing.

- Fouling behavior of the tubular ceramic membrane set-up operated at constant flux was consistent with results obtained with flat-sheet membranes operated at constant pressure (with the same membrane material, MWCO, and manufacturer) and a backwash. This is an important finding because the design, setup, and operation of flat-sheet membranes is much simpler and in particular, allows for surface characterization without sacrificing membrane modules.
- Employing a unique approach that utilizes a sequence of several backwashes consecutively can be a potentially effective fouling mitigation tool.
- A short maintenance clean with sodium hypochlorite was very effective in recovering additional clean water permeability for both humic acid and bovine serum albumin, which had the highest rates of hydraulically irreversible fouling. This suggests that if frequent maintenance cleans are performed, these ceramic membranes can potentially be used for waters with a high fouling potential without pretreatment. The significance of this finding translates into considerable savings on capital and operating costs.

In drinking water treatment, foulant mitigation is crucial for sustainable operations and maximizing efficiency and membrane lifetimes. The challenge is in collecting accurate and representative fouling behavior data without having to run experiments at full scale. Future steps would be to relate the fouling behavior observed with model solutions, in particular the combinations, to surface water fouling behavior for both tubular and flat-sheet membranes. This would help identify possible gaps of using flat-sheet membranes at constant pressure. Overall, the results from the current study are encouraging and hold promise for creative solutions to the issue of fouling of membranes in drinking water treatment.

Chapter 6
Stage 4: Sustainable Flux Experiments and NOM Rejection in Natural Waters with a Tubular Ceramic Membrane

This chapter may be considered for publication in the future. Cited references are included in the consolidated list of references at the end of the thesis.

This chapter discusses results obtained from the long-term operation of a ceramic ultrafiltration at a sustainable flux using the method determined in Chapter 3. The discussion also focuses on the rejection of different organic matter fractions in surface water with the use of LC-OCD analyses.

6.1 Introduction

The sustainable flux method established in Chapter 3 for a polymeric membrane was applied to a tubular ceramic ultrafiltration membrane. Ultimately, the goal was to run the tubular ceramic and polymeric membranes at their respective sustainable flux over 5 days using the same batch of water to compare the fouling behavior of both membranes. Furthermore, the rejection of different NOM fractions in natural waters was investigated to identify foulants of concern and compare the natural water results to the previous model foulant experiments using the same tubular ceramic membrane (Chapter 5).

As research is never straightforward, this collection of experiments took this investigator on twists and turns and required the cunning of a Sherlock Homes type detective sleuth mind. J_{sus} (aka sustainable flux) was a dodgy character and often slipped right through the grip of scientific logic. Despite several attempts, each time with enhanced artillery, J_{sus} was never captured. But, some clues were left behind and the efforts were not all in vain.

A significant portion of time was put into designing, implementing, and optimizing the tubular ceramic setup to operate at constant flux using a feedback loop. An intricate Labview program was designed to allow for a fully automated constant flux process. Inherently, with any new setup, several rounds of trial and error were required to reach an optimized and well performing setup and

procedure. Therefore, this process was also a design process that included implementation, modification, and optimization. The model solution experiments discussed in the previous chapter were performed after the work described in this chapter.

6.2 Materials and methods

The details of the tubular ceramic membrane, the final setup, and the TOC/DOC and LC-OCD instrument are provided in Section 5.2.2. A picture of the tubular membrane and the physical setup are provided in Appendix A Figure 5 and a screen shot of the Labview program is shown in Appendix D Figure 1. To maintain a constant flux operation, the Labview program monitored the permeate flux and adjusted the pump accordingly to maintain the flux within a desired flux range.

Grand River water was used for all the experiments and a 200 μm prefilter (reusable filtration cartridge – 10 gpm - Cole Palmer) was the only pretreatment. The water was stored at 4°C for a maximum of 2 weeks to minimize inconsistencies in the raw water quality due to organic matter degradation.

For each experiment, the sustainable flux was first determined using the methodology developed in Chapter 3. Remember that the sustainable flux determined is a function of the specific membrane and water quality tested. Then the membrane was operated at that sustainable flux for 5 days if possible. Throughout each experiment, the transmembrane pressure (TMP) and temperature were monitored, as well as water quality, which included LC-OCD, TOC/DOC and turbidity. Samples of the feed water, the permeate, and the backwash water were taken each day to monitor the water quality and the rejection of organic matter.

Turbidity was measured using a calibrated turbidimeter and the Standard Methods #2130. Alkalinity and hardness were determined using titration as outlined in method Standard Methods #2320 and #2340 respectively. UV absorbance at 254 nm was determined using a spectrophotometer (HP 8453, Palo Alto, CA) with a 1 cm quartz cell. No sample preparation is required prior to measurement. Specific UV absorbance (SUVA) is an indicator of the aromaticity of the organic matter and was calculated using equation 3.1.

A backwash procedure similar to that of another ceramic membrane manufacturer, Metawater, which currently provides ceramic membranes for drinking water was designed because the backwashing procedure for TAMI membranes is not established for drinking water treatment applications. This backwash was performed every 30 minutes. The procedure for the backwash, the 6-BW sequence and the maintenance clean is described in Section 5.2.1. To calculate the effectiveness of these fouling mitigation techniques:

$$\%TMP_{recovered} = \frac{TMP_{fouled} - TMP_{cleaned}}{TMP_{fouled}} x\ 100 \qquad \textbf{Equation 6.1}$$

The TMP used was normalized by subtracting the starting TMP.

A mass balance on biopolymers and humic acid was performed during the long-term sustainable flux experiment #4. A diagram of where the samples were taken is shown in Figure 5.2. Samples were taken from the feed, the permeate, the feed channel water, and the backwash water once every cycle during the first 4 cycles of filtration. Samples were weighed to determine total volume and then analyzed with the LC-OCD to calculate the mass. The feed channel water (i.e. retentate) was taken separately in order to determine the mass that was rejected but does not contribute to reversible or irreversible fouling. Calculations used in the mass balance are discussed in Section 5.2.4.

6.3 Results

6.3.1 The sustainable flux story: A series of confounding events

This section discusses the results of several attempts to use the sustainable flux method established in Chapter 3 with the tubular ceramic membrane using surface water. Six sustainable flux method experiments were performed using Grand River water, four of which were run for several days. For sustainable flux experiments #1-4, water was taken from the Kaufmann Flats in Waterloo, while for

#5 and #6 it was taken from the intake at the Manheim Treatment Plant in Hidden Valley, Kitchener. The goal was to operate at a sustainable flux for 5 days without exceeding 50% of the ceramic membrane's maximum operating transmembrane pressure (TMP), which is 72.5 psi (the maximum operating TMP given by the manufacturer is 10 bar or 145 psi). This allows for a comparison of fouling behavior and operating performance between the ceramic tubular membrane and the polymeric membrane within an acceptable fouling rate.

Each experiment shed light on something new about the sustainable flux method, the tubular setup, or the membrane. The lessons learned led to appropriate modifications, followed by an additional experiment. Experiments #1-3 were preliminary experiments with the tubular ceramic membrane in order to optimize the setup (including the physical setup, the Labview program, and the backwash procedure). The results are described in more detail in Appendix D Section 1.0. After changes were made to the setup, flux stepping with ultrapure water was done to assess the stability of the flux without fouling and to establish that flux stepping can be performed with the tubular setup (Figure 6.1). The setup was able to maintain the desired flux with ultrapure water within ±1 mL/min.

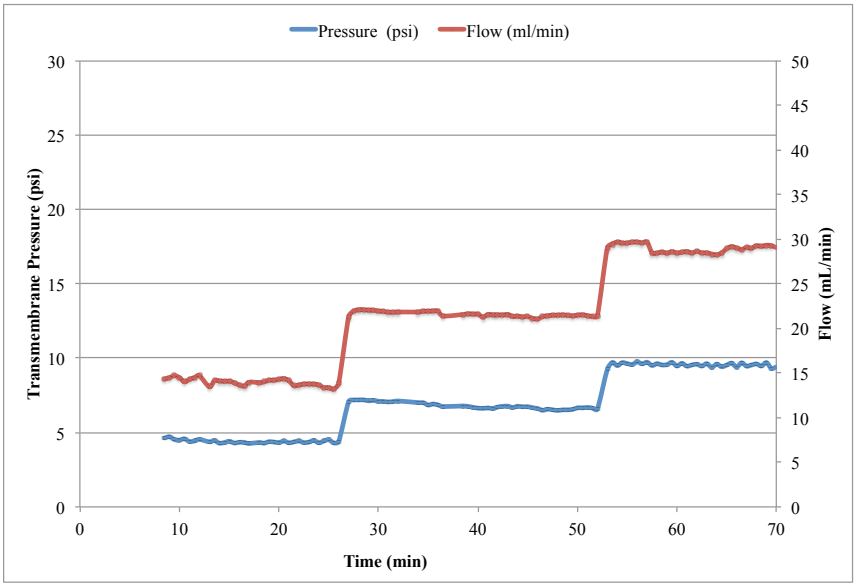

Figure 6.1: Flux stepping with ultrapure water for the tubular ceramic membrane

6.3.1.1 Long-term sustainable flux experiment #4

Once modifications and upgrades were made to the tubular ceramic membrane setup and operation, a long-term sustainable flux experiment was performed. For this experiment, the flux stepping method to determine sustainable flux started at a lower initial flux and used smaller flux increments than experiments #1-3 (42, 70, 90, 115, 140, 165, 185 LMH or 6, 11, 14, 18, 22, 26, 29 mL/min). The flux stepping results are shown in Figure 6.2. The sustainable flux determined was 141 LMH (22 mL/min) and is shown in Figure 6.3. This was the highest sustainable flux determined thus far, and considering the previous issues with long-term operation and that the fouling curve was quite steep, it seemed best to err on the side of caution. Therefore, the long-term experiment was operated at a slightly lower flux of approximately 128 LMH (20 mL/min).

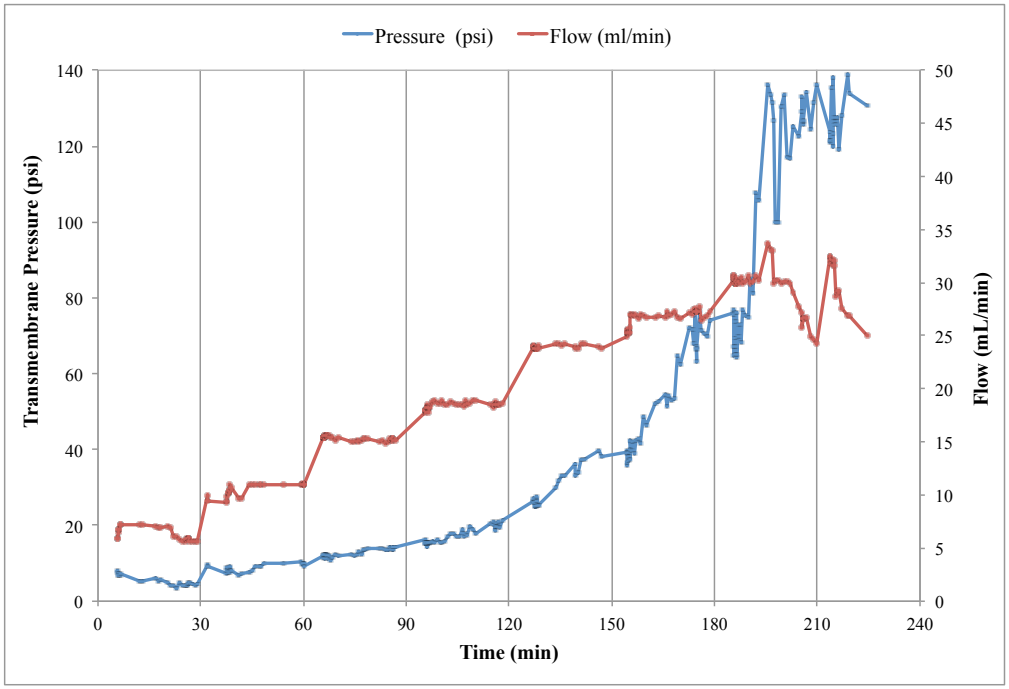

Figure 6.2: Flux stepping results for sustainable flux experiment #4

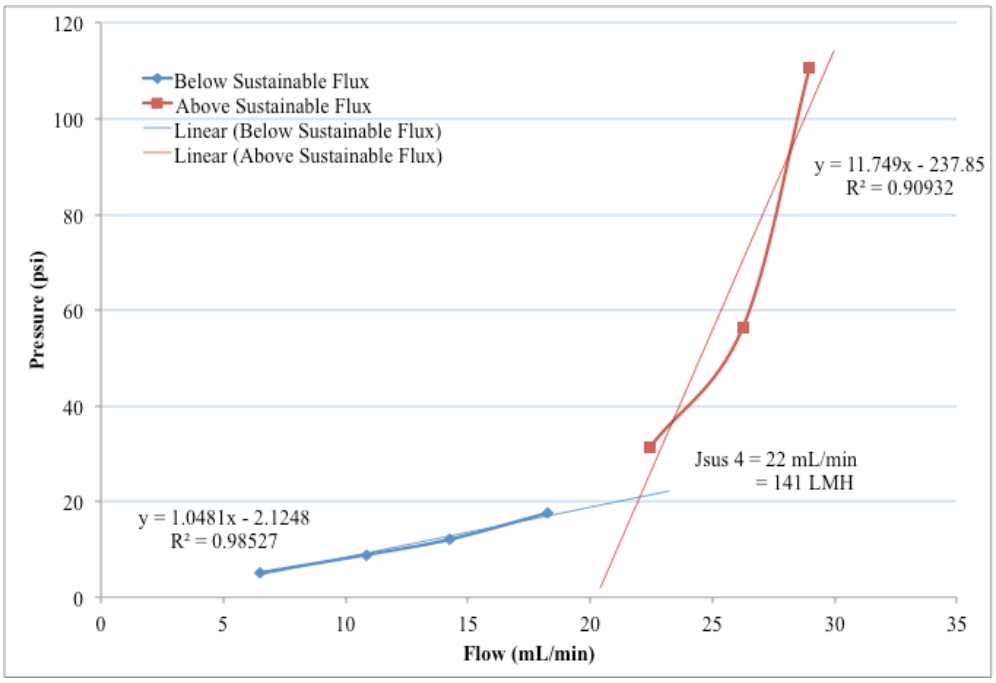

Figure 6.3: Sustainable flux determination for experiment #4

The long-term experiment at a flux of 128 LMH showed a rather rapid rate of fouling and after approximately 17 hours the membrane was completely fouled and the experiment had to be stopped (Figure 6.4). After 12 hours the transmembrane pressure had already reached and exceeded 50% of the ceramic membrane's maximum operating TMP (72.5 psi).

The membrane was chemically cleaned at this point to restore the clean water permeability. Since enough water had been collected to operate the membrane over 5 days, there was still a lot of water remaining from the same batch of water collected. Therefore, another long-term experiment was performed at a much lower flux of 64 LMH (10 mL/min) to observe the fouling trend (Figure 6.4). At this flux, the membrane was able to operate for almost 3 days before it reached 50% of the ceramic membrane's maximum operating TMP (72.5 psi).

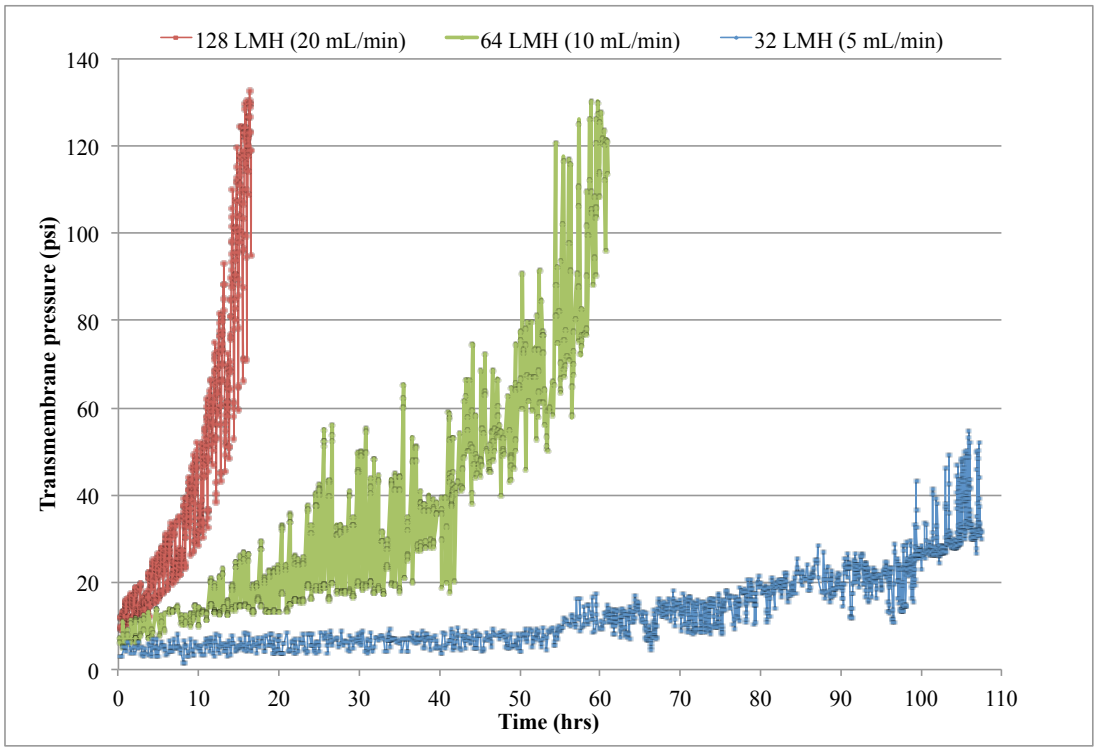

Figure 6.4: Long-term experiment #4 at different fluxes

Enough water was available to perform another long-term experiment at an even lower flux of 32 LMH (5 mL/min) for around 106 hours. At this flux the fouling rate was initially low and the TMP remained below approximately 10 psi (Figure 6.4). However, halfway through this experiment, after 60 hours, the fouling rate began to increase more rapidly. The TOC remained constant throughout the days for this batch of water while the turbidity slightly decreased from 3.6 to 2.8.

Conclusions for experiment #4

The results of these experiments clearly indicated that the method to determine a sustainable flux developed in Chapter 3 did not work for this ceramic membrane under these conditions. Such a conclusion was unexpected because the method is conceptually based and the sustainable flux determined is a direct function of a specific membrane and water quality. The aim of determining sustainable flux is simply to calculate a flux that is within a moderately acceptable rate of fouling.

Therefore, although the factorial design was performed using a polymeric hollow fiber membrane, it should in principle, work on any membrane with any water. A more in-depth discussion regarding this conclusion is covered in Section 6.3.2.

6.3.1.2 Long-term sustainable flux experiment #5

In this set of experiments, the plan was to operate the polymeric and ceramic membranes simultaneously with the same batch of water at the same flux. The polymeric membrane was used to determine the sustainable flux, which was the flux that was then used to run both membranes for 5 days.

The water quality for these side-by-side experiments was not typical and was challenging to treat due to the high turbidity (7-11 NTU). Further discussion of water quality and NOM rejection can be found in Section 6.3.3. Additionally, the winter of 2012 had many freeze/thaw events and planning experiments around unpredictable water quality was not an option.

The sustainable flux method was performed with the polymeric membrane setup and determined to be 64 LMH (Appendix D Figure 7). The polymeric membrane results are shown in Appendix D Figure 8 and are also briefly discussed in the Appendix D Section 2.0. The results showed that the polymeric membrane was also unable to operate sustainably over 5 days and required regular maintenance cleanings. However, the sustainable flux methodology developed in Chapter 3 did not consider maintenance cleaning. Therefore, even for the polymeric membrane, the methodology to determine a sustainable flux does not seem to apply for all water qualities. Further discussion on the sustainable flux methodology is included in Section 6.3.2.

There were 3 different attempts at running at 64 LMH flux with the ceramic membrane, each with different operational settings.

1st attempt at 64 LMH (10 mL/min)

The first attempt of running at 64 LMH resulted in extremely high fouling rates (Figure 6.5). The fouling rate was 3 psi/h in the first 10 hours, 8.7 psi/h from 10 to 18 hours, 14.5 psi/h from 18 to 24 hours, and 12.8 psi/h from 24 to 29 hours. At 18 and 24 hours a 6-BW sequence was performed and recovered 71% and 74% of the TMP respectively. The advantage of the ceramic membrane backwash is that it allows for a high-pressure pulse, which can be effective in dislodging the cake layer on the membrane surface. The effectiveness of this technique can be observed from the significantly decreased transmembrane pressure (Figure 6.5). However, the fouling rate continued to be very high and eventually this backwash sequence was needed again within 6 hours. The second 6-BW sequence performed showed a similar recovery followed by a similarly high fouling rate.

At this point a maintenance clean or a full cleaning could have been beneficial but was not done. One reason is that the use of chemicals had not been incorporated in the initial design and the polymeric membrane had not needed a maintenance clean after the same hours of filtration. Therefore, a different approach was needed. The new approach was to investigate the impact of operational conditions on membrane fouling, since pursuing maintenance cleanings would not have had an impact on the fouling rate.

Attempt #2: The 15-minute filtration cycle at 64 LMH (10 mL/min)

The filtration cycle was shortened from 30 to 15 minutes, which would allow for four backwashes per hour as opposed to two. A much slower rate of fouling was observed with this approach (Figure 6.5); the fouling rate was 2 psi/h for the first 23 hours and 1.4 psi/h from 23 to 50 hours. The more frequent backwashes may have minimized the thickness of the cake (i.e. over an hour, more mass was removed). A maintenance clean was performed once a day i.e. after 23 and 50 hours, which recovered 93% and 80% of the TMP, respectively. A maintenance clean was chosen over the 6-BW sequence because the frequency of backwashes had already been increased. This operational mode (i.e. regular maintenance cleans) seemed to be sustainable, which is similar to what was observed for the polymeric membrane.

Unfortunately, after 57 hours of filtration, the Labview program crashed and no data was being recorded from thereon. It also meant that there was no feedback loop from the flow meter and therefore, the pump continued running at the same setting. It was observed that the flux was maintained relatively close to the desired flux without the need for increased pump speeds despite increased transmembrane pressures. A closer inspection of previous data showed a similar trend, in which the average pump setting remained relatively stable until high rates of fouling were encountered. Therefore, the feedback loop from the flow meter to the pump was only critical in maintaining the desired flux if the fouling rate was high. However, the aim of these experiments was to operate at low fouling rates, which would make the need for this feedback loop less critical. By removing this feedback loop both the flux noise (Appendix D Figure 9) and overall fouling rate decreased (Figure 6.5).

Attempt #3: Constant pump filtration with 30 minute cycles at 64 LMH (10 mL/min)

Consequently, a final attempt at running a long-term experiment at a constant pump setting was performed at a flux of 64 LMH (Figure 6.5) with 30 minute filtration cycles. The rate of fouling was still less than the previous 2 attempts (Figure 6.5). The fouling rate was 0.4 psi/h for the first 19 hours, 0.7 psi/h for 19 to 39 hours, 1.3 psi/h for 39 to 58 hours, and 2.1 psi/h for 58 to 70 hours. Total operation time lasted for almost 70 hours before all the collected water had been used. A 6-BW sequence was performed every 20 hours at 20, 40, and 60 hours into filtration and the TMP recovered was 91%, 90%, and 89%, respectively. Therefore, since a significant portion of the TMP was recovered with additional backwashes the majority of the fouling observed was actually hydraulically reversible. However, the rate of irreversible fouling did seem to be increasing with each consecutive day. Over those 3 days the flux did not exceed 40 psi and the 6-BW sequence was successful in mitigating fouling, therefore, no chemical maintenance cleaning was required. Additionally, this attempt showed to be the most stable and least erratic in terms of TMP and flux fluctuations. It would be expected that if this experiment continued for another 2 days that the TMP would likely not exceed 50% of the ceramic membrane's maximum operating TMP or 72.5 psi.

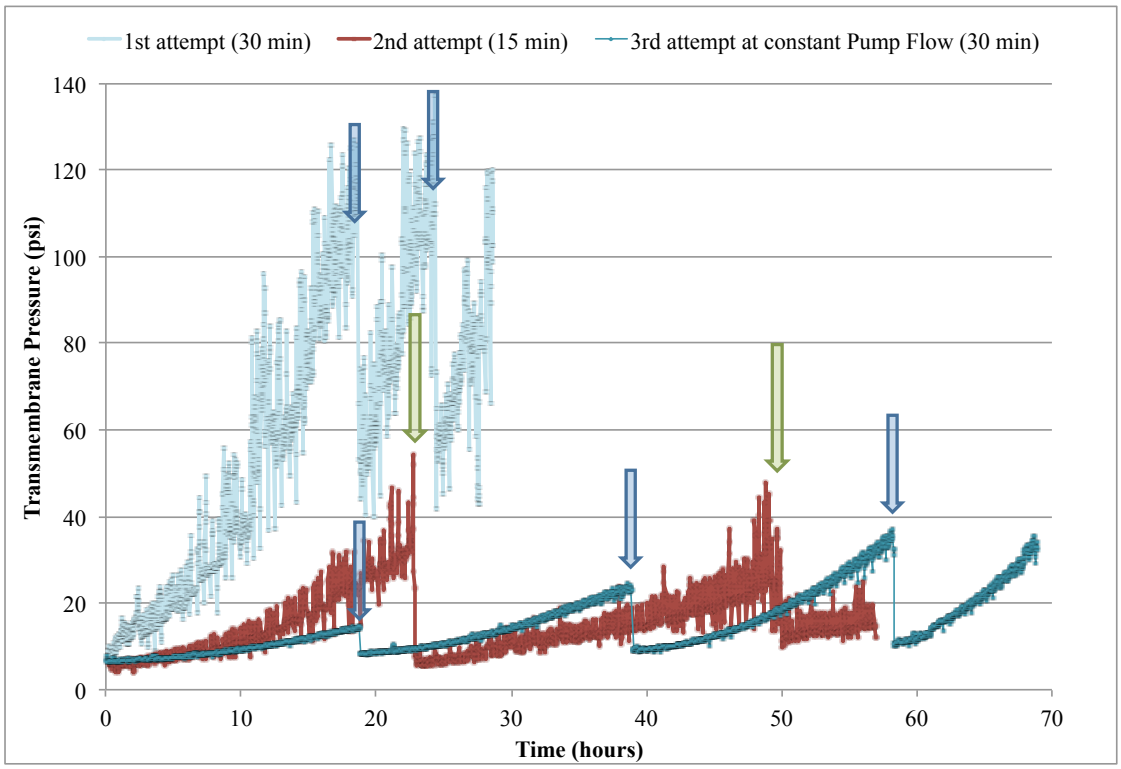

Figure 6.5: Long-term sustainable flux experiment #5 with different operating procedures at 64 LMH (10 mL/min).

Blue arrows indicate a 6-BW sequence and green arrows indicate a maintenance clean.

Conclusions for experiment #5

The main conclusions were:

- It was possible to operate the ceramic membrane sustainably with the updated operating procedure
- Operational conditions greatly influenced the membrane fouling rates, in particular the length of the filtration cycles and the pump setting
- Fouling could be controlled by a 6-BW sequence or regular maintenance cleaning

Another long-term experiment would be needed to confirm that changing the operational conditions (i.e. running at constant pump) would allow the sustainable flux method to work.

6.3.1.3 Long-term sustainable flux experiment #6: The Final Frontier

The purpose of this sustainable flux experiment was to confirm whether or not the inability of the membrane to run sustainably at the calculated sustainable flux was a function of the system operation, the membrane, or the sustainable flux method. During this experiment, the feedback loop to the pump was not used, and only occasional, slight adjustments to the pump speed were required to maintain the desired flux and these were done manually.

A sustainable flux stepping experiment was performed (Figure 6.6) and the sustainable flux determined was 109 LMH (17 mL/min) (Figure 6.7). At this flux, the membrane could only operate for a little over 13 hours before it was completely fouled (Figure 6.8). At this point a 6-BW sequence was performed and recovered 92% of the TMP. Note that the flux was also simultaneously decreased down to 77 LMH (12 mL/min). This flux was chosen because it was on the upper end of the "below sustainable flux" curve (Figure 6.7). The reason for this decrease is that since the membrane had fouled very rapidly at the previous flux of 109 LMH, no further information would be gathered by continuing to run at the same flux except to confirm that this flux is in fact unsustainable. This essentially confirmed that the approach to determine the sustainable flux did not work even with the improved set-up operation.

The 6-BW sequence seemed to be initially effective at removing a considerable amount of fouling (Figure 6.8). Nevertheless, after around 22 hours another 6-BW sequence was performed because it seemed that once the TMP exceeded approximately 25-30 psi, the rate of fouling increased more rapidly. However, this time a much smaller percentage of the TMP was recovered (33%). At the time, it was hypothesized that the additional backwashes may be only effective after sufficient fouling had occurred, which would require higher transmembrane pressures to be reached before a 6-BW sequence would be necessary. Therefore, once significant fouling had occurred (TMP of ~60 psi), another 6-BW sequence was performed after 31 hours with only a slightly higher TMP recovery (50%). Consequently, a maintenance clean had to be performed after 32 hours.

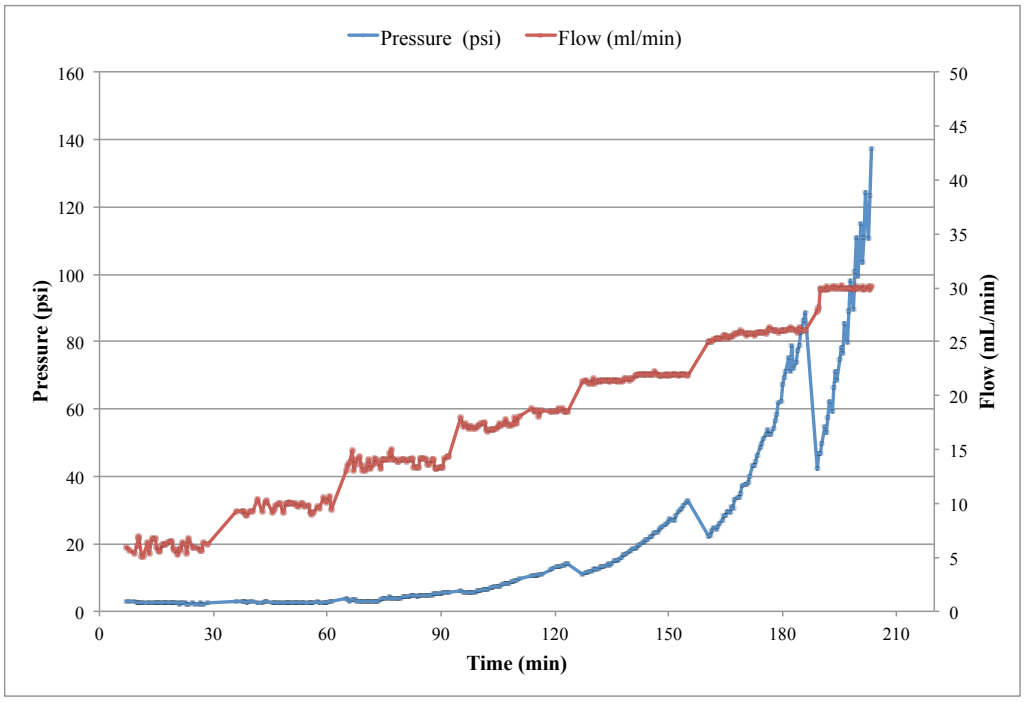

Figure 6.6: Flux stepping results for sustainable flux experiment #6

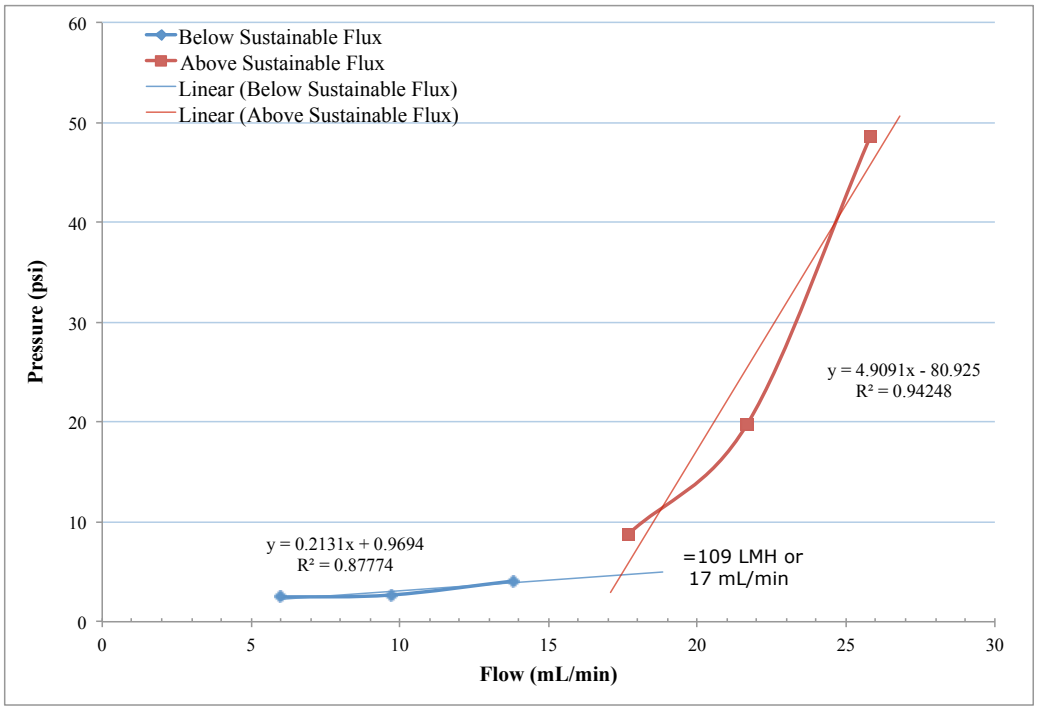

Figure 6.7: Sustainable flux determination for experiment #6

The flux had to be decreased again (down to 64 LMH) after 51 hours since the TMP had almost reached 50% of the ceramic membrane's maximum operating transmembrane pressure (72.5 psi) in less than 24 hours. At this flux, a maintenance clean performed every 20 hours allowed for sustainable operation and the TMP remained below 40 psi for 5 days. Throughout these 5 days, the 6-BW sequence was performed a few times, however, with little to no improvement. Table 6.1 summarizes the TMP recovered with either a 6-BW sequence or a maintenance clean throughout the long term experiment. Overall, the average TMP recovered with a maintenance clean was 95% (±5) and 49% (±21) with the 6-BW sequence. Therefore, the maintenance clean was more effective and more consistent.

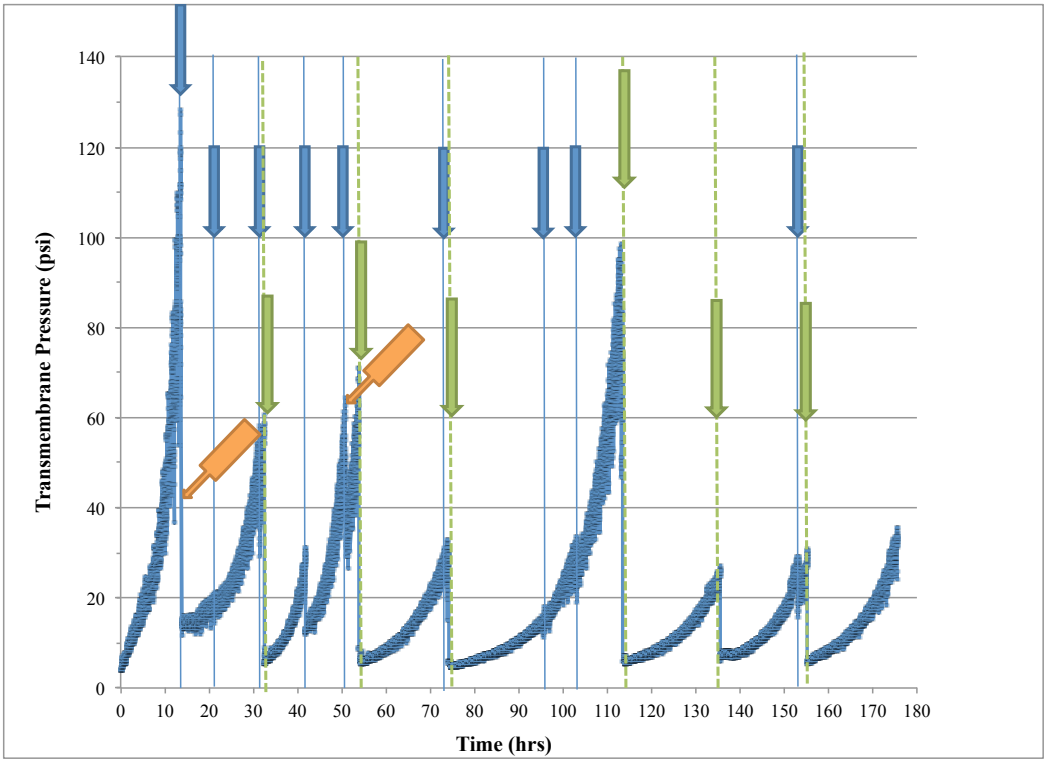

Figure 6.8: TMP during long-term experiment #6 starting at 109 LMH (17 mL/min).
Blue arrows indicate a 6 BW sequence, green arrows indicate a maintenance clean and orange arrows indicate a decrease in the operating flux (down to 77 LMH at 15 hours then down to 64 LMH at 50 hours).

Table 6.1:%TMP recovered with either a series of 6 backwashes or a maintenance clean

Time (h)	TMP recovered with a 6-BW sequence (%)	TMP recovered with MC (%)
13	92	-
22	33	-
31	50	-
32	-	98
42	70	-
51	52	-
54	-	97
74	34	-
75	-	96
95	25	-
103	42	-
113	-	97
135	-	86
153	41	-
155	-	96

BW: Backwash
MC: Maintenance clean

Conclusions for experiment #6

The main conclusions after this last long-term experiment were:

- Despite operating the pump at a constant setting, the ceramic membrane could not operate sustainably at the determined sustainable flux of 109 LMH. Therefore, the root cause for why the sustainable flux method is unsuccessful is still not fully understood or known.
- The 6-BW sequence was not necessarily an effective fouling mitigation method. This method may only be useful in cases in which the water is highly turbid, such as was observed in sustainable flux experiment #5 (Figure 6.5).
- The maintenance clean, however, was consistently successful in recovering TMP and allowed for sustainable operation at 64 LMH for 5 days without exceeding 40 psi. Therefore, a regular maintenance clean can be effective at maintaining a sustainable fouling rate, particularly in the case of a high biopolymer concentration. Consequently, a chemically enhanced backwash could potentially be a useful fouling mitigation tool.

Overall, the outcomes of this experiment and the many previous attempts to operate at the determined sustainable flux for many days were not successful despite trying several different operating procedures and fouling control measures. Unfortunately, this made it difficult to compare the operation of the ceramic and polymeric membrane at their respective sustainable fluxes as had been initially planned.

6.3.2 Discussion on the limitations of the sustainable flux method

There are a few hypotheses as to possible reasons that may be contributing factors to the sustainable flux method not working in this scenario:

- Different hydrodynamics for the polymeric membrane, which is a submerged module.
- The rate of irreversible fouling is not constant or that it is exponential or cumulative.
- The backwash procedure.
    - Possibility that high pressure backpulse used for the ceramic membrane allows it to be more effective, which delays the onset of fouling during the sustainable flux experiments and thus overestimates the sustainable flux.

The sustainable flux method approach that is used in these experiments accounts for both reversible and irreversible fouling. At lower fluxes the TMP increases very little during each cycle, which indicates minimal reversible and irreversible fouling, and little to no TMP is recovered after backwash (some of the TMP increase between cycles during a flux stepping experiment is simply the result of the increased membrane resistance at higher operating fluxes). However, at higher fluxes, the majority of fouling is in fact hydraulically reversible and often the rate of this reversible fouling is so high that a consistent flux is difficult to maintain and the pump reaches its maximum speed very rapidly. Therefore, in this case, it is difficult to differentiate between the two types of fouling. The importance in differentiating between the two types of fouling can be seen from the model solution experiments in which the combination ABHS had an extremely high rate of hydraulically reversible fouling but little to no hydraulically irreversible fouling (Figure 5.5). Since the rate of hydraulically irreversible fouling was so small for ABHS, the flux could potentially be sustained over longer

filtration times. Consequently, a different approach that only accounts for hydraulically irreversible fouling could potentially be used.

A closer look at the mathematical approach to determining the sustainable flux indicates that the mathematical approach is not the underlying issue. For example, the only flow that was capable of sustaining acceptable fouling rates over 5 days without any intervention was at 32 LMH (5 mL/min) during experiment #4 (Figure 6.4). From Figure 6.3 it can be observed that this flux is on the extremely low end of the "below sustainable flux" curve. Similar results are observed for experiment #6 in which only a flux of 64 LMH (10 mL/min) could be sustained for 5 days but with the use of regular maintenance cleans (Figure 6.7 and Figure 6.8). The water quality of both of these was, however, quite different (discussed in Section 6.3.3). Therefore, a more sensitive mathematical approach would not necessarily have identified these lower fluxes as the sustainable flux. However, since there is more fouling occurring at higher fluxes, it may be beneficial to incorporate more data points by decreasing the flux increments at these higher fluxes. Thus, a more detailed fouling curve can be obtained if the sustainable flux required needs to be more precise.

A possible alternative to this method would be to run at a particular flux over several cycles (as opposed to only one cycle), and doing this at several fluxes. This way a more representative picture of the fouling occurring can be obtained and rates of reversible and irreversible fouling can be calculated at different fluxes. The downside would be that this approach would take much longer and whether or not a chemical cleaning between each flux is needed would need to be considered. This method was not tested due to time constraints. However, the data obtained from the long-term experiments could be used to explain how such an approach might work.

The membrane resistance following backwash can be calculated from the first few cycles of each long-term experiment, thus giving the rate of irreversible fouling. The idea is that by determining the rate of irreversible fouling, an estimate can be made on the number of filtration hours that would have to occur before reaching a specific transmembrane pressure (or target TMP), at which a chemical cleaning would be required. In order to estimate the fouling behavior, a linear relationship (i.e. rate of fouling) is assumed. In this case, the estimated time to reach a specific or target TMP can be compared to the actual results of the long-term experiments at different fluxes (Table 6.2). The figures for the fouling rate estimations are included in Appendix D (Figures 10-16). For the long-term

sustainable flux experiment (LTJ) #4, at a flux of 128 LMH (20 mL/min), it was estimated that approximately 20 hours of filtration would be needed before reaching 50% of the ceramic membrane's maximum operating transmembrane pressure or 72.5 psi (5 bar). The actual time it took to reach that pressure was approximately 12 hours. At a flux of 64 LMH (10 mL/min), the predicted time to reach 72.5 psi was closer to approximately 100 hours, with the actual time being approximately 60 hours.

For some experiments (e.g. LTJ #4 at 32 LMH, LTJ #5 with 15 minute filtration cycles, and LTJ #5 at constant pump), the target TMP (i.e. 50% of the ceramic membrane's maximum operating TMP of 72.5 psi) was not reached within the filtration time available. Furthermore, during LTJ #5, different fouling mitigation techniques were used in addition to regular hydraulic backwashes, such as the 6-BW sequence and maintenance cleans. Therefore, if the target TMP was lowered (and before these additional fouling mitigation techniques were used), then an estimate could be compared to the actual results. As a result, a target TMP of 30 psi was chosen for LTJ #4 at 32 LMH and LTJ #5 with 15 minute filtration cycles, and a target TMP of 10 psi for LTJ #5 at the constant pump setting. The fouling rate predictions and the actual fouling data are summarized in Table 6.2. Additionally, to assess this estimation technique, the difference between the predicted value and the actual results is included.

Table 6.2: Fouling rate prediction using membrane resistance after backwash

	Experiment	Flow in mL/min (Flux in LMH)	Target TMP to reach (psi)	Predicted (h)	Actual (h)	Difference
LTJ #4	Attempt #1	20 (128)	72.5	20	12	+8
	Attempt #2	10 (64)	72.5	100	60	+40
	Attempt #3	5 (32)	30	53	100	-47
LTJ #5	Attempt #1	10 (64)	72.5	15	12	+3
	Attempt #2: 15-min filtration cycle	9 (58)	30	33	18	+15
	Attempt #3: constant pump setting	9 (58)	10	7	12	-5
LTJ #6		17 (109)	72.5	31	10	+21

LTJ: Long-term sustainable flux experiment; All experiments have 30 minute filtration cycles unless otherwise stated

From Table 6.2, it is apparent that this fouling rate prediction method tends to overestimate the amount of filtration time before reaching a specific transmembrane pressure. This is likely the result of the method assuming a linear fouling rate, which is not valid as the fouling rate increases. Therefore, the fact that this method only accounts for irreversible fouling to predict long-term fouling has its limitations as well. However, it does give a relative indication of when severe fouling will occur.

Ultimately, the root cause for the unsuccessful application of the sustainable flux method to the tubular ceramic membrane is still unknown.

6.3.3 Rejection of different NOM fractions in surface water

The water quality of the different experimental runs is summarized in Table 6.3. The LC-OCD chromatogram of the raw water for all the experimental runs is shown in Figure 6.9. Additional LC-OCD chromatograms for permeates during experiment #3 and #5 are included in Appendix D (Figures 17 to 19).

Table 6.3: Summary of raw water quality for all experimental runs*

	#1	#3	#4	#5	#6
pH	7.5	8.2	8.77	8.1	8.15
Turbidity (NTU)	0.84	3.18	3.61	7-11	2 - 3
TOC (mg C/L)	6.5	7.1	6.2	6-13	7.2
DOC (mg C/L)	5.5	6.7	5.5	6-11	7.08
Alkalinity (mg $CaCO_3$/L)	198	180	170	160	168
Hardness (mg $CaCO_3$/L)	230	220	230	220	200
Conductivity (mS/s)	600	595	620	589	635
Biopolymers (µg C/L)[1]	495	661	215	188	844
Humics (µg C/L)[2]	3324	3856	3664	3134	3457
SUVA (L/mg.L)	3.5	3.65	4.19	3.3	2.76
% Protein in biopolymers	26	27	n.q.	n.q.	10

* Experiment #2 is not included due to a high level of contamination present in the river water
[1] Average biopolymer concentration of the raw waters is 481 µg C/L
[2] Average humics concentration of the raw waters is is 3487 µg C/L
n.q. not quantifiable (<1 ppb calculated)

The water quality for experiment #1, which was performed in July 2011, was typical for Grand River water, with an average biopolymer concentration, but with a very low turbidity. The humics concentration was slightly below average (Table 6.3).

The water for experiment #3, taken during September 2011, had a relatively high concentration of biopolymers (with ~25% of it proteins – similar to experiment #1) and an average turbidity. It also had the highest humics concentration of all waters (Figure 6.10).

Although the turbidity for experiment #4, taken during November 2011, was relatively similar to experiment #3, the biopolymer content was almost 70% less and there was no protein detected; therefore, this may have been a contributing factor to the higher sustainable flux value obtained in experiment #4 (141 LMH vs. 109 LMH).

The raw water for experiment #5, taken during January 2012, had a relatively low biopolymer concentration (similar to that for experiment #4), however, for most days it also had an unknown peak in the low molecular weight region (Figure 6.11). Assumingly, this is from some contamination in the Grand River water, and it also seems to be declining the longer it is stored (i.e. with each consecutive day). Experiment #5 also had the lowest humics content and a very high turbidity.

Water for experiments #4 (November) and #5 (January) were both taken in winter and both had low biopolymer concentrations compared to the other experiments and no protein content. However, the turbidity was much higher in experiment #5 compared to #4 and overall.

Water for experiment #6, which was taken during April 2012, had the highest biopolymer concentration with 10% coming from proteins (Figure 6.12).

Although adjustments to the setup were still being made during experiments 1 and 3, interesting results were obtained regarding rejection of NOM fractions with the tubular ceramic membrane.

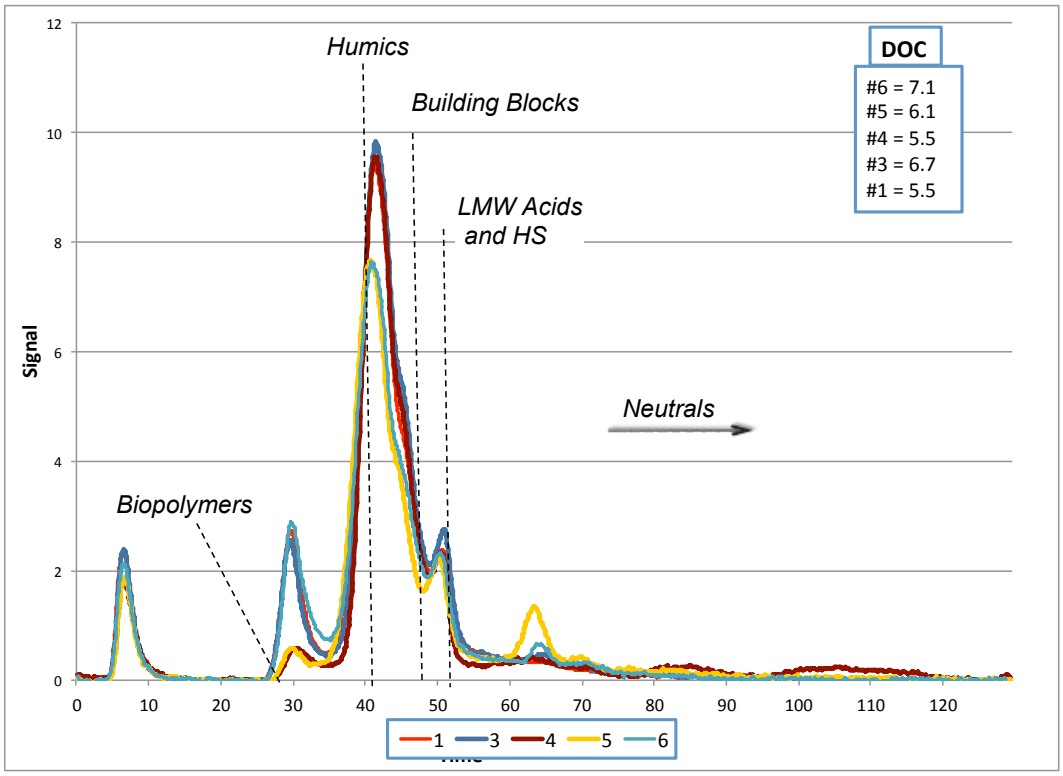

Figure 6.9: LC-OCD chromatograms of raw waters for all experiments

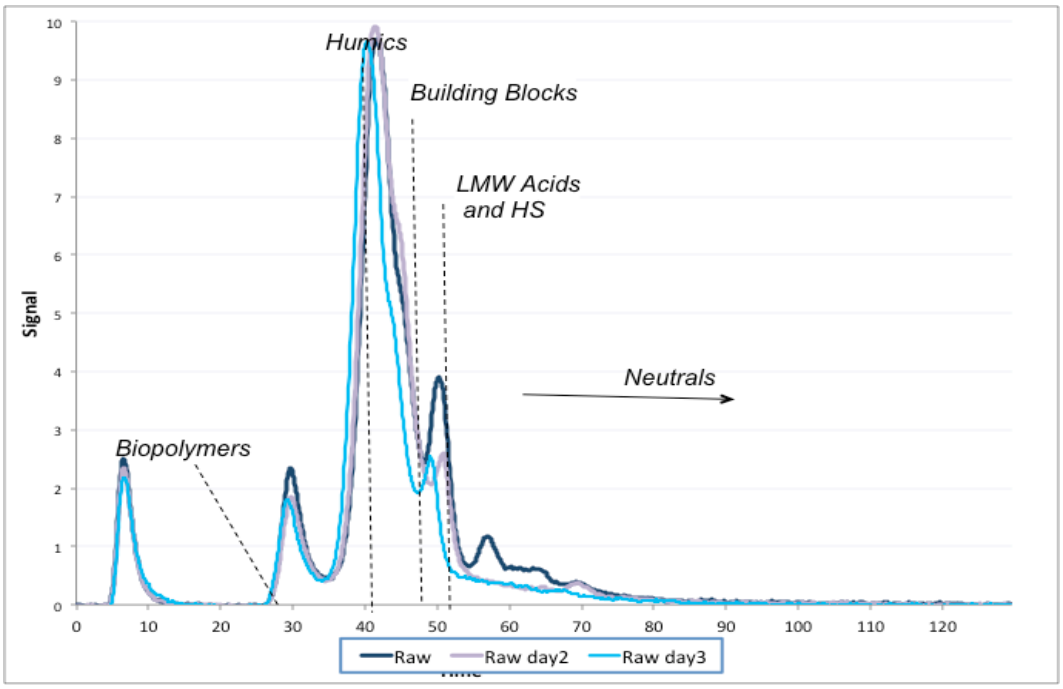

Figure 6.10: LC-OCD chromatograms for raw water during experiment #3

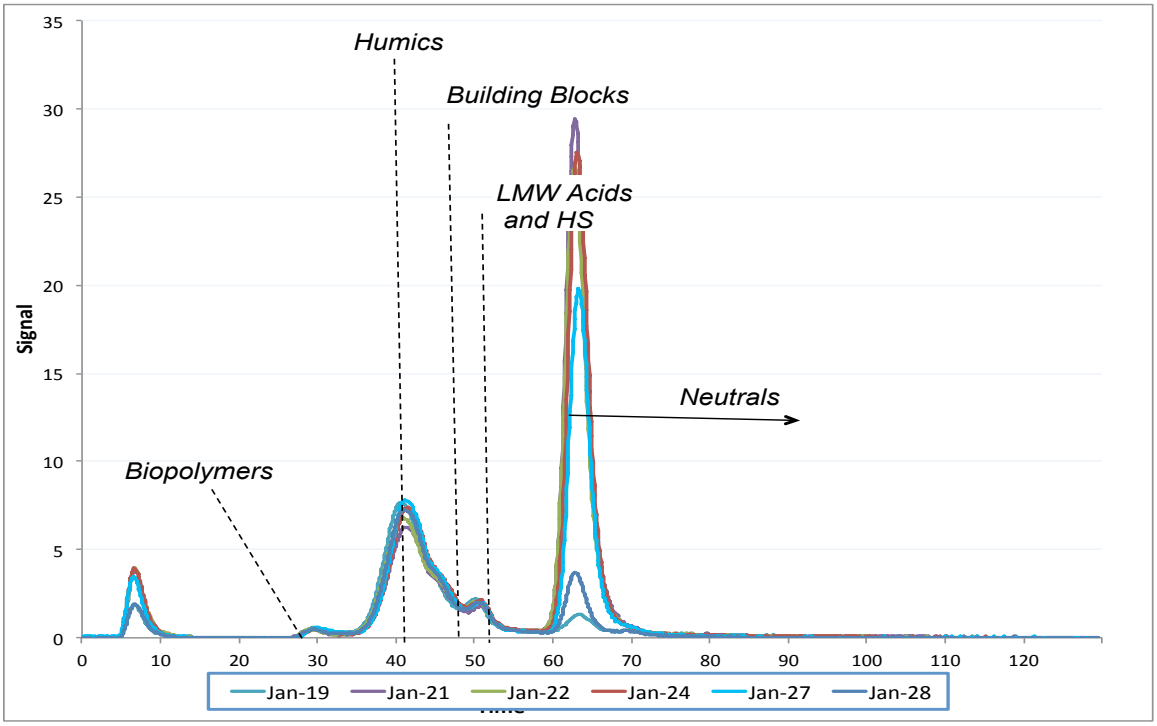

Figure 6.11: LC-OCD chromatograms for raw water in experiment #5

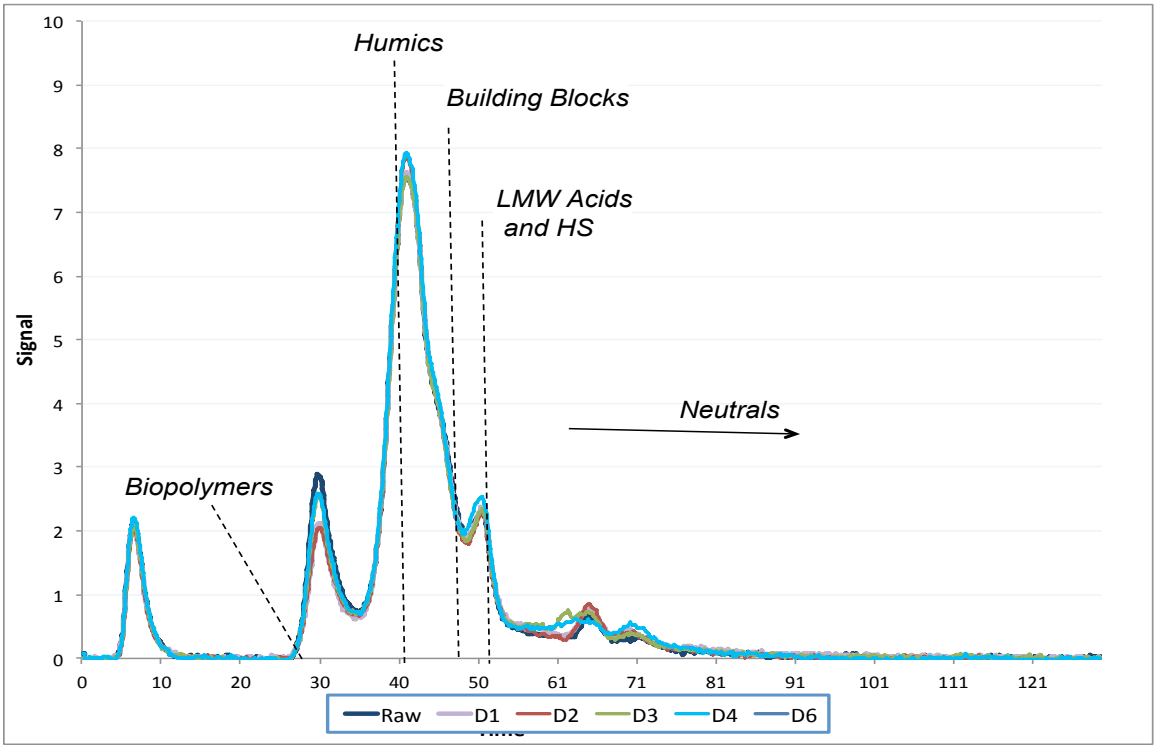

Figure 6.12: LC-OCD chromatograms for raw water during experiment #6 (D: Day)

6.3.3.1 NOM rejection

In experiment #1 a significant finding was the extremely high removal of all the organics during the initial stages of the first cycle (Figure 6.13). This suggests that organics have a strong affinity to the cleaned ceramic membrane surface. The second permeate cycle continued to have a good rejection of biopolymers but showed a drastic decrease for the humics.

In experiment #3, NOM rejection at the beginning and end of the filtration cycle was investigated. The permeates at the beginning of the cycle were taken after a backwash (except for cycle 1, which was after the membrane had been chemically cleaned). Table 6.4 compares the DOC values of the beginning of the first cycle, and the beginning and end of the cycle for subsequent permeates. The first permeate sample taken at the beginning of cycle 1 had a very low DOC (0.85 mg C/L), and thus a very high rejection. The results in Figure 6.14 show the average rejection of different NOM fractions at the beginning and end of the cycle using LC-OCD and confirm the DOC results of Table 6.4. The rejection at the beginning of the cycles showed an average 62% humics removal and 85% biopolymers removal. The difference between the rejection at the beginning and end of cycle was much larger for humic substances and other NOM fractions than it was for biopolymers. By the end of the filtration cycle the rejection of humics declined to below 20% while the biopolymer rejection averaged at 72% and remained relatively consistent. By the end of the cycle there was no removal of building blocks and little low molecular weight removal. The surprisingly high DOC rejections for the humics at the beginning of the cycle may be explained by a removal mechanism of adsorption, which is supported by the results obtained with the model foulant experiments (Table 5.4). Furthermore, the fact that humics rejection was higher at the beginning of the cycle than at the end of a cycle, even after several days of filtration, suggests that the humics adsorption is to some extent reversible (Figure 6.15 and Figure 6.16).

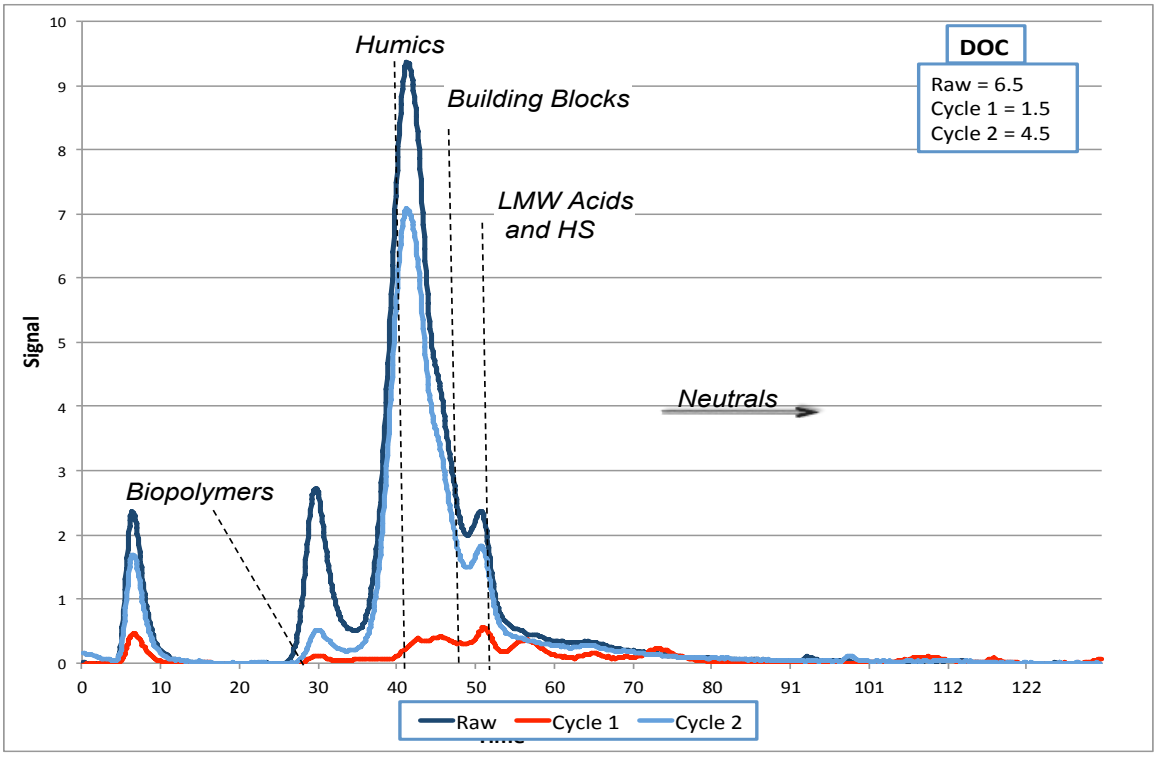

Figure 6.13: Raw and permeate LC-OCD chromatograms for cycle 1 and 2 for experiment #1

Table 6.4: Summary of DOC (mgC/L) values for the permeates

		Average of other permeates	
Raw	**Beginning of 1st Cycle**	**Beginning of cycle**	**End of Cycle**
6.9	0.85	2.5 n=4	6.2 n=6

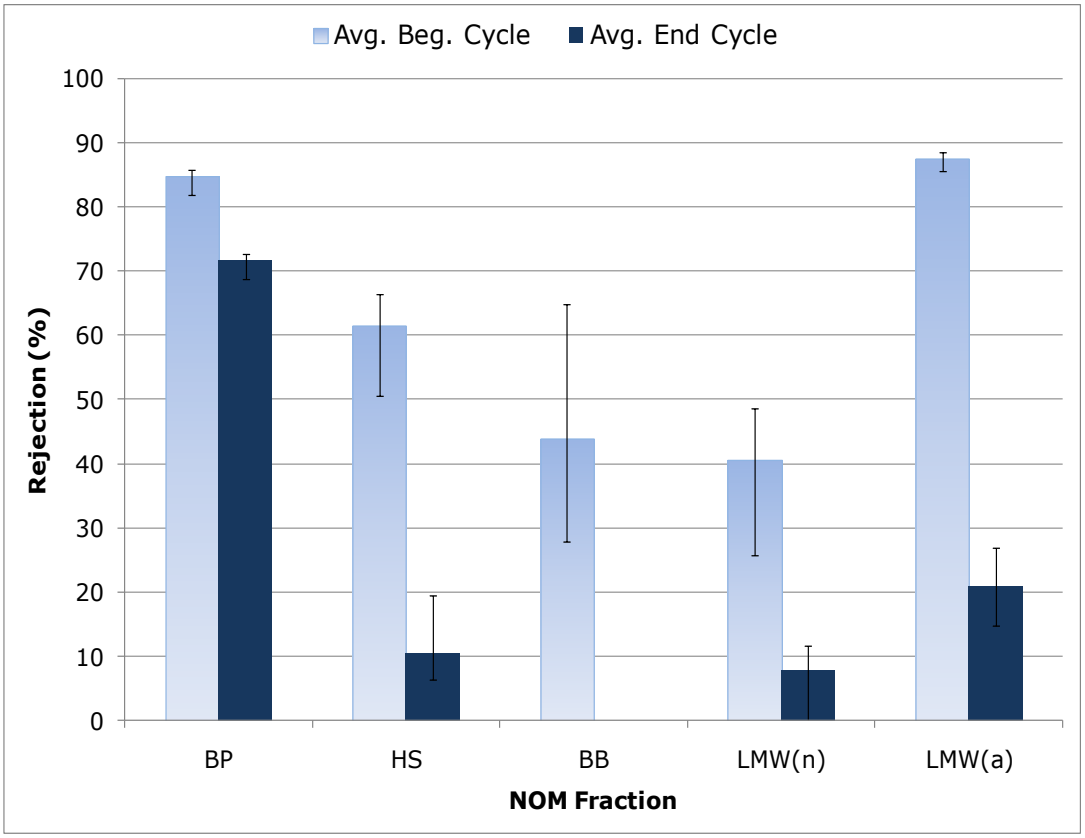

Figure 6.14: Comparison of rejections at the beginning to the end of the filtration cycle for experiment #3.

The error bars indicate range of values (n=3) (cycle 2 and 3, and Day 3). Note that the permeate at the beginning of cycle 1 is not included because it behaves differently than the following cycles as demonstrated in Figure 6.13.

The general rejection trend over time was characterized by a very high rejection for all NOM fractions in the first cycle, followed by a decreased rejection in subsequent cycles and days (Figure 6.15 and Figure 6.16). The extremely high rejection during the first cycle was also observed in the sustainable flux experiment #1 (Figure 6.13). Although the humics rejection at the beginning of the cycle continued to decrease with each filtration cycle, the biopolymer rejection remained relatively stable throughout the cycles, suggesting that the likely removal mechanism is through size exclusion.

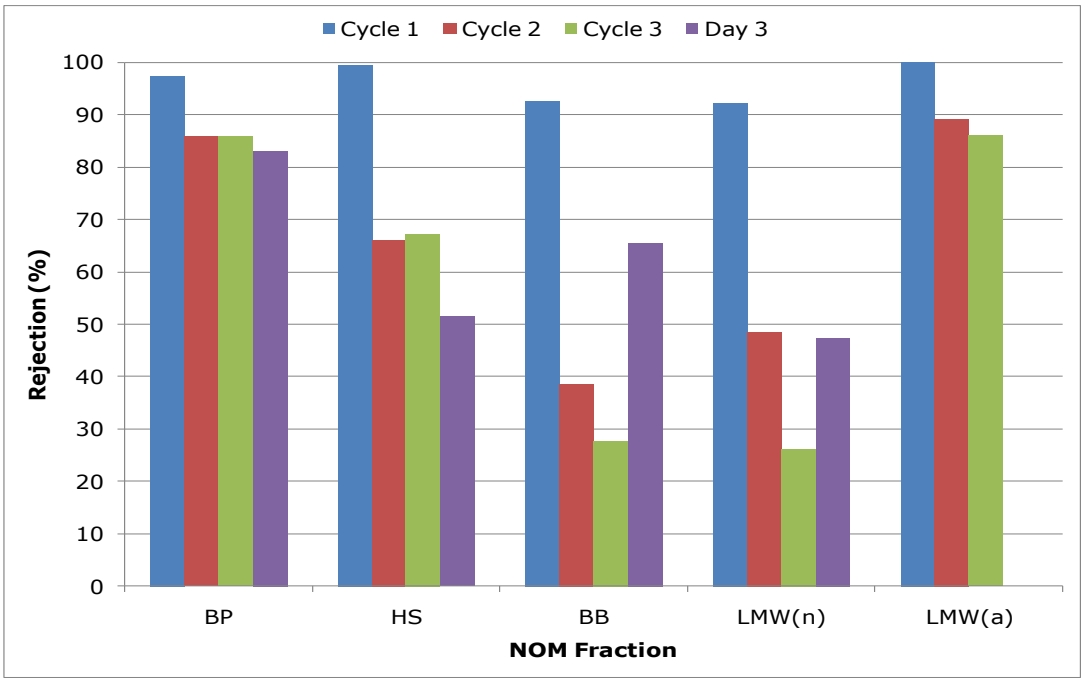

Figure 6.15: Rejection at the beginning of the cycle during experiment #3

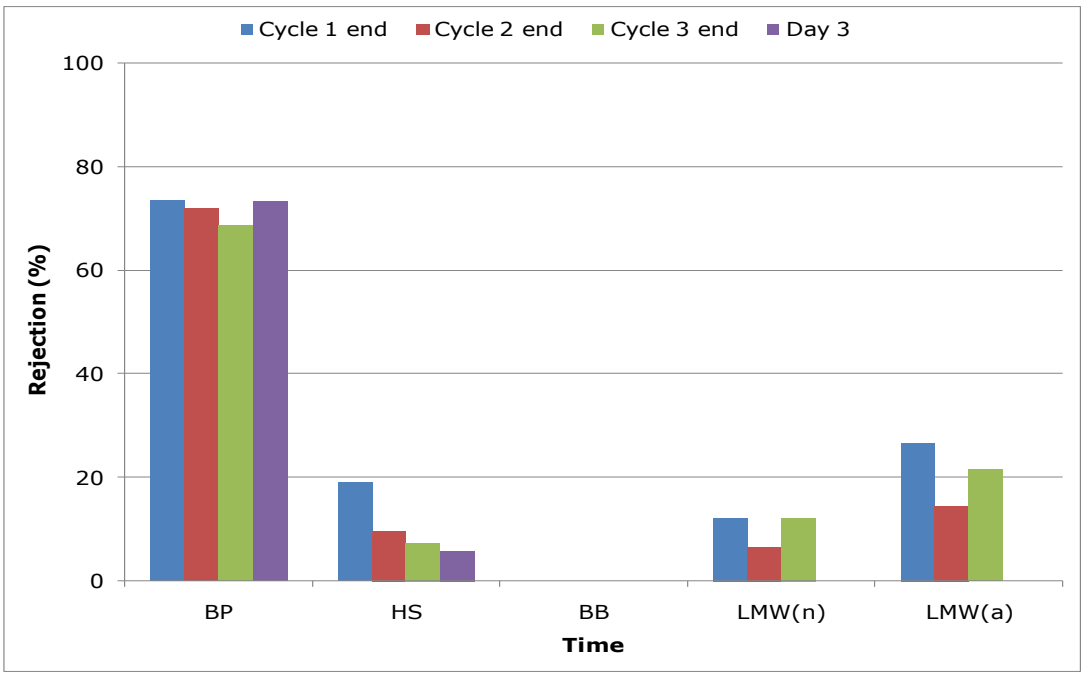

Figure 6.16: Rejection at the end of the cycle during experiment #3

The rejection results for experiment #5 were taken during the 15 minute filtration cycle run (Figure 6.17) and were taken a few cycles after the maintenance clean at the beginning of the cycle. The rejection trends are relatively similar to previous results (Figure 6.14). Therefore, despite the different operating parameters (i.e. shorter filtration cycles), the rejection trends remained consistent. The LC-OCD chromatograms for the permeate during experiment #5 are shown in Appendix D Figure 19.

The rejections of different NOM fractions during experiment #6 is shown in Figure 6.18. All permeate samples were taken during the third cycle after a chemical cleaning (Day 1) or maintenance clean (Day 2 and 3). It can be seen that for Day 1 and 3, the samples that are taken at the beginning of the cycle, the rejection is higher for humics initially. Nevertheless, there is a decrease in rejection from 82% down to 64% from Day 1 to 3, despite the samples being taken during a similar time window of a filtration cycle. This suggests that the maintenance clean, although effective, cannot fully remove humics adsorption. Therefore, there is likely a diminishing rejection with each consecutive cycle after a maintenance clean, which over time, even with regular maintenance cleans could ultimately lead to a need for a full chemical cleaning. Furthermore, after the first 5 minutes of filtration, the humics rejection dropped below 50%. This trend supports the results observed in previous experiments (Figure 6.14). Additionally, biopolymer rejection was consistently high between days and throughout the filtration cycle, and considering that the water collected for experiment #6 had the highest biopolymer concentration of all the experiments, the theory of rejection through size exclusion is supported.

The rejection results for natural waters with tubular ceramic membranes are somewhat similar to the results obtained with both flat-sheet and tubular ceramic membranes using model solutions. Compared to the flat-sheet experiments, humics had a lower rejection than BSA or alginate. With the tubular experiments all model foulants showed a very high rejection, however, humic acid rejection seemed to have a decreasing trend (Table 5.4).

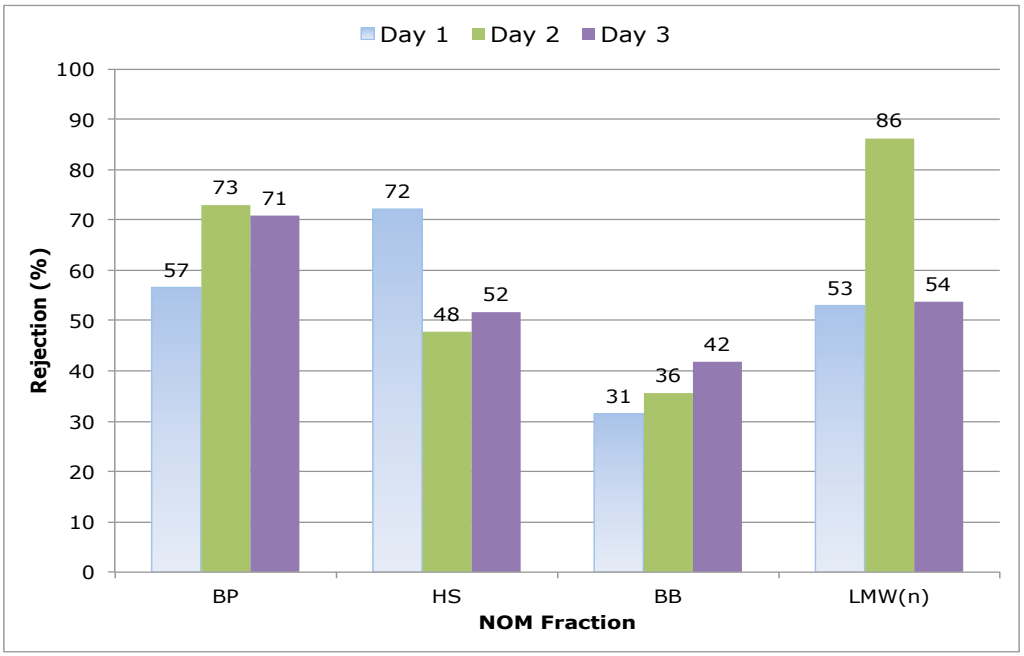

Figure 6.17: Ceramic rejection of different NOM fractions during experiment #5 with a 15 minute filtration cycle

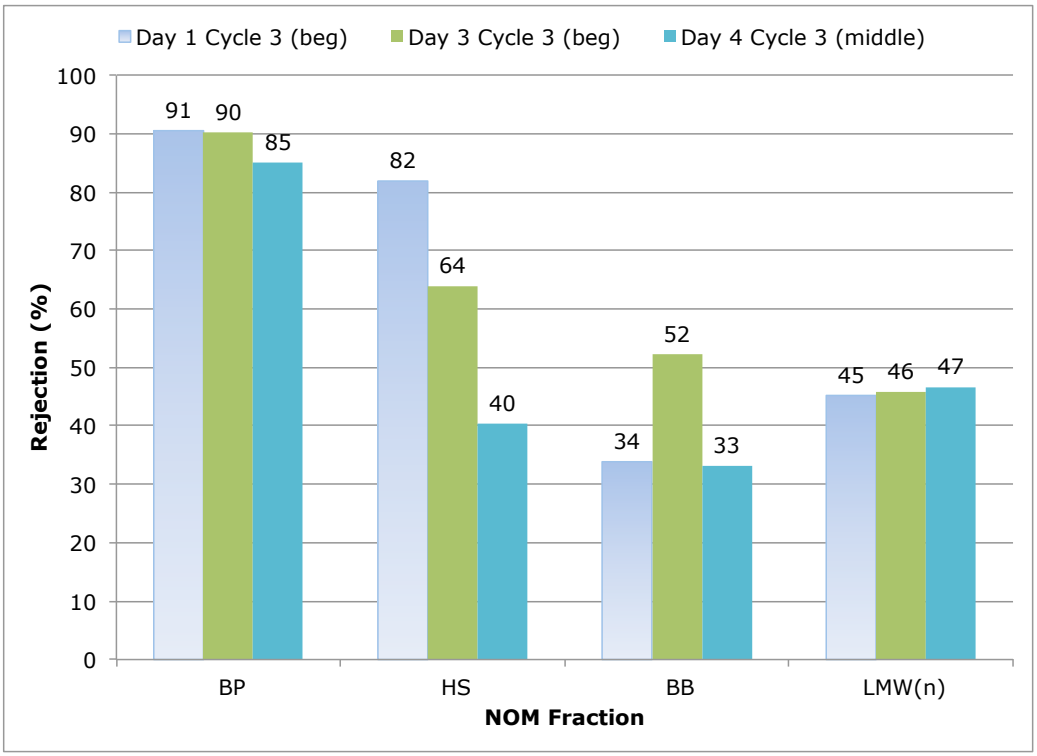

Figure 6.18: Rejection for experiment #6

Beg: beginning which is 1-4 minutes into filtration cycle; middle is 10-13 minutes into filtration cycle

Overall, the main conclusions that can be drawn from the LC-OCD results of the permeate are:

- The first filtration cycle has very high removals of all organic fractions, which suggests that there is a strong affinity of organics onto virgin ceramic membrane.
- Biopolymer rejection is stable and high throughout all filtration cycles, which indicates that size exclusion is likely the dominant removal mechanism.
- The removal of humics is much higher during the first cycle and at the beginning of each filtration cycle (following a backwash).
    - Rejection decreases from the beginning to the end of the filtration cycle and with each day.
    - Adsorption is likely the most dominant removal mechanism.
    - Some adsorption is reversible.

6.3.3.2 NOM in backwash

The backwash water was analyzed to determine which NOM components are removed with a hydraulic backwash. Table 6.5 summarizes the result from experiment #3 and shows that the composition of the backwash water remained relatively consistent. However, the first backwash is different and has less than half the DOC of the later backwashes. This trend is also consistent with the increased rejection observed in the first cycle. There is also a possibility that the membrane is initially conditioned with the foulants and eventually the cake layer builds and thus the backwash is more effective in subsequent cycles.

The biopolymer and humics fraction do seem to be slightly increasing over time (Figure 6.19 and Table 6.5). As discussed for Figure 6.14, the backwash can impact subsequent rejection in early stages of filtration, particularly for humics. However, the biopolymers were the least affected and the rejection remained consistent between and throughout cycles, which was also indicated by the constant concentration of biopolymers in the backwash water after the initial 2 cycles (Table 6.5).

Table 6.5: The %NOM for different fractions in the backwash water for experiment #3*

		Cycle				
	Raw	**1**	**2**	**3**	**Avg of BW after cycle 3[1]**	**Std. deviation**
DOC (mg/L)	6.9	1.3	2.9	2.9	3.2	0.2
Biopolymers (%)	9	18	25	28	28	1.1
Humics (%)	58	31	33	36	38	2.4
Bldg. Blocks (%)	11	7	9	9	9	0.7
LMW (n) (%)	12	13	12	14	8	2.6
LMW (a) (%)	2	0	0	0	0	0.3

* The hydrophobic portion of organic matter is not included, therefore, the organic matter fractions listed here do not add up to 100%

[1] n=4

The LC-OCD results of the backwashes for experiment #5 with a 15 minute filtration cycle are shown in Figure 6.20. Unlike previous results with 30 minute filtration cycles (Figure 6.19), this experiment showed similar biopolymer concentrations in the backwash water and the feed water. Therefore, it is possible that the biopolymers did not concentrate as much during the 15 minute filtration cycle. Additionally, the biopolymer concentration for the water in experiment #5 was the lowest (Table 6.3).

The LC-OCD backwash chromatograms for experiment #6 are shown in Figure 6.21, which shows higher biopolymer and humics removal at the beginning of the day. The concentrations are summarized in Table 6.6. These were single measurements, therefore, a significance test could not be performed. The result suggests that either there is less adsorption occurring on the membrane surface later on in the day or the backwash becomes less effective. Note that for all backwashes in this experiment, the feed channel water was not extracted prior to backwash (unlike experiment #4). Therefore, the concentration of biopolymers in the feed channel partially contributes to the elevated concentration of biopolymers observed in the backwash. Furthermore, there is probably very little of humics being removed during backwash. Figure 6.22 shows that the feed channel water does not have an increased concentration of humics compared to that of the raw water. Therefore, the decreased concentration of humics in the backwash compared to the feed water is likely simply a result of dilution, since the backwash is done with ultrapure water.

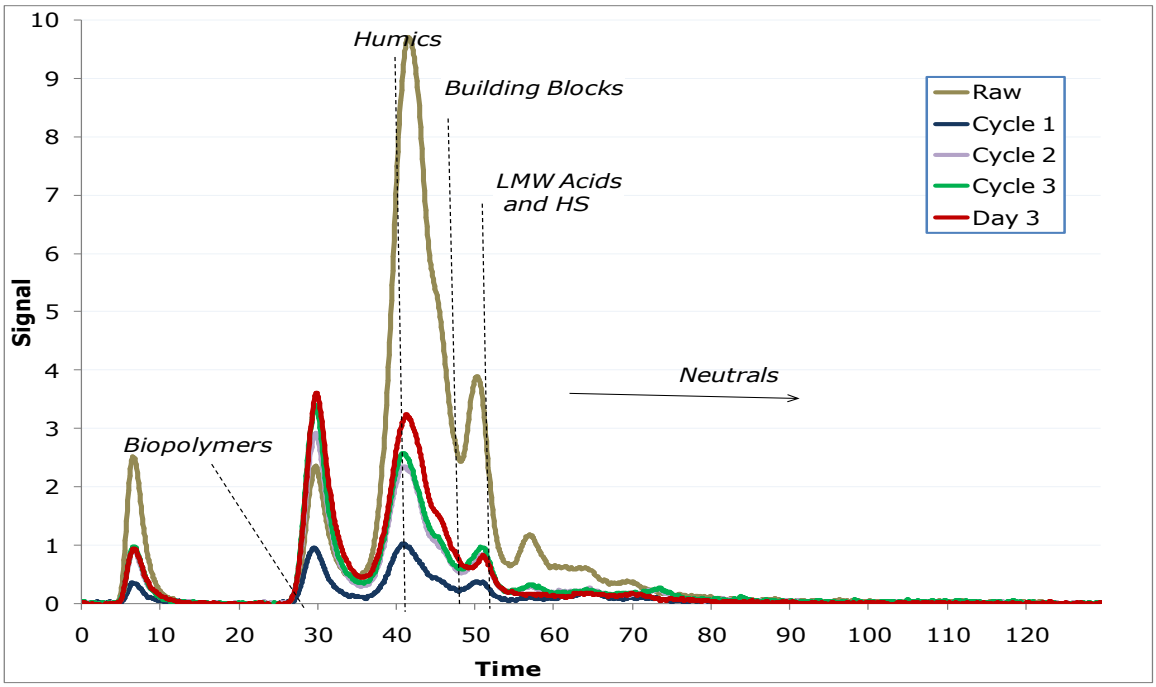

Figure 6.19: LC-OCD chromatograms for backwash water in experiment #3

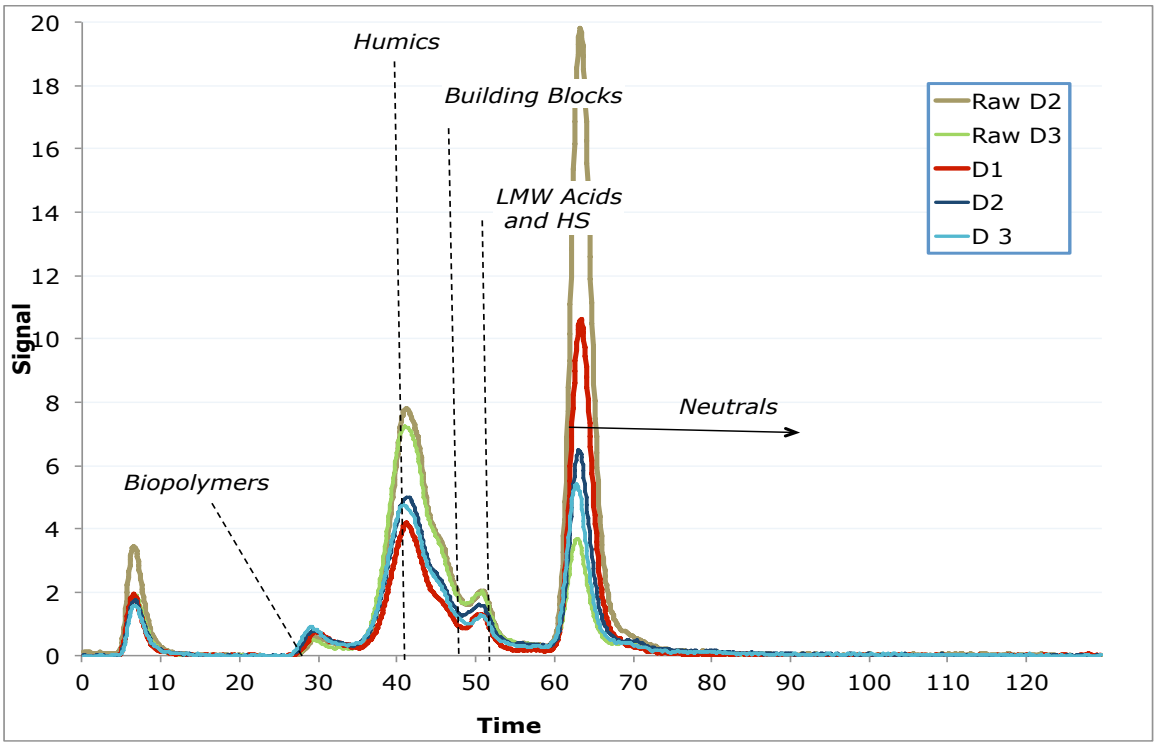

Figure 6.20: LC-OCD chromatograms for backwash water during experiment #5 with a 15 minute filtration cycle. *D: Day*

Table 6.6: Concentration of biopolymers and humics in ugC/L in the backwash water at the beginning and end of the day for experiment #6

	Day 1			Day 3		
	Raw	*Beginning*	*End*	*Raw*	*Beginning*	*End*
Biopolymers	655	3579	3192	734	4057	2430
Humics	3412	2145	1760	3449	2812	1186

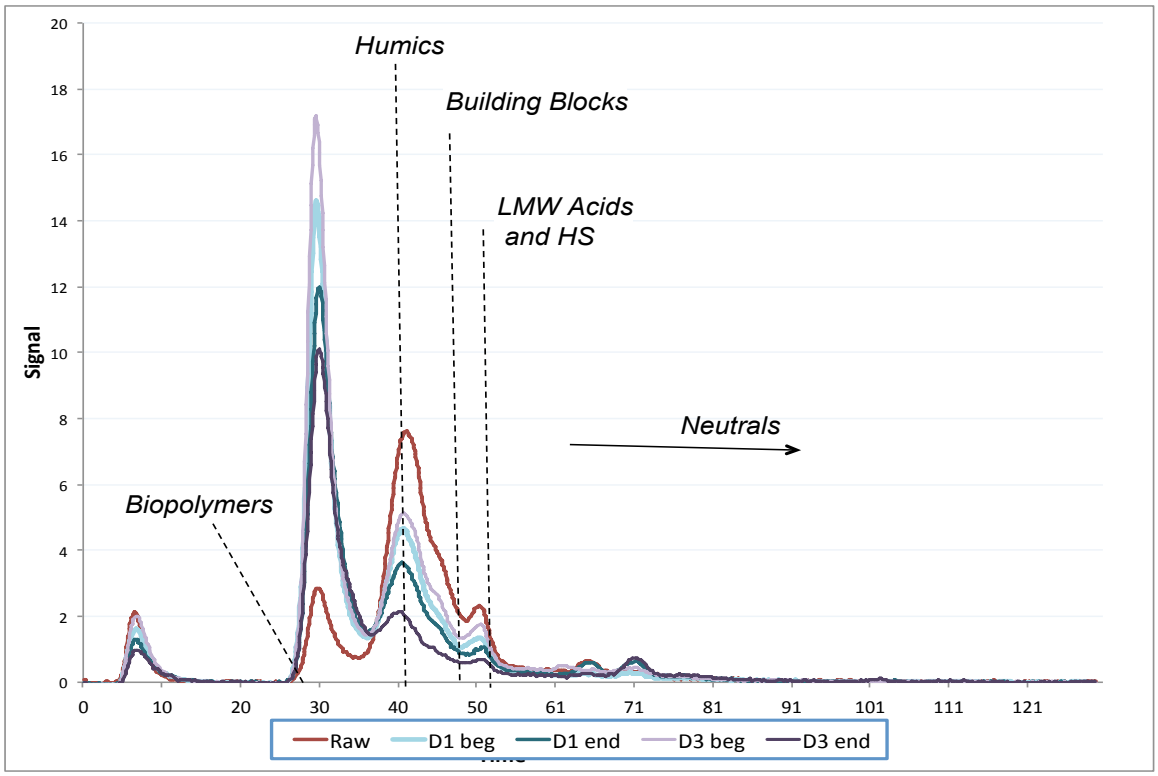

Figure 6.21: LC-OCD chromatograms for backwash water in experiment #6

Beg: Beginning; and D: Day

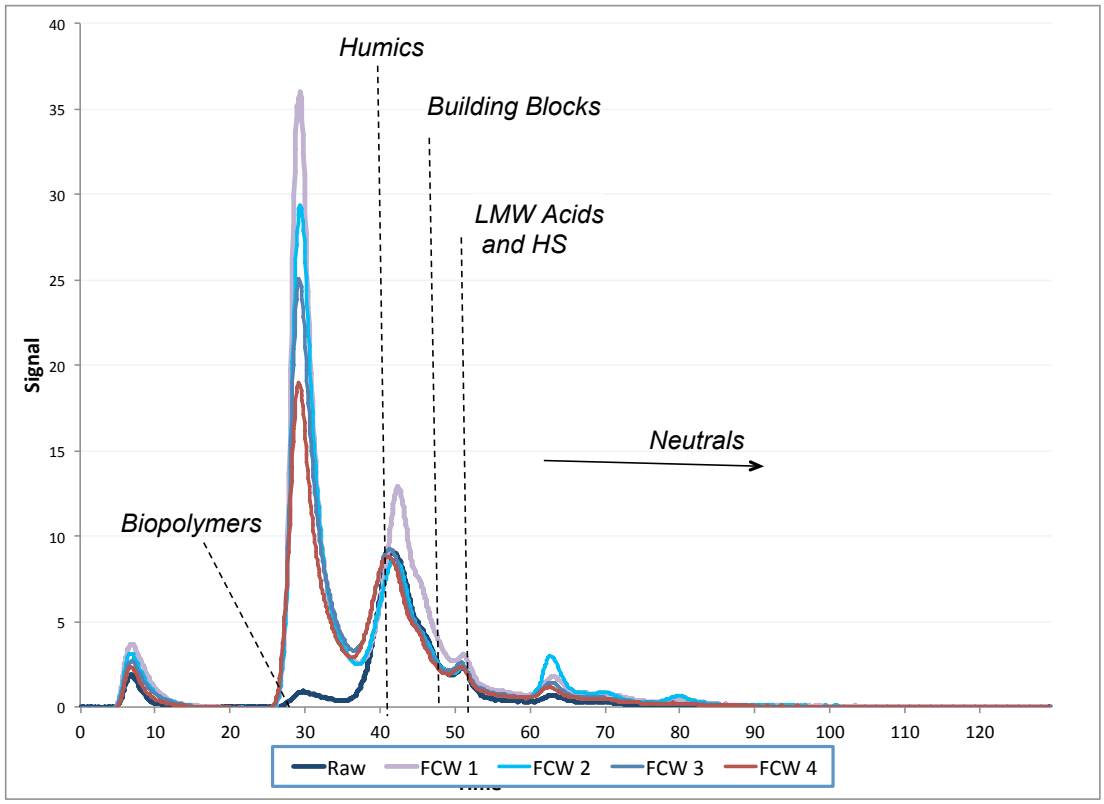

Figure 6.22: LC-OCD chromatograms for feed channel water during the mass balance in experiment #4

FCW: Feed Channel Water

Overall, the main conclusions that can be drawn from the LC-OCD results of the backwash water are as follows:

- Overall backwash composition remained relatively consistent.
- Shorter filtration cycles seemed to minimize biopolymer accumulation in the feed channel water.
- Humics adsorption is partially reversible.
- Biopolymers concentrate in the feed channel water.

6.3.4 Mass balance

A mass balance was performed during experiment #4. In order to quantitatively evaluate the changes occurring during the initial stages of filtration, samples were taken from the first 4 cycles of filtration during Day 1. The approach is described in detail in Section 5.2.4.

Unfortunately, the first cycle had a citric acid contamination from the last cleaning step (of the chemical cleaning) and its peak is in the same range as that of the humic peak (at 43 minutes); this was the first time that this occurred. Therefore, it is best to disregard cycle 1 for this the mass balance as it skews the results. The biopolymer concentration of this raw water was also much lower than previous experiments. However, this was expected since the experiment was run during November and in the past, biopolymer concentrations for this water have been shown to be lower during the winter months (Peldszus *et al.* 2012).

It is also important to note that after Experiment #3 the backwash tank was changed, which allowed the backwash pressure to be increased from 40 psi to 70 psi.

Obtaining good mass balance results can be challenging due to many possible sources of error arising from sampling to instrumental error. One example is, in order to extract feed channel water prior to backwash, which would include mass of organic matter that was rejected but not adsorbed on the membrane, required the use of a syringe. This might inadvertently result in some permeate being pulled back from the housing and through the membrane into the feed channel, which may slightly simulate a backwash. Furthermore, the very small volume available (10 mL or less), restricted the analysis that could be performed; only LC-OCD analysis could be performed since it requires less sample volume but could also provide DOC values.

From the mass balance results shown for biopolymers and humics (Figure 6.23), several interesting observations can be made. Biopolymer concentrations in the permeate remained constant at around 30% in all cycles, which is consistent with previous rejection results. The irreversible fouling remained within the same range for all cycles. Only a small proportion of biopolymers contributed to irreversible fouling (4-10%), and is therefore likely getting irreversibly incorporated into the fouling layer. The biopolymer concentration in the feed channel water (FCW) increased with each cycle, suggesting that biopolymers contribute less and less to membrane fouling, because if it is in the

retentate, then it is not part of fouling. This increase is mirrored by a decrease in the concentration of biopolymers in the backwash water indicating that reversible fouling is decreasing rapidly within the first few cycles.

Humics were mostly present in the permeate as was reflected in previous results, showing very low rejections (Figure 6.14). The much lower rejection of humics for surface water as compared to the model solution results (Table 5.4) is likely due to a function of both a higher concentration and flow for the surface water experiment. Additionally, the composition and characteristics of the humics in the model solution will differ from the humics in surface water and may be larger in size. Furthermore, the humics concentrations are also much higher than the biopolymer concentration in the feed water (Table 6.3), therefore, the mass involved in the reversible fouling for humic acids is higher than the mass of the biopolymers involved in reversible fouling. Also, there is no negative number, meaning that the total mass measured in the permeate, backwash, and FCW add up to less than the total feed mass.

The FCW generally had similar concentrations to the raw water of all organic components except the biopolymers (Figure 6.22). The biopolymer concentration was much higher in the FCW than the raw water as opposed to humics, which were lower in the FCW than the raw water (Figure 6.22). This suggests that the biopolymers were being rejected and becoming highly concentrated in the feed channel. It seems that the majority of the biopolymers were not adsorbed or incorporated in the fouling layer; they were simply rejected (Figure 6.23). This further suggests humics adsorption and that the biopolymers are largely rejected through size exclusion and likely do not contribute significantly to fouling.

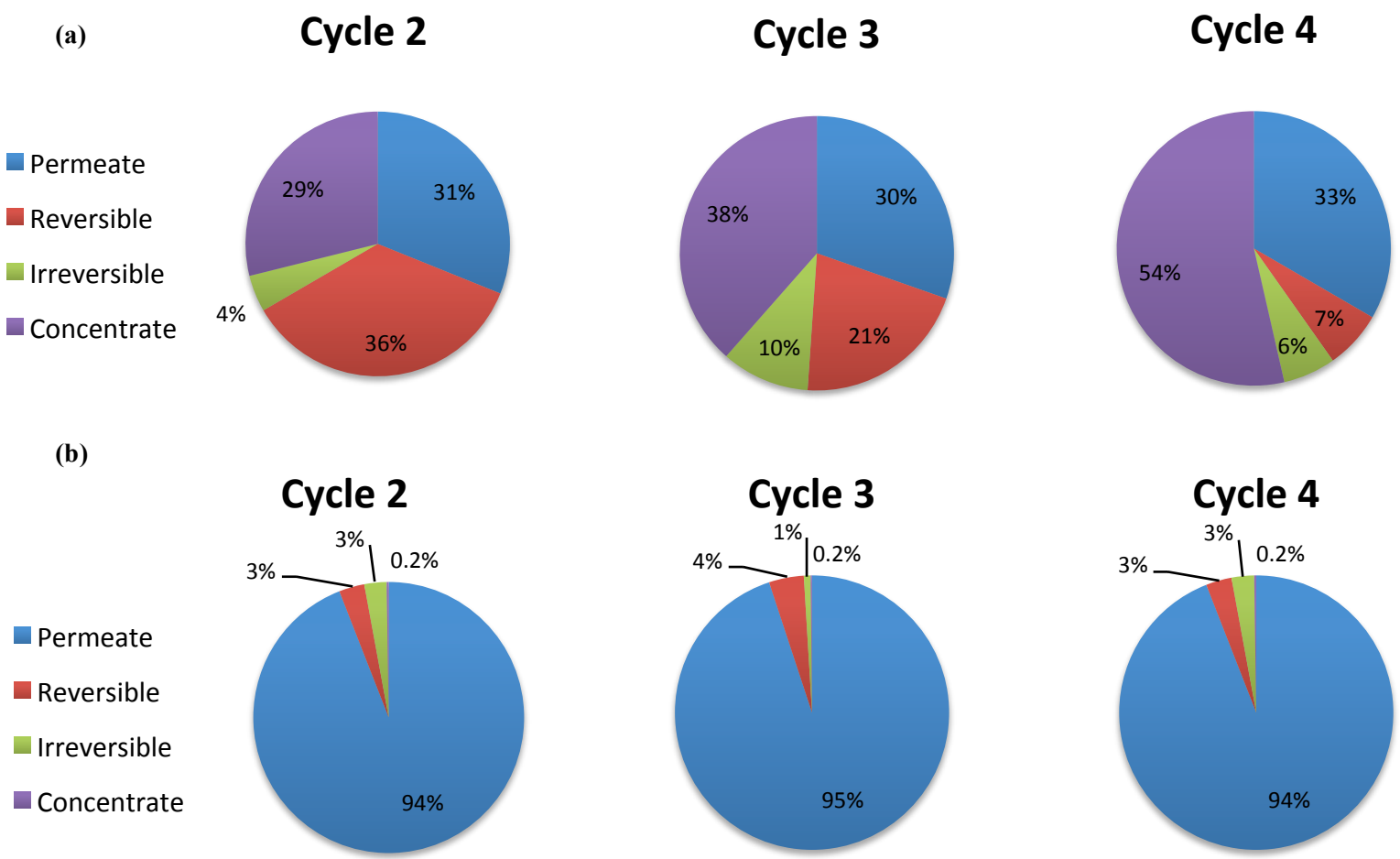

Figure 6.23: Mass balance results for biopolymers and humics with LC-OCD analysis of natural waters in experiment #4. a) Biopolymers b) Humics

6.4 Conclusions

Despite both setup and operational optimization, the sustainable flux method established earlier with a polymeric membrane did not work for this tubular ceramic membrane under the conditions employed or for the same polymeric membrane with highly turbid water. Considering that the underlying concepts behind determining the sustainable flux for a particular membrane and water quality are conceptually sound, and the results should be water and membrane specific, this outcome was unexpected. Consequently, there still remains a need for further investigations into the different factors or variables that need to be included or considered when developing a procedure to determine sustainable flux. Furthermore, this may help in determining the underlying causes or reasons why the sustainable flux method established from the factorial experiment was not applicable for all membranes or water qualities.

From these results, several conclusions can be made:

- Biopolymer rejection was constant throughout cycles and between days, implying size exclusion, which is consistent with the results from the model solution experiments.
- There is a very high initial rejection of all organic matter at the onset of filtration indicating a high affinity of organics to the virgin ceramic membrane surface.
- Humic acid rejection decreased throughout each filtration cycle and increased after backwash. This points to at least in some part reversible fouling behavior. Humic acid model fouling reversibility was generally low but improved with the 6-BW sequence, which confirms the slight reversibility of humic acid adsorption. Note that the humic acid in the model fouling is from Aldrich and the composition and characteristics of surface water humics can vary greatly.
- The 6-backwash sequence proved to be most effective for a highly turbid water with a lower concentration of biopolymers.

Ultimately in full-scale operation, the water quality will often vary from day to day or season-to-season, especially if the primary source is surface water. Thus, operating at a sustainable flux may require constant readjustment, which may not be practical in full-scale treatment plants. Therefore, the ability to employ fouling mitigation tools such as more frequent backwashes (i.e. shorter filtration

cycles), several consecutive backwashes, or a maintenance clean without compromising membrane integrity or performance is vital to long-term sustainable operations.

Chapter 7
Summary, Conclusions and Recommendations

The results of the work discussed in this thesis largely focused on identifying foulants of concern for a ceramic ultrafiltration membrane that are often present in surface water using both model solutions and surface water.

The research presented in this thesis is divided into four main stages. The first stage involved an investigation of different approaches to determine sustainable flux through a factorial design based on three main variables (Chapter 3). The purpose was to establish a method with which to compare the fouling behavior of two different membranes while operating at their own respective sustainable fluxes. This process helped identify which variables were most influential for sustainable flux determination. The aim was to maximize the efficiency of this method to accurately reflect fouling behavior and minimize the amount of time required to determine the sustainable flux. A unique aspect to this method was the incorporation of a backwash step, which is generally not included but common practice in full-scale drinking water treatment plants. By including a backwash between flux steps, the reversibility of fouling was integrated into the sustainable flux determination.

The second stage investigated fundamental fouling behavior with a flat-sheet ceramic membrane with model solutions, combined with surface characterization (Chapter 4). This step was important because it laid the groundwork for future fouling behavior analysis in more complex scenarios. This is the only stage in which membrane surface characterization was performed, which was not an option for the tubular membrane without sacrificing the membrane. Since the flat-sheet membrane is of the same composition and molecular weight cut-off as the tubular membrane, it can be assumed that the interactions between the foulants and membrane surface would be similar and therefore, the results obtained for the flat-sheet membranes are anticipated to be applicable to the tubular membrane. Nevertheless, hydrodynamic conditions will differ due to configuration and different operating procedures. The model solution experiments investigated three organic compounds (alginate, bovine serum albumin, and humic acid) and an inorganic colloidal suspension of silica. These model foulants were filtered at different pressures for single solutions and at 40 psi for

combinations to simulate likely foulants in a drinking water treatment setting. Additionally, hydraulic backwash and chemical cleaning were investigated to identify hydraulically and chemically reversible and irreversible foulants.

The third stage investigated the same model compounds used in Chapter 4 but with a tubular ceramic membrane employing constant flux, which is closer to membrane operations employed in full-scale practice. The main purpose of this step was to determine if the fouling behavior of these model solutions was similar in both the flat-sheet and tubular membrane configuration (Chapter 5). The results helped identify if representative fouling behavior could be obtained with simpler experiments that could be performed at lower costs and required less time. This stage also serves as an intermediary between the flat-sheet model solution experiments and the tubular surface water experiments.

The fourth and last stage investigated the fouling behavior of a tubular ceramic membrane with surface water (Chapter 6). These experiments built on the fundamental fouling results from Chapter 4 and Chapter 5 to identify foulants of concern that contribute to reversible and irreversible fouling. Different organic fractions were identified with the use of Liquid Chromatography with Organic Carbon Detection (LC-OCD). Natural organic matter in water can be extremely complex and waters with the same total organic carbon can result in different fouling trends. Therefore, the use of the LC-OCD, which can differentiate between different organic matter fractions, was able to highlight the importance of properly characterizing the organic matter present in the water. Additionally, the sustainable flux method established in Stage 1 was attempted with the tubular ceramic membrane. The results were unexpected.

7.1 Summary of findings and conclusions

A summary of conclusions from individual chapters is discussed followed by overall conclusions, which examines the results and concepts derived from the research as a whole in order to identify overarching principles.

The concept of sustainable flux was applied in order to compare the performance of a polymeric and ceramic membrane (Chapter 3). A factorial design was used to develop the sustainable flux method using flux stepping. The following conclusions were made:

- Of the three variables investigated in the factorial design (interval length, increment increase between flux intervals, and the use of backwash between intervals), the interval length and backwash component were identified to be significant through statistical analysis, however, the latter had the most significant impact on the sustainable flux determination.
- An interval length of 30 minutes is needed in the sustainable flux approach to more accurately predict fouling behavior.
- The increment increase between flux steps is the least significant variable for determining sustainable flux.
- Therefore, the sustainable flux method resulting from this stage is flux stepping with intervals of 30 minutes, with a 100% (of initial flux) increment increase in flux between intervals, and a backwash between intervals.
- The sustainable flux methodology was verified using a polymeric ultrafiltration membrane filtering surface water. After the sustainable flux was established, the membrane was operated at this sustainable flux for a 5-day period, in which the transmembrane pressure (TMP) did not exceed 50% of the membrane's maximum TMP.

Four model solutions representing problematic foulants for polymeric membranes in drinking water treatment were filtered through a flat-sheet ceramic ultrafiltration membrane at constant pressure (Chapter 4). These model solutions comprised three different organic matter compounds and an inorganic colloid; they were filtered in single solutions and in all possible combinations. The following conclusions were made:

- Colloidal silica is significantly influential in determining the extent and type of fouling that occurs. It both increases the rate of fouling and the extent to which that fouling is hydraulically reversible.
- Humic acid and bovine serum albumin generally had slower rates of fouling but were largely hydraulically irreversible. The likely removal mechanism is through adsorption.
- In some cases synergistic fouling occurred when model foulants are combined.

- When colloidal silica was included in the solution, the resulting foulant layer remained relatively hydrophilic, even in the presence of bovine serum albumin, which was the only solution that greatly increased the hydrophobicity of the membrane.
- All single solutions and combinations showed fouling by cake layer filtration, except for humic acid alone and humic acid combined with bovine serum albumin; the fouling mechanism was intermediate and complete pore blocking filtration, respectively.
- Although hydrophilic membrane surfaces have been linked to lower rates of fouling, a hydrophilic fouled membrane surface was neither a reflection of the extent or reversibility of fouling.

Building on the previous model solution experiments, a tubular ceramic ultrafiltration membrane operating in dead-end mode and at constant flux was used to investigate fouling behavior (Chapter 5). The effectiveness of a unique backpulse approach as well as a maintenance clean were also incorporated into this stage. The following conclusions were made:

- The combination of all the organics and colloidal model foulants showed the highest rate of flux decline, similar to that observed with the flat-sheet membranes. Additionally, the fouling was mostly hydraulically reversible and the rate of fouling remained consistent throughout the cycles.
- When bovine serum albumin was filtered alone, the greatest overall rate of fouling was observed, with the majority of fouling being hydraulically irreversible. Therefore, some form of chemical cleaning would be required to mitigate this fouling. Nevertheless, the extreme fouling effect of bovine serum albumin was significantly reduced in the presence of other model foulants.
- Humic acid fouling was also largely hydraulically irreversible, however, the rate of fouling was very low.
- A unique backwash approach employing a series of 6 backpulses in succession is predominantly effective in the presence of a higher concentration of particles and organic matter.
- A maintenance clean with sodium hypochlorite is particularly effective in the event of humic acid or bovine serum albumin fouling.

- An important conclusion is that the results obtained from these experiments are qualitatively very similar to those obtained from the flat-sheet experiments. Therefore, this indicates that it is possible to study fundamental fouling behavior using less complex setups and still obtain representative fouling results, particularly if a backwash is incorporated into these experiments, which is often not done.

The last stage built on all the previous experiments by using the sustainable flux method to investigate the fouling behavior of a tubular ceramic membrane with natural water (Chapter 6). The sustainable flux method was also used to compare to fouling behavior obtained with a polymeric membrane. The results of these experiments can also be related back to the model solution results in Chapter 4 and Chapter 5. The following conclusions were made:

- Even after several modifications were made to both setup and operation, the sustainable flux method established could not be applied to the tubular ceramic membrane. The method was also not applicable for the polymeric membrane for highly turbid water. This finding elucidates the need for more in-depth research into different or additional variables that may need to be included when determining sustainable flux.
- NOM rejection was also investigated using LC-OCD analysis, which provided interesting observations regarding fouling behavior. In all the experiments it was apparent that biopolymers are consistently rejected at a high percentage initially, and even after many days of filtration, thereby indicating a primary removal mechanism through size exclusion.
- All organic matter was highly rejected at the initial stages of filtration indicating a high affinity of organics to the membrane surface. Higher than expected total organic carbon removals were also observed for the model solution experiments.
- Humic acid rejection was initially high but rapidly decreased during the filtration cycle, indicating at least some hydraulically reversible adsorption of humic acid. This theory is further supported by the increased effectiveness of a series of 6 backpulses (as compared to a single backwash) to remove fouling by the model foulant humic acid in Chapter 5. Adsorption was postulated to be the primary removal mechanism for humic acid using model solutions.
- A series of 6 backpulses in succession can be especially effective when fouling is a result of highly turbid waters and possibly a lower concentration of biopolymers.

- A maintenance clean used at regular intervals may be essential for maintaining a sustainable flux, particularly in the case of a high concentration of biopolymers. This result highlights the potential application of chemically enhanced backwashes as a useful fouling mitigation tool for ceramic membranes.

7.2 Experimental approach guidelines and recommendations

It is important to run bench-scale experiments under conditions as similar to full-scale operation as possible. This is clearly not always realistic or feasible; consequently, the ideal should always be strived for if possible. Factors to consider when planning model solution fouling experiments and the ideal choice are given in Table 7.1. Additionally, the main drawback or limitation associated with not incorporating the ideal conditions is mentioned. This table can serve as a basic guideline.

Table 7.1: Best practices approach to bench-scale studies for maximizing data from model solutions of low-pressure membranes in drinking water treatment (DWT) applications

Factor	Options	Ideal	Main drawback if not ideal
Configuration	Flat-sheet; tubular; hollow fiber	Tubular or hollow-fiber	Significant hydrodynamic differences can affect foulant-foulant & foulant-membrane interactions
Operating condition	Constant pressure; constant flux	Constant flux	Constant flux conditions are used in full-scale DWT plants and the hydrodynamic conditions will differ from constant pressure filtration
Backwash procedure	Yes or no	Yes	If hydraulically reversible foulants are not determined, it is not possible to predict sustainable operation and can make fouling data insignificant if applying it to DWT conditions
Model solution concentrations	A wide range	Within range of typical surface water concentrations	Extent of fouling can be over/under estimated.
Number of model foulants used	Single solutions; combinations of more than one model foulant	Combinations of several foulants	Foulant-foulant interactions can play a significant role in fouling behavior and single solutions only give information on foulant-membrane interactions
Membrane material	Wide range	As similar to current or expected in full-scale DWT plant	To a certain extent, membrane material can play a role in membrane fouling behavior, especially in shorter experiments, which may make results less relevant for practice
Duration	Can range from minutes to days	Days	High adsorption affinity of a model foulant can give misleading information regarding long-term rejection capabilities of the membrane

7.3 Overall significant conclusions and contributions

Significant conclusions regarding ceramic membrane filtration for drinking water treatment were made in the course of this research. The key contributions of this research are:

- The use of the concept of sustainable flux to compare two extremely different membranes has not been previously investigated. Most comparison studies have operated the membranes at the same flux or have strived to operate at similar hydrodynamic conditions. The limitation with these mentioned approaches is that they would retract from the key advantage of the ceramic membrane's ability to operate at higher fluxes and pressures. Therefore, the application of this concept for comparing a polymeric and ceramic membrane allows both membranes to operate as they normally would.

- Since the sustainable flux method could not be applied to the ceramic membrane as well as the polymeric membrane this indicates that more variables may need to be included in the sustainable flux methodology.

- Simplified studies such as the flat-sheet membrane experiments with model solutions can obtain representative qualitative fouling behavior of more complex and larger-scale systems/setups. However, a few essential factors in these types of experiments are the inclusion of a backwash, the use of representative foulant concentrations, the use of combinations of foulants, and the incorporation of a chemical cleaning regime.

- Since it is essential to minimize hydraulically irreversible fouling, implementing pretreatment strategies that target the removal of foulants having characteristics similar to that of proteins and humics will be crucial for long-term operational sustainability. Proteins, particularly without the presence of particulates seem to be especially troublesome.

    - Alternatively, the implementation of an efficient and optimized maintenance cleaning strategy may be just as effective depending on the water quality.

- Ultimately, to achieve an ideal treatment process a balance is needed between appropriate fouling mitigation techniques (i.e. pretreatment or backwashing) and chemical usage.

- The interactions between the water matrix components (e.g. silica and protein) are at least as important or maybe even more important in determining fouling behavior than the interaction of foulants with the membrane surface. However, this highly depends on the different water matrix constituents and further research is warranted.

- A series of 6 consecutive backpulses proved effective for a highly turbid water with a low biopolymer concentration. Since the ceramic membrane is quite robust, it allows for some creativity regarding fouling mitigation techniques, particularly backwashes and chemical cleaning. Therefore, this opens the door to some more unique future investigations.

7.4 Implications and recommendations for future ceramic membrane work for drinking water treatment

Several unexpected results along the course of this research clearly indicate that further work is still needed before ceramic membranes can really break into the drinking water treatment market and compete with polymeric membranes.

An inherent disadvantage of ceramic membranes is their relatively large footprint due to smaller surface areas compared to polymeric membranes. As a result (and to potentially drive down costs of ceramic membranes), manufacturers have experimented with a plethora of configurations, anywhere from circular to rectangular to even star shaped feed channels, as well as hollow fiber membranes. These can affect the hydrodynamics and potentially the fouling behavior of the membrane. With polymeric membranes, configurations are generally flat-sheet or hollow fiber, and the complicating factor is the numerous membrane surface modifications. Furthermore, membrane properties such as the pore size distribution and surface charge can also play a role in fouling behavior and need to be studied in more detail, particularly for ceramic membranes.

Nevertheless, it can be argued that the virgin membrane properties may only have an initial influence on fouling, and once fouling occurs, the cake layer characteristics will dictate subsequent fouling behavior. Consequently, the myriad of polymeric membrane materials will likely have a lower impact on fouling throughout the membrane's lifetime as opposed to the effects of configuration, which would be a continuous influence on fouling behavior throughout filtration.

A unique advantage of the ceramic membranes is the ability to operate high-pressure backwashes that work like a pulsing action. From the results achieved using a sequence of 6 backpulses, as opposed to one extended backwash suggests that, particularly in highly turbid waters, a creative investigation of different backwash procedures and techniques could be beneficial.

The ability of these ceramic membranes to tolerate higher pressures and more challenging water qualities makes them ideal candidates for severely polluted surface waters. Therefore, these membranes may potentially find a specific niche in this area of drinking water treatment. Also, with the increased incidence of indirect water reuse and a decrease in the availability of easily treatable surface waters and groundwater, drinking water treatment processes need to be even more robust. Possible niche applications for ceramic membranes include brackish or highly turbid waters, backwash or concentrate water, and potentially in areas with extreme changes in water quality. Northern areas such as Alaska and northern Canada are the most sensitive to the effects of climate change and can in some cases experience severely challenging raw water quality for different reasons. With such a robust membrane, treatment goals could still be met without concern for the membrane's integrity or lifetime.

Ultimately, cost will always be a driving factor. Despite estimations that suggest that ceramic membranes are becoming cost competitive with polymeric membranes, the short-term, higher capital costs will often be enough of a deterrent for ceramic membranes. However, with the higher costs of ceramic membranes does come higher quality. Although risk can often be difficult to quantify, the uncertainty of water quality and quantity bring forth a new variable that needs to be considered when designing drinking water treatment plants and calculating lifetime costs. A robustness factor, which provides flexibility of the system, should be considered when accounting for risk. Overall, the opportunity for creative applications and techniques that can be used with ceramic membranes may be the key advantage in a time when the only certainty in the future of water is the uncertainty.

Copyright Permissions

American Water Works Association

6666 West Quincy Avenue
Denver, CO 80235-3098
T (303) 794-7711
F (303) 794-7310
www.awwa.org

The Authoritative Resource on Safe Water®

May 8, 2013

Advocacy
Communications
Conferences
Education and Training
Science and Technology
Sections

Leila Munla
Dept. of Civil & Environmental Engineering
NSERC Chair in Water Treatment
University of Waterloo
Waterloo, Ontario

Dear Ms. Munla:

We are pleased to grant a one-time use permission to reproduce the following AWWA material:

> "Reversible and Irreversible of Ultrafiltration Ceramic Membranes by Model Solutions Relevant for Drinking Water Treatment" from *Journal AWWA* Vol. 104 No. 10 (Oct 2012) published by the American Water Works Association.

Reproduction is authorized for the following stated purpose:

> Inclusion in PhD thesis for Department of Civil & Environmental Engineering at University of Waterloo.

Please use the following citation when you credit AWWA:

> Reprinted from *Journal AWWA* Vol. 104 No.10 by permission. Copyright © 2013 the American Water Works Association.

Thank you for your attention to this matter.

ELSEVIER LICENSE
TERMS AND CONDITIONS

May 10, 2013

This is a License Agreement between Leila Munla ("You") and Elsevier ("Elsevier") provided by Copyright Clearance Center ("CCC"). The license consists of your order details, the terms and conditions provided by Elsevier, and the payment terms and conditions.

All payments must be made in full to CCC. For payment instructions, please see information listed at the bottom of this form.

Supplier	Elsevier Limited The Boulevard,Langford Lane Kidlington,Oxford,OX5 1GB,UK
Registered Company Number	1982084
Customer name	Leila Munla
Customer address	University of Waterloo Waterloo, ON N2L 3G1
License number	3142550328355
License date	May 05, 2013
Licensed content publisher	Elsevier
Licensed content publication	Desalination
Licensed content title	Ultrafiltration of protein mixtures: measurement of apparent critical flux, rejection performance, and identification of protein deposition
Licensed content author	Robert Chan,Vicki Chen,Martin P. Bucknall
Licensed content date	10 September 2002
Licensed content volume number	146
Licensed content issue number	1–3
Number of pages	8

Start Page	83
End Page	90
Type of Use	reuse in a thesis/dissertation
Portion	figures/tables/illustrations
Number of figures/tables/illustrations	1
Format	both print and electronic
Are you the author of this Elsevier article?	No
Will you be translating?	No
Order reference number	
Title of your thesis/dissertation	A study of fouling on ceramic ultrafiltration membranes by model solutions and natural waters
Expected completion date	May 2013
Estimated size (number of pages)	200
Elsevier VAT number	GB 494 6272 12
Permissions price	0.00 USD
VAT/Local Sales Tax	0.0 USD / 0.0 GBP
Total	0.00 USD
Terms and Conditions	

INTRODUCTION

1. The publisher for this copyrighted material is Elsevier. By clicking "accept" in connection with completing this licensing transaction, you agree that the following terms and conditions apply to this transaction (along with the Billing and Payment terms and conditions established by Copyright Clearance Center, Inc. ("CCC"), at the time that you opened your Rightslink account and that are available at any time at http://myaccount.copyright.com).

GENERAL TERMS

2. Elsevier hereby grants you permission to reproduce the aforementioned material subject to the terms and conditions indicated.

3. Acknowledgement: If any part of the material to be used (for example, figures) has appeared in our publication with credit or acknowledgement to another source, permission must also be sought from that source. If such permission is not obtained then that material may not be included in your publication/copies. Suitable acknowledgement to the source must be made, either as a footnote or in a reference list at the end of your publication, as follows:

"Reprinted from Publication title, Vol /edition number, Author(s), Title of article / title of chapter, Pages No., Copyright (Year), with permission from Elsevier [OR APPLICABLE SOCIETY COPYRIGHT OWNER]." Also Lancet special credit - "Reprinted from The Lancet, Vol. number, Author(s), Title of article, Pages No., Copyright (Year), with permission from Elsevier."

4. Reproduction of this material is confined to the purpose and/or media for which permission is hereby given.

5. Altering/Modifying Material: Not Permitted. However figures and illustrations may be altered/adapted minimally to serve your work. Any other abbreviations, additions, deletions and/or any other alterations shall be made only with prior written authorization of Elsevier Ltd. (Please contact Elsevier at permissions@elsevier.com)

6. If the permission fee for the requested use of our material is waived in this instance, please be advised that your future requests for Elsevier materials may attract a fee.

7. Reservation of Rights: Publisher reserves all rights not specifically granted in the combination of (i) the license details provided by you and accepted in the course of this licensing transaction, (ii) these terms and conditions and (iii) CCC's Billing and Payment terms and conditions.

8. License Contingent Upon Payment: While you may exercise the rights licensed immediately upon issuance of the license at the end of the licensing process for the transaction, provided that you have disclosed complete and accurate details of your proposed use, no license is finally effective unless and until full payment is received from you (either by publisher or by CCC) as provided in CCC's Billing and Payment terms and conditions. If full payment is not received on a timely basis, then any license preliminarily granted shall be deemed automatically revoked and shall be void as if never granted. Further, in the event that you breach any of these terms and conditions or any of CCC's Billing and Payment terms and conditions, the license is automatically revoked and shall be void as if never granted. Use of materials as described in a

revoked license, as well as any use of the materials beyond the scope of an unrevoked license, may constitute copyright infringement and publisher reserves the right to take any and all action to protect its copyright in the materials.

9. Warranties: Publisher makes no representations or warranties with respect to the licensed material.

10. Indemnity: You hereby indemnify and agree to hold harmless publisher and CCC, and their respective officers, directors, employees and agents, from and against any and all claims arising out of your use of the licensed material other than as specifically authorized pursuant to this license.

11. No Transfer of License: This license is personal to you and may not be sublicensed, assigned, or transferred by you to any other person without publisher's written permission.

12. No Amendment Except in Writing: This license may not be amended except in a writing signed by both parties (or, in the case of publisher, by CCC on publisher's behalf).

13. Objection to Contrary Terms: Publisher hereby objects to any terms contained in any purchase order, acknowledgment, check endorsement or other writing prepared by you, which terms are inconsistent with these terms and conditions or CCC's Billing and Payment terms and conditions. These terms and conditions, together with CCC's Billing and Payment terms and conditions (which are incorporated herein), comprise the entire agreement between you and publisher (and CCC) concerning this licensing transaction. In the event of any conflict between your obligations established by these terms and conditions and those established by CCC's Billing and Payment terms and conditions, these terms and conditions shall control.

14. Revocation: Elsevier or Copyright Clearance Center may deny the permissions described in this License at their sole discretion, for any reason or no reason, with a full refund payable to you. Notice of such denial will be made using the contact information provided by you. Failure to receive such notice will not alter or invalidate the denial. In no event will Elsevier or Copyright Clearance Center be responsible or liable for any costs, expenses or damage incurred by you as a result of a denial of your permission request, other than a refund of the amount(s) paid by you to Elsevier and/or Copyright Clearance Center for denied permissions.

LIMITED LICENSE

The following terms and conditions apply only to specific license types:

15. **Translation**: This permission is granted for non-exclusive world **English** rights only unless your license was granted for translation rights. If you licensed translation rights you may only translate this content into the languages you requested. A professional translator must perform all translations and reproduce the content word for word preserving the integrity of the article. If this license is to re-use 1 or 2 figures then permission is granted for non-exclusive world rights in all languages.

16. **Website**: The following terms and conditions apply to electronic reserve and author websites:
Electronic reserve: If licensed material is to be posted to website, the web site is to be password-protected and made available only to bona fide students registered on a relevant course if:
This license was made in connection with a course,
This permission is granted for 1 year only. You may obtain a license for future website posting,
All content posted to the web site must maintain the copyright information line on the bottom of each image,
A hyper-text must be included to the Homepage of the journal from which you are licensing at http://www.sciencedirect.com/science/journal/xxxxx or the Elsevier homepage for books at http://www.elsevier.com , and
Central Storage: This license does not include permission for a scanned version of the material to be stored in a central repository such as that provided by Heron/XanEdu.

17. **Author website** for journals with the following additional clauses:

All content posted to the web site must maintain the copyright information line on the bottom of each image, and the permission granted is limited to the personal version of your paper. You are not allowed to download and post the published electronic version of your article (whether PDF or HTML, proof or final version), nor may you scan the printed edition to create an electronic version. A hyper-text must be included to the Homepage of the journal from which you are licensing at http://www.sciencedirect.com/science/journal/xxxxx . As part of our normal production process, you will receive an e-mail notice when your article appears on Elsevier's

online service ScienceDirect (www.sciencedirect.com). That e-mail will include the article's Digital Object Identifier (DOI). This number provides the electronic link to the published article and should be included in the posting of your personal version. We ask that you wait until you receive this e-mail and have the DOI to do any posting.

Central Storage: This license does not include permission for a scanned version of the material to be stored in a central repository such as that provided by Heron/XanEdu.

18. **Author website** for books with the following additional clauses:
Authors are permitted to place a brief summary of their work online only.
A hyper-text must be included to the Elsevier homepage at http://www.elsevier.com . All content posted to the web site must maintain the copyright information line on the bottom of each image. You are not allowed to download and post the published electronic version of your chapter, nor may you scan the printed edition to create an electronic version.

Central Storage: This license does not include permission for a scanned version of the material to be stored in a central repository such as that provided by Heron/XanEdu.

19. **Website** (regular and for author): A hyper-text must be included to the Homepage of the journal from which you are licensing at http://www.sciencedirect.com/science/journal/xxxxx. or for books to the Elsevier homepage at http://www.elsevier.com

20. **Thesis/Dissertation**: If your license is for use in a thesis/dissertation your thesis may be submitted to your institution in either print or electronic form. Should your thesis be published commercially, please reapply for permission. These requirements include permission for the Library and Archives of Canada to supply single copies, on demand, of the complete thesis and include permission for UMI to supply single copies, on demand, of the complete thesis. Should your thesis be published commercially, please reapply for permission.

21. **Other Conditions**:

v1.6

If you would like to pay for this license now, please remit this license along with your payment made payable to "COPYRIGHT CLEARANCE CENTER" otherwise you will be

invoiced within 48 hours of the license date. Payment should be in the form of a check or money order referencing your account number and this invoice number RLNK501014509. Once you receive your invoice for this order, you may pay your invoice by credit card. Please follow instructions provided at that time.

Make Payment To:
Copyright Clearance Center
Dept 001
P.O. Box 843006
Boston, MA 02284-3006

For suggestions or comments regarding this order, contact RightsLink Customer Support: customercare@copyright.com or +1-877-622-5543 (toll free in the US) or +1-978-646-2777.

Gratis licenses (referencing $0 in the Total field) are free. Please retain this printable license for your reference. No payment is required.

ELSEVIER LICENSE
TERMS AND CONDITIONS

May 10, 2013

This is a License Agreement between Leila Munla ("You") and Elsevier ("Elsevier") provided by Copyright Clearance Center ("CCC"). The license consists of your order details, the terms and conditions provided by Elsevier, and the payment terms and conditions.

All payments must be made in full to CCC. For payment instructions, please see information listed at the bottom of this form.

Supplier	Elsevier Limited The Boulevard,Langford Lane Kidlington,Oxford,OX5 1GB,UK
Registered Company Number	1982084
Customer name	Leila Munla
Customer address	University of Waterloo Waterloo, ON N2L 3G1
License number	3142550645386
License date	May 05, 2013
Licensed content publisher	Elsevier
Licensed content publication	Journal of Membrane Science
Licensed content title	Sustainable flux enhancement in non-circular ceramic membranes on wastewater using the Fenton process
Licensed content author	T.Y. Chiu,A.E. James
Licensed content date	1 August 2006
Licensed content volume number	279
Licensed content issue number	1–2
Number of pages	7
Start Page	347

End Page	353
Type of Use	reuse in a thesis/dissertation
Intended publisher of new work	other
Portion	figures/tables/illustrations
Number of figures/tables/illustrations	2
Format	both print and electronic
Are you the author of this Elsevier article?	No
Will you be translating?	No
Order reference number	
Title of your thesis/dissertation	A study of fouling on ceramic ultrafiltration membranes by model solutions and natural waters
Expected completion date	May 2013
Estimated size (number of pages)	200
Elsevier VAT number	GB 494 6272 12
Permissions price	0.00 USD
VAT/Local Sales Tax	0.0 USD / 0.0 GBP
Total	0.00 USD
Terms and Conditions	

INTRODUCTION

1. The publisher for this copyrighted material is Elsevier. By clicking "accept" in connection with completing this licensing transaction, you agree that the following terms and conditions apply to this transaction (along with the Billing and Payment terms and conditions established by Copyright Clearance Center, Inc. ("CCC"), at the time that you opened your Rightslink account and that are available at any time at http://myaccount.copyright.com).

GENERAL TERMS

2. Elsevier hereby grants you permission to reproduce the aforementioned material subject to the terms and conditions indicated.

3. Acknowledgement: If any part of the material to be used (for example, figures) has appeared in our publication with credit or acknowledgement to another source, permission must also be sought from that source. If such permission is not obtained then that material may not be included in your publication/copies. Suitable acknowledgement to the source must be made, either as a footnote or in a reference list at the end of your publication, as follows:

"Reprinted from Publication title, Vol /edition number, Author(s), Title of article / title of chapter, Pages No., Copyright (Year), with permission from Elsevier [OR APPLICABLE SOCIETY COPYRIGHT OWNER]." Also Lancet special credit - "Reprinted from The Lancet, Vol. number, Author(s), Title of article, Pages No., Copyright (Year), with permission from Elsevier."

4. Reproduction of this material is confined to the purpose and/or media for which permission is hereby given.

5. Altering/Modifying Material: Not Permitted. However figures and illustrations may be altered/adapted minimally to serve your work. Any other abbreviations, additions, deletions and/or any other alterations shall be made only with prior written authorization of Elsevier Ltd. (Please contact Elsevier at permissions@elsevier.com)

6. If the permission fee for the requested use of our material is waived in this instance, please be advised that your future requests for Elsevier materials may attract a fee.

7. Reservation of Rights: Publisher reserves all rights not specifically granted in the combination of (i) the license details provided by you and accepted in the course of this licensing transaction, (ii) these terms and conditions and (iii) CCC's Billing and Payment terms and conditions.

8. License Contingent Upon Payment: While you may exercise the rights licensed immediately upon issuance of the license at the end of the licensing process for the transaction, provided that you have disclosed complete and accurate details of your proposed use, no license is finally effective unless and until full payment is received from you (either by publisher or by CCC) as provided in CCC's Billing and Payment terms and conditions. If full payment is not received on a timely basis, then any license preliminarily granted shall be deemed automatically revoked and shall be void as if never granted. Further, in the event that you breach any of these terms and conditions or any of CCC's Billing and Payment terms and conditions, the license is automatically revoked and shall be void as if never granted. Use of materials as described in a revoked license, as well as any use of the materials beyond the scope of an unrevoked license, may constitute copyright infringement and

publisher reserves the right to take any and all action to protect its copyright in the materials.

9. Warranties: Publisher makes no representations or warranties with respect to the licensed material.

10. Indemnity: You hereby indemnify and agree to hold harmless publisher and CCC, and their respective officers, directors, employees and agents, from and against any and all claims arising out of your use of the licensed material other than as specifically authorized pursuant to this license.

11. No Transfer of License: This license is personal to you and may not be sublicensed, assigned, or transferred by you to any other person without publisher's written permission.

12. No Amendment Except in Writing: This license may not be amended except in a writing signed by both parties (or, in the case of publisher, by CCC on publisher's behalf).

13. Objection to Contrary Terms: Publisher hereby objects to any terms contained in any purchase order, acknowledgment, check endorsement or other writing prepared by you, which terms are inconsistent with these terms and conditions or CCC's Billing and Payment terms and conditions. These terms and conditions, together with CCC's Billing and Payment terms and conditions (which are incorporated herein), comprise the entire agreement between you and publisher (and CCC) concerning this licensing transaction. In the event of any conflict between your obligations established by these terms and conditions and those established by CCC's Billing and Payment terms and conditions, these terms and conditions shall control.

14. Revocation: Elsevier or Copyright Clearance Center may deny the permissions described in this License at their sole discretion, for any reason or no reason, with a full refund payable to you. Notice of such denial will be made using the contact information provided by you. Failure to receive such notice will not alter or invalidate the denial. In no event will Elsevier or Copyright Clearance Center be responsible or liable for any costs, expenses or damage incurred by you as a result of a denial of your permission request, other than a refund of the amount(s) paid by you to Elsevier and/or Copyright Clearance Center for denied permissions.

LIMITED LICENSE

The following terms and conditions apply only to specific license types:

15. **Translation**: This permission is granted for non-exclusive world **English** rights only unless your license was granted for translation rights. If you licensed translation rights you may only translate this content into the languages you requested. A professional translator must perform all translations and reproduce the content word for word preserving the integrity of the article. If this license is to re-use 1 or 2 figures then permission is granted for non-exclusive world rights in all languages.

16. **Website**: The following terms and conditions apply to electronic reserve and author websites:
Electronic reserve: If licensed material is to be posted to website, the web site is to be password-protected and made available only to bona fide students registered on a relevant course if:
This license was made in connection with a course,
This permission is granted for 1 year only. You may obtain a license for future website posting,
All content posted to the web site must maintain the copyright information line on the bottom of each image,
A hyper-text must be included to the Homepage of the journal from which you are licensing at http://www.sciencedirect.com/science/journal/xxxxx or the Elsevier homepage for books at http://www.elsevier.com , and
Central Storage: This license does not include permission for a scanned version of the material to be stored in a central repository such as that provided by Heron/XanEdu.

17. **Author website** for journals with the following additional clauses:

All content posted to the web site must maintain the copyright information line on the bottom of each image, and the permission granted is limited to the personal version of your paper. You are not allowed to download and post the published electronic version of your article (whether PDF or HTML, proof or final version), nor may you scan the printed edition to create an electronic version.
A hyper-text must be included to the Homepage of the journal from which you are licensing at http://www.sciencedirect.com/science/journal/xxxxx . As part of our normal production process, you will receive an e-mail notice when your article appears on Elsevier's online service ScienceDirect (www.sciencedirect.com). That e-mail will include the article's Digital Object Identifier (DOI). This number provides the electronic link to the published article and should be included in the posting of your personal version. We ask that you wait until you receive this e-mail and have the DOI to do any posting.

Central Storage: This license does not include permission for a scanned version of the material to be

stored in a central repository such as that provided by Heron/XanEdu.

18. **Author website** for books with the following additional clauses:
Authors are permitted to place a brief summary of their work online only.
A hyper-text must be included to the Elsevier homepage at http://www.elsevier.com . All content posted to the web site must maintain the copyright information line on the bottom of each image.
You are not allowed to download and post the published electronic version of your chapter, nor may you scan the printed edition to create an electronic version.

Central Storage: This license does not include permission for a scanned version of the material to be stored in a central repository such as that provided by Heron/XanEdu.

19. **Website** (regular and for author): A hyper-text must be included to the Homepage of the journal from which you are licensing at http://www.sciencedirect.com/science/journal/xxxxx. or for books to the Elsevier homepage at http://www.elsevier.com

20. **Thesis/Dissertation**: If your license is for use in a thesis/dissertation your thesis may be submitted to your institution in either print or electronic form. Should your thesis be published commercially, please reapply for permission. These requirements include permission for the Library and Archives of Canada to supply single copies, on demand, of the complete thesis and include permission for UMI to supply single copies, on demand, of the complete thesis. Should your thesis be published commercially, please reapply for permission.

21. **Other Conditions**:

v1.6

If you would like to pay for this license now, please remit this license along with your payment made payable to "COPYRIGHT CLEARANCE CENTER" otherwise you will be invoiced within 48 hours of the license date. Payment should be in the form of a check or money order referencing your account number and this invoice number RLNK501014510.
Once you receive your invoice for this order, you may pay your invoice by credit card. Please follow instructions provided at that time.

Make Payment To:

Young-june Choi May 5, 2013

Dear Leila,

You can use any figures and tables in the thesis with the reference if not for commercial purpose.
In addition, can I get the file of your thesis when it is completed? I'm leading research group here in Seoul and I'm interested in ceramic membrane. Your thesis would be very interesting to my researchers as well as I.

Thank you for your interest in my work.
Sincerely yours,

Young-june Choi 최영준

Director 서기관

Chief R&D Officer
Waterworks Research Institute
Seoul Metropolitan Government

2013/5/6 Leila Munla
Hi,

I am writing to request permission to reprint Figure 2.6 part b from your PhD thesis "Critical flux, resistance, and removal of contaminants in ultrafiltration of natural organic materials" in 2003. I am planning to include this figure in my PhD thesis titled "A study of fouling on ceramic ultrafiltration membranes by model solutions and natural waters" to be submitted by the end of May 2013. Unless you request otherwise, I will use the conventional scholarly form of acknowledgement, including author and title, publisher's name, and date. If permission is granted, please respond to this email indicating so. If permission is denied, please inform me by responding to this email address as well.
Thank you for your consideration of this request,

Leila Munla

References

Abdullah, S., Bérubé, P. 2012. Effects of chemical cleaning on membrane operating lifetime. Proceedings, American Water Works Association Membrane Technology Conference Proceedings. Online, Wed 2d-1.

Abrahamse, A.J., Lipreau, C., Li, S., & Heijman, S.G.J. 2008. Removal of divalent cations reduces fouling of ultrafiltration membranes. Journal of Membrane Science, **323**: 1: 153-158.

Al-Amoudi, A. 2010. Factors affecting natural organic matter (NOM) & scaling fouling in NF membranes: A review. Desalination, **259**: 1-10

Alpatova, A., Davies, S., Masten, S. 2013. Hybrid ozonation- ceramic membrane filtration of surface waters: The effect of water characteristics on permeate flux and the removal of DBP precursors, dicloxacillin and ceftazidime. Separation and Purification Technology, **107:** 179-186.

Aoustin, E., Schäfer, A.I., Fane, A.G., and Waite, T.D. 2001. Ultrafiltration of natural organic matter. Separation and Purification Technology, **22-23**: 63-78.

AWWA. 2005. Microfiltration and Ultrafiltration Membranes for Drinking Water. First Edition. American Water Works Association, Denver, Colorado.

Bacchin, P., Aimar, P., and Field, R.W. 2006. Critical and Sustainable fluxes: Theory, experiments and applications. Journal of Membrane Science, **281**: 42-69.

Batsch, A., Tyszler, D., Brügger, A., Panglisch, S., and Melin, T. 2005. Foulant analysis of modified and unmodified membranes for water and wastewater treatment with LC-OCD. Desalination, **178**: 63-72.

Bellona, C., Drewes, J.E., Xu, P., and Amy, G. 2004. Factors Affecting the rejection of organic solutes during NF/RO treatment – a literature review. Water Research, **38**: 2795-2809.

Bodzek, M., and Konieczny, K. 1998. Comparison of ceramic and capillary membranes in the treatment of natural waters by means of ultrafiltration and microfiltration. Desalination, **119**: 191-198.

Boerlage, S.F.E., Kennedy, M.D., Aniye, M.P., Abogrean, E., Tarawneh, Z., & Schippers, J.C. 2003. The MFI-UF as a water quality test & monitor. Journal of Membrane Science, **211**: 271-289.

Bottino, A., Capannelli, C., Borghi, A.D., Colombino, M., and Conio, O. 2001. Water Treatment for Drinking Purpose: Ceramic Microfiltration Application. Desalination, 141: 75-79.

Burggraaf, A.J., and Cot, L., 1996. Fundamentals of Inorganic Membrane Science and Technology. Elsevier Science, Amsterdam.

Calvo, J.I., Bottino, A., Capannelli, G., & Hernández, A. 2008. Pore size distribution of ceramic UF by liquid-liquid displacement porosimetry. Journal of Membrane Science, **310**: 531-538.

Carrère, H., Blaszkow, F., and Balmann, H. 2001. Modeling the clarification of lactic acid fermentation broths by cross-flow microfiltration. Journal of Membrane Science, **186**: 219-230.

Carroll, T., King, S., Gray, S.R., Bolto, B.A., and Booker, N.A. 2000. The fouling of microfiltration membranes by NOM after coagulation treatment. Water Research, **34**: 11: 2861-2868.

Chan, R., Chen, V., and Bucknall, M.P. 2002. Ultrafiltration of Protein Mixtures: Measurement of Apparent Flux, Rejection Performance, and Identification of Protein Deposition. Desalination, **146**: 1: 83-90.

Chen, V., Fane, A.G., Madaeni, S., & Wenten, I.G. 1997. Particle deposition during membrane filtration of colloids: transition between concentration polarization & cake formation. Journal of Membrane Science, **125**: 109-122.

Chiu, T.Y., and James, A.E. 2006. Sustainable flux enhancement in non-circular ceramic membranes on wastewater using the Fenton process. Journal of Membrane Science, **279**: 347-353.

Cho, B.D., and Fane, A.G. 2002. Fouling Transients in Nominally Subcritical Flux Operation of a Membrane Bioreactor. Journal of Membrane Science, **209**: 391.

Cho, J., Amy, G., and Pellegrino, J. 2000. Membrane filtration of natural organic matter: factors and mechanisms affecting rejection and flux decline with charged ultrafiltration (UF) membrane. Journal of Membrane Science, **164**: 1-2: 89-110.

Cho, M.-H., Lee, C.-H., and Lee, S. 2005. Effect of flocculation conditions on membrane permeability in coagulation-microfiltration. Desalination, **191**: 386-396.

Choi, K.Y., and Dempsey, B.A. 2005. Bench-scale evaluation of critical flux and TMP in low-pressure membrane filtration. Journal of American Water Works Association, **97**: 7: 134-143.

Choi, Y.-j., 2003. Critical Flux, Resistance, and Removal of Contaminants in Ultrafiltration (UF) of Natural Organic Materials. PhD Thesis. Pennsylvania State University, Pennsylvania.

Cornelissen, E.R., Moreau, N., Siegers, W.G., Abrahamse, A.J., Rietveld, L.C., Grefte, A., Dignum, M., Amy, G., and Wessels, L.P. 2008. Selection of anionic exchange resins for removal of natural organic (NOM) fractions. Water Research, **42**: 413-423.

Costa, A.R., de Pinho, M.N., & Elimelech, M. 2006. Mechanisms of colloidal natural organic matter fouling in ultrafiltration. Journal of Membrane Science, **281**: 716-725.

Daufin, G., Escudier, J.-P., Carrère, H., Berot, S., Fillaudeau, L., and Decloux, M. 2001. Review Paper: Recent and Emerging Applications of Membrane Processes in the Food and Dairy Industry. Food and Bioproducts Processing, **79**: C2: 89-102.

Decloux, M., and Tatoud, L. 2000. Importance of the control mode in ultrafiltration: case of raw cane sugar remelt. Journal of Food Engineering, **44**: 119-126.

Defrance, L., and Jaffrin, M.Y. 1999. Comparison between filtrations at fixed transmembrane pressure and fixed permeate flux: application to a membrane bioreactor used for wastewater treatment. Journal of Membrane Science, **152**: 203-210.

De la Rubia, Á., Rodríguez, M., and Prats, D. 2006. pH, ionic strength, and flow velocity effects on the NOM filtration with TiO2/ZrO2 membranes. Separation and Purification Technology, **52**: 325-331.

Dramas, L., Croué, J.P. 2012. Interaction of soluble organic matter with metal oxides used as ceramic membrane for drinking water treatment. AWWA Membrane Technology Conference Proceedings, pages 103-114.

Espinasse, B., Bacchin, P., and Aimar, P. 2002. On an experimental method to measure critical flux in ultrafiltration. Desalination, **146**: 91-96.

Fakhfakh, S., Baklouti, S., Baklouti, S., and Bouaziz, J. 2010. Preparation, characterization, and application in BSA solution of silica ceramic membranes. Desalination, **262**: 188-195.

Fan, L., Harris, J.L., Roddick, F.A., and Booker, N.A. 2001. Influence of the characteristics of natural organic matter on the fouling of microfiltration membranes. Water Research, **35**: 18: 4455-4463.

Fane, A.G., Yeo, A., Law, A., Parameshwaran, K., Wicaksana, F., and Chen, V. 2005. Low pressure membranes ~ doing more with less energy. Desalination, **185**: 159-165.

Field, R.W., Wu, D., Howell, J.A., and Gupta, B.B. 1995. Critical flux concept for microfiltration fouling. Journal of Membrane Science, **100**: 259-272.

Foley, G. 2006. A review of factors affecting filter cake properties in dead-end microfiltration of microbial suspensions. Journal of Membrane Science, **274**: 1-2: 38-46.

Fujiura, S., Tomita, Y., Kanaya, S., Lehman, S.G., Chiu, K.-P., and Hudson, B., 2006. Ceramic Membrane Microfiltration with Coagulation. Proc. AWWA Annual Conference and Exposition. San Antonio, TX.

Gao, Y., Chen, D., Weavers, L.,Walker, H. 2012. Ultrasonic control of UF membrane fouling by natural waters: Effects of calcium, pH, and fractionated natural organic matter. Journal of Membrane Science, **401-402:** 232-240.

Garmash, E.P., Kryuchkov, Y.N., and Pavlikov, V.N. 1995. Ceramic Membranes for Ultra- and Microfiltration (Review). Glass and Ceramics, **52**: 6: 150-152.

Gesan-Guiziou, G., Wakeman, R.J., and Daufin, G. 2002. Stability of latex crossflow filtration: cake properties and critical conditions of deposition. Chemical Engineering Journal, **85**: 27-34.

Gray, S.R., Ritchie, C.B., Tran, T., and Bolto, B.A. 2007. Effect of NOM characteristics and membrane type on microfiltration performance. Water Research, **41**: 3833-3841.

Gray, S. R., Dow, N., Orbell, J. D., Tran, T., &Bolto, B. A. 2011. The significance of interactions between organic compounds on low pressure membrane fouling. Water Science and Technology, **64** (3), 632-639.

Guerra, K., Pellegrino, J. 2012. Comparison of fouling potential and cleaning efficiency of ceramic and polymeric membranes for water treatment applications. Proceedings, American Water Works Association Membrane Technology Conference. Online, Tues 3b-2.

Guerra, K., Pellegrino, J., Drewes, J. 2012. Impact of operating conditions on permeate flux and process economics for cross flow ceramic ultrafiltration of surface water. Separation and Purification Technology, **87:** 45-53.

Haberkamp, J., Ernst, M., Makdissy, G., Huck, P.M., & Jekel, M. 2008. Protein fouling of ultrafiltration membranes - Investigation of several factors relevant for tertiary wastewater treatment. Journal of Environmental Engineering and Science, **7**: 6: 651-660.

Hallé, C., Huck, P.M., Peldszus, S., Haberkamp, J., & Jekel, M. 2009. Assessing the performance of biological filtration as pretreatment to low pressure membranes for drinking water. Environmental Science and Technology, **43**: 10: 3878-3884.

Harman, B.I., Koseoglu, H., Yigit, N.O., Sayilgan, E., Beyhan, M., and Kitis, M. 2010. The removal of disinfection by-product precursors from water with ceramic membranes. Water Science and Technology, **62**: 3: 547-555.

Heidenreich, S. 2011. Ceramic membranes: High filtration area packing densities improve membrane performance. Filtration and Separation, **48**: 3: 25-27.

Hermia, J. 1982. Constant Pressure Blocking Filtration Laws-Application to Power-Law Non-Newtonian Fluids. Trans Inst Chem Eng, **60**: 3: 183-187.

Hester, J.F., and Mayes, A.M. 2002. Design and performance of foul-resistant PVDF membranes prepared in a single-step by surface segregation. Journal of Membrane Science, **202**: 119-135.

Hilal, N., Ogunbiyi, O.O., Miles, N.J., and Nigmatullin, R. 2005. Methods employed for control of fouling in MF and UF membranes: A comprehensive review. Separation Science and Technology, **40**: 10: 1957-2005.

Hofs, B., Ogier, J., Vries, D., Beerendonk, E., Cornelissen, E. 2011. Comparison of ceramic and polymeric membrane permeability and fouling using surface water. Separation and Purification Technology, **79**:365-374.

Hong, S., & Elimelech, M. 1997. Chemical and Physical Aspects of Natural Organic Matter (NOM) Fouling of Nanofiltration Membranes. Journal of Membrane Science, **132**: 159-181.

Howe, K.J., and Clark, M.M. 2002. Fouling of Microfiltration and Ultrafiltration Membranes by Natural Waters. Environmental Science and Technology, **36**: 16: 3571-3576.

Howe, K.J., Marwah, A., Chiu, K.-P., & Adham, S. 2007. Effect of membrane configuration on bench-scale MF & UF fouling experiments. Water Research, **41**: 3842-3849.

Hsieh, H., 1996. Inorganic membranes for separation and reaction. Elsevier Science, BV, Amsterdam.

Huisman, I.H., Vellenga, E., Tragardh, G., and Tragardh, C. 1999. The influence of the zeta potential on the critical flux for crossflow microfiltration of particle suspensions. Journal of Membrane Science, **156**: 1: 153-158.

Jermann, D., Pronk, W., and Boller, M. 2008a. Mutual Influences between Natural Organic Matter and Inorganic Particles and Their Combined Effect on Ultrafiltration Membrane Fouling. Environmental Science and Technology, **42**: 24: 9129-9136.

Jermann, D., Pronk, W., Kägi, R., Halbeisen, M., and Boller, M. 2008b. Influence of interactions between NOM and particles on UF fouling mechanisms. Water Research, **42**: 3870-3878.

Jermann, D., Pronk, W., Meylan, S., and Boller, M. 2007. Interplay of different NOM fouling mechanisms during ultrafiltration for drinking water production. Water Research, **41**: 1713-1722.

Jucker, C., and Clark, M.M. 1994. Adsorption of aquatic humic substances on hydrophobic ultrafiltration membranes. Journal of Membrane Science, **97**: 37-52.

Jung, C.-W., and Kang, L.-S. 2003. Application of Combined Coagulation-Ultrafiltration Membrane Process for Water Treatment. Korean Journal of Chemical Engineering, **20**: 5: 855-861.

Jung, C.-W., Son, H.-J., and Kang, L.-S. 2006. Effects of membrane material and pretreatment coagulation on membrane fouling: fouling mechanism and NOM removal. Desalination, **197**: 154-164.

Kanaya, S., Fujiura, S., Tomita, Y., and Yonekawa, H., 2007. The World Largest Ceramic Membrane Drinking Water Treatment Plant. American Water Works Association Membrane Technology Conference. American Water Works Association, Tampa, Florida, USA.

Katsoufidou, K., Sioutopoulos, D.C., Yiantsios, S.G., and Karabelas, A.J. 2010. UF membrane fouling by mixtures of humic acids and sodium alginate: Fouling mechanisms and reversibility. Desalination, **264**: 220-227.

Katsoufidou, K., Yiantsios, S.G., and Karabelas, A.J. 2005. A study of ultrafiltration membrane fouling by humic acids and flux recovery by backwashing: Experiments and modeling. Journal of Membrane Science, **266**: 1-2: 40-50.

Katsoufidou, K., Yiantsios, S.G., and Karabelas, A.J. 2008. An experimental study of UF membrane fouling by humic acid and sodium alginate solutions: the effect of backwashing on flux recovery. Desalination, **220**: 214-227.

Katsoufidou, K., Yiantsios, S.G., and Karabelas, A.J. 2007. Experimental study of ultrafiltration membrane fouling by sodium alginate and flux recovery by backwashing. Journal of Membrane Science, **300**: 137-146.

Konieczny, K., Bodzek, M., and Rajca, M. 2006. A coagulation-MF system for water treatment using ceramic membranes. Desalination, **198**: 92-101.

Kosmulski, M. 2009. Compilation of PZC and IEP of sparingly soluble metal oxides and hydroxides from literature. Advances in Colloid and Interface Science, **152:** 14-25.

Laabs, C., Amy, G., and Jekel, M. 2006. Understanding the Size and Character of Fouling-Causing Substances from Effluent Organic Matter (EfOM) in Low-Pressure Membrane Filtration. Environmental Science and Technology, **40**: 14: 4495-4499.

Lahoussine-Turcaud, V., Wiesner, M.R., and Bottero, J.-Y. 1990. Fouling in Tangential-flow Ultrafiltration: The Effect of Colloid Size and Coagulation Pretreatment. Journal of Membrane Science, **52**: 2: 173-190.

Law, C.M.C., Li, X.Y., & Li, Q. 2010. The combined colloid-organic fouling on NF membrane for wastewater treatment and reuse. Separation Science and Technology, **45**: 7: 935-940.

Lee, E.K., Chen, V., and Fane, A.G. 2008. Natural organic matter (NOM) fouling in low pressure membrane filtration - effect of membranes and operation modes. Desalination, **218**: 257-270.

Lee, N., Amy, G., Croue, J.-P., & Buisson, H. 2005. Morphological analyses of natural organic matter fouling of low-pressure membranes (MF/UF). Journal of Membrane Science, **261**: 7-16.

Lee, S., and Cho, J. 2004. Comparison of ceramic and polymeric membranes for natural organic (NOM) removal. Desalination, **160**: 3: 223-232.

Lee, S., Dilaver, M., Park, P., Kim, J. 2013. Comparative analysis of fouling characteristics of ceramic and polymeric microfiltration membranes using filtration models. Journal of Membrane Science. **432:** 97-105.

Lee, S., Park, G., Amy, G., Hong, S., Moon, S.-Y., Lee, D.-H., and Cho, J. 2002. Determination of membrane pore size distribution using fractional rejection of nonionic and charged macromolecules. Journal of Membrane Science, **201**: 191-201.

Lehman, S.G., Adham, S., Liu, L. 2008. Performance of new generation ceramic membranes using hybrid coagulation pretreatment. Journal of Environmental Engineering and Management, **18**: 4: 257-260.

Lehman, S.G., Adham, S., Liu, L., Fujuira, S., and Kanaya, S., 2007. Performance of New Generation Ceramic Membranes Using Coagulation and Ozonation Pretreatment. Membrane Technology Conference. American Water Works Association, Tampa, Florida, USA.

Leong, Y.K., Katiforis, N., Harding, D.B.O., Healy, T.W., Boger, D.V. 1993. Role of rheology in colloidal processing of ZrO_2. Journal of Materials Processing and Manufacturing Science, **1:** 445-453.

Lerch, A., Panglisch, S., Buchta, P., Tomita, Y., Yonekawa, H., Hattori, K., and Gimbel, R. 2005. Direct river water treatment using coagulation/ceramic membrane filtration. Desalination, **179**: 41-50.

Levitsky, I., Duek, A., Arkhangelsky, E., Pinchev, D., Kadoshian, T., Shetrit, H., Naim, R., Gitis, V. 2011. Understanding the oxidative cleaning of UF membranes. Journal of Membrane Science. **377:** 206-213.

Li, S., Heijman, S.G.J., & Van Dijk, J.C. 2010. A pilot-scale study of backwashing ultrafiltration membrane with demineralized water. Journal of Water Supply: Research and Technology-AQUA, **59**: 2-3: 128-133.

Liu, C., Caothien, S., Hayes, J., Caothuy, T., Otoyo, T., and Ogawa, T. 2001. Membrane Chemical Cleaning: From Art to Science. AWWA Membrane Technology Conference, San Antonio.

Loi-Brügger, A., Panglisch, S., Buchta, P., Hattori, K., Yonekawa, H., Tomita, Y., and Gimbel, R. 2006. Ceramic membranes for direct river water treatment applying coagulation and microfiltration. Water Science and Technology: Water Supply, **6:** 4: 89-98.

Loi-Brügger, A., Panglisch, S., Hattori, K., Yonekawa, H., Tomita, Y., and Gimbel, R., 2007. Open Up New Doors in Water Treatment with Ceramic Membranes. Membrane Technology Conference. American Water Works Association, Tampa, Florida, USA.

Mallevialle, J., Odendaal, P.E., and Wiesner, M.R., 1996. Water Treatment Membrane Processes. AWWA and AWWA Research Foundation.

Mao, M., Fornasiero, D., Ralston, J., Smart, R.S.C, Sobieraj, S. 1994. Electrochemistry of the zircon-water interface. Colloids and Surfaces A: Physicochemical and Engineering Aspects, **85:** 37-49.

Matsushita, T., Matsui, Y., Shirasaki, N., and Kato, Y. 2005. Effect of membrane pore size, coagulation time, and coagulant dose on virus removal by a coagulation-ceramic microfiltration hybrid system. Desalination, **178**: 21-26.

Meylan, S., Hammes, F., Traber, J., Salhi, E., Gunten, U.v., and Pronk, W. 2007. Permeability of low molecular weight organics through nanofiltration membranes. Water Research, **41**: 3968-3976.

Mourouzidis-Mourouzis, S.A., and Karabelas, A.J. 2006. Whey protein fouling of microfiltration ceramic membranes - Pressure effects. Journal of Membrane Science, **282**: 124-132.

Mullet, M., Fievet, P., Reggiani, J.C., Pagetti, J. 1997. Surface electrochemical properties of mixed oxide ceramic membranes: zeta potential and surface charge density. Journal of Membrane Science, **123:** 255-265.

Munla, L., S. Peldszus, and P.M. Huck, 2012. Reversible and Irreversible Fouling of Ultrafiltration Ceramic Membranes by Model Solutions. Journal of American Water Works Association, (Peer-reviewed - online only). **104** (10): E540-E554.

Munla, L.D., S. Peldszus and P.M. Huck, 2011. Fouling Characterization of Ultrafiltration Ceramic Membranes with Model Solutions: Surface Characterization and Solute Rejection. Proceedings, AWWA Membrane Technology Conference & Exposition, Long Beach, CA. Online, THU05-2.

MWH, 2005. Water Treatment: Principles and Design. Second Edition. John Wiley and Sons, New Jersey.

Nakao, S.-i. 1994. Determination of pore size and pore size distribution 3. Filtration membranes. Journal of Membrane Science, **96**: 131-165.

Nghiem, L.D., Schäfer, A.I., and Elimelech, M. 2005. Pharmaceutical Retention Mechanisms by Nanofiltration Membranes. Environmental Science and Technology, **39**: 7698-7705.

Pearce, G., and Field, R.W. 2007. Development of the Sustainable Flux Concept to Provide Guidelines for Fouling Control in UF/MF System Design. Proceedings AWWA Membrane Technology Conference and Exposition, Tampa, Florida, pp. CD-ROM, paper Mon 2-2.

Peiris, R.H., Budman, H., Moresoli, C., & Legge, R.L. 2010. Understanding fouling behavior of ultrafiltration membrane processes & natural water using principal component analysis of fluorescence excitation-emission matrices. Journal of Membrane Science, **357**: 1-2: 62-72.

Peldszus, S., J. Benecke, M. Jekel, and P.M. Huck, 2012. Direct Biofiltration Pretreatment for Fouling Control of Ultrafiltration Membranes. Journal of American Water Works Association, (Peer-reviewed - online only). **104:** 7: E430-E445.

Peldszus, S., C. Hallé, R.H. Peiris, M.A. Hamouda, X. Jin, R.L. Legge, H. Budman, C. Moresoli, & P.M. Huck, 2011. Reversible & Irreversible Low-pressure Membrane Foulants in Drinking Water Treatment: Identification by Principal Component Analysis of Fluorescence EEM & Mitigation by Biofiltration Pretreatment. Water Research, **45:** 16: 5161-5170.

Sano, S., Banno, T., Maeda, M., Oda, K., Shibasaki, Y. 1996. Slip casting and sintering of silicon carbide (part 1) – slip preparation of silicon carbide powder produced by Acheson method. Journal of the Ceramic Society of Japan, **104:** 984-988.

Singh, S., Khulbe, K.C., Matsuura, T., and Ramamurthy, P. 1998. Membrane characterization by solute transport and atomic force microscopy. Journal of Membrane Science, **142**: 1: 111-127.

Sioutopoulos, D.C., Yiantsios, S.G., & Karabelas, A.J. 2010. Relation between fouling characteristics of RO & UF membranes in experiments with colloidal organic & inorganic species. Journal of Membrane Science, **350**: 1-2: 62-82.

Van der Bruggen, B., Vandecasteele, C., Van Gestel, T., Doyen, W., and Leysen, R. 2003. A Review of Pressure-Driven Membrane Processes in Wastewater Treatment and Drinking Water Production. Environmental Progress, **22**: 1: 46-56.

Vrijenhoek, E.M., Hong, S., & Elimelech, M. 2001. Influence of membrane surface properties on initial rate of colloidal fouling of reverse osmosis & nanofiltration membranes. Journal of Membrane Science, **188**: 1: 115-128.

Vyas, H.K., Bennett, R.J., and Marshall, A.D. 2002. Performance of cross-flow microfiltration during constant transmembrane pressure and constant flux operations. International Dairy Journal, **12**: 473-479.

Wang, X.H., Hirata, Y. 2004. Colloidal processing and mechanical properties of SiC with Al_2O_3 and Y_2O_3. Journal of the Ceramic Society of Japan, **112:** 22-28.

Weber, R., Chmiel, H., and Mavrov, V. 2003. Characteristics and application of new ceramic nanofiltration membranes. Desalination, **157**: 1-3: 113-125.

Wu, D., Howell, J.A., & Field, R.W. 1999. Critical flux measurement for model colloids. Journal of Membrane Science, **152**: 1: 89-98.

Yamamura, H., Kimura, K., & Watanabe, Y. 2007. Mechanism involved in the evolution of physically irreversible fouling in microfiltration & ultrafiltration membranes used for drinking water treatment. Environmental Science and Technology, **41**: 19: 6789-6794.

Yan, L., Li, Y.S., and Xiang, C.B. 2005. Preparation of poly(vinylidene fluoride) (pvdf) ultrafiltration membrane modified by nano-sized alumina (Al_2O_3) and its antifouling research. Polymer, **46**: 7701-7706.

Yao, M., Zhang, K., & Cui, L. 2010.Characterization of protein-polysaccharide ratios on membrane fouling. Desalination, **259**: 1-3: 11-16.

Yeh, S.H., Wan, C.C. 1994. Codeposition of SiC powders with nickel in a Watts bath. Journal of Applied Electrochemistry, **24:** 993-1000.

Yonekawa, H., Tomita, Y., and Watanabe, Y. 2004. Behavior of micro-particles in monolith ceramic membrane filtration with pre-coagulation. Water Science and Technology, **50**: 12: 317-325.

Yuan, W., & Zydney, A.L. 1999. Humic acid fouling during microfiltration. Journal of Membrane Science, **157**: 1: 1-12.

Xiao, K.; Wang, X.; Huang, X.; Waite, T.D.; & Wen, X., 2009. Analysis of Polysaccharide, Protein, and Humic Acid Retention by Microfiltration Membranes Using Thomas' Dynamic Adsorption Model. Journal of Membrane Science, **342:** 1-2: 22.

Zhang, J., Chua, H.C., Zhou, J., & Fane, A.G. 2006. Factors affecting the membrane performance in submerged membrane bioreactors. Journal of Membrane Science, **284**: 54-66.

Zhang, M., and Song, L. 2000. Mechanisms and Parameters Affecting Flux Decline in Cross-flow Microfiltration and Ultrafiltration of Colloids. Environmental Science and Technology, **34**: 3767

Zhao, Y.-H., Qian, Y.-L., Zhu, B.-K., and Xu, Y.-Y. 2008. Modification of porous PVDF membrane using amphiphilic polymers with different structures in phase inversion process. Journal of Membrane Science, **310**: 567-576.

Zhu, H., Wen, X., Huang, X. 2012. Characterization of membrane fouling in a microfiltration ceramic membrane system treating secondary effluent. Desalination. **284:** 324-331

.

Appendix A

Pictures of the Membranes Used and Their Setups

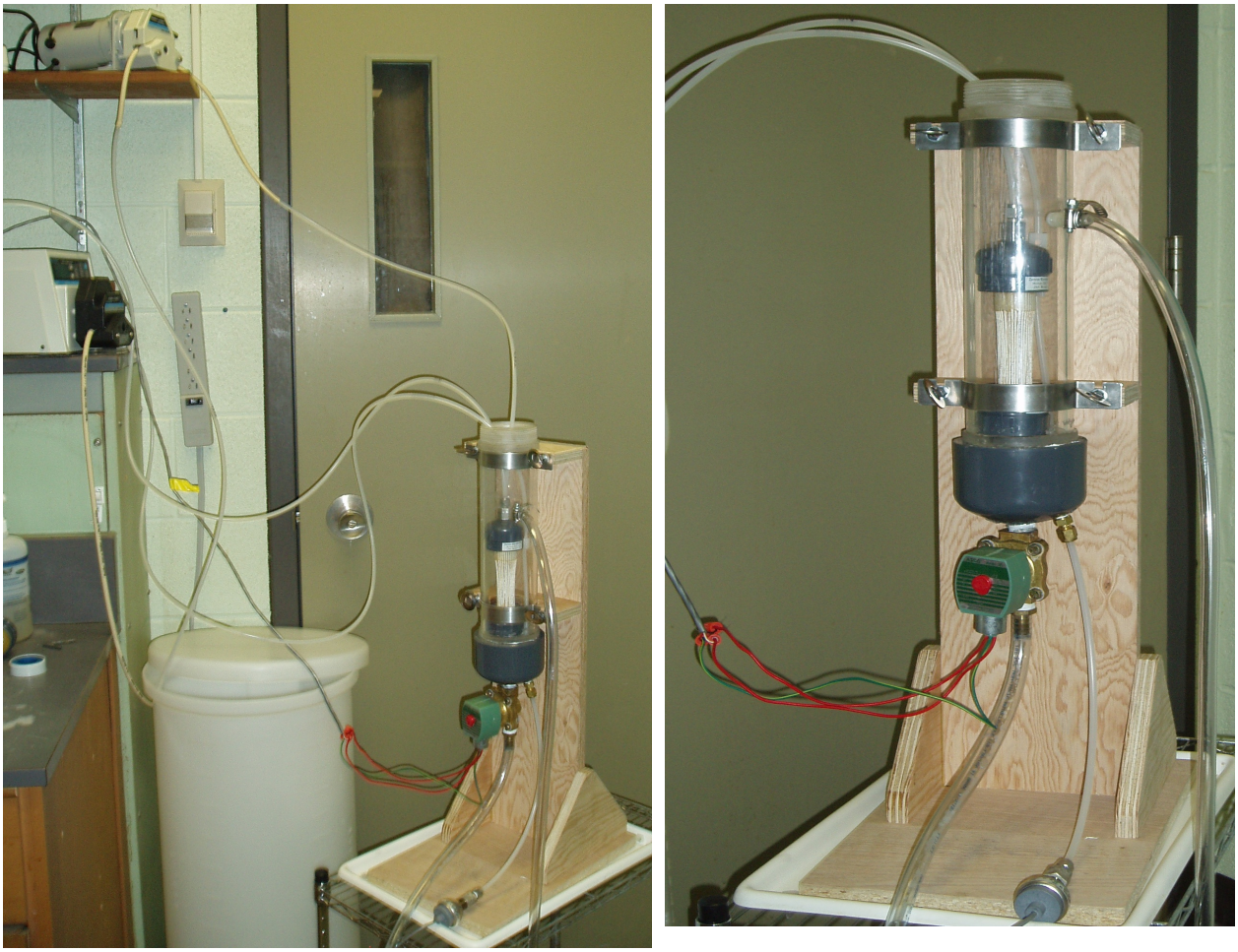

Appendix A Figure 1: Picture of polymeric membrane setup

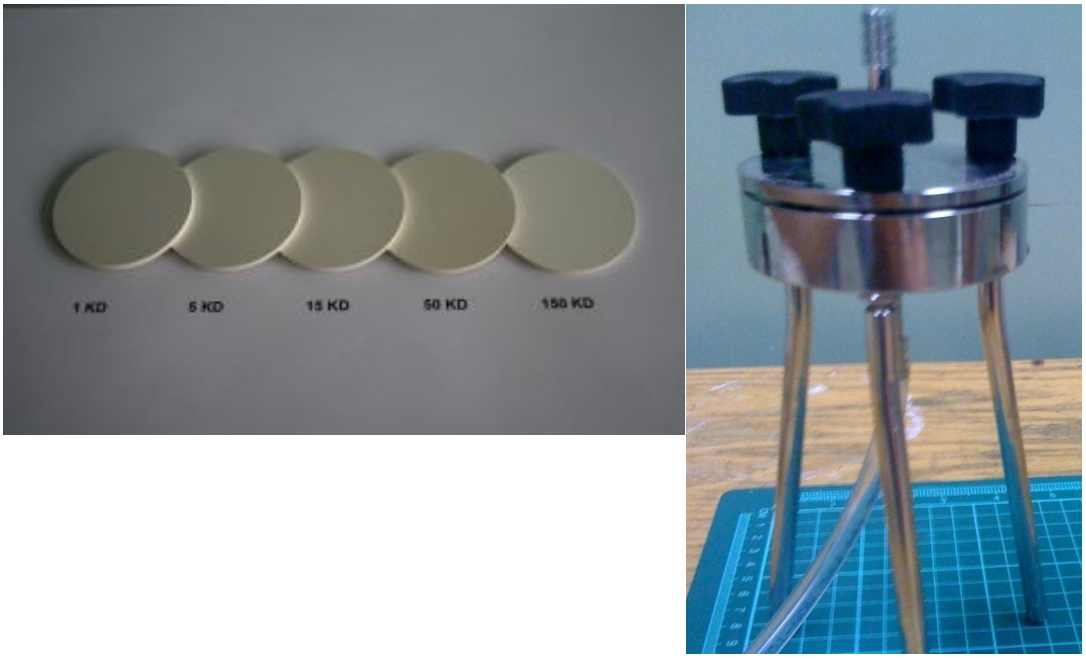

Appendix A Figure 2: Picture of the flat-sheet ceramic membrane and the housing

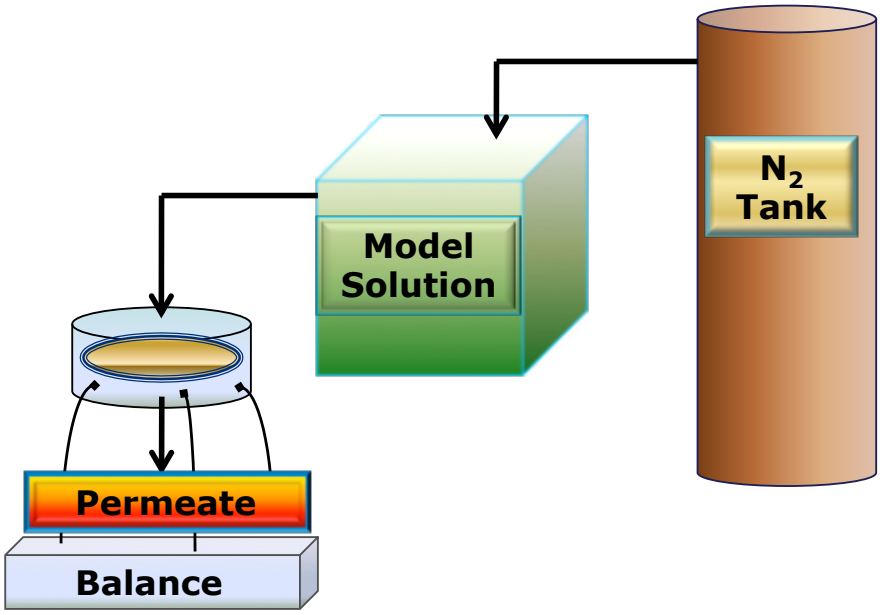

Appendix A Figure 3: Schematic of flat-sheet membrane filtration

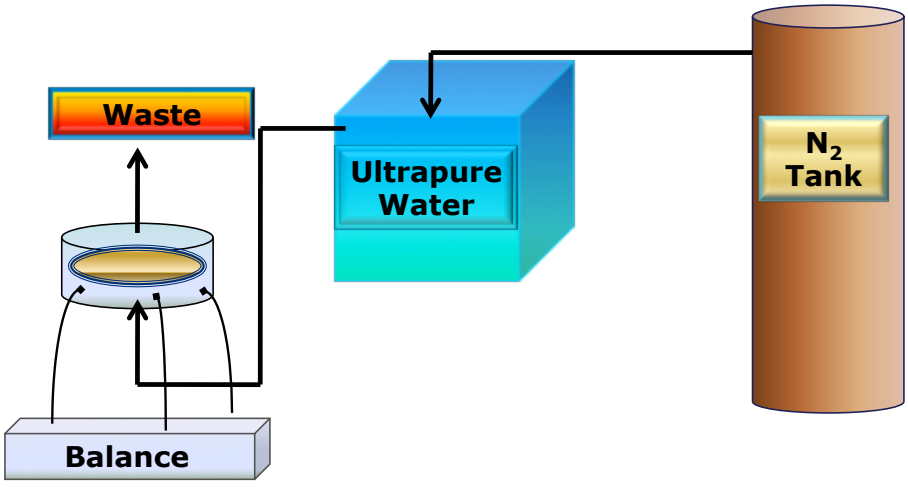

Appendix A Figure 4: Schematic of the flat-sheet membrane backwash

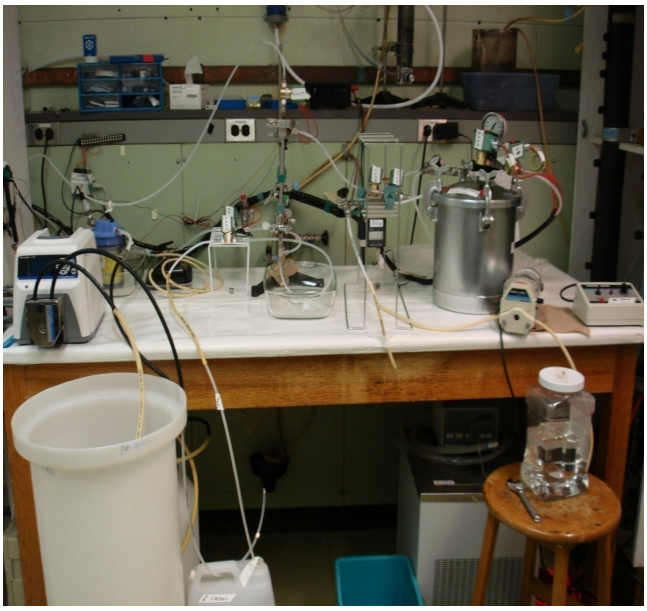

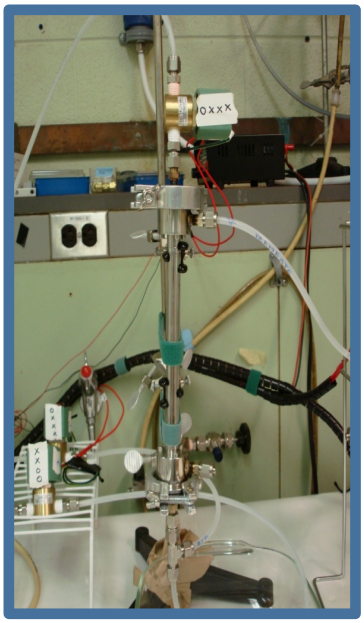

Appendix A Figure 5: Pictures of the tubular membrane and the setup

Appendix B

Additional Figures for Chapter 3: Sustainable Flux Factorial Results

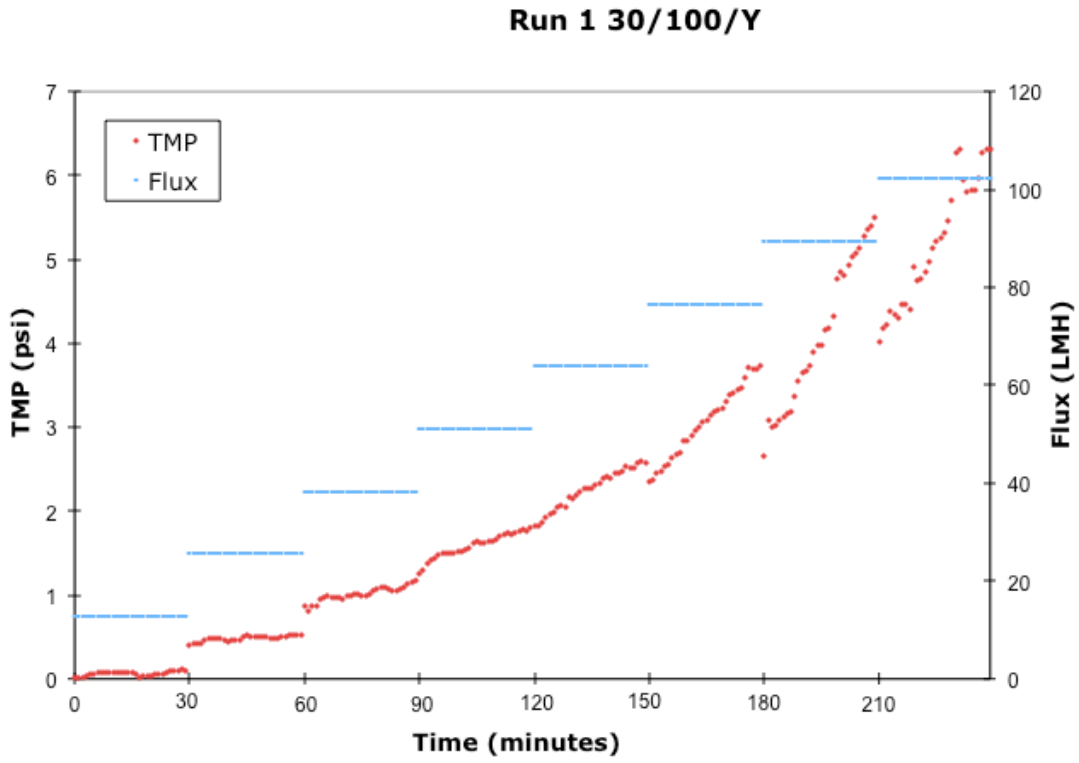

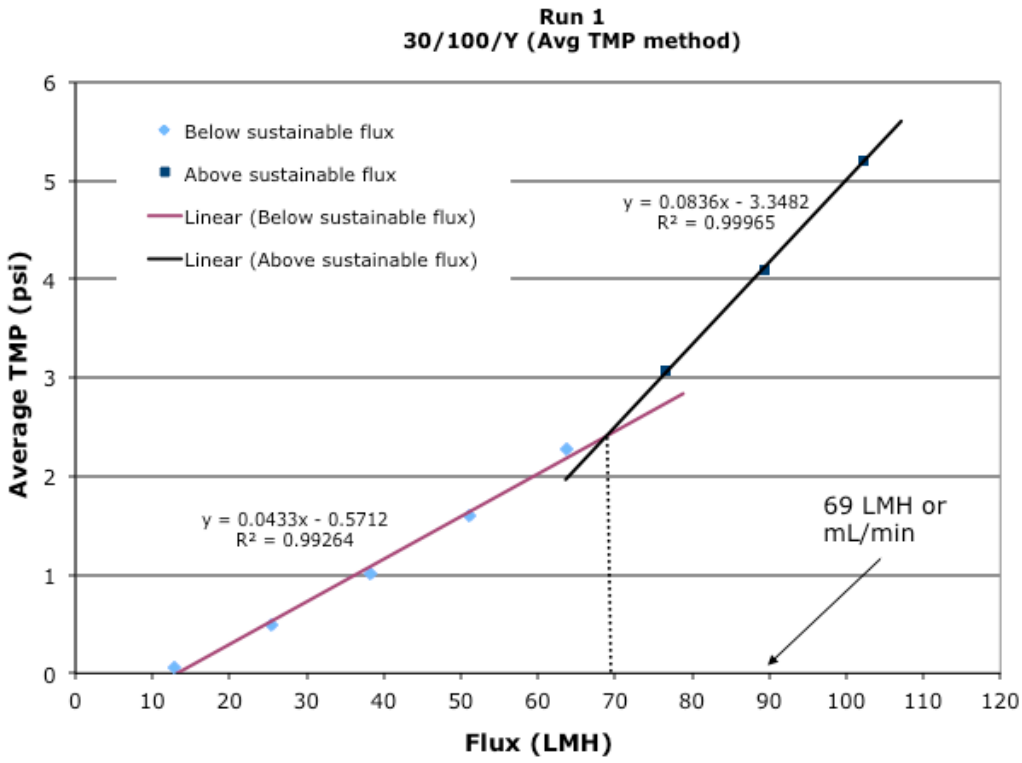

The results for Run 2 are in Chapter 3.

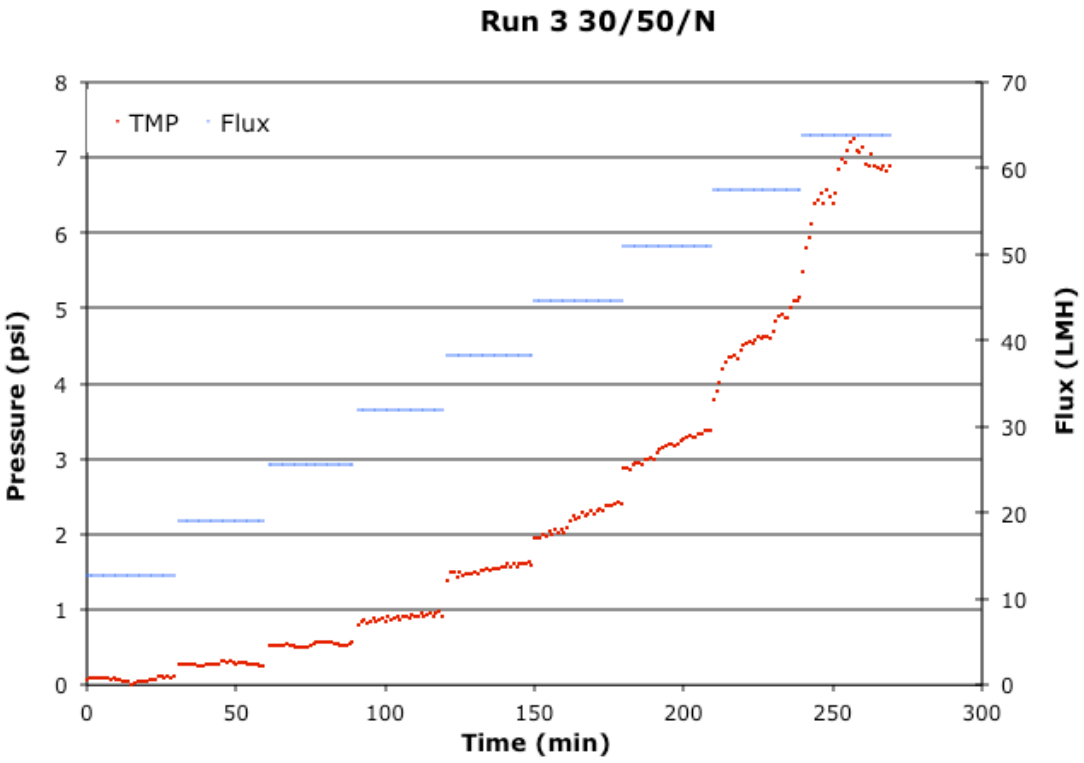
Run 3 30/50/N
TMP
Flux
Pressure (psi)
Flux (LMH)
Time (min)
0
1
2
3
4
5
6
7
8
10
20
30
40
50
60
70
0
50
100
150
200
250
300

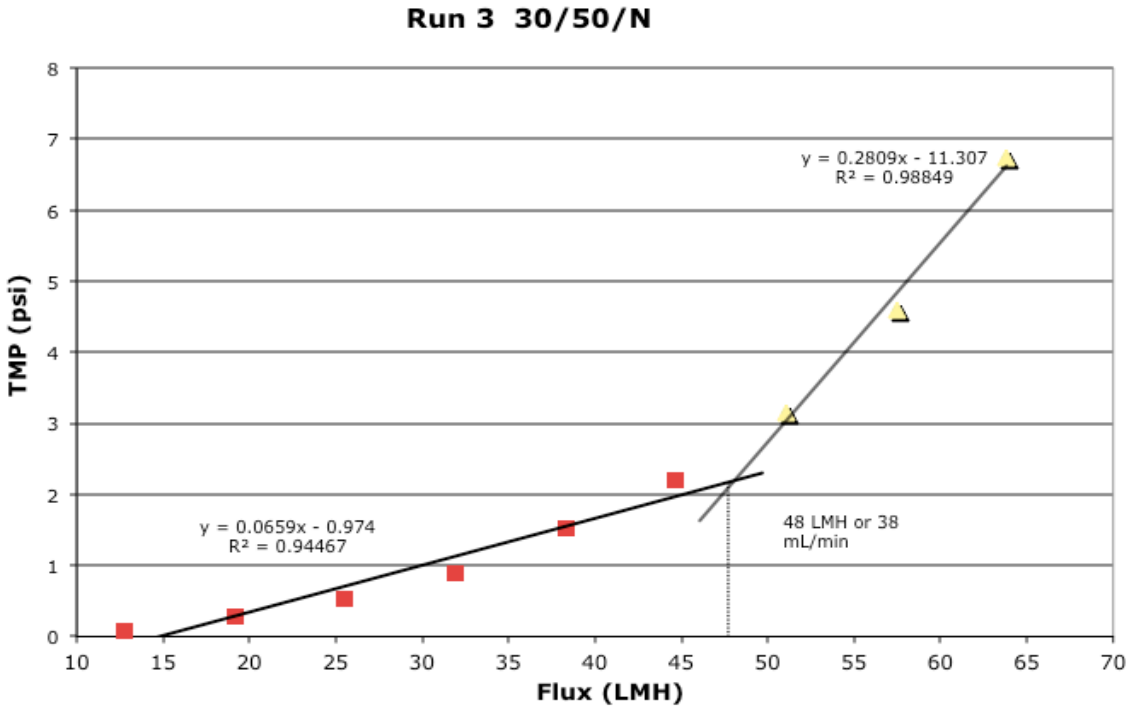
Run 3 30/50/N
y = 0.2809x - 11.307
R² = 0.98849
y = 0.0659x - 0.974
R² = 0.94467
48 LMH or 38
mL/min
TMP (psi)
Flux (LMH)
0
1
2
3
4
5
6
7
8
10
15
20
25
30
35
40
45
50
55
60
65
70

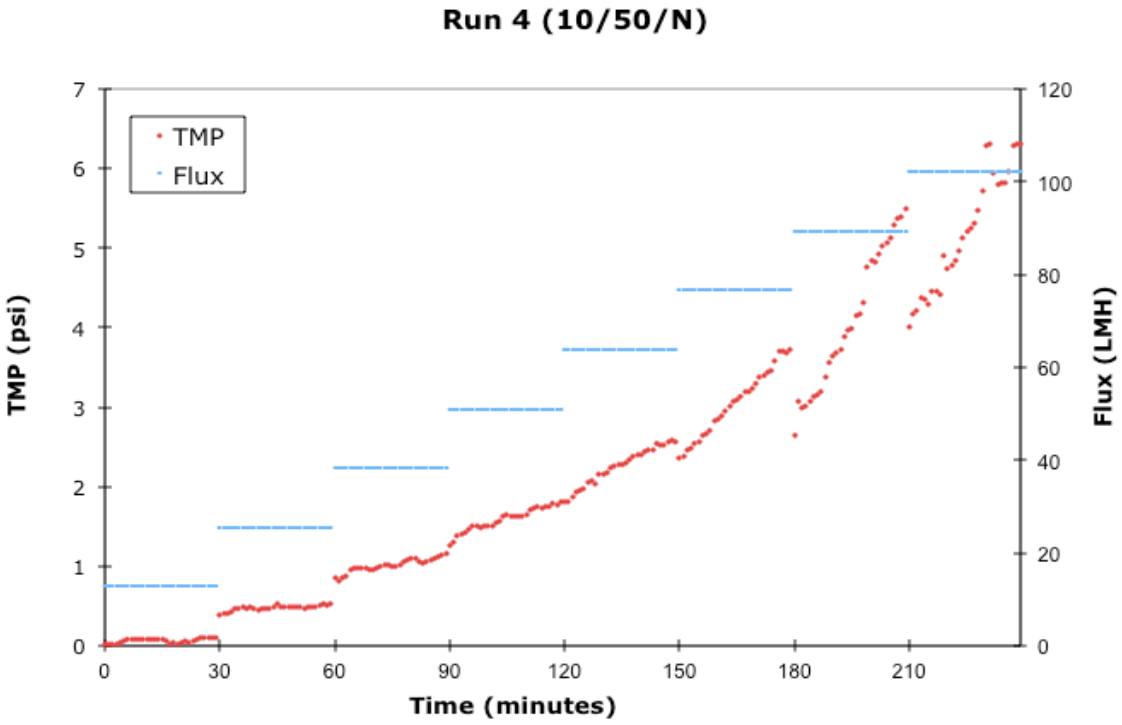
Run 4 (10/50/N)
TMP
Flux
TMP (psi)
Flux (LMH)
Time (minutes)
0
1
2
3
4
5
6
7
0
20
40
60
80
100
120
0
30
60
90
120
150
180
210

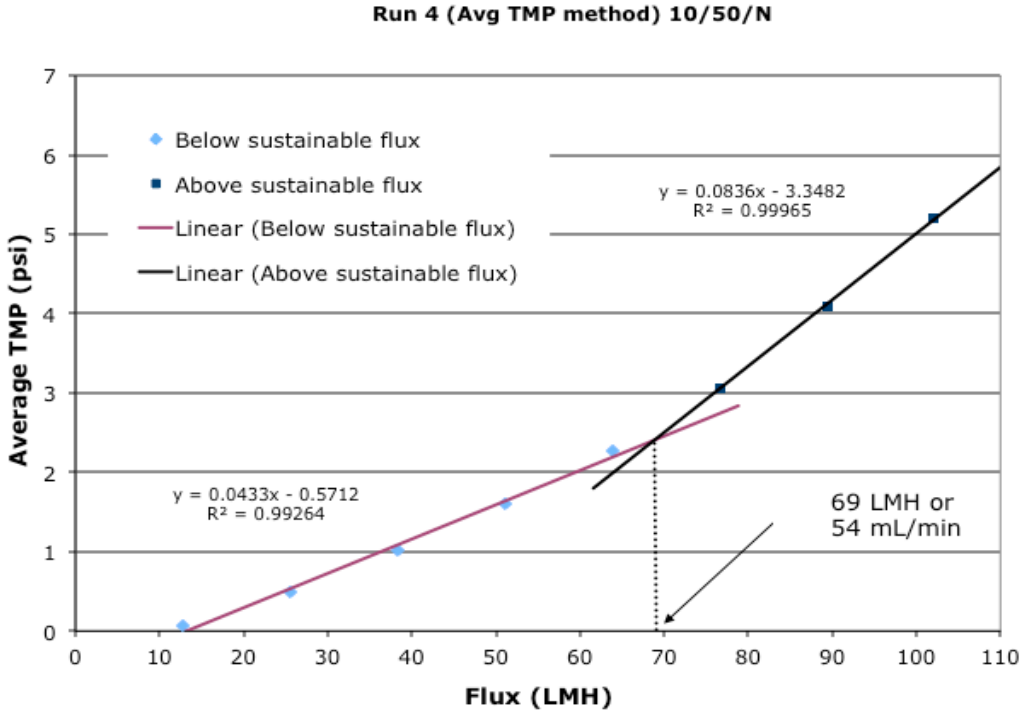
Run 4 (Avg TMP method) 10/50/N
Below sustainable flux
Above sustainable flux
Linear (Below sustainable flux)
Linear (Above sustainable flux)
y = 0.0836x - 3.3482
R² = 0.99965
y = 0.0433x - 0.5712
R² = 0.99264
69 LMH or
54 mL/min
Average TMP (psi)
Flux (LMH)
0
1
2
3
4
5
6
7
0
10
20
30
40
50
60
70
80
90
100
110

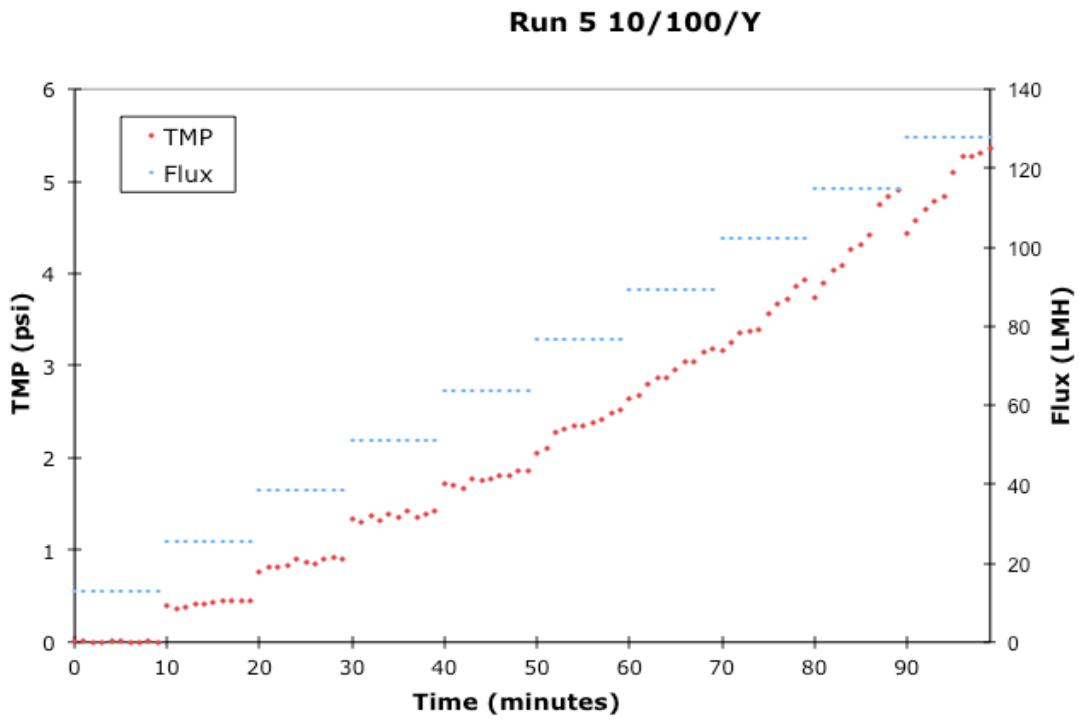
Run 5 10/100/Y
TMP
Flux
TMP (psi)
Flux (LMH)
Time (minutes)
0
1
2
3
4
5
6
0
20
40
60
80
100
120
140
0
10
20
30
40
50
60
70
80
90

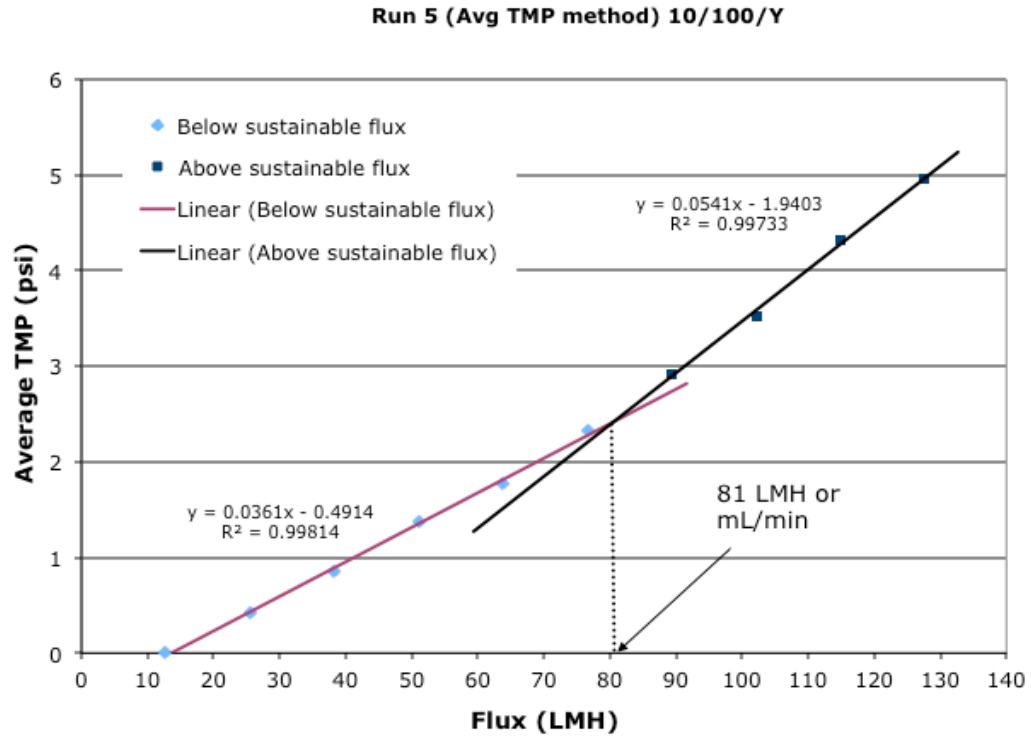
Run 5 (Avg TMP method) 10/100/Y
Below sustainable flux
Above sustainable flux
Linear (Below sustainable flux)
Linear (Above sustainable flux)
y = 0.0541x - 1.9403
R² = 0.99733
y = 0.0361x - 0.4914
R² = 0.99814
81 LMH or
mL/min
Average TMP (psi)
Flux (LMH)
0
1
2
3
4
5
6
0
10
20
30
40
50
60
70
80
90
100
110
120
130
140

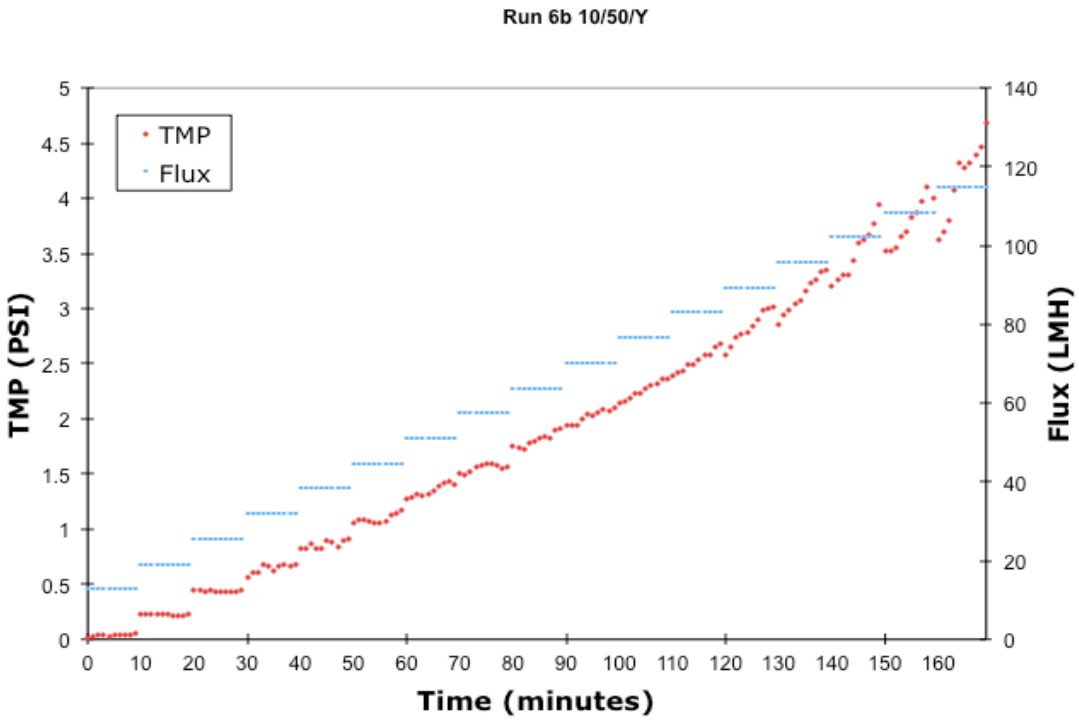
Run 6b 10/50/Y
TMP
Flux
TMP (PSI)
Flux (LMH)
Time (minutes)
0
0.5
1
1.5
2
2.5
3
3.5
4
4.5
5
0
20
40
60
80
100
120
140
0
10
20
30
40
50
60
70
80
90
100
110
120
130
140
150
160

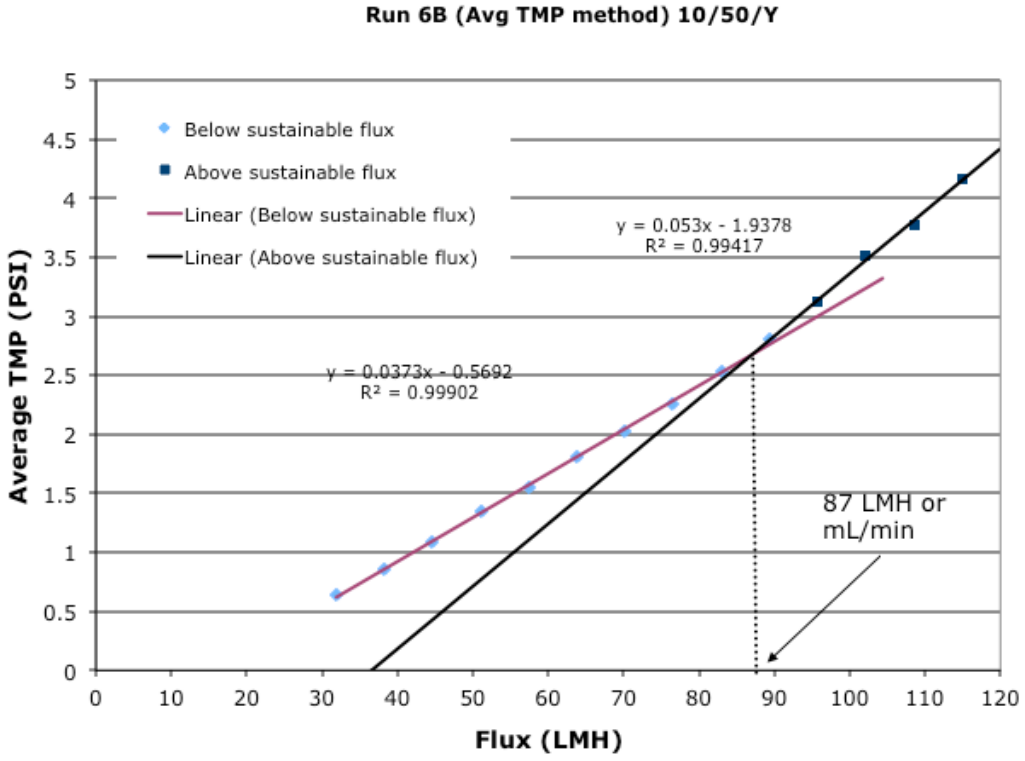
Run 6B (Avg TMP method) 10/50/Y
Below sustainable flux
Above sustainable flux
Linear (Below sustainable flux)
Linear (Above sustainable flux)
y = 0.053x - 1.9378
R² = 0.99417
y = 0.0373x - 0.5692
R² = 0.99902
87 LMH or
mL/min
Average TMP (PSI)
Flux (LMH)
0
0.5
1
1.5
2
2.5
3
3.5
4
4.5
5
0
10
20
30
40
50
60
70
80
90
100
110
120

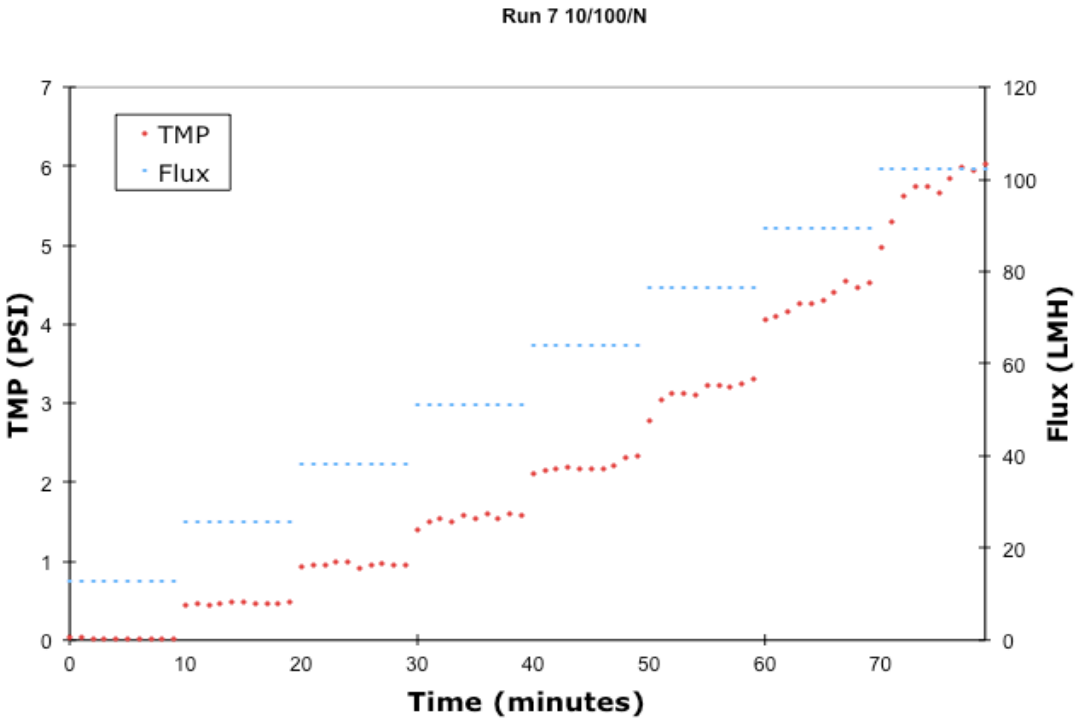
Run 7 10/100/N
TMP
Flux
TMP (PSI)
Flux (LMH)
Time (minutes)
0
1
2
3
4
5
6
7
0
20
40
60
80
100
120
0
10
20
30
40
50
60
70

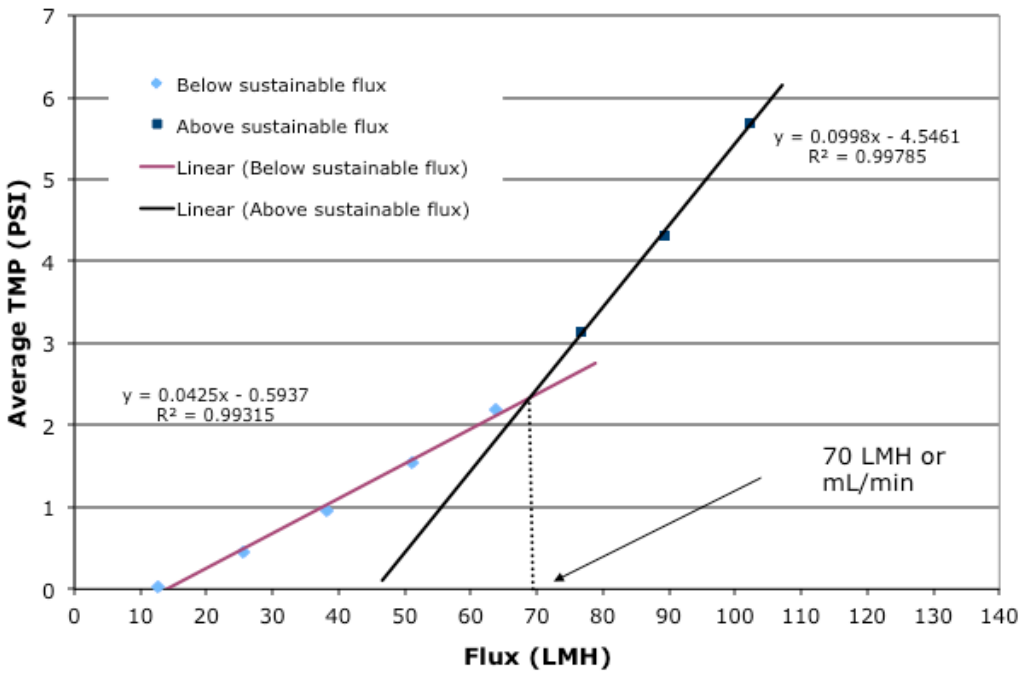
Run 7 (Avg TMP method) 10/100/N
Below sustainable flux
Above sustainable flux
Linear (Below sustainable flux)
Linear (Above sustainable flux)
y = 0.0998x - 4.5461
R² = 0.99785
y = 0.0425x - 0.5937
R² = 0.99315
70 LMH or
mL/min
Average TMP (PSI)
Flux (LMH)
0
1
2
3
4
5
6
7
0
10
20
30
40
50
60
70
80
90
100
110
120
130
140

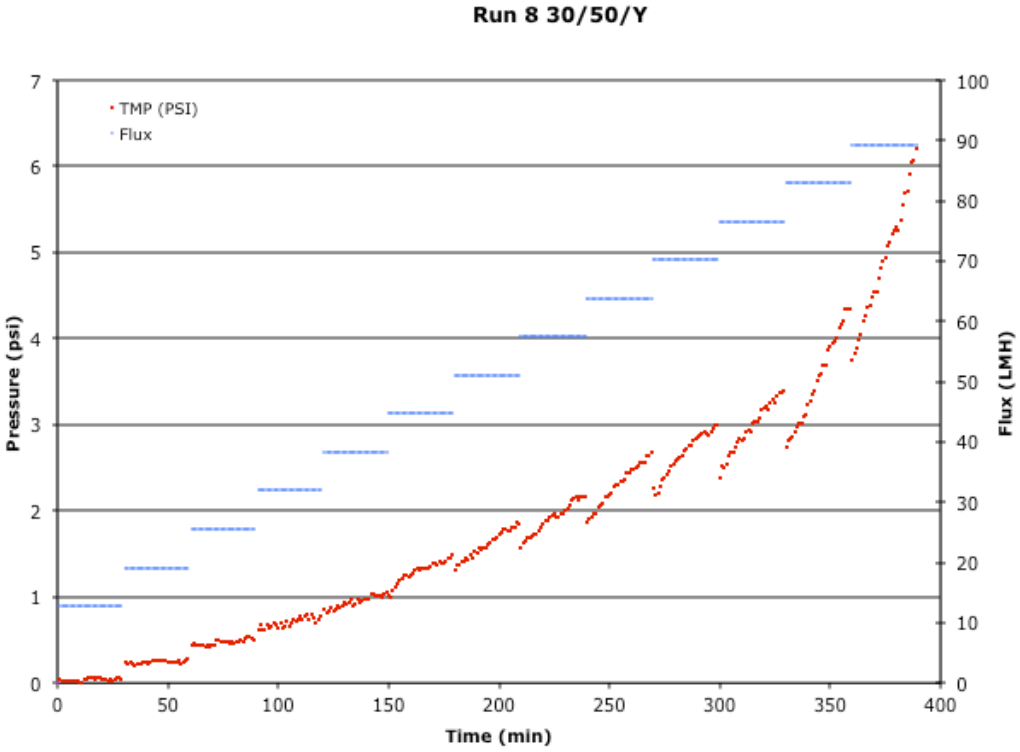
Run 8 30/50/Y
TMP (PSI)
Flux
Pressure (psi)
Flux (LMH)
Time (min)
0
1
2
3
4
5
6
7
0
10
20
30
40
50
60
70
80
90
100
0
50
100
150
200
250
300
350
400

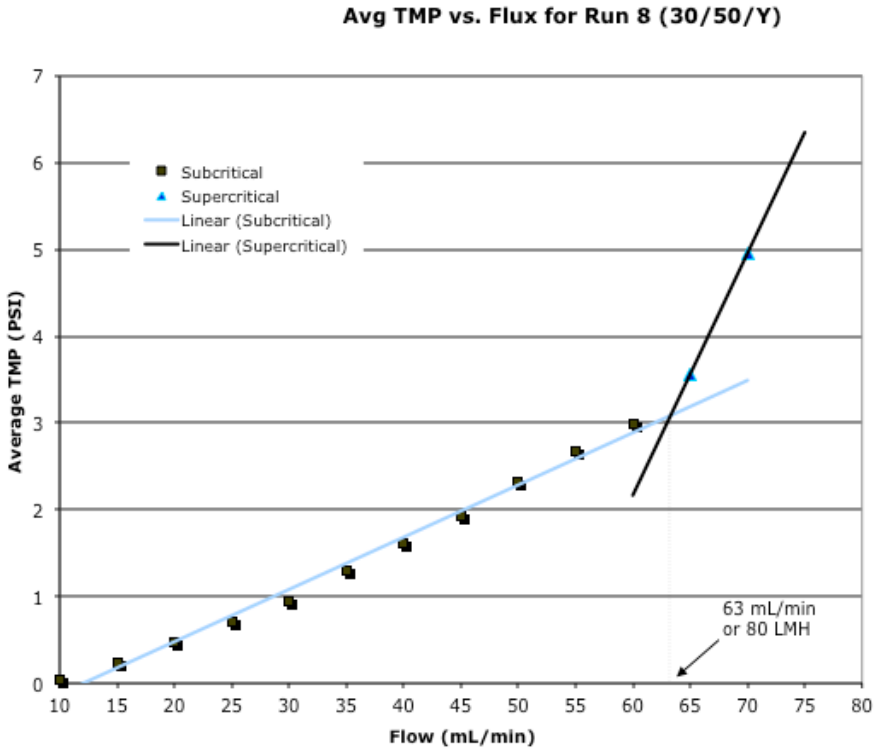
Avg TMP vs. Flux for Run 8 (30/50/Y)
Subcritical
Supercritical
Linear (Subcritical)
Linear (Supercritical)
Average TMP (PSI)
Flow (mL/min)
63 mL/min
or 80 LMH
0
1
2
3
4
5
6
7
10
15
20
25
30
35
40
45
50
55
60
65
70
75
80

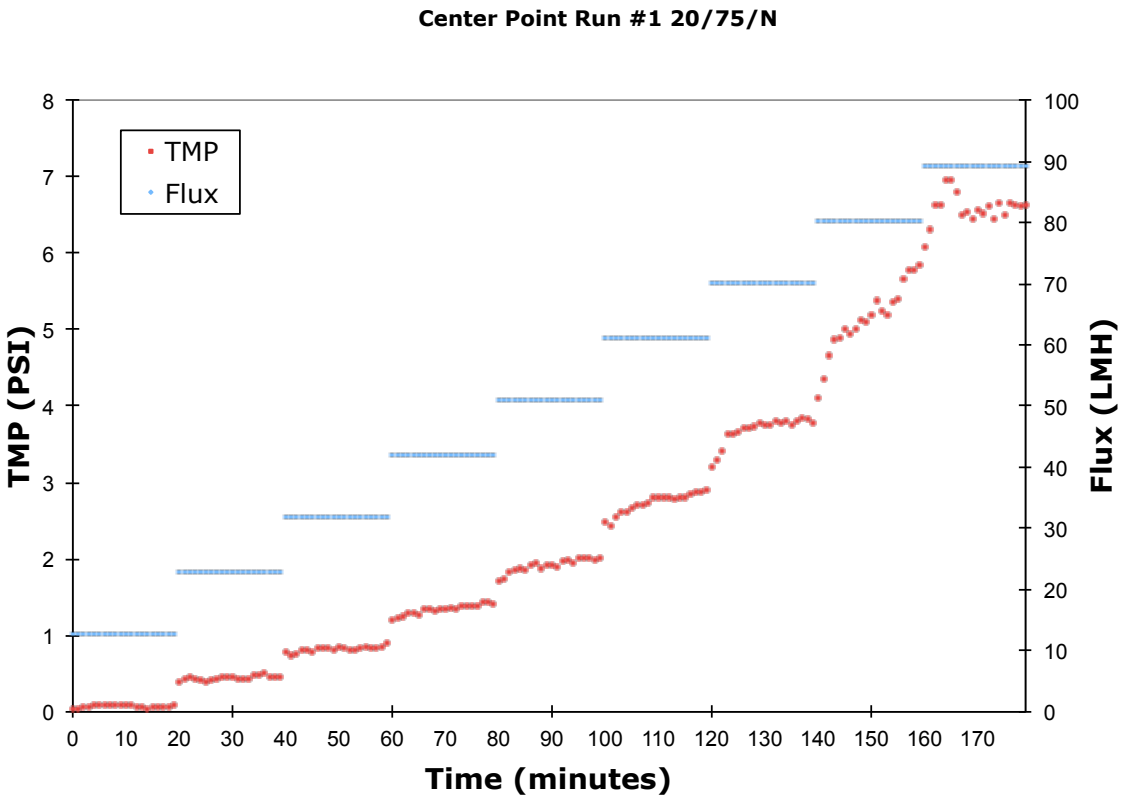
Center Point Run #1 20/75/N
TMP
Flux
TMP (PSI)
Flux (LMH)
Time (minutes)
0
1
2
3
4
5
6
7
8
0
10
20
30
40
50
60
70
80
90
100
0
10
20
30
40
50
60
70
80
90
100
110
120
130
140
150
160
170

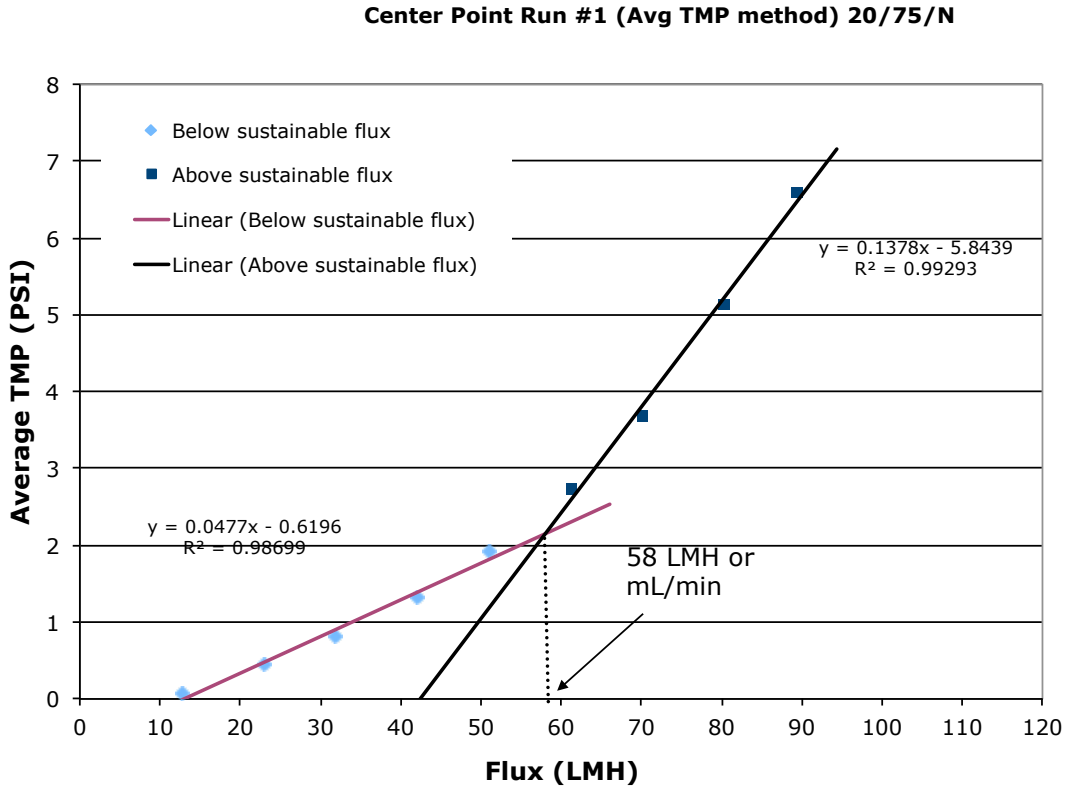
Center Point Run #1 (Avg TMP method) 20/75/N
Below sustainable flux
Above sustainable flux
Linear (Below sustainable flux)
Linear (Above sustainable flux)
y = 0.1378x - 5.8439
R² = 0.99293
y = 0.0477x - 0.6196
R² = 0.98699
58 LMH or
mL/min
Average TMP (PSI)
Flux (LMH)
0
1
2
3
4
5
6
7
8
0
10
20
30
40
50
60
70
80
90
100
110
120

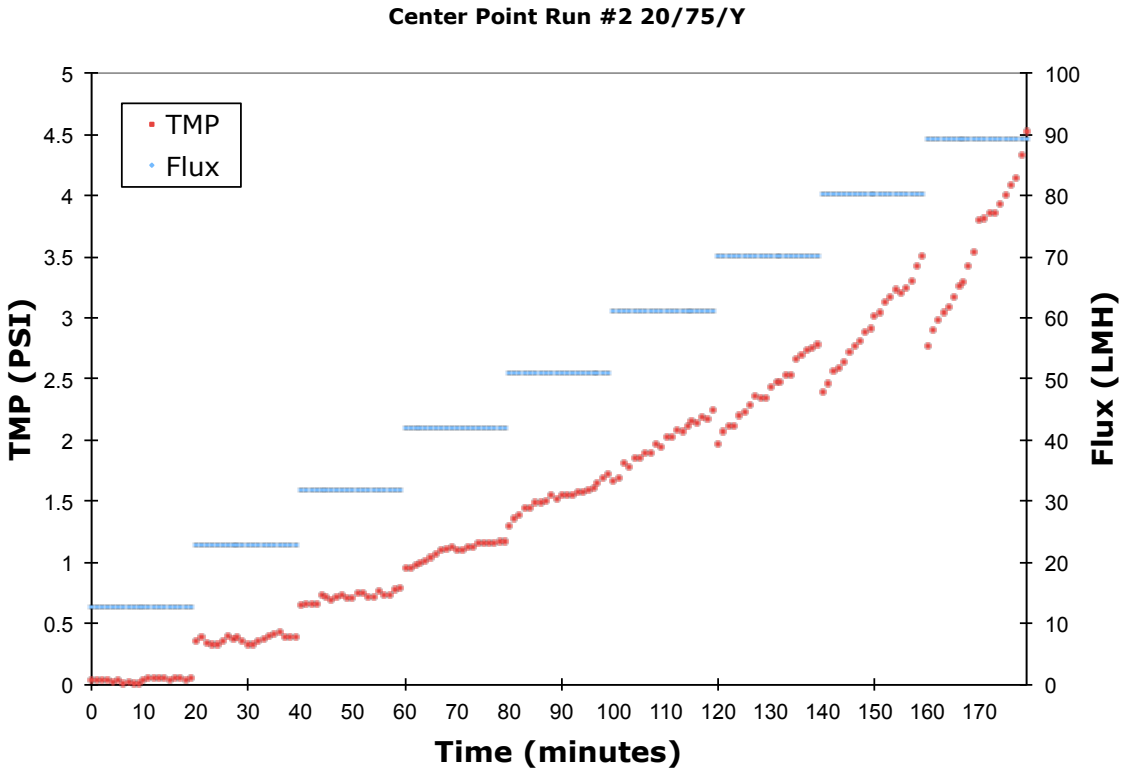
Center Point Run #2 20/75/Y
TMP
Flux
TMP (PSI)
Flux (LMH)
Time (minutes)
0
0.5
1
1.5
2
2.5
3
3.5
4
4.5
5
0
10
20
30
40
50
60
70
80
90
100
110
120
130
140
150
160
170

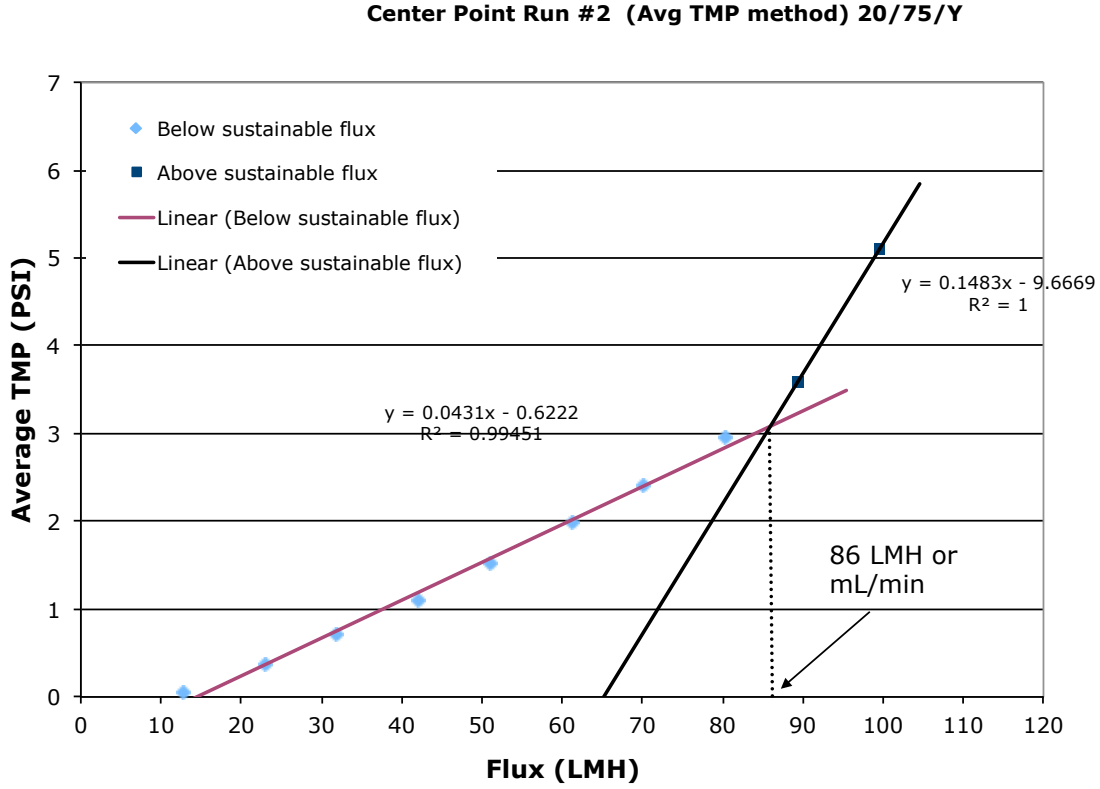
Center Point Run #2 (Avg TMP method) 20/75/Y
Below sustainable flux
Above sustainable flux
Linear (Below sustainable flux)
Linear (Above sustainable flux)
y = 0.1483x - 9.6669
R² = 1
y = 0.0431x - 0.6222
R² = 0.99451
86 LMH or
mL/min
Average TMP (PSI)
Flux (LMH)
0
1
2
3
4
5
6
7
0
10
20
30
40
50
60
70
80
90
100
110
120

Appendix C

Additional Information and Figures for Chapter 5: Tubular Ceramic Membranes with Model Solution Filtration

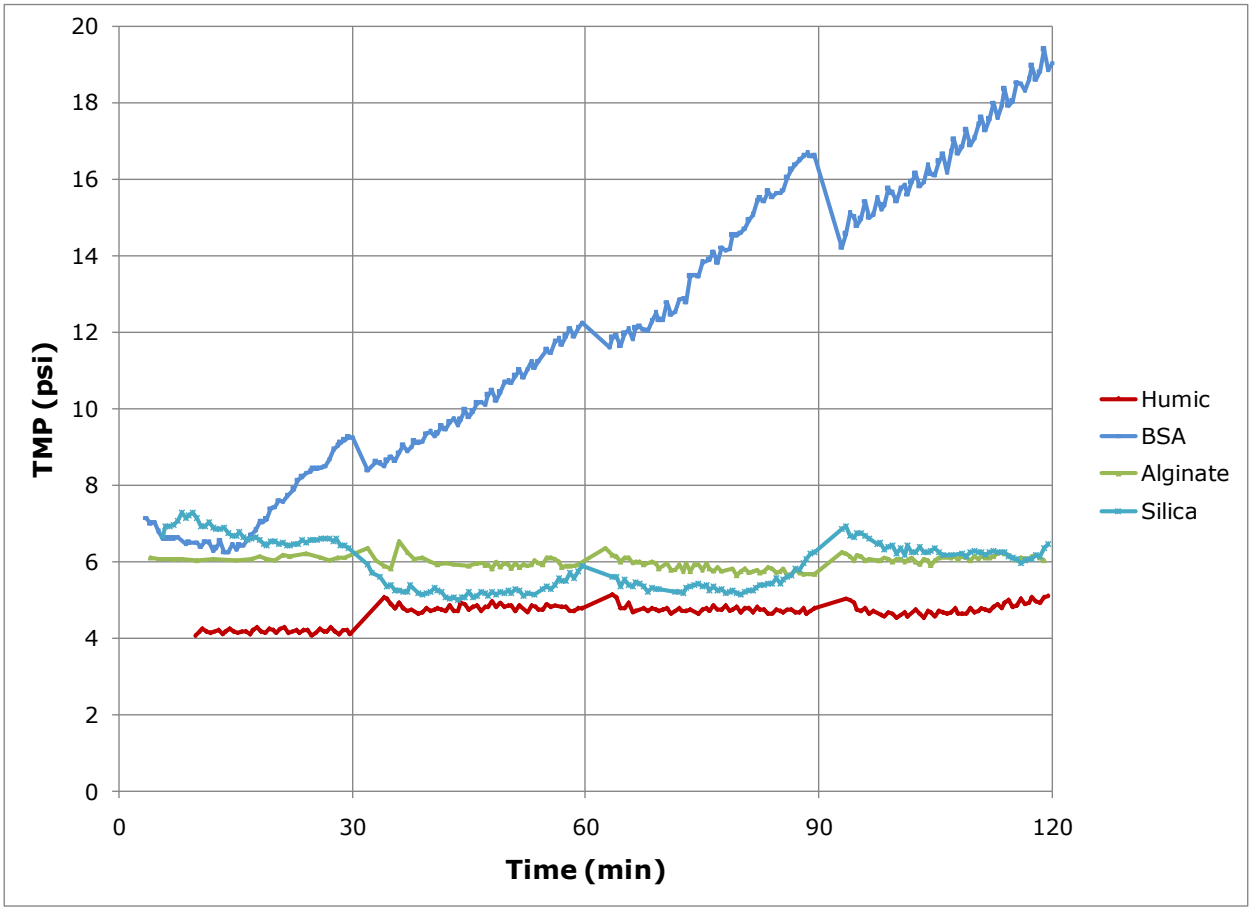

Appendix C Figure 1: Transmembrane pressure profile for tubular ceramic membranes with model solutions at lower flux of 60 LMH

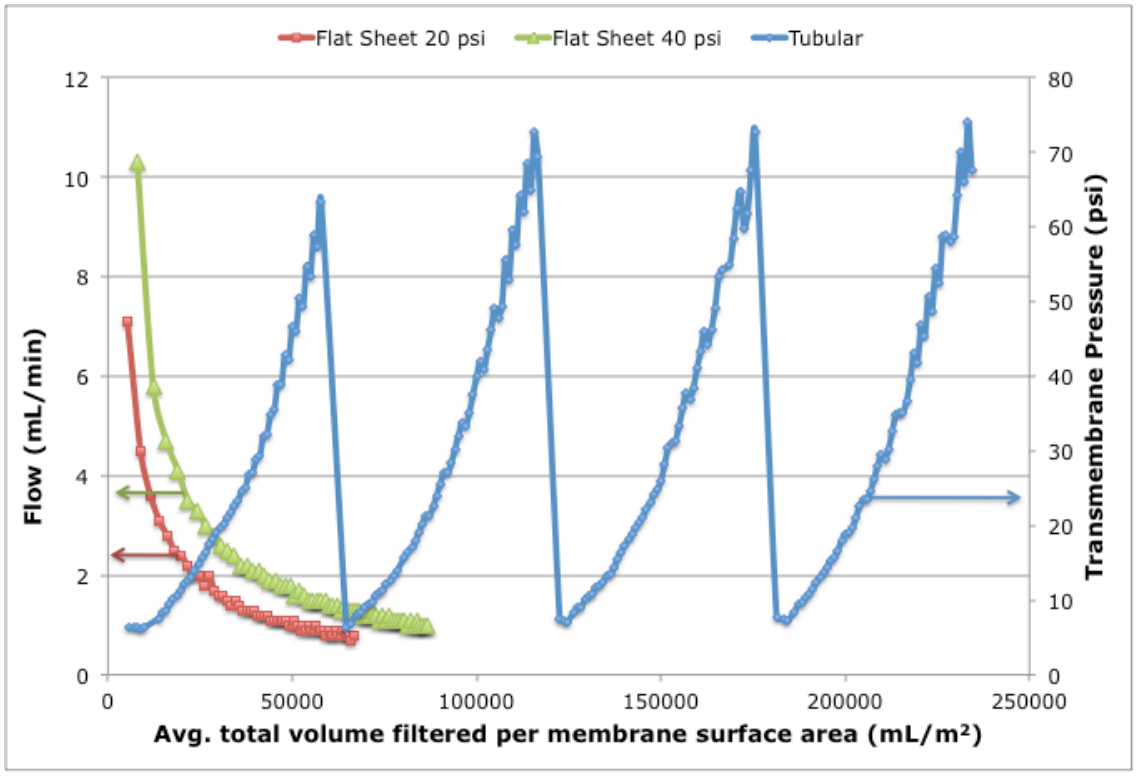

Appendix C Figure 2: A comparison of the fouling rate data for ABHS obtained between constant pressure and constant flux

Appendix C Figure 2 shows the flux decline or the transmembrane pressure increase for the constant pressure (at 20 and 40 psi) and constant flux studies, respectively, versus the average total volume filtered per membrane surface area for the ABHS combination. This combination was investigated at both 20 and 40 psi for the flat-sheet study. The purpose of the figure is to illustrate the large difference in data that is collected between the flat-sheet study at constant pressure for 1 hour without backwashing compared to the current study using tubular membranes at constant flux with backwashing every 30 minutes. Since the corresponding flux or TMP is plotted as a function of volume and not time and since the same concentrations of model foulants were used in both studies, it is an indication of the comparable mass/quantity of model foulants that has reached the membrane surface. An important difference between these two operating procedures is that since the TMP is changing throughout the filtration cycle during constant flux filtration, the hydrodynamics are also continuously changing.

Appendix D

Additional Information and Figures for Chapter 6: Tubular Ceramic Membranes with Natural Water

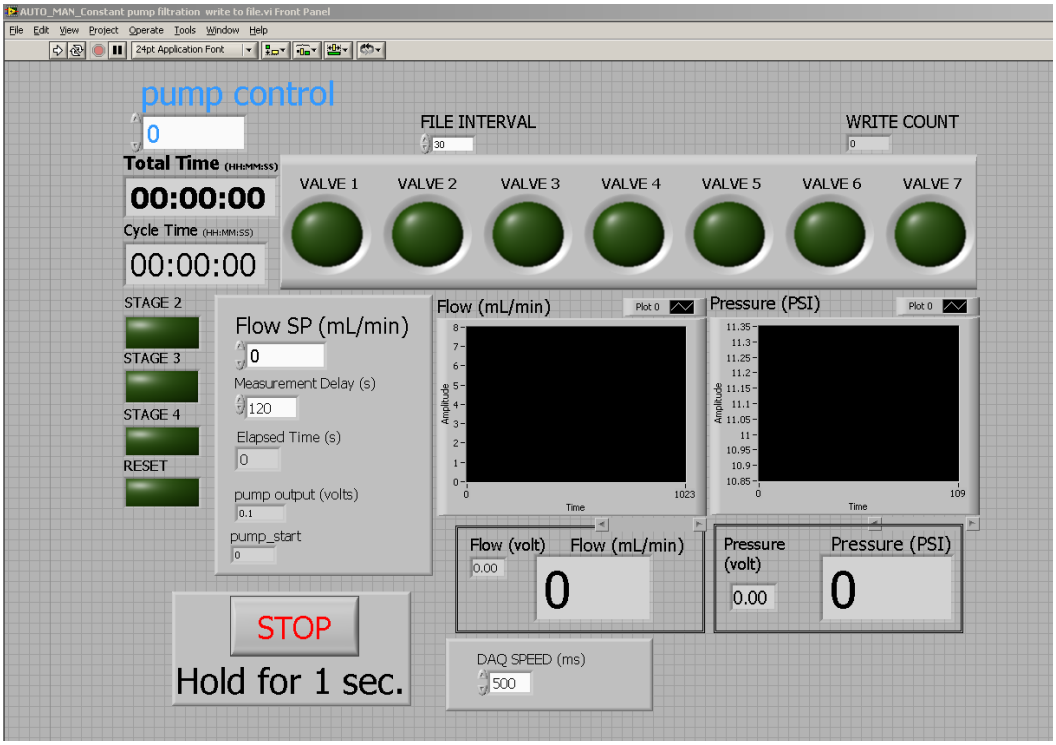

Appendix D Figure 1: Labview screenshot for operating at constant pump.

It takes approximately one minute from the time the pump is adjusted until the change is reflected in the permeate flux, therefore a "measurement delay" parameter, during which no additional pump changes can be made is included.

Appendix D 1.0 Preliminary sustainable flux experiments #1-3

Appendix D 1.1 Sustainable flux experiment #1:

This was the first experiment that was run with the tubular membrane and thus, the main issues encountered during this experiment were regarding the functionality of the setup. The biggest issue was related to the pump and flow. Although these experiments are discussed after the previous chapter on model solutions with tubular membranes, they were performed prior to the model solutions and the set-up was optimized using natural waters.

Firstly, the pump is peristaltic and will inherently have inconsistent flows due to pulsing action; therefore, the system needs to be flexible for some minor variations in the flow. Additionally, once the pump flow is increased (as a result of the flow meter detecting a decrease in flow), it takes a minimum of 1-2 minutes before the permeate flow actually increases. This meant that a wait period needed to be incorporated into the Labview program once a pump adjustment had been made (Appendix D Figure 1).

From Appendix D Figures 2 and 3 it can be observed that the flow is not very stable and can easily spike up and down. It is particularly sensitive at lower flows. At this point, adjustments were made to the setup to optimize the system and minimize the length of tubing that the water would need to travel from the feed tank to the flow meter on the permeate side of the membrane (Figure 5.1).

Unfortunately, since adjustment were being made to the setup, a long-term experiment could not be run because the water had exceeded the recommended storage maximum time of 2 weeks.

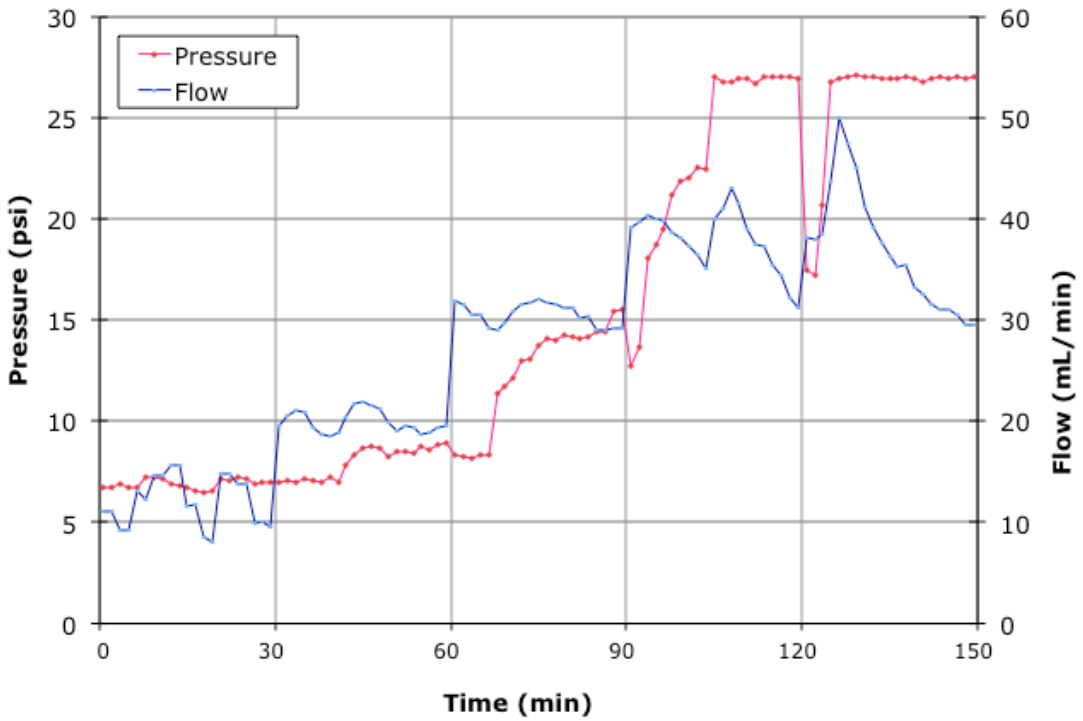

Appendix D Figure 2: Flux stepping results for sustainable flux experiment #1

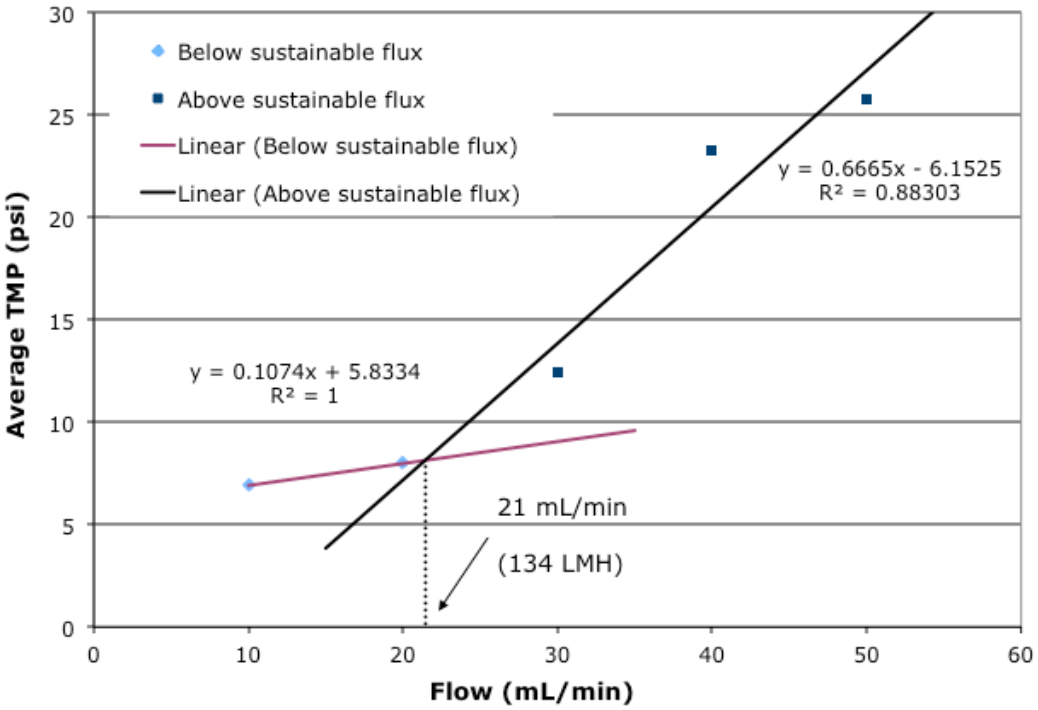

Appendix D Figure 3: Sustainable flux determination for Experiment #1

Appendix D 1.2 Sustainable Flux Experiment #2:

The results are not discussed because there was a contamination in the Grand River water and a long-term experiment was not performed. Although no data is presented or discussed for this experiment, it is included here to prevent confusion or possible errors resulting from renumbering several files.

Appendix D 1.3 Sustainable Flux Experiment #3:

Flux stepping for this experiment is shown in Appendix D Figure 4. The sustainable flux was then determined to be 17 mL/min or 109 LMH (Appendix D Figure 5). The long-term sustainable flux experiment was then performed, however, the fouling rate was very rapid and therefore, the membrane could not be operated longer than 10 hours (Appendix D Figure 6). The flux also becomes quite erratic at the higher fouling rates. Therefore, some adjustments to the Labview program and the way the feedback loop works were made. From the pressure data, it seems that the pressure transducer reaches a maximum at around 27 psi although it is rated up to at least 100 psi. This was suspicious (also the pump is rated up to at least 100 psi) and after further investigation it seemed that the pressure transducer had been compromised and malfunctioning. Therefore, the pressure results are unreliable. Although the pressure transducer data cannot be used, it is not part of the feedback loop that controls the pump speed. Therefore, the fact that the pump could not operate sustainably past 10 hours is still valuable information because it is a direct result of increased fouling.

Since operating at a flux of 109 LMH caused the membrane to foul extremely fast and there was enough water for more experimentation, another long-term experiment was performed at a lower flux of 64 LMH (10 mL/min). This additional run could help confirm that the membrane could operate sustainably for several days. The membrane was still operating sustainably into the 3rd day when the computer crashed and unfortunately the data could not be retrieved and cannot be shown. Nevertheless, the data from the LC-OCD samples that were taken are still useful and discussed in Section 6.3.3.

For the sustainable flux stepping method, only 4 data points could be used because the last flux step could not be maintained (50 mL/min or 320 LMH) (Appendix D Figure 5). Upon further observation of the results shown in Appendix D Figure 5 it seemed plausible that the sustainable flux had been

overestimated due to such few data points. Therefore, it was concluded that more data points were needed as well as a lower initial starting flux in order to acquire more detailed fouling data.

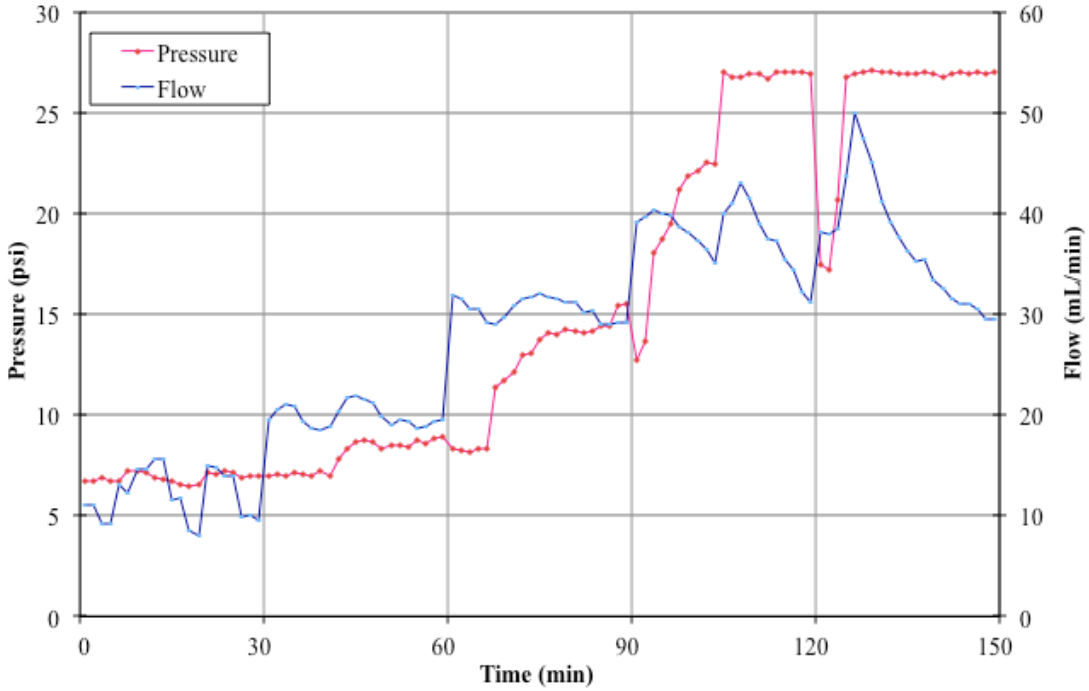

Appendix D Figure 4: Flux stepping results for sustainable flux experiment #3

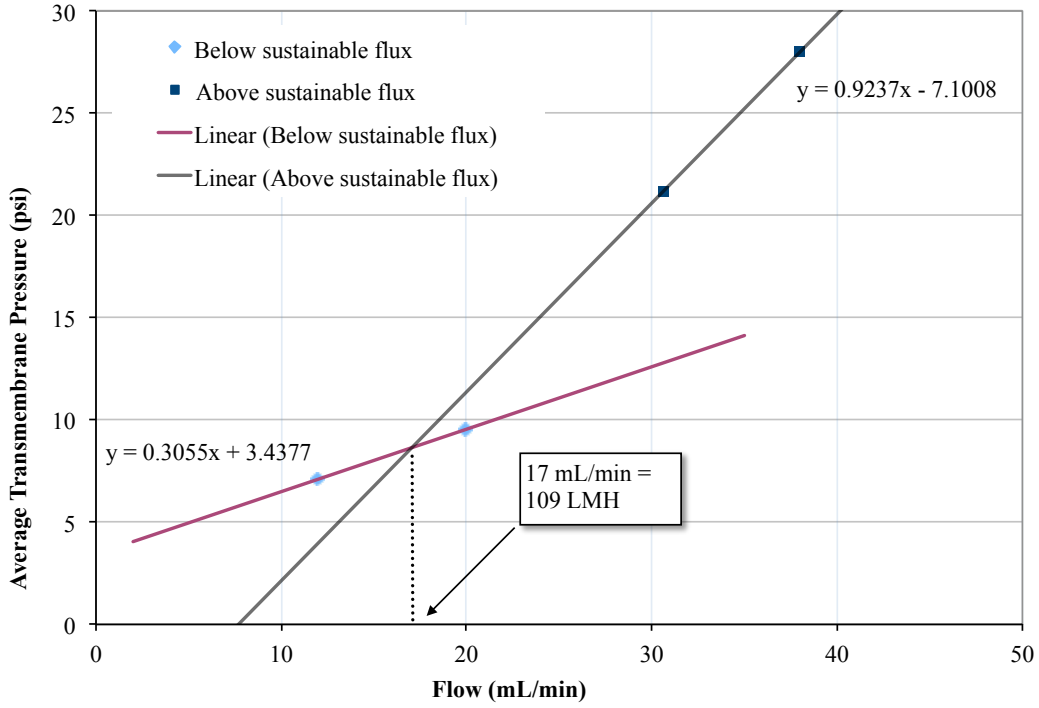

Appendix D Figure 5: Sustainable flux determination for experiment #3

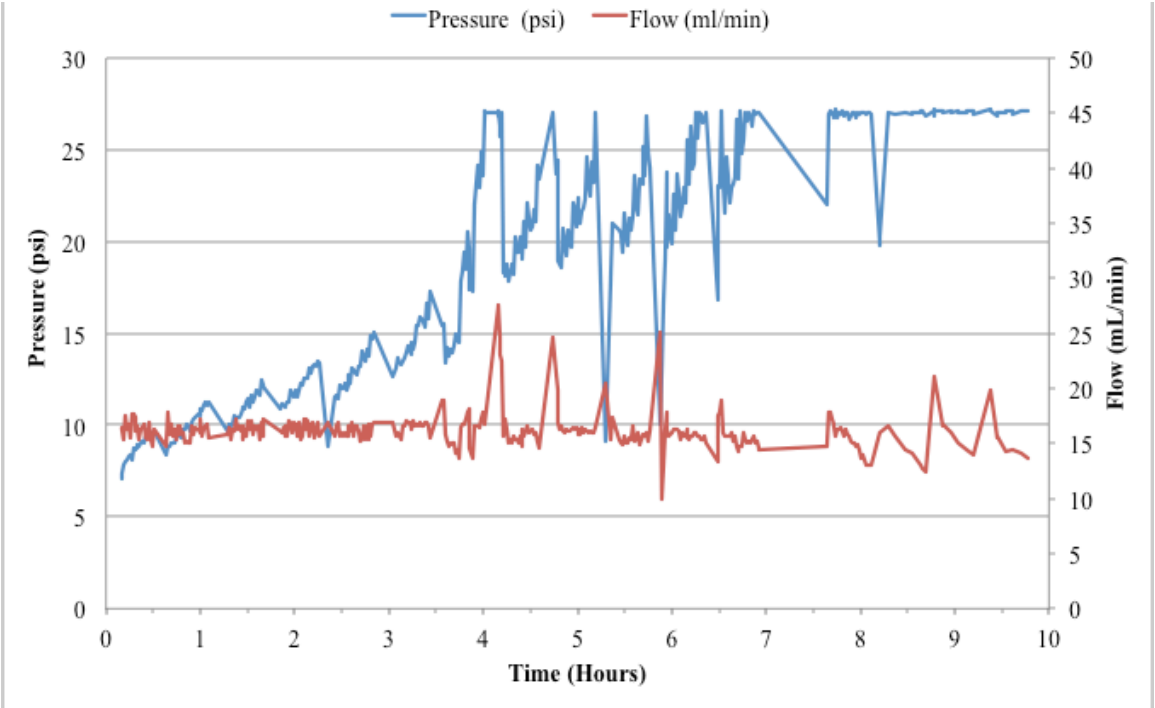

Appendix D Figure 6: Long-term Sustainable Flux Experiment #3 at 109 LMH (17 mL/min)

Conclusions

The results of this sustainable flux experiment indicated the need for the following:

- The pressure transducer was compromised and needed replacement.
- The sustainable flux method needed to be adjusted to incorporate more flux increments and start at a lower initial flux.

Ultimately, after this experiment it was concluded that the reason the membrane did not operate sustainably at the determined flux was method related and not membrane related.

Appendix D 2.0 Polymeric membrane results during experiment #5

The flux used for both membranes during this experiment was determined by using the sustainable flux method with the polymeric membrane (Appendix Figure 7). It was assumed at this point that the method worked for the polymeric membrane (due to positive results in Chapter 3 with this membrane) and possibly not the ceramic membrane. The results of the polymeric membrane are difficult to interpret because they are impacted by the fact that the pump could not maintain the desired flux and since this could only be manually measured, constant adjustments to the pump were required. Furthermore, with the highly turbid water, fouling was much more extreme/rapid and the flux dropped significantly over short periods of time. Therefore, the TMP readings do not reflect constant flux since a constant flux could not be maintained once high fouling is experienced. Except for the initial 24 hours, the polymeric membrane experienced very high fouling rates, which could only be mitigated through regular maintenance cleans (Appendix D Figure 8). Nevertheless, maintenance cleans were not considered or incorporated into the development of the sustainable flux methodology. Therefore, since operation of the polymeric membrane without maintenance cleans was not sustainable it seems that the sustainable flux methodology developed in Chapter 3 is not appropriate even for the polymeric membrane.

When backwash samples were taken, the tank was fully drained and filled with ultrapure water, then the permeate was backwashed through the membrane. This was done in order to determine which foulants were hydraulically reversible and to allow for a comparison to the ceramic membrane, which also uses ultrapure water for backwashing. This step resulted in noticeable TMP decreases (indicated by the blue arrows) that were greater than the normal backwash. When taking BW samples TMP decrease was 80% after 2 hours, 75% after 26 hours, 31% after 48 hours, and 34% after 71 hours. The first backwash sample was taken soon after filtration had started, therefore, there was not much time for fouling to accumulate and form a significant cake layer. This may explain why at 26 hours backwash sampling had a greater effect on the TMP. The next sample was taken shortly after a maintenance clean and the last sample was taken approximately 5 hours after a maintenance clean; therefore, again there was likely not as much time for cake accumulation. With a maintenance clean the TMP decrease was 68% after 45.5 hr, 72% after 67 hours, 72% after 72 hours, and 82% after 99 hours. Therefore, it seems that an average of a 50-60% decrease in TMP with a maintenance clean can be expected under these conditions.

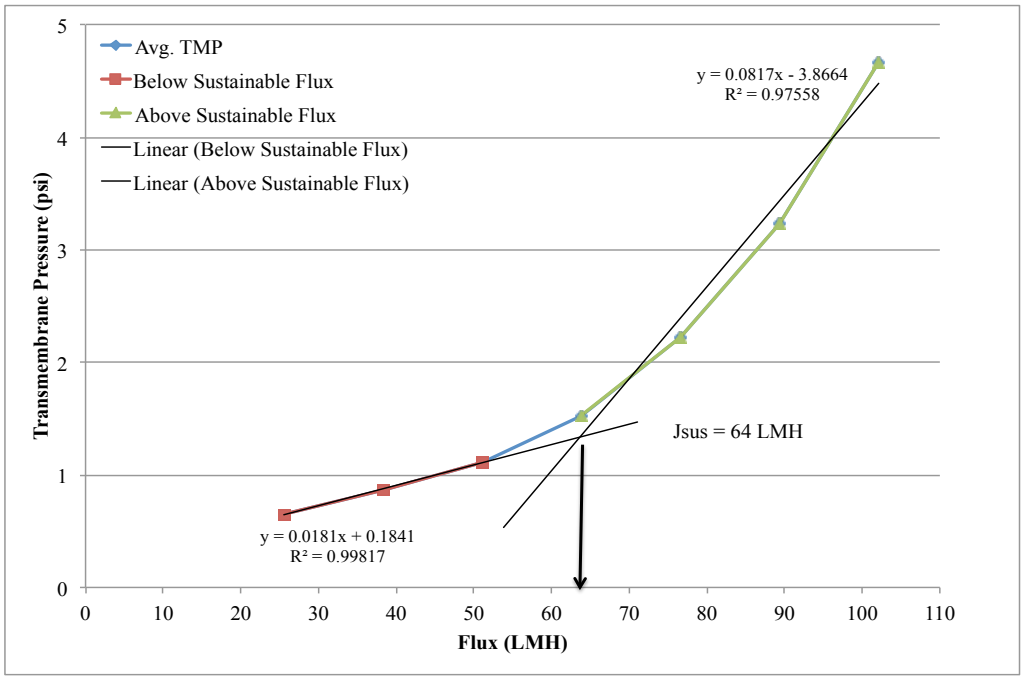

Appendix D Figure 7: Sustainable flux determination for experiment #5 with the polymeric membrane setup

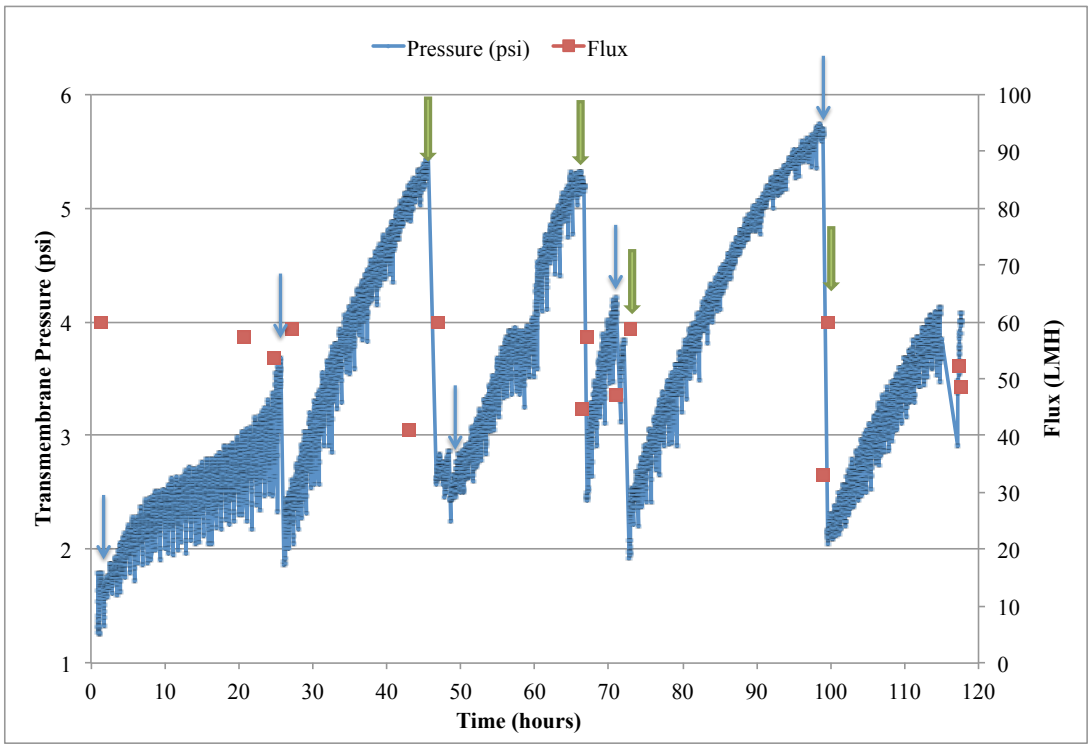

Appendix D Figure 8: TMP and flux data for the long-term experiment with the polymeric membrane setup. Blue arrows indicate when a backwash sample was taken and green arrows indicate a maintenance

Appendix D 3.0 Additional figures

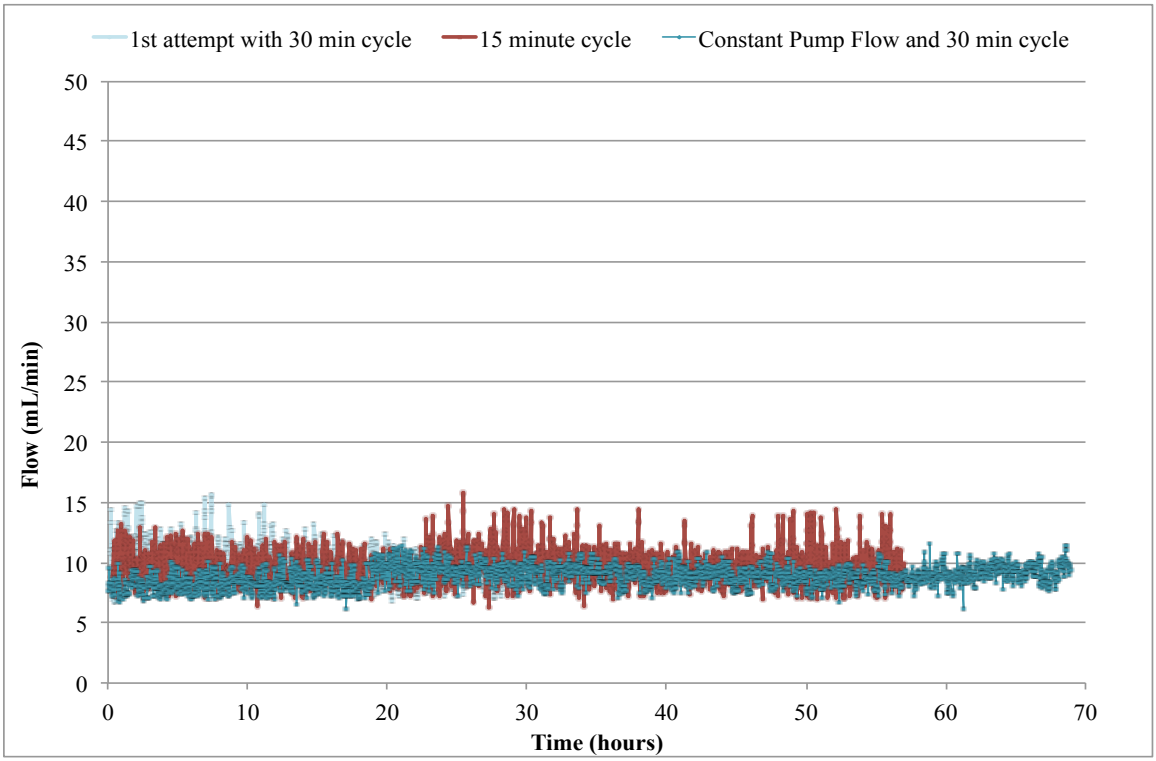

Appendix D Figure 9: The flow for all three attempts at sustainable flux experiment #5

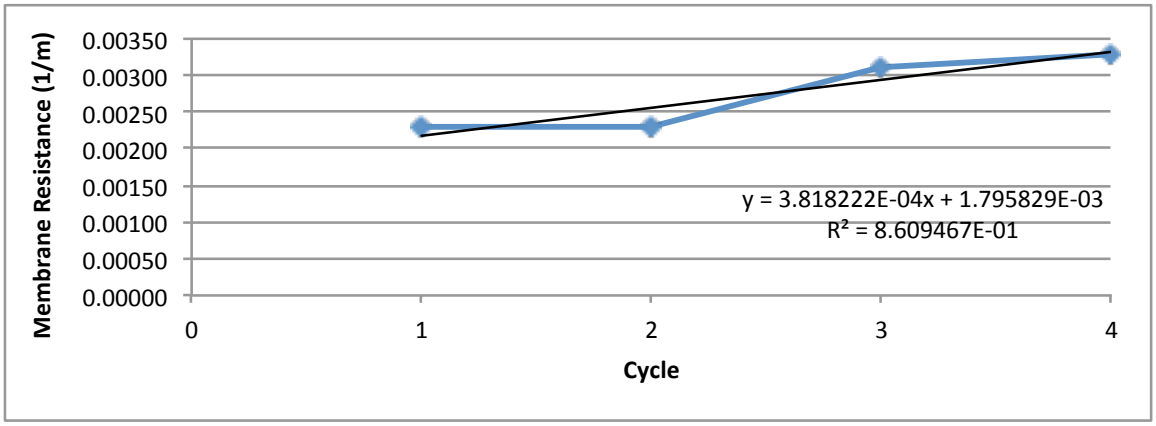

Appendix D Figure 10: Membrane resistance following backwash for experiment #4 at 20 mL/min (128 LMH)

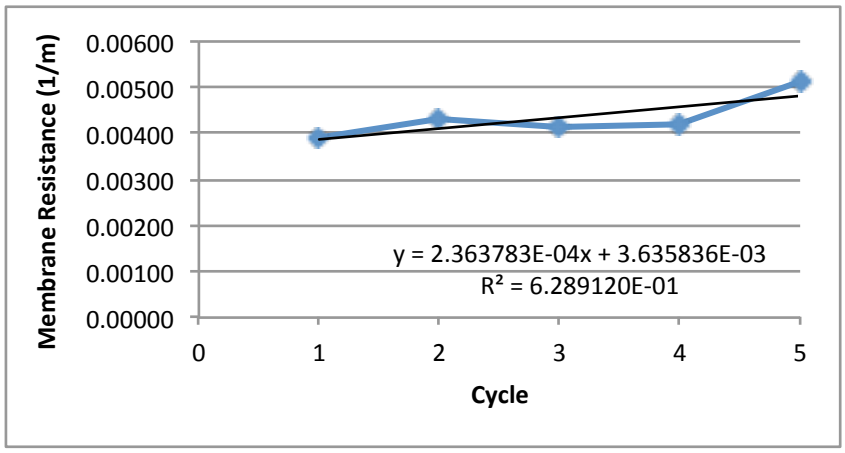

Appendix D Figure 11: Membrane resistance following backwash for experiment #4 at 10 mL/min (64 LMH)

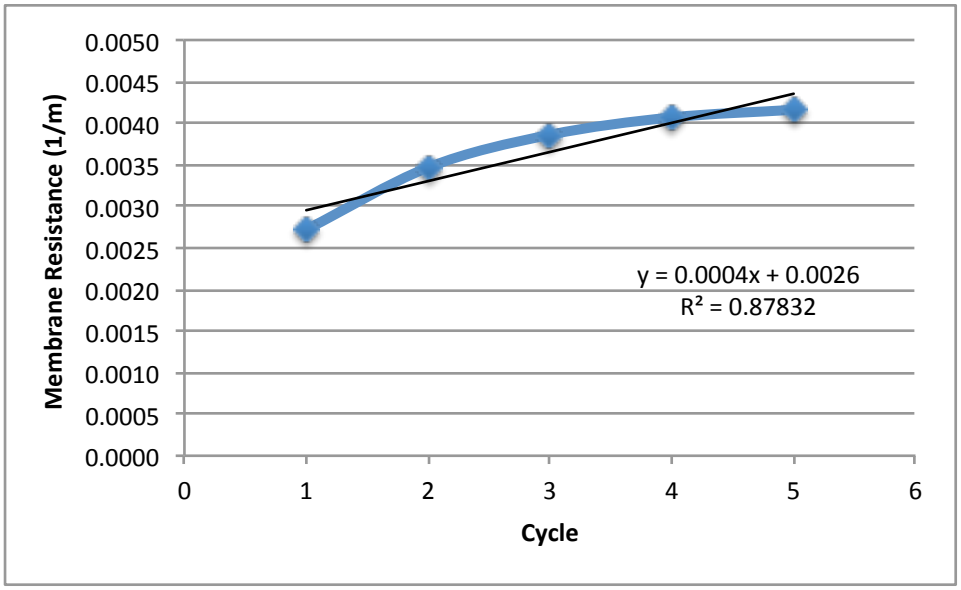

Appendix D Figure 12: Membrane resistance following backwash for experiment #4 at 5 mL/min

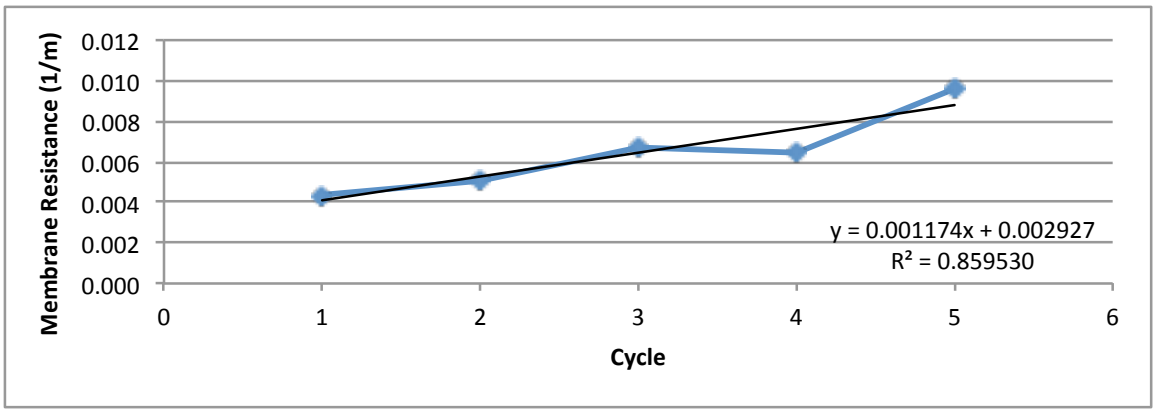

Appendix D Figure 13: Membrane resistance following backwash for experiment #5 at 10 mL/min (64 LMH)

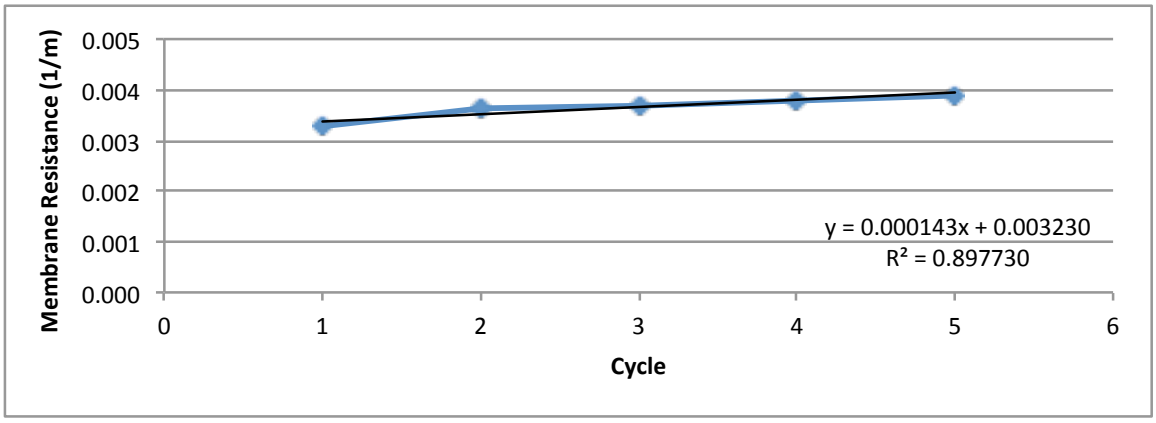

Appendix D Figure 14: Membrane resistance following backwash for LTJ5 at 10 mL/min (64 LMH) at constant pump setting

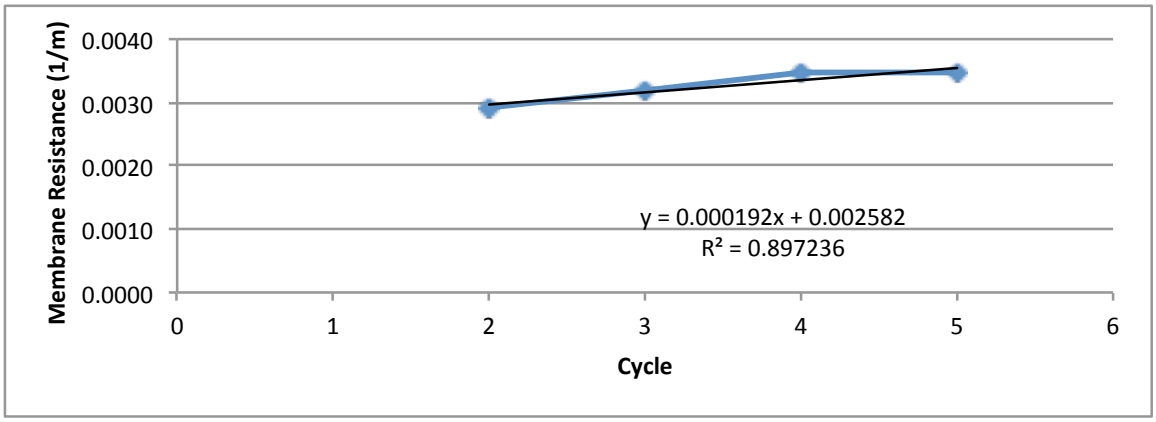

Appendix D Figure 15: Membrane resistance following backwash for experiment #5 at 10 mL/min (64LMH) with 15 minute filtration cycles

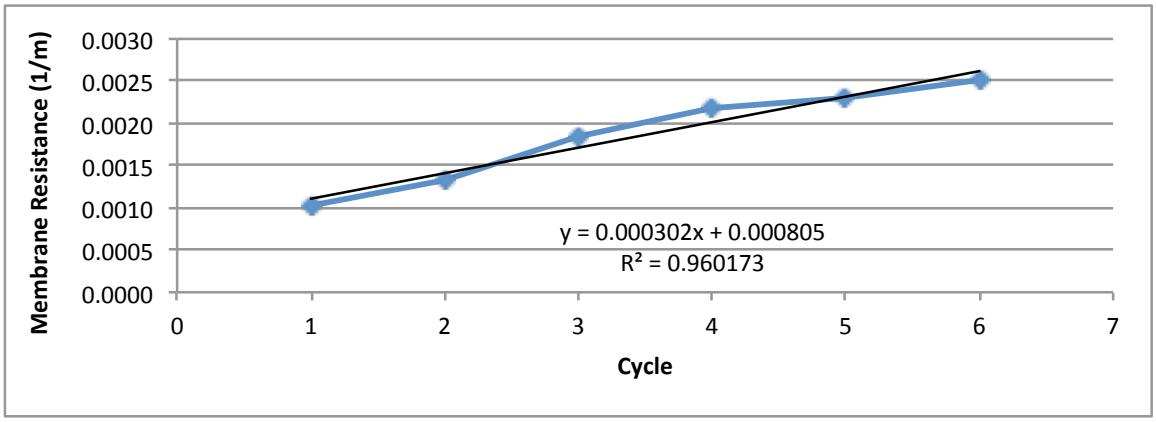

Appendix D Figure 16: Membrane resistance following backwash for experiment #6 at 17 mL/min

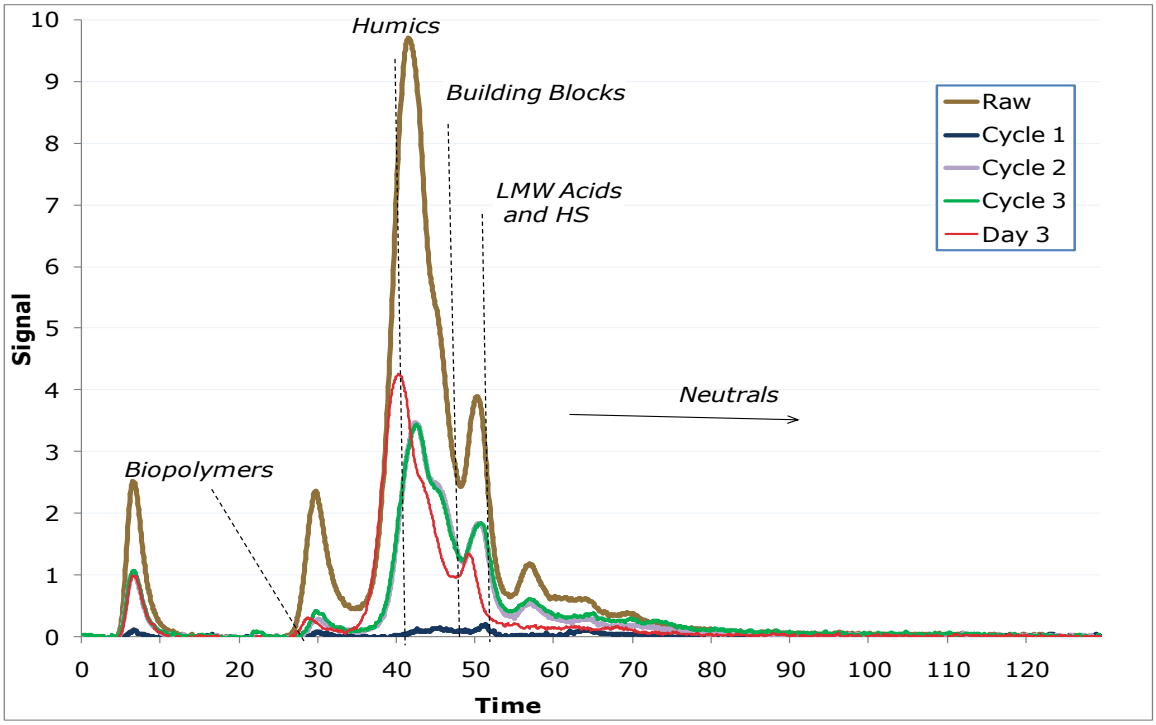

Appendix D Figure 17: Experiment #3 permeates at the beginning of the cycle

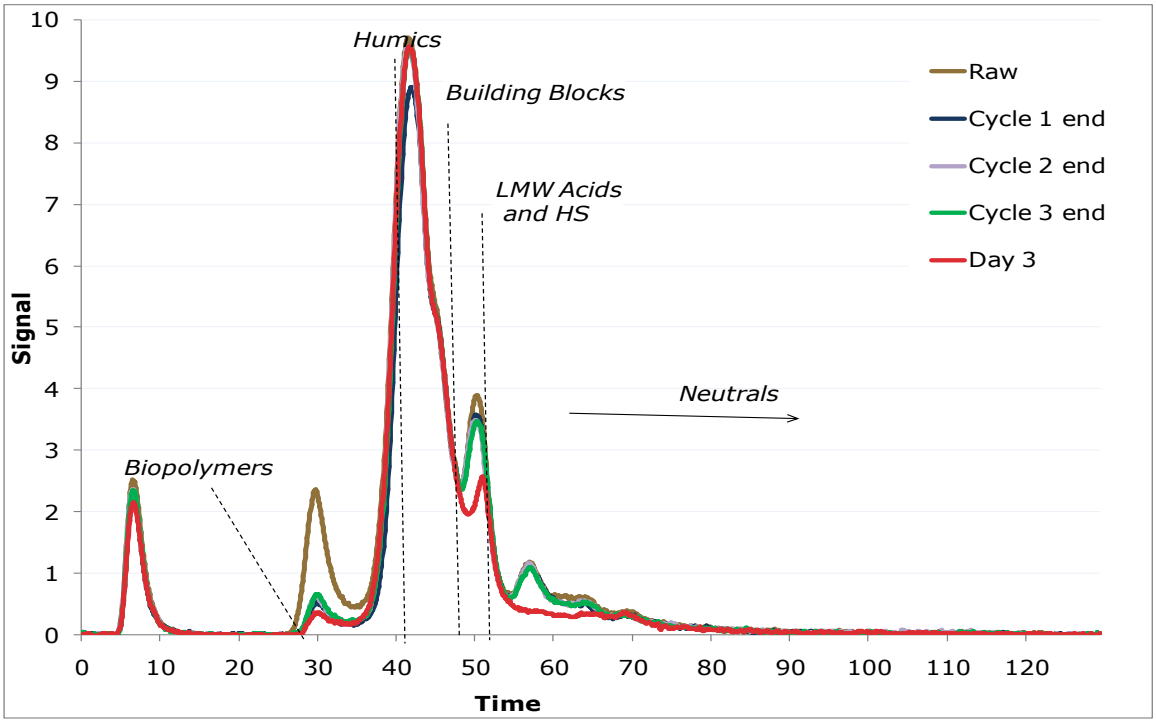

Appendix D Figure 18: Experiment #3 permeates at the end of the cycle

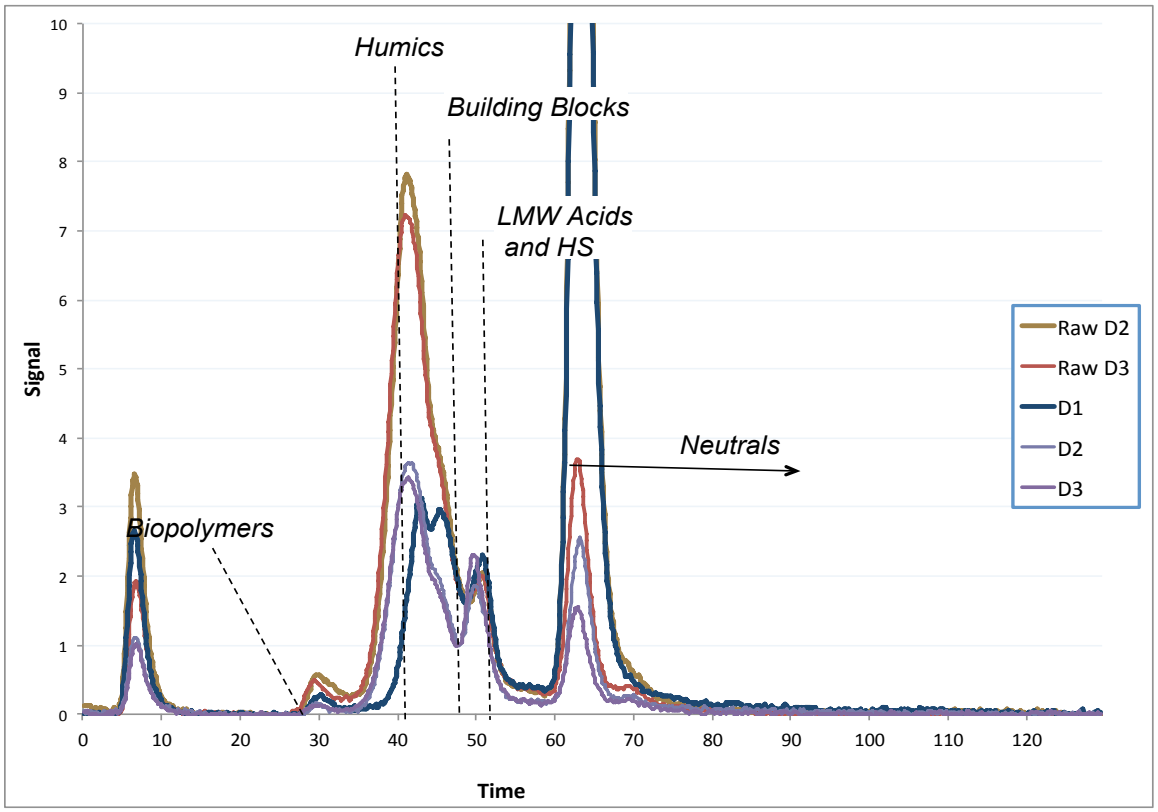

Appendix D Figure 19: Ceramic permeate chromatograms for experiment #5 with a 15 minute filtration cycle (D=Day)